Deriving Spatial Patterns of Severe Rainfall in Southern Ontario From Rain Gauge and Radar Data

by

Graham J. Smith

A thesis
presented to the University of Waterloo
in fulfillment of the
thesis requirement for the degree of
Master of Environmental Studies
in
Geography

Waterloo, Ontario, Canada, 2010

Author’s Declaration

I hereby declare that I am the sole author of this thesis. This is a true copy of the thesis, including any required final revisions, as accepted by my examiners.

I understand that my thesis may be made electronically available to the public.

Abstract

Severe weather is a natural product of the earth's atmosphere. Water delivered by storms sustains important biophysical functions whereas from a human perspective severe weather can have negative effects when damage is caused to material assets and health. Modern society has acquired knowledge and technological know-how to deal with the effects of severe weather on human activity. In Canada storm water management infrastructure and land management practices reflect decades of analysis of weather data. In Ontario the engineering of storm water management infrastructure has assumed a long term climate 'normal' to guide specifications for safely operating during severe storm events. Water resource managers also consider long term climate records to guide decision-making for water use and allocation. However, given the measured and predicted effects of global warming, climate normals generated from data from the past may not be suitable for planning for the climate of the future.

From the Fourth Assessment by the Intergovernmental Panel on Climate Change it is generally accepted that one of the predicted effects of climate change will be shifts in the intensity, the frequency and the spatial distribution of severe storm events. Human activity in regions affected by these changes will be required to make adjustments to their water and land management practices and to make better strategic decisions about the use of existing knowledge and technology to adapt to change.   The climate in Southern Ontario is expected to shift to earlier snow melt, earlier spring storms and increased storm severity throughout the summer season. The region is particularly vulnerable to the combined effects of these climate parameters in the spring months of March, April and May when the risk of flooding and erosion is at its greatest. The predicted increase in summer rainfall intensity will have negative impacts for soil erosion and flood damage.

This paper presents an analysis of 46 years of climate data in Southern Ontario. The spatial distribution of intense rainfall is examined to determine the extent to which rainfall exhibits localized patterns and whether there have been changes in the patterns over the period of data. The spatial patterns of severe rainfall between the months of March and September are also examined with the use of 13 years of radar data.   A comparison of one hour rainfall measured from NEXRAD radar data to Environment Canada's intensity duration frequency (IDF) data demonstrates a technique of spatial analysis that could aid in revising IDF values and indentifying areas that experience a higher frequency of intense rainfall events.

Acknowledgements

I would like to thank George Sousa and Dwight Boyd from the Grand River Conservation Authority for supporting my work on this project and for providing guidance and inspiration. Thank you to Environment Canada staff, specifically Joan Klassen for her continued enthusiasm toward my research, Norman Donaldson for sharing his radar expertise, Edson Paixao for incorporating the radar analysis into his own IDF research, as well as, for being a reader, and Linda Mortsch from the Adaptation and Impacts Research Division, for being a reader and providing helpful feedback. Thank you to my advisor Dr. Peter Deadman for his patience and encouragement as I gradually brought this project to fruition, Dr. Doug Dudycha for first introducing me to GIS in the early 1990's during my undergraduate degree, and for being a reader for this paper, and also to Dr. Brent Hall who over a number of courses and projects challenged and mentored me on concepts related to GIS that lead to new insights and perspectives. Lastly, but most importantly, thank you to my family, Seven, Vari, Tom and Ryan for their patience and unconditional support, especially when I struggled at times to find the right balance for life's priorities.

Table of Contents

Author's Declaration ii
Abstract iii
Acknowledgements iv
Table of Contents v
List of Figures viii
List of Tables xi
Chapter 1 Introduction 1
1.1 Living with Severe Storms 1
1.2 Problem Statement: Monitoring Weather and Climate Change 3
1.3 Objectives – Spatial Analysis of Severe Rainfall Patterns in Southern Ontario 8
1.4 Study Area 9
1.5 Structure of Thesis 10
Chapter 2 Climate Change and Severe Storms in Ontario 11
2.1 Intergovernmental Panel on Climate Change (IPCC) 11
2.1.1 The Connection Between Increased CO2 Concentration and Precipitation 12
2.2 Impacts of Climate Change on Southern Ontario 13
2.2.1 Spring Susceptibility 15
2.2.2 Water Runoff, Infiltration and Evapotranspiration 15
2.2.3 Soil Erosion 17
2.3 Severe Weather of Southern Ontario 18
2.3.1 Climate Regions of Southern Ontario 19
2.3.2 Types of Storms 20
2.3.2.1 Winter and Tropical Storms 21
2.3.2.2 Convection 22
2.3.2.3 Rainfall Intensity-Duration-Frequency 22
2.3.2.4 What Is Normal? 27
2.3.3 Severe Local Storms 29
2.3.4 Local Factors 32
2.3.4.1 Lake Breeze and Convergence 32
2.3.4.2 Terrain 35
2.3.4.3 Urban Heat Island and Pollution 37
2.3.4.4 Soil and Land Cover 38

Chapter 3 Weather Monitoring Data 40
3.1 Environment Canada Climate Data 40
3.1.1 Climate Stations 40
3.1.2 Decreasing Number of Climate Stations 42
3.2 Radar Data 44
3.2.1 Overview of NEXRAD System 45
3.2.1.1 Radar Principles 45
3.2.1.2 Digital Precipitation Array Data 46
3.2.2 Data Acquisition 47
3.2.3 Differences Between NEXRAD and Environment Canada Radar 48
3.2.4 Limitations and Sources of Error in Radar Data 49
Chapter 4 Spatial Analysis Methodology 53
4.1 Deriving Daily Climate Surfaces 53
4.1.1 Spline Interpolation 54
4.2 Analysis of Climate Surfaces 56
4.3 NEXRAD Radar Processing 56
4.4 NEXRAD Radar Analysis 58
4.4.1 Anomalous Propagation Handling 58
Chapter 5 Spatial Analysis Results 60
5.1 Rainfall Mapped from Spline Versus Radar – Case Study of July 14, 1997 60
5.2 Spline Interpolation Results 64
5.2.1 Monthly Temperature Trends 1960 to 2005 64
5.2.2 Monthly Precipitation Trends 1960 to 2005 70
5.2.3 Average Annual Precipitation 72
5.2.4 Patterns of Changing Rainfall Averages 74
5.2.5 Spatial Patterns of Severe Rainfall Events 75
5.2.6 Number of Rainfall Days 78
5.3 NEXRAD Radar Analysis 81
5.3.1 Spatial Patterns of Severe Rainfall Events 1996 to 2005 81
5.3.1.1 Getis Clustering of the Severe Rainfall Patterns 83
5.3.2 Number of Rainfall Days 86

5.3.3 One Hour Rainfall Intensity Analysis ... 87
5.3.4 Comparison of Radar to 1 Hour IDF Values from Environment Canada ... 92
5.3.5 Comparison of NEXRAD and Rain Gauge – Case Study of July 2008 ... 95
5.4 Summary of Results and Findings ... 103
5.4.1 Normals for Monthly Temperature and Precipitation ... 103
5.4.2 Rainfall Patterns ... 104
5.4.3 Rainfall Intensity Analysis of NEXRAD Radar Data ... 105
5.4.4 Implications of Results for Land Management and Planning ... 107
Chapter 6 Discussion and Conclusions ... 109
6.1 Review of Thesis and Objectives ... 109
6.2 Research Outcome and Contribution ... 110
6.2.1 Climate Surfaces ... 110
6.2.2 Radar Data ... 111
6.2.3 Uncertainty and Limitations ... 111
6.2.4 Future Research Potential ... 112
6.3 Concluding Remarks ... 115

Appendices

Appendix A Daily Minimum and Maximum Temperature 1960 to 2005 ... 118
Appendix B Monthly Precipitation 1960 to 2005 ... 125
Appendix C Maps Showing Change in Average Monthly Precipitation Between 1960 to 1982 and 1983 to 2005 ... 129
Appendix D Maps Showing Number of Occurrences of Daily Precipitation Over 25 Millimetres between 1960 to 2005 ... 133
Appendix E Maps Showing Number of Occurrences of Daily Precipitation Over 50 Millimetres between 1960 to 2005 ... 136
Appendix F Number of Raindays 1960 to 2005 Based on Spline Surfaces ... 138
Appendix G Maps Showing Number of Occurrences of Daily Precipitation Over 50 and 75 Millimetres between 1996 to 2008 based on NEXRAD ... 140
Appendix H Number of Rain-days From 1996 to 2008 Based on NEXRAD ... 143
Appendix I 1 Hour Rainfall Intensity Based on NEXRAD Radar 1996 to 2008 ... 145
Appendix J Difference Between Environment Canada 1 Hour IDF Maximums and 1 Hour Rainfall Intensity Based on NEXRAD Radar 1996 to 2008 ... 148
Appendix K Spline Algorithm ... 152
Bibliography ... 157

List of Figures

Figure 1-1: Severe storm over Cambridge, Ontario, as detected by NEXRAD radar 6
Figure 1-2: Map of study area in southern Ontario 9
Figure 2-1: Climate regions of Southern Ontario (Brown, McKay, Chapman 1968). 19
Figure 2-2: Intensity duration frequency (IDF) curve for Cambridge rain gauge (Environment Canada 2007a) 25
Figure 2-3: Graph of monthly daily precipitation accumulation occurrences for Cambridge 27
Figure 2-4: Deviations from long term normal for Shand Dam (Farwell, Boyd, Ryan 2008) 29
Figure 2-5: Lake breeze circulation (adapted from Sumner 1988) 33
Figure 2-6: Composite of GOES-7 images from 1500 to 1730 EST on July 21, 1994. The image was formed by finding the minimum brightness of the six images at each pixel. Thus gray areas indicate the presence of cloud in each of the six images and, hence, persistence of convection at that location. (King and others 2003) 34
Figure 2-7: GOES image taken at 1640 EST on July 6, 2007. The image illustrates a northwesterly flow with lake breeze confining convection inland along a convergence line. 34
Figure 2-8: Terrain and climate regions of Southern Ontario 36
Figure 3-1: Climate stations across southern Ontario 41
Figure 3-2: Graph of the number of AES/MSC climate stations 1860 to 2005 44
Figure 3-3: Radar beam propagation errors 51
Figure 4-1: Effect of anomalous propagation shown in dark blue for Buffalo NEXRAD radar, March 1997 59
Figure 5-1: Daily precipitation surface for July 14, 1997 (value in millimeters) 60
Figure 5-2: 3-D perspective of spline surface for July 14, 1997, with data points shown. 61
Figure 5-3: 3-D perspective of daily precipitation surface from NEXRAD July 14, 1997 61
Figure 5-4: GOES images of 16:45 and 17:32 local time showing the development of the July 14, 1997 convection cell. Not the inverted Y cloud structures and the absence of cumulus clouds between the shoreline of the lakes and the storm cell. 62
Figure 5-5: GOES image of the July 14, 1997 storm at 18:45 local, at the peak of the maximum rainfall rate at Punkeydoodles Corners. 63

Figure 5-6: Daily minimum (left) and maximum (right) temperature surfaces, from July 14, 1997, generated from the spline interpolation....65
Figure 5-7: Graph of average daily minimum temperature 1960 – 2005 March to May 67
Figure 5-8: Graph of average daily minimum temperature 1960 – 2005 June to September....67
Figure 5-9: Graph of average daily maximum temperature 1960 – 2005 March to May....68
Figure 5-10: Graph of average daily maximum temperature 1960 – 2005 June to September....68
Figure 5-11: Graphs showing upward trend in daily minimum and maximum temperature between 1960 and 2005....70
Figure 5-12: Graph of overall changes in monthly precipitation....72
Figure 5-13: Map of average annual precipitation between March and September for the years 1960 to 2005....73
Figure 5-14: Change in average precipitation between 1960-1982 and 1983-2005....74
Figure 5-15: Total occurrences of 25 mm or more of daily precipitation from 1960-2005 and the change in the number of occurrences between 1960-1982 and 1983-2005. Blue means more occurrences and brown fewer in the most recent 23 year period. 76
Figure 5-16: Total occurrences of 50 mm or more of daily precipitation from 1960-2005 and the change in the number of occurrences between 1960-1982 and 1983-2005. 76
Figure 5-17: Total occurrences of 75 mm or more of daily precipitation from 1960-2005 and the change in the number of occurrences between 1960-1982 and 1983-2005. These events primarily occurred between June and September and no monthly maps are in the appendices. 77
Figure 5-18: Number of days per year between March and September that rainfall threshold values occurred. 80
Figure 5-19: Maps of daily rainfall occurrences of 50mm or more from 1996-2005, radar on left and spline surfaces on right....82
Figure 5-20: Maps of daily rainfall occurrences of 75mm or more from 1996-2005, radar on left and spline surfaces on right....82
Figure 5-21: Spatial clustering of 50 mm rainfall 1996-2005 (radar left, spline right)....84
Figure 5-22: Spatial clustering of 50 mm rainfall 1983-2005 based on spline....84
Figure 5-23: Spatial clustering of 75 mm rainfall 1996-2005 (radar left, spline right)....85
Figure 5-24: Spatial clustering of 75 mm rainfall 1983-2005 based on spline....85

Figure 5-25: Number of rain-days for 12.5, 25, 50 and 75 mm events 1996-2008 based on NEXRAD 86
Figure 5-26: Maximum 1 hour rainfall intensity measured between March – September for the years 1996 to 2008, based on NEXRAD radar 87
Figure 5-27: Average of annual maximum 1 hour rainfall intensity between March – September for the years 1996 to 2008, based on NEXRAD radar 88
Figure 5-28: Distribution by area of the years contributing to the 1 hour maximum 89
Figure 5-29: Distribution by study area of the years contributing to the 1 hour maximum 89
Figure 5-30: Distribution by area of the months contributing to the 1 hour maximum 90
Figure 5-31: Distribution by study area of the months contributing to the 1 hour maximum 90
Figure 5-32: Distribution by area of the local time, rounded to the nearest hour, when the 1 hour maximum was detected 91
Figure 5-33: Distribution by study area of the local time, rounded to the nearest hour. 91
Figure 5-34: Difference between radar 1 hour maximum and IDF 10 year value 93
Figure 5-35: Difference between radar 1 hour maximum and IDF 100 year value 94
Figure 5-36: Graph of 1 hour maximum between radar and 10, 100 and average IDF 94
Figure 5-37: Comparison of GRCA rain gauge to NEXRAD for July 2008 96
Figure 5-38: Comparison of Environment Canada rain gauge stations to NEXRAD radar for July 2008 97
Figure 5-39: Percent Difference between Environment Canada rainfall and NEXRAD for July 2008, plotted against distance from the radar station 98
Figure 5-40: Map show total accumulation of rainfall for July 2008 from Buffalo NEXRAD 98
Figure 5-41: Rainfall total from July 11, 2008 storm from NEXRAD radar. 99
Figure 5-42: Graph of radar and gauge measurements from July 11, 2008 101
Figure 5-43: Map showing location of gauges and radar values from July 11, 2008 102

List of Tables

Table 2-1: Percent land cover classes across study area 20
Table 2-2: Seasonal distribution of daily rainfall accumulation occurrences for Cambridge 1960-1998 (Schroeter 2007) 26
Table 3-1: Statistics of distance between climate stations from 1860-2005 43
Table 4-1: Detected and fixed occurrences of anomalous propagation 59
Table 5-1: Change in the monthly normals for daily minimum temperature 69
Table 5-2: Change in the monthly normals for daily maximum temperature 69
Table 5-3: Change in monthly precipitation averages between 1960 and 2005 71
Table 5-4: Rainfall measures from radar compared to private measurements, GRCA and Environment Canada for July 11, 2008 100

Chapter 1
Introduction

"I'm 70 years old and I've never seen it rain so hard
for so long," Fred Butler, Brantford, Ontario (Pearce 2008)

1.1 Living with Severe Storms

In 2005 world-wide weather related disasters including heat waves, cold snaps, hurricanes, floods, winter storms, and tornados caused damages totaling $216.6 billion and 12,081 deaths (Worldwatch Institute 2006). While Canada may experience all these weather phenomena, the nation generally does not bear the brunt of the worst damage. This is due in part to mid-northern latitudes, a relatively sparse distribution of populated areas and a predominately modern infrastructure. However, concentrated along the southern-most latitudes of Canada medium to densely populated landscapes are vulnerable to extreme weather events. For example, according to the Institute for Catastrophic Loss Reduction it is estimated that on average the annual loss in the Province of Ontario due to flood damage is $30 million (Cumming Cockburn Limited. 2000).

Southern Ontario is a susceptible region due to a complex mix of climate patterns, physiography and a highly managed landscape covered with a wide range of land uses. From intense agriculture, densely urbanized areas and managed drainage systems, land use activities rely on a combination of infrastructure and water management practices to minimize damage from severe rainfall and run-off from major storm events. Infrastructure systems for flood and flow control, hydroelectric production, and water use have been engineered using standards that account for weather patterns and known variability in their vicinity. Structures are designed in a manner to minimize the risk of failure from extreme weather.

Extreme weather events draw particular attention in meteorological terms since they can have hazardous and far reaching effects. Society attempts to control the impact of severe events by monitoring synoptic, macro-scale atmospheric variables, predicting storm tracks, issuing warnings in the geographic vicinity and designing infrastructure to cope with the physical manifestations of water, wind and temperature. Climatologists have measured, analyzed and assembled a great deal of data about climate and weather in order to understand weather patterns in short time frames of hours to weeks and longer periods of months to years. Applying statistical analysis on weather records of extreme events over many years, climatologists are able derive a probable return interval for future re-occurrence of events of similar extreme magnitudes. Over seven billion observations of Canada's climate have been recorded, beginning in the mid-19th century (Environment Canada 2001). An immense volume of data has been analyzed to understand the variability of climatic extremes and the stationarity of climate averages over time. A climate average or 'normal' refers to a statistical calculation of observed weather data at a given location over a specified time period (Environment Canada 2008). The World Meteorological Organization (WMO) requires the calculation of averages to use data covering a period of 30 consecutive years, for example 1961 to 1990. Thirty years was deemed an appropriate duration to eliminate year-to-year variations and imply stationarity, the assumption that natural systems fluctuate around an unchanging mean (Milley et al. 2008). A normal is an abstract concept in that it could refer to any parameter of weather or upper or lower limits of a parameter, such as the average maximum daily rainfall for any given month of the year. Normals are statistical devices used to describe the climatic characteristics of a location and often compared to short-term extreme values to describe how far from the 'normal' the weather is on any given day. For example, measurements of daily rainfall or temperature are often compared to the climate average for a location and date to determine how far it deviates from the long term average for that date. Normals for multiple locations are used for characterizing patterns of seasonal and annual weather phenomena in regions across the country.

Analysis of climate data has played an important role in guiding the design specifications of modern storm-water infrastructure built in the 20th century. Structures like dams, bridges, sewers, flood control structures, such as levees and spillways were constructed to engineering specifications that applied knowledge of local weather extremes and normals available during their design. (National Research Council of Canada. Associate Committee on Hydrology and others 1989)

Water management and land management practices in Canada have also evolved with a knowledge and application of climate normals. The hydrologic cycle is the perpetual transport of water via atmospheric and terrestrial mechanisms. Water is diverted and extracted from natural systems of the hydrologic cycle for use by society for municipal drinking water, industrial supply, irrigation, waste disposal, hydro-electric generation, navigation, fish and wildlife production and recreation (Nuttle 1993). In order to ensure ecosystems are not negatively affected and that the hydrologic cycle is sustainable, water managers must understand the inputs and outputs, or the water budget, of the entire system in order to balance and optimize human extraction and use of water resources.

Thus for any given locality, to effectively plan, prepare and mitigate the impact of intense rainfall on infrastructure like dams or assets like fertile soil, it is critical to understand the temporal and spatial characteristics of the climate average and storm extremes. Maintaining an understanding of weather and climate patterns over a long period of time not only requires a lineage of climate records from the past but also the continuous monitoring of weather phenomena in the present and into the future.

1.2 Problem Statement: Monitoring Weather and Climate Change

Members of the scientific community participating on the working groups of the Intergovernmental Panel on Climate Change (IPCC) have made a clear assertion that climate change is a tangible threat to the planet and that there needs to be a strong will amongst the global political community to address the issue. According to the Fourth Assessment Report of the Intergovernmental Panel on Climate Change (IPCC), Working Group 1 (IPCC 2007) the effects of climate change due to global warming have already begun to manifest themselves in shifting weather systems and patterns. To project climate change impacts the IPCC employs a range of greenhouse gas emission scenarios that are based on the Special Report on Emission Scenarios (SRES) (IPCC 2000). The scenarios are driven by variables including population, governance, mitigation strategies and policies, with key scenarios linked to atmospheric CO_2 concentrations ranging between 600 to 1550 ppm. Global Climate Model (GCM) analysis was run out to year 2100 to derive predictions for precipitation and temperature changes related to those CO_2 concentrations. Whereas there are differences in scenarios, leaving some room for some uncertainty about the amount of warming and timing of it, there is universal agreement amongst the scientific community that the global climate is in the process of change due to increasing concentrations of CO_2. Given that atmospheric processes are undergoing change the necessity for continuous monitoring and analysis of weather data is critical in order to understand, predict and prepare for the future climate. One would reasonably conclude that the overall effort by governments to monitor weather should be increased, or at minimum, maintained at present levels. In southern Ontario, however, this paper will present data that shows the number of weather monitoring stations operated by Environment Canada has in fact substantially decreased in recent decades.

1.2.2. Intensity Duration Frequency of Rainfall

In Ontario the primary source of precipitation data used in climate analysis comes from ground-based monitoring stations operated by the Meteorological Service of Canada (MSC), renamed from the Atmospheric Environment Service (AES) in 1999, a branch of Environment Canada. The federal agency has built its archive of daily and hourly weather measurements from thousands of stations across Canada. From this data climatologists have acquired an understanding of seasonal patterns and generated statistics to characterize the intensity, the duration and the return frequency of severe rainfall for monitoring stations. The longer the continuous record of monitoring data at a site, the higher the confidence in long term predictions derived from the data. During the design of water management structures engineers use rainfall intensity, frequency and duration (IDF) curves to model the hydrologic parameters of the locality. IDF values are calculated from multiple years of climate data to estimate the return interval of severe rainfall events of different durations and intensities. For a structure within a given watershed, IDF data are used to model the hydrologic response of the watershed to a rainfall event. This is then used to predict the hydraulic regime that the structures will operate within. In Canada, IDF data has been generated for a sub-set of weather monitoring stations where there is a continuous record and a local requirement, such as a dam or an urbanized floodplain (Hogg, Carr, Routledge 1989).

However, over the last two decades while intensified land-use has grown outward from urban centres across Ontario's landscape, the number of active weather stations operated by Environment Canada has decreased substantially. Between 1990 when the IPCC released its first assessment on report climate change and 2005 there were 37 percent fewer active weather stations measuring precipitation in southern Ontario. This decrease in monitoring may impair continued local understanding of weather and climate, especially if the stations closed collect data for IDF calculations. An IDF graph characterizes extremes of rainfall accumulation along a temporal spectrum of light rain rates in duration of days, to moderate rain rates in duration of hours, to short-duration extremely intense deluges in the order of minutes to an hour. The spectrum of the areal extent of storms of different durations varies from covering large geographic areas ranging in thousands of square kilometers to small storms of hundreds of square kilometers and less. However, since IDF data represents a single point location in space the spatial character of storm events is not represented. During the summer months in Ontario the most intense rainfall is typically the result of convective storms. While ranging in size, the core of a convective storm where the rain is heaviest is often relatively small in comparison to the gaps between rain gauge stations. This means that ground-based measurements can at best only partially characterize summer rainfall activity since the core or entire storms will invariably pass between stations. Even when a storm core passes over one or more stations, accurately determining the storm's spatial extent is difficult based on point locations alone. Given this and an increasingly sparser network of monitoring stations, the collection of data from local storms is being missed by ground-based climate stations. This creates a problem if climate change alters the nature of storm activity since there may insufficient data to sufficiently identify and characterize change.

As an example to illustrate this problem, the Grand River Conservation Authority reported an intense storm that occurred on September 12, 2006 that delivered over 80 millimetres of rainfall in less than 2 hours over the north end of the City of Cambridge (Grand River Conservation Authority 2008). As shown in Figure 1-1, the intense core of the storm passed between automatic rain gauges and thus missed detection by ground sensors. The heaviest rainfall was only detectable by radar. The storm caused damage to sewers and culverts leading to road failures and other local flood damage within the city. This type of event highlights the need for a new approach for detecting and capturing rainfall data to support the continuous improvement of IDF information in the vicinity of vulnerable areas such as urban centres.

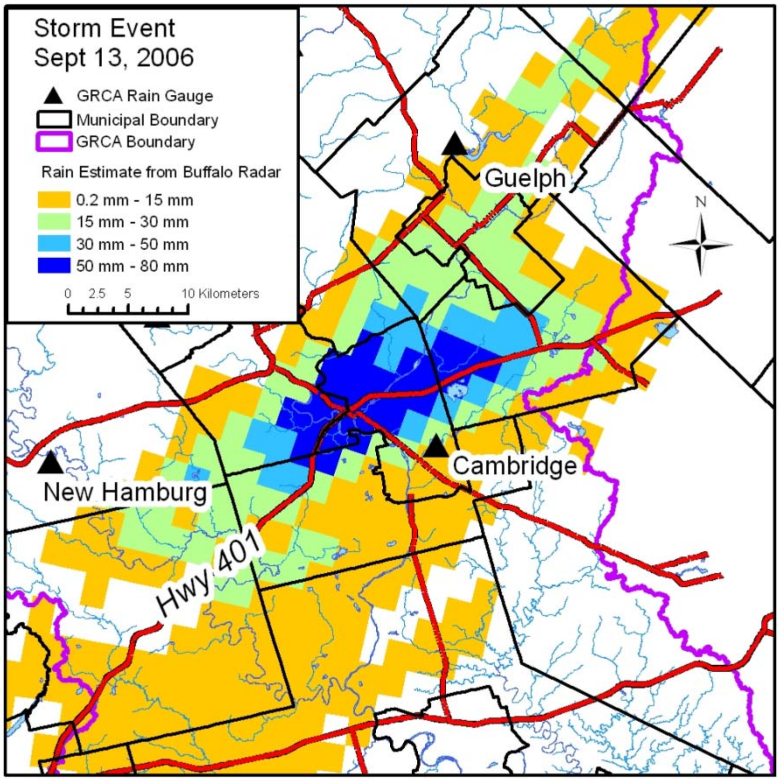

Figure 1-1: Severe storm over Cambridge, Ontario, as detected by NEXRAD radar

The problem of fewer monitoring stations is compounded by the fact that the IDF curves may be out-of-date if the climate has undergone change since their last calculation. Of the 42 monitoring stations with IDF curves in the vicinity of the study area for this thesis, the average end year of the IDF analysis was 1993, fifteen years ago. The last major update of Canadian IDF curves was released in 1991 with records up to 1990. Across Canada only 25 percent of 549 stations with IDF curves have been updated with data up to 2003 (Environment Canada 2007a). IDF curves are based on the analysis of historical rate-of-rainfall data and they do not incorporate any projected future trends due to a climate change. However, according to data sources obtained by the World Meteorological Organization global temperature measurements during the decade of 1998-2007 were the warmest recorded (Science Daily 2007). Whatever impact these warm years had on regional climate and storm patterns are not represented in most of the official IDF data currently maintained by Environment Canada.

There are two driving needs for maintaining a system to monitor weather. The first is to sustain a record of continuous data so that trends and the predicted effects of climate can be identified over time. If trends are detected it may be possible to more accurately estimate the true impacts in the future and conduct infrastructure planning to safely handle a new climate regime. The second requirement for monitoring is the operational requirements for water managers to respond to event based precipitation either for flooding, surface run-off control or for dealing with drought and low water conditions.

In addition to maintaining a continuous climate record to monitor long terms trends, it would also be valuable to understand the patterns of storm events. If the pattern of intense rainfall from storms has spatial heterogeneity in southern Ontario, and if the predicted intensification of storms due to climate change is assumed to occur, knowledge of the storm patterns could aid in adaptation strategies. This is based on the assumption that the underlying physical processes that drive storm patterns would continue to function in the future and the resulting storms will be stronger in response to changing atmospheric conditions. According to climate change predictions, areas that have had a higher frequency of intense storms are going to have even stronger storms under global warming.

1.3 Objectives – Spatial Analysis of Severe Rainfall Patterns in Southern Ontario

The objective of this thesis is to present research in the use of spatial analysis of rainfall data collected from ground-based stations from Environment Canada and radar data from the American NEXRAD system for the purpose of analyzing severe storm activity in southern Ontario. Under this broad objective the following are specific goals:

- To derive continuous climate surfaces for daily temperature and rainfall using spatial interpolation and to examine trends in monthly statistics from 1960-2005
- To analyze the spatial patterns of rainfall events derived from interpolated rainfall surfaces and to examine changes in patterns between the first and second halves of the data record, 1960-1982 and 1983-2005, each sub-period representing 23 years.
- To analyze the spatial patterns of severe rainfall events derived from NEXRAD radar data between 1996 and 2008.
- To compare resulting spatial patterns from interpolated surfaces and from radar data and examine whether there are similar or dissimilar clustering patterns.
- To build a spatial characterization of severe storm activity in southern Ontario by creating a spatial mean of 1 hour rainfall intensity using NEXRAD radar data.
- Assess if the results from the analysis could be applied to help guide planning of weather monitoring, and to help direct adaptation efforts for applying land management practices to reduce the damaging impact of intense rainfall from severe storms on flooding, erosion and water quality.

1.4 Study Area

The study area covers southern Ontario bounded by the Lake Huron, Lake Erie and Lake Ontario, the southern extent of Algonquin Provincial Park and east to Trenton. The area covered by the radar data, as shown in a darker shade of brown on Figure 1.2, is limited to the extent of coverage provided by the Buffalo and Detroit NEXRAD radar stations. While Environment Canada radar stations at Exeter and King City provide overlapping coverage and extend radar coverage to the northern part of the study area, Canadian radar data was not used for this project. This will be discussed further in Chapter 3.

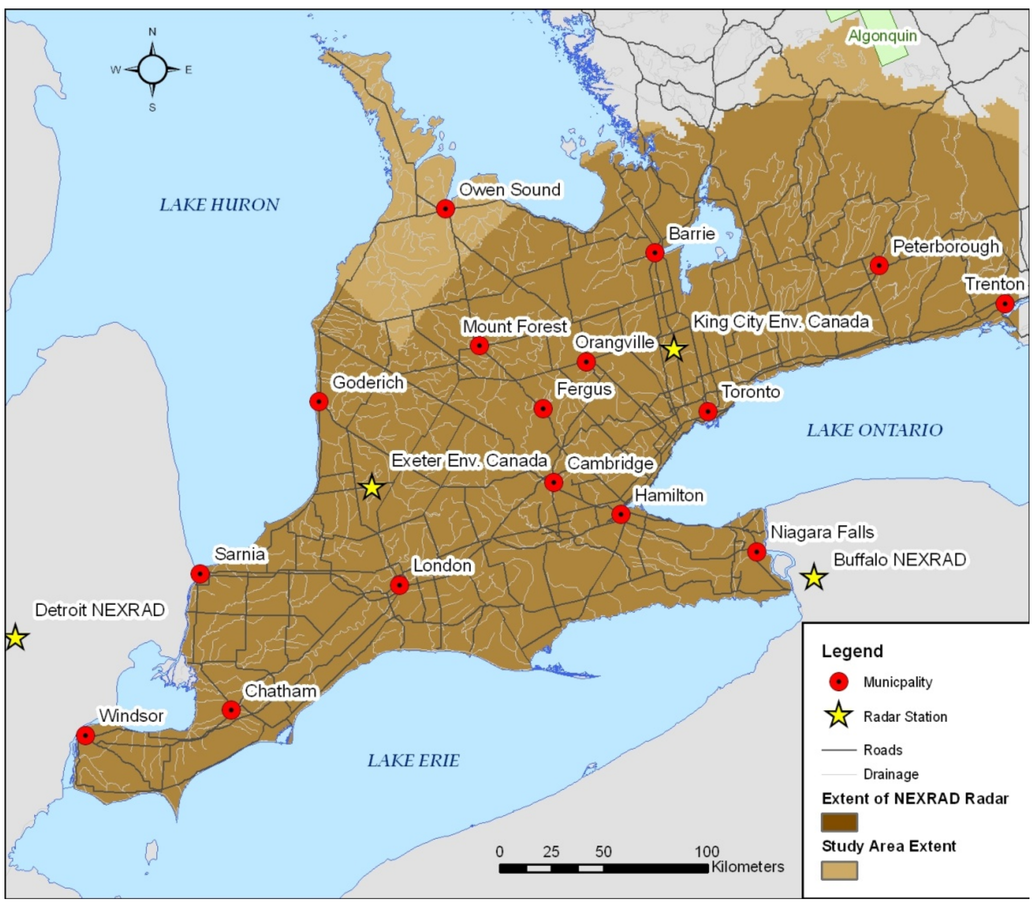

Figure 1-2: Map of study area in southern Ontario

1.5 Structure of Thesis

The remainder of this paper is organized under the following chapters:

Chapter 2 will provide a literature review on aspects of climate change and the implications of severe weather in relation to southern Ontario.

Chapter 3 will provide details on the data used for the analysis, the data sources, the known weaknesses and assumptions about the data.

Chapter 4 outlines the methodology of preparing, processing and analyzing the two main sources of climate data.

Chapter 5 presents the results and findings of the data analysis. Additional maps and graphs are referred to in the Appendices.

Chapter 6 discusses the outcomes realized in the context of the research objectives. The results are examined for their strengths and weaknesses. The overall context of the work is explored in relation to the broader issue of weather monitoring and climate change. Recommendations for future work and enhancements are provided.

Chapter 2
Climate Change and Severe Storms in Ontario

2.1 Intergovernmental Panel on Climate Change (IPCC)

The empirical evidence accumulated by global monitoring data shows that the global climate is changing, and that warming temperatures recorded over the past fifty years do not fit with what would be expected under natural variability (National Oceanic and Atmospheric Administration, Ocean Service Education 2009) and (IPCC 2007). According to the IPCC authors, the warming trend adheres to the scientific understanding of how the climate should respond to the increase in greenhouse gases that has occurred since the late nineteenth century. Whereas the warming is not consistent with the science of how the climate should respond to natural external factors such as variability in solar output and volcanic activity. Working Group I of the Fourth Assessment Report of the Intergovernmental Panel on Climate Change (IPCC) (IPCC 2007) has expressed with a high degree of confidence that climate change is due to the increasing concentration of greenhouse gases in the atmosphere. Other forcings related to natural phenomena, such as solar activity, are far lesser factors. Anthropogenic effects are attributed as the primary cause.

Working Group II of the Fourth Assessment Report of the Intergovernmental Panel on Climate Change (Parry 2007) stated that detectable shifts have been recorded across a wide range of climatic, terrestrial and oceanic systems. The authors further stated that the expected impacts of a warming climate, changes in water regimes and temperature extremes, pose the greatest risk to human populations. The direct impacts include rising ocean levels, more frequent events of extreme precipitation, droughts and more frequent and intense heat waves. Indirectly, the biological systems that humans depend on for resources from forests, aquaculture, and agricultures will also suffer adverse effects. While regionally, such as in the mid-latitudes of Canada, there are areas that may benefit due to a longer growing season (Environment Canada 2001), the net effect on a global scale is a negative one.

2.1.1 The Connection Between Increased CO2 Concentration and Precipitation

Climate change figures reported by Environment Canada (Environment Canada 2001) state that the average global temperature rose 0.6^{o}C in the past century, and the 10 warmest years worldwide, since measurements began 140 years ago, have all occurred since 1980. Canada's average temperature rose 0.9 ^{o}C between 1948 and 2000.

Carbon dioxide concentration in the earth's atmosphere increased from 316.9 ppm to 375.61 ppm, or 18 percent, during the period of 1960 to 2003 (Keeling and Whorf 2004). The annual rate at which the concentration of CO2 is rising has also increased from 1.4 ppm between 1960 and 2005 to 1.9 ppm as measured between 1995 and 2005 (Connor 2007). The accelerating rate of annual increases in CO2 could be an indicator of positive feedback whereby increased CO2 concentration decreases the uptake of carbon from terrestrial and ocean sinks.

Global warming also accelerates due to the increased uptake of water vapour in the atmosphere. As temperatures warm the carrying capacity of the atmosphere for water vapour also increases and as a greenhouse gas it further adds to the warming effect. From the standpoint of precipitation more water stored in the atmosphere simply means more will eventually fall back to the earth. As stated by the Working Group I of the Third Assessment Report:

> "the influence of warmer temperatures and increased water vapour in the atmosphere are not independent events, and are likely to be jointly related to increases in heavy and extreme precipitation events." (Houghton 2001)

This connection between global warming, increased rates of evapotranspiration and increased availability of water vapour within the atmosphere is the catalyst for increasing precipitation delivered by weather systems that would have naturally done so anyway.

Between the latitudes of 30°N and 85°N it has been reported that precipitation over land increased during the 20th century, however, decreases have also occurred in the past 30 to 40 years, according to the Technical Paper of the Intergovernmental Panel on Climate Change and Water (Bates and others 2008). In chapter 2 of the report, the authors stated that direct attribution of changes in overall global precipitation is uncertain, due in part to large-scale patterns of natural variability which tend to mask long-term trends. In North America, however, since 1901 annual precipitation has increased and the contribution from very wet days has also been increasing per decade since 1951. This finding is significant and suggests that both storm frequency and magnitude have been increasing. Monitoring data show widespread increases in events of extreme precipitation (the 95th percentile and above) across North America and Europe, including areas where total annual precipitation has decreased. In the United States the largest increases in extreme precipitation events have been observed during the warm season, suggesting convective storms as the primary delivery process. The authors of the report stated that the increases in observed precipitation are associated with increased amounts of water vapour in the atmosphere due to warming. Climate models have suggested that under a warmer climate that a greater increase is expected in the extremes of precipitation versus changes to the mean. They conclude that increases in the frequency and the relative contribution from heavy rainfall is likely to have occurred over most land during the 20th century, and that the increases are more likely than not to have been influenced by anthropogenic factors.

2.2 Impacts of Climate Change on Southern Ontario

According to the Fourth IPCC Report, Working Group 1 (IPCC 2007) climate change research suggests that the North American climate in the area of southern Ontario will experience the following effects from global warming:

Precipitation Effects

- Increased winter precipitation and spring runoff
- Decreased summer and fall precipitation
- Longer and more frequent summer droughts
- Increased severity of summer storms and intensified precipitation

Temperature Effects

- Average 1.5 to 2.0 degrees warming between 2020-2029
- Average 3.0 to 6.0 degrees warming between 2090-2099
  (based on ranges between SRES B1 and A2 scenarios) (Houghton 2001)
- Shift to earlier spring snow melt
- Shift to more extreme temperature events

Research in Canada using the Canadian Coupled Global Climate Model (CGCM) suggests that the probability of daily extreme precipitation events in Ontario will double by 2100 (Kharin and Zwiers 2005) and that total annual precipitation will increase by 15% by the 2050s (Mortsch et al. 2005). Under a doubling of atmospheric CO2 some models indicate heavy rainfall will become more frequent and light rainfall less frequent (Francis and Hengeveld 1998).

Any significant long term changes in precipitation and temperature will affect the water cycle and thus impact the interaction of water with regard to human interests. While naturally having variability, Ontario's economy has relied on its relatively stable and predictable climate (Smith and Lavender 1998) to sustain its socio-economic wealth. A sustained and clean supply of water to meet the needs of society is one of the main risk factors related to the effects of climate change. Whereas excessive water in the form of heavy precipitation events pose challenges insofar as the need to control the damage from flooding and runoff while retaining water on the landscape to support ecosystems. As suggested by De Loë and Kreutzwiser (2000) changes to extremes in climate variability, wet years versus dry years, rather than changes in the climate averages may pose the greatest challenge for water management. Rainfall delivered from strong storms separated by lengthened drier periods would force changes to how water is managed. In general terms, the effects of climate change suggest a much greater degree of seasonal variability with winter being wetter and summer being drier, and summer rainfall being delivered by increasingly severe storm events.

2.2.1 Spring Susceptibility

The effect of climate change on the hydrologic cycle during spring is a particular concern. Changes in spring climate will have an impact on groundwater infiltration and runoff. While in the Great Lakes basin annual runoff is expected to decrease, winter and spring runoff is expected to increase (De Loë and Berg 2006). This is due to higher accumulation of snow according to Global Climate Models (GCM) predictions. Spring represents a transition period between frozen ground and water fixed in the snow pack and water mobility from warming days and shifts in precipitation from snow to rain. It is also a period of pre-green up when deciduous vegetation is defoliated from the previous autumn and agricultural fields are bare. Heavy rain falling onto frozen ground results in greater surface runoff than under summer conditions. Soil moisture tends to be high due to melting snow and greater groundwater mobility from a thawing ground. All these factors combine to make the spring a period when the landscape is the least capable to store water from rain and the most vulnerable to erosion and sedimentation from runoff.

2.2.2 Water Runoff, Infiltration and Evapotranspiration

Anthropogenic modification of the land by clearing forests, draining of wetlands, creation of paved impervious surfaces, and diversion of precipitation by engineered infrastructure, such as urban storm-sheds and drains, has disrupted the natural water cycle and impacted the response of the landscape to severe rainfall events (De Loë and Berg 2006). These modifications favor the reduction in the storage of water on the landscape and the faster transport of water into streams and rivers, leading to higher rates of erosion and a greater risk of flooding. An additional impact of reduced storage and more runoff is a reduction to infiltration and groundwater recharge. According to Southam et al. (1999) the susceptibility of the Grand River watershed to decreased groundwater recharge poses a risk to its residents due to the major dependency on groundwater resources for rural and municipal use. On the other hand Mikko and Sykes (2007) suggest that groundwater infiltration may actually increase in the Grand River basin. They suggest that due to milder winters and less frozen ground conditions will support winter groundwater recharge. However, they also state that greater seasonal variability is expected and that increased runoff from severe rainfall events, as well as, increased evapotranspiration due to warmer temperatures could offset the winter increases in recharge.

Higher evapotranspiration rates could counteract the predicted annual increases in precipitation. According to analysis done using the Canadian Climate Centre model (Sanderson and Smith 1993) the Grand River watershed could be in a deficit of its water balance by 2041 due to much higher rates of evapatranspiration due to climate warming.

Differing views in the literature leave room for uncertainty about the effects of climate change in Ontario insofar as runoff and infiltration and the overall water balance. It is likely that annual variability in winter, spring and summer weather patterns will play a large role in determining the runoff potential from year to year. Since precipitation is the only input of water to the surface and groundwater water cycles, any changes in long term trends in snow and rainfall will have repercussions despite short-term variability. To help offset wider variability between dry and wet extremes, efforts need to be taken to decrease runoff and increase natural storage of water on the landscape. Some of the steps to building resiliency on the landscape include planting trees, enhancing and restoring wetlands, and riparian buffers (Farwell, Boyd, Ryan 2008).

2.2.3 Soil Erosion

Foliage from vegetation is a natural obstacle to falling raindrops and buffers the impact of water droplets on the ground. The roots of vegetation stabilize soils and thus reduce erosive power of rainfall and surface water movement. When vegetation is disturbed or under a management regime that leaves soil bare, rates of erosion increase. As mentioned above, spring is a particularly vulnerable period for erosion due to a lack of vegetation, especially on bare agricultural fields. The Working Group II from the Fourth IPCC states the following in regard to the impact that climate change may have on erosion and sediment transport:

> "All studies on soil erosion have suggested that increased rainfall amounts and intensities will lead to greater rates of erosion unless protection measures are taken. Soil erosion rates are expected to change in response to changes in climate for a variety of reasons. The most direct is the change in the erosive power of rainfall." (Parry 2007)

The IPCC authors further note that a shift in winter precipitation from non-erosive snow to erosive rainfall due to increasing winter temperatures is one of the contributing factors supporting the prediction of higher soil erosion. For southern Ontario, climate changes related to precipitation will increase the risk and exposure of erosion sedimentation, non-point source pollution and flooding hazard. According to a report by Conservation Ontario (Conservation Ontario 2009) on average there has been a 4 percent increase per decade since 1960 in the frequency of heavy rainfall events between March and May. A shift to earlier and more frequent rainfall events in the months of March, April and May will stress landscapes already saturated from snow melt and lacking protective vegetation. Another impact of climate change in southern Ontario will be on agricultural lands due to the increased severity of storm events. Spring storms delivering water under increasingly severe rates of rainfall will have greater erosive potential on soil and will lead to more runoff.

Increases in sediment loads and pollution transported by higher run-off will negatively impact water quality for aquatic habitats and human intake from surface water sources (Murdoch, Baron, Miller 2000).

Whereas in Ontario annual rainfall totals are predicted to increase, primarily due to increased precipitation as snow during winter months, periodic severe rainfall events are a disproportionate contributing factor to soil erosion throughout the year. Working Group I of the Third IPCC Assessment Report (Houghton 2001) noted for Canada, and in all other global regions studied, that the magnitude of change in heavy precipitation is higher than the change in the average precipitation total. The authors of Working Group II, chapter 3, (Parry 2007) further suggest that conservation measures should be targeted at extreme storm events. Research in soil erosion in Ontario (Bruce and others 2006) has shown that approximately 85 percent of soil erosion occurs in spring and summer months. Erosion rates are highly event driven whereby a single intense event in the summer could account for up to 60 percent of the annual total. Farming practices will need to apply adaptation techniques to adjust to the new climate reality in order to preserve soil and crop systems. In terms of southern Ontario an improved understanding of seasonal patterns of when and where severe rainfall is a risk to vulnerable soils and land cover would be useful to help guide the application of conservation practices.

2.3 Severe Weather of Southern Ontario

The climate of southern Ontario is controlled by a number of large-scale (synoptic) factors, including its latitude, which controls direct solar input, physiography and continental weather systems that are influenced by the prevailing westerly flow of the jet stream. Intense precipitation events are most often associated with the mixing of warm, humid tropical air masses drawn northward to the region by low pressure systems with dry, cool arctic air masses drawn southward into the region. Local climate conditions are influenced by landscape terrain characteristics and juxtaposition in relation to the Great Lakes and prevailing winds.

2.3.1 Climate Regions of Southern Ontario

The climate of Southern Ontario is also influenced by a number of meso-scale (local) factors that affect both weather systems and regional conditions. The physiography of the landscapes and the influence of the three Great Lakes that surround southern Ontario to the south and the west are dominant characteristics. Figure 2-1 shows the climate regions as sketched by Brown, McKay, and Chapman (1968). The regions are defined by a combination of terrain elevation or proximity to terrain changes, such as the Oak Ridges moraine, proximity to the coastal areas of the Great Lakes and higher elevation defined by the Dundalk Upland region.

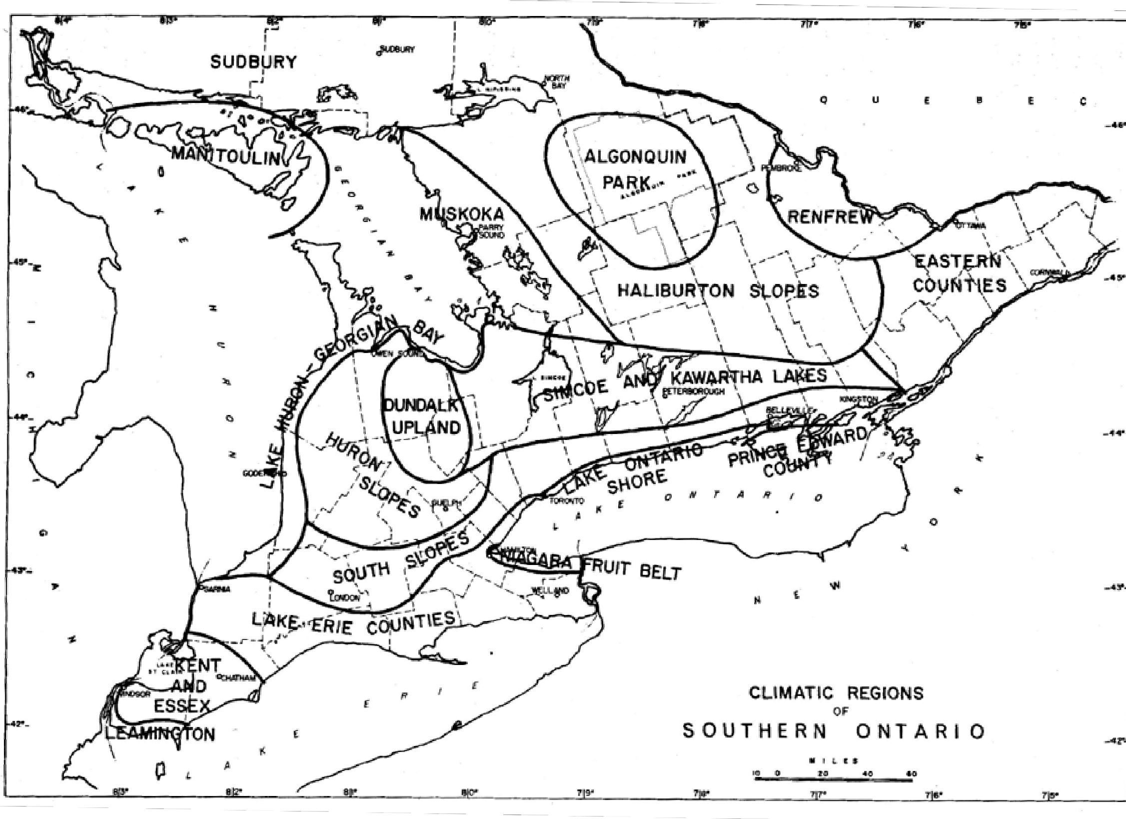

Figure 2-1: Climate regions of Southern Ontario (Brown, McKay, Chapman 1968).

An area-based summary of the Southern Ontario Land Resource Information System (SOLRIS) (Ontario Ministry of Natural Resources 2008) showed that 64 percent of the land cover across the study area is open land used primarily for agricultural. Forest and swamp represent 26.5 percent of the land. Table 2-1 lists the percentages of land cover classes across the study area. Differences in the surface-energy budget of these land cover types, the influence of terrain and cover types to airflow can lead to pressure gradients that influence local convection processes. In this region the most notable gradient is formed between the large water bodies of the lakes and the in-land coastal margins. Daily surface heating over the land sets up a sea breeze or lake breeze circulation. When synoptic scale conditions are conducive to strong convection these locally forced precipitation processes can lead to the development of extreme meso-scale events (Sumner 1988).

Land Cover	**Percent Cover**
Agriculture - Undifferentiated	64.0
Urbanized	5.5
Transportation	3.5
Extraction (pits and quarries)	0.3
Forest	14.4
Swamp/Marsh	12.1

Table 2-1: Percent land cover classes across study area

2.3.2 Types of Storms

The type of weather systems that deliver precipitation to southern Ontario are frontal, convection and tropical depressions. These processes can intermingle and affect each other‘s occurrence and movement across North America. An in-depth review of the meteorology behind weather systems that pass across southern Ontario is beyond the scope of this thesis. However, in basic terms suitable for subsequent sections and the results and findings the following is a summary of the seasonal variations of dominate weather systems.

2.3.2.1 Winter and Tropical Storms

During the winter season storm deriving weather is dominated by frontal depressions that draw moist warm air from the Gulf of Mexico, the Pacific or Atlantic Oceans which mixes with arctic air drawn south along frontal systems moving west to east across North America. Frontal storms are generally large and can deliver precipitation over wide areas over a duration lasting up to several days. Winter weather is not examined in this paper.

Tropical hurricanes directly affect Ontario relatively infrequently. However their ability to deliver sustained rainfall and powerful winds present a severe damage potential. Based on data starting in 1887, 5.5 percent of hurricanes originating in the western Atlantic have passed close to or over Ontario with approximately 2 percent of storms delivering extreme rainfall and wind (Phillips and O'Donnell 1975). The most notable storm to date has been Hurricane Hazel which occurred on October 15th and 16th, 1954. The storm stands out because its 12 hour total rainfall was greater than any 12 hour maximum across all of southern Ontario (Cumming Cockburn Limited 2000). The storm dropped 280 millimetres (mm) of rain in 48 hours in the Toronto area, which caused widespread flood damage and human casualties. The storm represented a major turning point in Ontario by bringing political awareness to flooding, leading to the implementation of new programs to reduce future losses due to flood damage (Cumming Cockburn Limited 2000).

Hurricanes and tropical storms present the greatest threat because they have the potential to deliver heavy rainfall over a large spatial extent for a long duration. The Ontario Ministry of Natural Resources adopted Hurricane Hazel to represent the “Regional Storm” for southern and southwestern Ontario (Ontario Ministry of Natural Resources 1985). The Regional Storm specification assumes a 100 year return interval of a storm of similar magnitude. In Ontario the riverine flooding hazard limit is delineated to an extent that is calculated from the precipitation that was delivered by Hurricane Hazel. While the path of Hazel was just west of Toronto it was assumed that it could have occurred anywhere between Windsor and Trenton. The design standard to handle 12 to 48 hour maximum rainfall totl accounts for the future potential of a repeat event in the engineering design of structures and the planning of land use in and adjacent to floodplain areas.

2.3.2.2 Convection

Fortunately, hurricanes are the least frequent type of storm affecting southern Ontario. The highest seasonal rainfall intensity is most commonly associated with convective storm events which reach their peak in the summer months. Under the correct circumstances and atmospheric conditions, surface heating leads to a deep column of vertical air movement in the troposphere carrying up with it warm moist air from the surface into cool to sub-zero temperatures. This type of storm is capable of short-lived but extremely high rainfall intensity at the earth's surface as the moisture laden column is released by the cloud. The nature and organization of convective storms differ in time and space in comparison to longer duration, more moderate precipitation rates as produced by frontal depressions (Sumner 1988). The area affected by a convective storm ranges in the size of hundreds of square kilometers whereas frontal systems may impact tens-of-thousands. Sumner (1988) further suggests that the intensity and the spatial organization of convective storms depend on the strength and duration of convection whereas the internal storm structure is contingent on the availability of moisture, temperature stratification of the air mass and the vertical wind structure of the atmosphere. Both synoptic conditions as well as local factors such as variable surface heating determine the outcome of convective storm activity.

2.3.2.3 Rainfall Intensity-Duration-Frequency

The maximum rate of rainfall intensity from convective storms typically occurs over a duration lasting several minutes to approximately one hour (Sumner 1988). Longer duration convective rainfall can occur due to a stationary storm or multiple storm events. A squall line, associated with cold fronts, can form a sequence of multiple storm cells that can pass over the same area.

Environment Canada provides short-duration rainfall intensity statistics in the form of intensity duration frequency (IDF) curves which are produced from statistical analysis of extreme values using at least 10 years of rate-of-rainfall data from a single climate station. IDF information is typically provided as tables and graphs that show the frequency of extreme rainfall rates and accumulation amounts for the following durations: 5, 10, 15, 30 and 60 minutes, and 2, 6, 12, and 24 hours. Return periods are used as a measure of the reoccurrence of the same intensity in numbers of years. The return period is defined as the annual probability that a rainfall accumulation will occur or be exceeded. For example, a 50-year return period storm event has a 1 in 50 chance or 2% probability of occurring in any given year. The return period represents the average time between occurrences of a given event. Return periods are calculated by fitting a series of annual maximum rainfall rates for the corresponding durations to the Gumbel extreme value distribution using the method of moments (Environment Canada 2007a). Most of the data used to calculate rainfall intensity rates for IDF curves are derived from observations taken from automatic tipping bucket rain gauges (TBRGs) with a shortest duration of 5 minutes. It is important to distinguish the subset of IDF stations from the majority of climate stations. Most climate stations in the network have been operated manually and report values once or twice daily. Their data cannot be used to derive IDF values. While mostly TBRG-based, a small portion of IDF curves are generated from Fischer & Porter weighing precipitation gauges that have a shortest duration of 15 minutes.

Figure 2-2 represents the IDF curve for the City of Cambridge rain gauge. According to Boyd (2008), as a general rule of thumb, as the rainfall intensity decreases and the duration increases from left to right on the IDF graph, the types of storms represented transition from convection to frontal to tropical. The transition zones on the graph are not distinct but rather overlap and are dependent on other factors. However, between 1 hour and

3 hours there is a notable drop of intensity whereby the storms expected to occur on a more frequent interval, 2 to 5 years, have expected rain accumulation below 50 mm. Whereas a 50 mm accumulation within a 3 hour period is only expected to occur every 5 years or more and 50 mm within 1 hour is only expected to occur every 25 years. These estimates for recurrence are statistical ratios of measured extreme rainfall events that occurred over the data period of 1980-1992 standardized to 100 years. Therefore a 5 year return period should be interpreted as meaning that in any given year there is a 1-in-5 chance of a given intensity-duration occurring. It does not imply a cycle of recurrence or predictable variability in the climate. In this example of an IDF curve for Cambridge, only 13 years of observational data has been used to statistically extrapolate the expected return cycle of storm events of varying intensity-duration to a 100 year period. It is reasonable to assume that the confidence of any IDF graph to accurately represent the recurrence intervals would improve over a longer period of observational record at that location. That assumes that the underlying climate normal is stationary, whereby the climate of the past represents the climate of today and the future. However, as mentioned earlier in this chapter, greater variability in climate extremes, as expected under climate change, will likely outweigh gradual changes in the climate normal.

Environment Canada issues rainfall warnings in both winter and summer. In the winter rainfall warnings are issued when 50 mm of rain or more is expected to fall within 12 hours but the ground is dry or covered in snow and is capable of absorbing much of the rain. However, in conditions typical for late winter a warning is given when 25 mm of rain or more is expected to fall within 24 hours and the ground is frozen or sodden with little snow on it (Environment Canada 2007b). In summer a rainfall warning is given when 50 mm or more of rain is expected to fall within 12 hours and a severe thunderstorm warning is issued when rainfall of 50 mm or more within one hour or 75 mm or more within three hours is forecast (Environment Canada 2005). It should be noted that Environment Canada considers the winter season in southern Ontario as the period between November and mid-April, depending on conditions for a specific year.

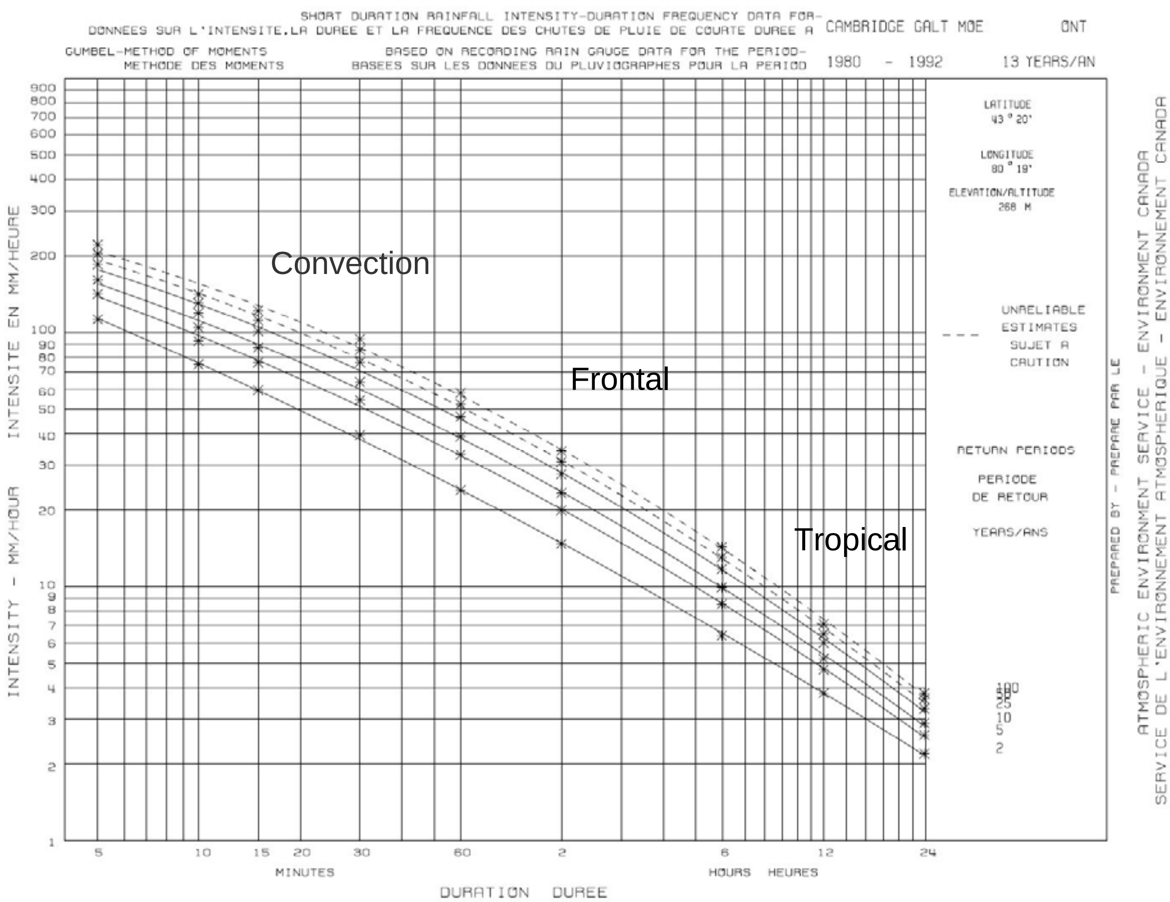

Figure 2-2: Intensity duration frequency (IDF) curve for Cambridge rain gauge (Environment Canada 2007a)

In the context of Environment Canada's rainfall warnings, the values for monthly occurrences of daily rainfall for the Cambridge station, shown in table 2-1, provide an indication for when in the year severe weather is likely a concern. For the 'winter' months there are no daily occurrences of 50 mm of rain; however November and April both have higher occurrences of daily accumulations of 25 mm. A forecast of 25 mm of rain triggers a rainfall warning from Environment Canada if the ground is frozen or saturated, a condition more likely to occur in April rather than November due to the melting of the snow pack.

mm/day	***JAN***	***FEB***	***MAR***	***APR***	***MAY***	***JUN***	***JUL***	***AUG***	***SEP***	***OCT***	***NOV***	***DEC***	***TOTAL***
>0	159	128	255	423	451	394	394	390	405	459	411	228	4097
>5	90	61	118	180	193	176	182	186	181	175	180	109	1831
>10	55	35	60	102	103	99	115	116	106	89	93	56	1029
>15	29	22	30	55	55	55	74	75	60	38	51	33	577
>20	15	13	11	27	32	28	49	49	35	19	29	16	323
>25	**8**	**6**	**6**	**17**	**13**	**21**	**30**	**29**	**18**	**10**	**13**	**6**	177
>40	**2**	**2**	0	0	**3**	**3**	**16**	**13**	**5**	**1**	**3**	0	48
>50	0	0	0	0	0	**1**	**4**	**7**	**3**	**1**	0	0	16
>60	0	0	0	0	0	0	**2**	**6**	**1**	0	0	0	9
>80	0	0	0	0	0	0	0	**3**	0	0	0	0	3

Table 2-2: Seasonal distribution of daily rainfall accumulation occurrences for Cambridge 1960-1998 (Schroeter 2007)

As for summer rainfall and thunderstorm warnings the Cambridge data show daily occurrences of 50 mm or more between June to October with a peak in July and August. It is also notable that the number of occurrences of daily rainfall of 25 mm or more doubles between March and April, nearly doubling again from June in July and August and then dropping by roughly half in September. Since the sun provides the energy behind the convective processes driving these storms, it's not surprising that highest angle of sun incidence is coincident to the highest frequency of intense rainfall events. There appears to be a delayed response after solar solstice through July and August. Figure 2-3 graphs the values in Table 2-1 showing the annual distribution of daily rainfall for the Cambridge station. It should be emphasized that these data represent one location, and while a similar trend would be expected across the study area, other factors that affect storm development and spatial orientation of storm tracks may affect changes in the values observed elsewhere.

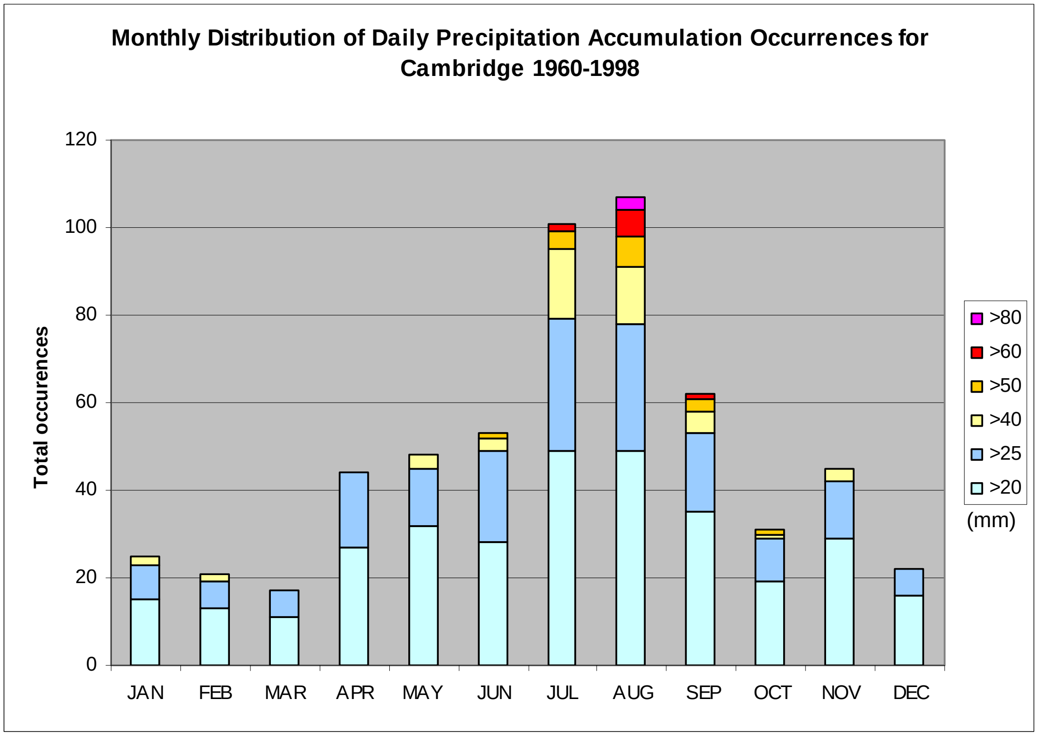

Figure 2-3: Graph of monthly daily precipitation accumulation occurrences for Cambridge

2.3.2.4 What Is Normal?

The impact of severe storms or droughts on annual total rainfall can represent large fluctuations from the long term average. The climate normal does not represent the variability of extremes that may occur above or below its value, but rather an averaging of those events. If under climate change extremes in weather are expected to swing further in amplitude, the meaningfulness of a 'normal' may diminish and more importantly the concept may become obsolete. On examination of the deviations of monthly precipitation from normal over ten years at the Shand Dam in Fergus, Figure 2-4, this hypothesis appears to have some validity based on recent observations. The differences between the red line, representing the long term average, which was calculated from data between 1960 and 2007, and the blue bars representing the actual accumulation show 27 months where rainfall was much higher than normal and another 38 months where it was considerably lower. These relatively large deviations from normal represent slightly more than half of the 127 monthly records. It is notable that the amplitude is greater for months with rainfall extremes than it is for months when precipitation was below normal. This graph suggests that extremes, when they occur, deviate much further from the mean than the long term normal may fluctuate. This concurs with the earlier statement made in section 2.2.3 whereby that magnitude of potential increases in extreme rainfall are much greater than the change in the overall normal.

In the article titled “Stationarity Is Dead: Whither Water Management?” (Milly et al. 2008), the authors rebuke the assumption of stationarity, the concept that natural systems fluctuate within an unchanging envelope of variability.   In the past, the concept was adopted in design standards since natural trends were considered insignificantly small. However, the authors’ assertion that the relevancy of stationarity is dead and should be abandoned in the practice of water management is based on the anthropogenic driven changes to the global climate that are altering the means and extremes of global weather phenomena. They further suggest that a new approach is needed, one that uses non-stationary probabilistic models to optimize the management of water systems, however, admit the daunting complexities of shifting to a new paradigm. It is noteworthy that the article concludes by stating that under a non-stationary climate, a continuous record of observations is critical.

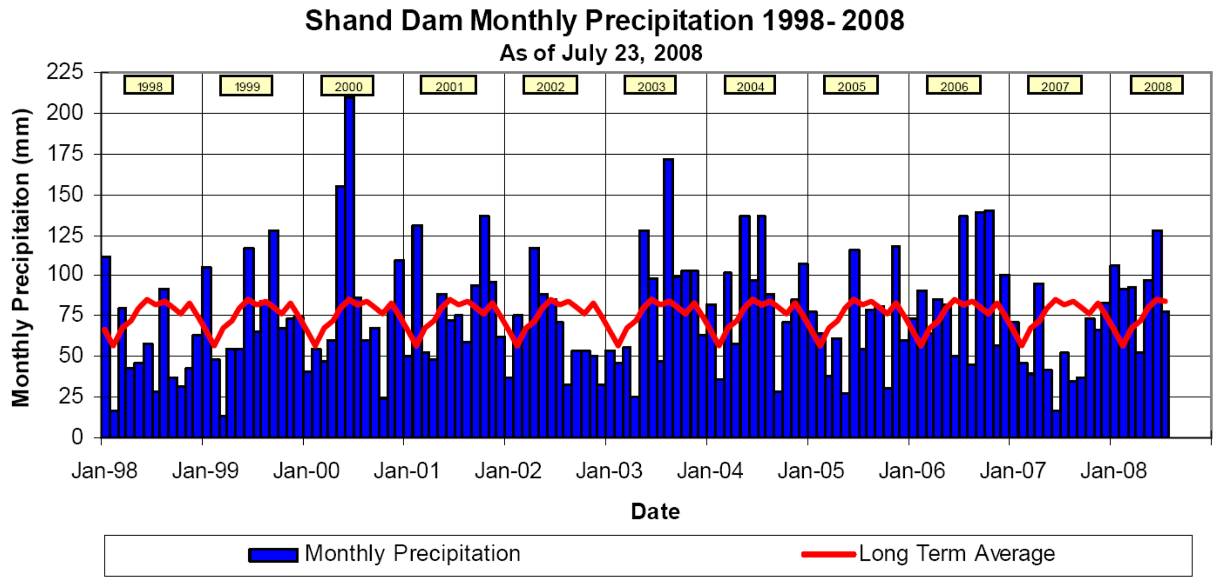

Figure 2-4: Deviations from long term normal for Shand Dam (Farwell, Boyd, Ryan 2008)

2.3.3 Severe Local Storms

Between 1998 and 2008 at the Shand Dam, 8 out of the 11 years had occurrences of much higher than normal monthly rainfall totals sometime between April and September, as shown graph in Figure 2-4. The years of 1998, 2001 and 2007 were comparatively drier. The relative consistency of the annual occurrence of extreme rainfall suggests that the processes that drive the storms that cause extreme rainfall events have some normality to them and that the long term average is actually a smoothing between extremes of wet and dry years rather than a representation of the expected weather.

Gaining an understanding of the processes that drive severe storm development may help to anticipate the long term effects climate change may have on enhancing or diminishing those processes. Global Climate Models and Regional Climate Models generate predictions about local effects of climate; however, spatially they are too generalized to provide specific patterns about local storms (Klaassen and Seifert 2004). The hypothesis of this research is that local patterns of severe rainfall will be detected through spatial analysis of data over time. If there is heterogeneity in the spatial distribution of severe rainfall, the question that follows is what causes one area to receive more severe weather than another?

As mentioned above, the most intense short duration rain is the result of convective storms. The large and small scale interactions between atmospheric and terrestrial processes affecting the genesis of convective storms are complex. The remaining sections of this chapter provide a summary of local factors for the purpose of giving context to convective storm development.

The movement of parcels of air upward and downward is a principal process triggering the development of convective rainfall. The motion occurs due to the isolated or combined effects of rising cells of heated moist air from surface heating or along squall lines in association with instability caused at the frontal zone of a cold air-mass (Barry and Chorley 1987). Mechanical lifting from topography can also be a trigger in mountainous areas. The difference in density of cool air versus warm is fundamental. As low level warm moist air rises into cooler layers of the troposphere aloft, the moisture condenses, forms a cloud mass, releasing latent heat to the cell which supports continued warming. The difference in density of the rising air mass to the surrounding air creates powerful updrafts that cause the column to rise as long as a temperature differential is maintained. Downdraughts of cool air also occur as air displaced by rising air is sent downward. For mid-latitude storms the minimum depth of the vertical development to cause rain is 4 to 5 km, whereas the largest storms reach towering heights of 11 km or more.

The engine behind weather in Ontario is the jet stream and its control over low and high pressure systems which lead to movement and mixing of air masses along frontal margins that move from west to east. In Ontario the conditions ideal to the development of thunderstorms occur when solar heating of the ground is at a maximum, before and after summer solstice, when warm moist air is drawn up from the Gulf of Mexico and cool air is drawn south. The atmospheric conditions in the summer of 2008 led to cooler than normal upper atmosphere conditions which permitted deep convection leading to frequent and severe storms. In June and July 2008 these conditions lead to frequent storm events and record breaking rainfall accumulations, conditions described by the Weather Network (2008) as follows:

> "Over Ontario sits an upper level low with two high pressure ridges sitting on either side. These ridges have been acting as a blocking pattern to the low, keeping it firmly in place for the last couple months. The upper level low is responsible for bringing down cool air to Southern Ontario, while hot, moist air is moving up from the Gulf of Mexico. This collision of cool and warm air causes instability, which leads to thunderstorms."

While individual thunderstorms can form as the result of local heating, widespread severe weather from multiple storms is typically related the formation of a meso-scale convective complex (Barry and Chorley 1987). Large complexes of convection storms setup self-perpetuating disturbances of down draughts that displace low-level warm air aloft setting up meso-scale high and low pressure zones that draw inflow of air, often causing convergence, furthering the upward development. These storms are enhanced by synoptic factors such as the jet stream that can draw warm moist air from the south and cooler air aloft from the north. These complexes are common to the mid-west United States, according to Barry and Chorley (1987), they last on average up to 12 hours, with initial organization occurring between 1800-1900 local time and reaching maximum extent within 7 hours. These storms are influenced by prevailing winds and can travel from various zones of genesis in the mid-west up to the Great Lakes basin. The process of self-propagation is weakened when synoptic scale factors no longer support the factors for convection. A supercell thunderstorm is similar to the meso-scale complex except it is characterized by a single primary zone of updraught that rotates the storm in manner that permits lengthened vertical development. The development of tornados is often associated with the formation of this type of system.

There is interconnectedness between scales of local to synoptic when it comes to the circumstances that lead to the probability of severe storms. Sumner (1988) states that storms will propagate in response to the combined local and meso-scale atmospheric circulation and localized convection. The next section will review some of the local factors that may influence storm tracks and thus lead to patterns in the occurrence of intense storms.

2.3.4 Local Factors

Southern Ontario is unique as a continental inland region since it is a peninsula surrounded by the water of the Great Lakes. The differences in the thermal regime of the Great Lakes versus the land mass influence weather in all seasons. The following sections will examine the summertime influences of sea-breeze, terrain, urban heat island effect and land cover.

2.3.4.1 Lake Breeze and Convergence

In a study of tornado development in southwestern Ontario researchers at the Meteorological Service of Canada (King et al. 2003) have demonstrated that lake breezes, interactions with the mean atmospheric flow and advancing cold fronts play a critical role in triggering and influencing severe storm events. According to their findings the strongest summer storms occur when the prevailing winds range from southwest to northwest, with the strongest storms favouring a prevailing southwest wind.

Figure 2-5 illustrates the basic lake breeze circulation resulting from day time surface heating. The inland penetration of the sea breeze can vary from 30 to 80 km in southern Ontario. Linear bands of cumulus clouds may form in lines parallel to the shoreline when interacting with prevailing winds. The lake breeze effect in Ontario is not dissimilar to the sea breezes in Florida. Ellis and Chen (2004) developed a meso-scale model to predict sea breeze and rainfall. Their model was validated using rain gauge and NEXRAD radar.

An additional effect unique to southern Ontario, is the convergence of lake breezes, primarily in the area between the southern extent of Lake Huron and Lake Erie, between

Point Pelee and Long Point.   The convergence of lake breezes seem to favour a southwest flow however also occur with northwesterly winds. In their study (King and others 2003) examined a number of severe convection events that show an inverted “Y” structure of lake breeze convection oriented in a southwest to northeast direction.

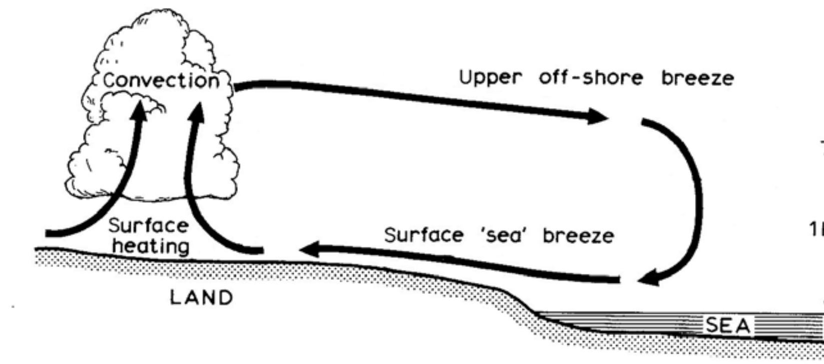

Figure 2-5: Lake breeze circulation (adapted from Sumner 1988)

The study concluded that long track storms occur in a line stretching between Lake St. Clair and Lake Simcoe. This route maximizes the travel time with surface heating. Lake breezes and their convergence may provide the trigger for storm development when atmospheric conditions are favourable for deep convection. The lake breeze circulation helps feed low level moisture into the convergence zone. The authors also noted a track favouring Lake Erie lake breeze storms when the prevailing winds are more west-southwest versus southwest that tended to shift storms south toward Lake Erie.

The GOES satellite image shown Figure 2-6 illustrates lake breezes from Lake Erie and Lake Huron and the convergence along a mid-peninsula line caused by a southwesterly flow. Note the inverted Y configuration of cumulus cloud along the convergence line. Conversely, Figure 2-7 shows a satellite image illustrating the effect of lake breeze and inland penetration from a northwesterly flow causing a convergence line from the northwest.

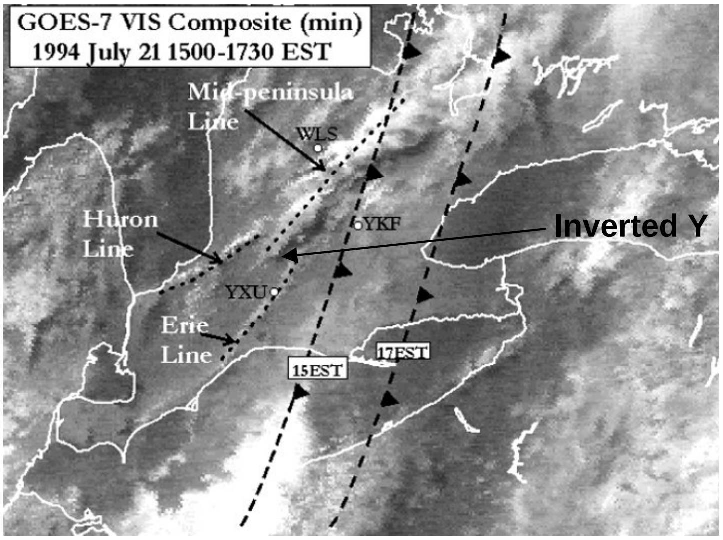

Figure 2-6: Composite of GOES-7 images from 1500 to 1730 EST on July 21, 1994. The image was formed by finding the minimum brightness of the six images at each pixel. Thus gray areas indicate the presence of cloud in each of the six images and, hence, persistence of convection at that location. (King and others 2003)

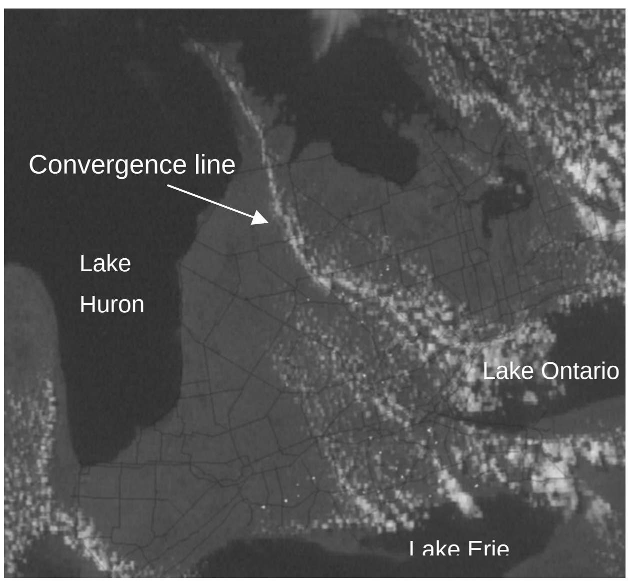

Figure 2-7: GOES image taken at 1640 EST on July 6, 2007. The image illustrates a northwesterly flow with lake breeze confining convection inland along a convergence line.

The lake breeze effect would be expected to influence convective storm patterns since in the zone between the shoreline and the lake breeze front (the zone of convergence with surface heating) generally there is little to no convective lifting of air parcels. This is due to relatively cool air being drawn from above the lake inland and thus causing a condition of a stable air mass. On days with deep inland penetration the lake-breeze zones of minimal convection would be expected to confine the geographic area that storms may form to areas in the convergence zone or beyond in the deeper inland areas.

2.3.4.2 Terrain

In southwestern Ontario there is nearly a 500 metre change in elevation between the surrounding Great Lakes and the Dundalk Upland region. The climate regions from Figure 2-1 are overlaid on an elevation map in Figure 2-6 to illustrate how their boundaries are influenced by transitions in terrain. The south and southwest facing upslopes along the lower Lake Huron, Lake Erie Counties and the Lake Ontario Shore regions are where daytime solar heating combined with onshore lake breezes can cause ascending winds. These areas are predominately composed of clay, till and sand plain surficial material under land used primarily for agriculture activity. According to Sills (2009) terrain does not have a significant influence on patterns of convective storms activity in southern Ontario compared to the effect of lake breezes. In other areas such as Texas and in Colorado research on the local effects terrain (Mead, Murdoch, Turnage 2008) suggest that complex terrain features can have an effect to enhance the severity and frequency of thunderstorms. In general the terrain in southwestern Ontario rises from the southwest toward the northeast peaking at the Niagara Escarpment in the Dundalk Highlands. Whether the rise in the land influences long track thunderstorms moving from southwest to northeast is uncertain and worthy of further investigation. At a more local level long ridges of glacial moraine features rise from 20-50 meters above the surrounding land. In most areas the ridges run parallel to the shores of Lake Erie and Lake Huron since they were formed on the edge of glacial ice masses retreating back to the Great Lake basins. Notably, the area of lake breeze convergence, roughly in the Strathroy and London area, coincides with the location where the moraine complexes from Lake Erie and Lake Huron are at their closest. It seems plausible that these features could act to assist the triggering mechanism for uplift of inland lake breezes and enhanced convection. Studies in Sweden have shown that low hills of 30 to 50 metres can affect precipitation during strataform cyclonic events (Barry and Chorley 1987). The effect of terrain on frontal systems is especially notable during winter storms. However, there does not seem be literature on the potential triggering effect that features such as glacial moraines may have on convective storms in the study area of Southern Ontario.

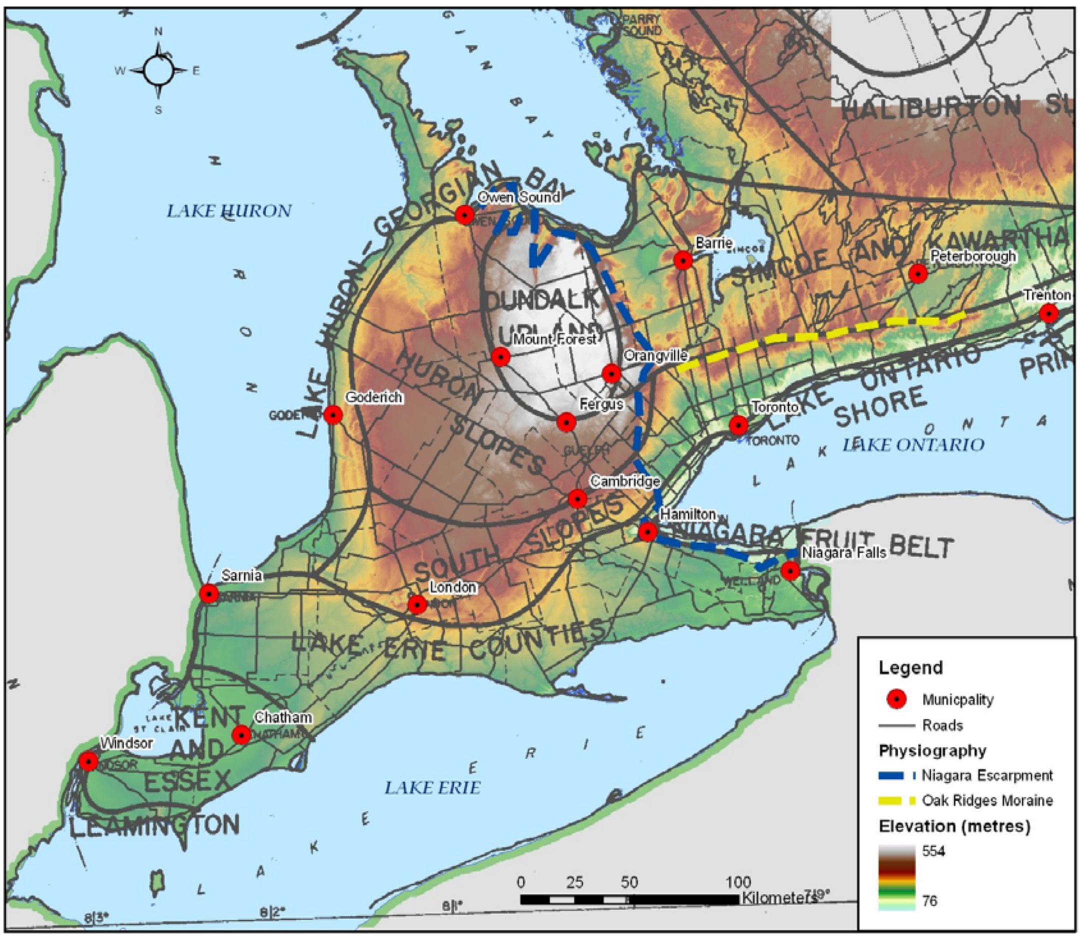

Figure 2-8: Terrain and climate regions of Southern Ontario

2.3.4.3 Urban Heat Island and Pollution

With vast areas of pavement, asphalt and other dark surfaces cities absorb solar radiation and emit thermal radiation to create urban heat islands. Urbanized areas can be 0.56 to 5.6 Celsius warmer than surrounding suburbs and rural areas (Ramanujan 2007). The rising warm air and the disturbed winds passing over large urban structures have been shown in various studies to increase severe weather and rainfall within and downwind of cities (National Weather Service 2008). During the summer, weaker winds move clouds slowly over urban areas lengthening the duration and intensity of the urban heat island influence. The effects of convective updrafts, increased air temperature and the interference of air pollution on raindrop formation together cause the clouds to intensify before producing precipitation. Increased airborne particulates from air pollution provide a greater number of cloud condensation nuclei which promote the formation of more abundant but smaller water droplets in clouds. The reduced size of water droplets delays the onset of precipitation, thus intensifying storm clouds that can build higher and suspend a larger volume of water before they start precipitating and subsequently dissipating. Building to large cumulus complexes these larger and more intense thunderstorm clouds eventually produce heavier rainfall over the city and areas downwind of the prevailing wind.

Compared to rural areas the urban heat island effect has been found to significantly increase summer convective activity with more frequent thuderstorms and hail downwind of industrial areas of St. Louis for a distance up to 40 km (Barry and Chorley 1987). Changnon's early work on the effect of Chicago on the LaPorte (Changnon 1980) and his work on St. Louis clearly demonstrate the urban heat island effect downwind. Changnon pointed out in the case of LaPorte that while industrial air pollution was a contributing factor to increased storm intensity, that the underlying circulation patterns pre-existed and were merely enhanced by the anthropogenic urban heat island effect. Rosenfeld (2000) has shown that tiny air particles, aerosols from cars and industry, also change local rainfall rates around cities. Rosenfeld suggests that small air pollution particles increase the available surfaces for water to collect on, preventing droplets from condensing into larger drops, and slowing the conversion of cloud water into precipitation. In summer, rain and thunder increases downwind of big cities, as rising air from urban heat islands combines with dispersed water in aerosol laced clouds, creating larger moisture laden clouds and eventually heavier rainfall. In other cases, Rosenfeld (2000) demonstrated with satellite data that pollution and aerosols can significantly reduce precipitation, primarily affecting strataform clouds whose temperature at their tops was -10 degrees Celsius or colder.

2.3.4.4 Soil and Land Cover

It has long been recognized in literature on severe weather that the heterogeneity of land cover is linked to convective activity. Brown (Brown and McCann 2004) suggested that the development of meso-scale circulations via differential heating may cause certain regions of the mid-western United States to experience enhanced severe weather. He further noted that a soil discontinuity in North Carolina was related to an increase to tornado activity as compared to nearby homogenous soil types. In his research of convection patterns in Mississippi, Brown (2004) found evidence that during weak synoptic flow meso-scale surface features contributed to the destabilization of boundary layer. He found statistical significance that initial convective uplift was enhanced over regions of sandy soils with the effect of advecting moisture from nearby regions dominated by clay soils. For southern Ontario this is a notable finding insofar as the juxtaposition of various large glacial deposits. Along the north shore of Lake Erie there is soil discontinuity between the Norfolk sand plain and a clay plain in the Haldimand area at the southern extent of the Grand River watershed.

As noted earlier, Southern Ontario is a heavily modified landscape with 64 percent of the area under some sort of agricultural activity. Research into the effects that agriculture has on weather and climate have found that important biophysical forcings with significant climate feedback exist as a result of agricultural-related land use change. Desjardins (Desjardins, Sivakumar, de Kimpe 2007) suggests that human disturbance of the earth’s surface that affect the energy budget might be as important climatologically as the greenhouse gas emissions arising from the land disturbance. There are complex interactions between agriculture land and the environment, and it is beyond the scope of this paper to explore them. However, at a local scale the land conversion of forest or grassland to crop production has shown several effects that could be relevant for southern Ontario. Raddatz (Raddatz 2007) summarizes the influence of agriculture on weather as follows:

> "The physiological and physical properties of the vegetation, along with the land cover's impact upon the level of available soil moisture, affect the weather and climate by influencing the transfer of heat, moisture and momentum from the land surface to the overlying air. Agriculture influences the availability of energy and water vapour mass for moist deep convection on the local and regional scales. By creating latent heat flux discontinuities, it may induce meso-scale circulations that initiate moist deep convection. Agriculture, by affecting the level of stored soil moisture, moisture that is available to the vegetation during a later period, may influence the level of convective activity within a region during a subsequent season. Thus agriculture, through the physiological and physical properties of the land cover, has had, and continues to have, an impact upon near surface weather elements and, more significantly, upon the regional hydrologic cycle."

With lake breeze effects, convergence zones, varied wet and dry soils, post-glacial terrain, urban environments and intense agriculture the southern Ontario region combines a complex arrangement of factors that likely impact local weather patterns. In consideration of the urban heat island effect and pollution, the urban and industrial influences of Detroit, Cleveland, Buffalo and Toronto likely have local influences on the weather in and downwind of their locations. Building an understanding of the interactions of these local factors and their net results on severe weather patterns should provide a fertile ground for future research.

Chapter 3
Weather Monitoring Data

This chapter will provide a description of the two sources of precipitation data used for the spatial analysis of rainfall patterns. The first is rainfall data collected by the Meteorological Service of Canada (MSC) and the second is Next Generation Radar (NEXRAD) data collected from the Buffalo and Detroit radar stations operated by the United States National Weather Service (NWS), an agency of the National Oceanic and Atmospheric Administration (NOAA).

3.1 Environment Canada Climate Data

The Canadian precipitation network is composed of weather observation sites that measure climate parameters using both manual and automated devices. The majority of sites have been operated by volunteer observers that report readings once or twice a day and send the data to MSC, with a smaller number of sites, such as airports, that operate automated tipping bucket rain gauges that measure rainfall at 5 minute and hourly intervals. The data are reviewed by MSC meteorologists to ensure data quality control and integrity. It is then centralized into the National Climate Archive, which MSC makes available via Internet for dissemination. The database of daily maximum and minimum temperature, and daily synoptic precipitation and temperature data used for analysis was downloaded from the Canadian Daily Climate Data (CDCD) from 1960 to 2005.

3.1.1 Climate Stations

A total of 1054 climate stations operated during the 46 year study period within the study area, these are shown on Figure 3-1. However, most stations were not in operation for the entire duration. Stations not reporting on any given date were excluded from the creation of the daily surface for that day. A value of zero measured precipitation was considered a valid value and was included in the interpolation.

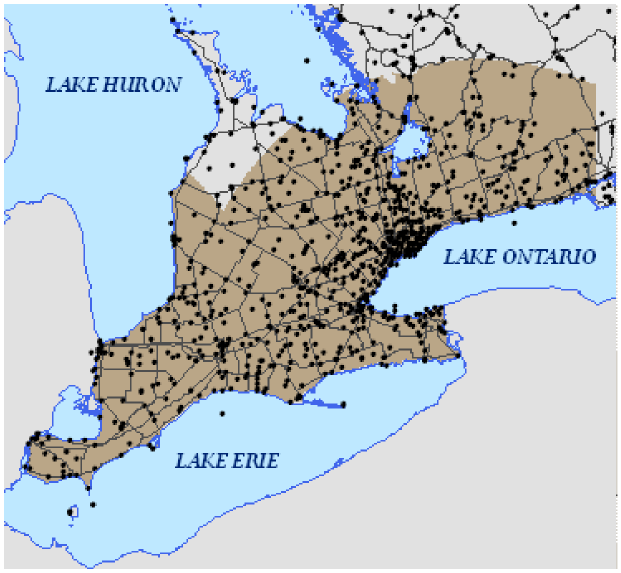

Figure 3-1: Climate stations across southern Ontario

For the precipitation data there is a difference in the time of day 24 hour rainfall accumulation is reported. For manual observers of rainfall the period of reporting is from 08:00 AM the day reported to 08:00AM the previous day (Klaassen 2008). However, for automated systems, the data is reported at 12 noon. This discrepancy is not adjusted for in the analysis, but should not have a significant impact since most convective storm events generally occur in the afternoon and evening. It should also be noted that the daily precipitation value used as the input was total daily precipitation including the rainfall equivalent for snowfall. Therefore the value stored for precipitation surfaces during months when snow could occur are considered a 'wet' total of precipitation. This is likely to only affect spring months and not expected to have an impact on the analysis of convective storms.

In Canada daily rainfall is measured using a standard rain gauge while short duration rainfall intensity is measured with tipping bucket rain gauges (TBRG) and weighing gauges. The standard rain gauge is a hollow metal tube with an open top that collects precipitation.

The observer measures the depth of the water in a small inner tube using a ruler. A TBRG is a mechanical device that automatically tips when a certain amount of precipitation accumulates inside of it. Rainfall rate is determined by the number of tips within a given interval and daily accumulations are calculated from TBRGs using a correction factor (National Research Council 1989). A Fischer and Porter gauge measures all types of precipitation by continuously collecting it into a bucket that is weighed every 15 minutes and recorded. All gauges are subject to a degree of error and uncertainty. Sources of error include observer error, instrument failure or malfunction, improper maintenance, instrument design flaw, and interaction of the measurement process with environmental factors, which include the site and location (National Research Council of Canada. Associate Committee on Hydrology and others 1989). The most significant error insofar as daily totals on manual measurements is the effect of wind. According to the National Research Council (1989) error resulting from wind can cause an underestimation bias between 5 to 15 percent. For severe storms this potential source of error can be significant. Tipping bucket rain gauges are further susceptible to underestimate during intense rainfall when the mechanical tipping device can become overwhelmed by the volume of water entering the device, and therefore have an under catch of the total accumulation of an event. These devices, since they are operated remotely, can also be affected by animal nests, spider webs, debris likes leaves, and other foreign objects that interfere with the mechanism. All MSC stations follow Canadian standards for both measuring devices and site and location considerations, which conform to the World Meteorological Organization for data measurements.

3.1.2 Decreasing Number of Climate Stations

The number of MSC stations actively collecting weather data reached its peak in Ontario in the years between 1960 and 1980. It seems contradictory that as southern Ontario experienced sustained development growth since 1980 that the number of climate monitoring sites has not grown, but instead decreased. Among the many uses of rain gauge data, the modeling of watershed hydrologic response to precipitation is particularly sensitive to location error caused by a sparse network of data collection sites (Troutman 1981). Surface runoff models use point locations to model precipitation across entire watershed basins. The amount of uncertainty that is introduced by interpolating finite point locations to represent precipitation between sites is a factor of the number of sites in an area, the distance between the data collection sites and the characteristics of the weather systems that deliver the precipitation. Fewer climate stations mean less reliability in the interpolation of rainfall values in the gaps between stations. Table 3-1 highlights the history of operational climate stations across the study area in southern Ontario. Most notably is the drop in the number of stations since the 1960 to 1980 period and most recently from the 1990 to 2000, whereas the number of operating stations in 2005 was only 47 percent of the peak of records. It is also notable the difference in the average distance between stations for the same periods changed from 7.5 km to 12.6 km, an increase of 40 percent on average. Figure 3-2 graphically illustrates that the number of operating stations most recently has dropped below the number operating between 1940 and 1960. In place of the disappearing MSC stations agencies such as conservation authorities, provincial ministries and other organizations have developed their own rain gauge networks. However, the outcome of this in-filling by non-MSC stations has led to the fragmentation of data holdings, less rigorous and consistent data collection standards and less accessibility of data for operational and research purposes.

Period	Average Distance (km)	Maximum Distance (km)	No. Stations
1860-1880	50.5	192	17
1880-1900	12.3	67	245
1900-1920	13.9	67	236
1920-1940	14.3	55	292
1940-1960	9.5	35	629
1960-1980	7.5	36	1137
1980-1990	8.8	36	840
1990-2000	9.1	38	841
2000-2005	12.6	74	532

Table 3-1: Statistics of distance between climate stations from 1860-2005

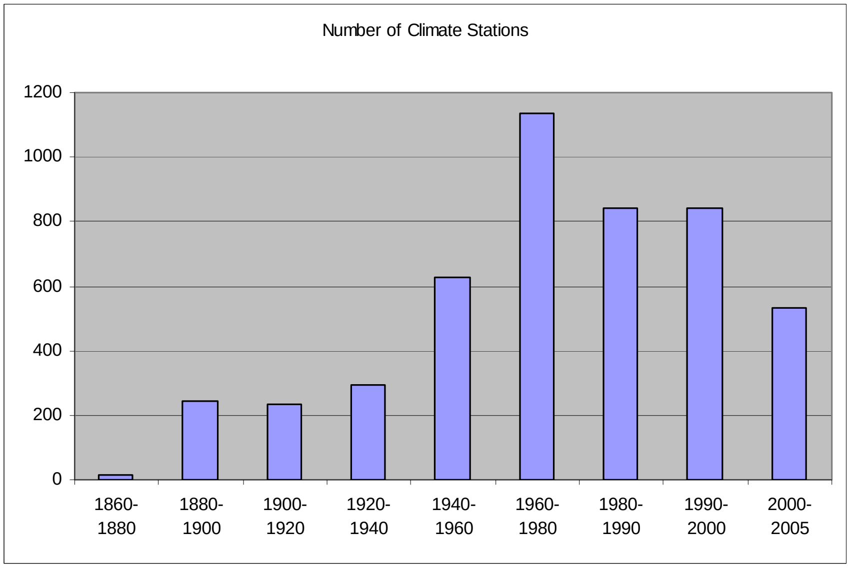

Figure 3-2: Graph of the number of AES/MSC climate stations 1860 to 2005

3.2 Radar Data

The second source of rainfall data used in this project was weather radar data from the American WSR-88D NEXRAD (Next generation Radar) network. Radar has had a long relationship with rainfall since it was first used for detecting aircraft during the Second World War. The ability to tune the pulse of the radio signal to reflect some of the energy back from water droplets in the sky has been the subject of ongoing research since the 1950s. One of the early breakthroughs for harnessing the ability of radar to detect the distance and intensity of water in the sky came from McGill University with the development of the Constant Altitude Plane Position indicator (CAPPI) (Atlas 1963). The CAPPI system scans the sky using regular intervals of radial distance and elevation angles to permit the automatic processing of volumetric data about water droplets in the atmosphere. The current radar systems operated by both Environment Canada and National Weather Service for WSR-88D use various atmospheric scanning strategies that have incorporated the original principles of the CAPPI approach.

In Canada the use of radar for qualitative rainfall estimates (QPE) has in general lagged behind the much wider range of users and applications of radar in the United States. There are marked differences in the technologies and the policies of the federal agencies that operate national radar networks across each country. These differences will be examined in section 3.2.3.

3.2.1 Overview of NEXRAD System

The NEXRAD system is composed of a series of sophisticated components of hardware, data processing algorithms and networks of data dissemination. This paper will primarily address issues related to being an informed consumer of radar data rather than delving into the technical aspects of the physics of radar reflectivity theory.

Southern Ontario is unique in Canada insofar as the coverage offered by NEXRAD radar stations located in Buffalo, Cleveland and Detroit. The overlap of coverage between Detroit and Buffalo was sufficient that Cleveland data was not considered in this project. The most built-up portions of south central and southwest Ontario have coverage from NEXRAD data. The data from the WSR-88D system is available from 1996 with continuous coverage up to the present.

3.2.1.1 Radar Principles

NEXRAD uses a 10cm or "S-band" wavelength to measure the reflectivity or density of water droplets in the atmosphere to a distance of 230 Km from the radar station. Beam wavelengths used to measure precipitation generally range between 1 cm to 10 cm, with 10 cm suffering the least from attenuation of signal over distance. As the wavelength used shortens, so does the effective range of the radar system.

The information product of radar is a calculated value for the rainfall rate (R) in depth per time interval as based on a relationship with the reflectivity (Z) measured as decibals (dBZ) from the sensor. The default convective Z/R relationship used by NEXRAD is $Z=300R^{1.4}$ with a maximum rate of 53 dBZ which equates to 103.8 mm/hour or 4.09 inches/hr (Story 2006). A maximum value is set to eliminate the contamination of the high reflectivity of hail within rainfall estimates.

Reflectivity is measured from radial scans of the atmosphere at different elevation angles. Estimating precipitation is complicated by the radar beam path of travel through various layers of a storm's vertical profile in the atmosphere at any given time and distance from the station. It is also complicated by the fact that the radar beam does not follow a straight path through the air relative to the ground. There are a number of factors affecting beam propagation that will be covered in section 3.2.4, however, under normal circumstances the beam bends away from the earth's surface due in part to the adiabatic lapse rate of cooling air in the troposphere and also in part due to the curvature of the earth away from the beam with greater distance from its source. Different beam scan angles are used to characterize the full volume of the scanning cone of the radar coverage leading to the generation of a composite reflectivity Z value that is used in the Z/R calculation.

The NEXRAD system uses several scan strategies or Volume Coverage Patterns (VCP) that are adjusted for different conditions. The completion of a full scan of the atmosphere within range of the station takes between 4 to 5 minutes when rainfall is detected in the swath. A 10 minute scan interval strategy is used during winter or during clear air to reduce usage of the equipment. There are a suite of different NEXRAD data products derived for each scan interval that include both the raw and composite reflectivity, as well as derivative products such as wind, total storm rainfall, and hourly rainfall.

3.2.1.2 Digital Precipitation Array Data

The NEXRAD Digital Precipitation Array (DPA) data product was used as the primary radar data input for the rainfall analysis of this project. The DPA data contains a 1 hour estimate of rainfall accumulation representing the average of the calculated rainfall from the volumetric scans over the previous hour. The DPA is generated for each scan interval, typically on a 4 or 5 minute VCP and is processed into a useable data product on 6 minute intervals.

The DPA data is arranged on a 4 Km by 4 Km grid, called the Hydrologic Rainfall Analysis Project (HRAP) grid, based on a stereographic map projection. For each 6 minute interval a DPA file is generated for each radar station with grid cells assigned a rainfall depth in inches, representing the average rainfall over the past hour. This moving average of rainfall accumulation is the most commonly used data product for flood forecasting and other hydrologic modeling purposes.

The DPA rainfall estimate is the output from five components or scientific sub-algorithms that include the initial data preprocessing, calculated rainfall rate based on Z/R relationship, rainfall accumulation, rainfall adjustment based on rain gauge data and generation of precipitation products (Story 2006). The DPA end product goes through several stages of quality control processing, which include checking for beam blockage and for anomalous propagation. One the key features of DPA data is an adjustment or bias factor that is applied to the estimate rainfall based on rainfall observations at automated tipping bucket rain gauges within the radar station coverage. A bias factor is calculated for each radar station for each hour based on a ratio of the sum of all positive rain gauge data to non-zero DPA values over set time interval (Story 2006). The time interval varies depending on the radar operator and the availability of rain gauge date. If the bias factor is 1.0 the rain gauge data and the radar are in agreement. When it is greater than 1.0 the radar is underestimating compared to ground measurements. The bias factor is used to adjust the radar's rainfall accumulation value, based on the initial Z/R relationship, so that radar and rain gauge accumulation are in closer agreement.

3.2.2 Data Acquisition

One of strengths of radar for tracking weather is the near real-time availability of the data for weather forecasters. For the general public both Environment Canada and the

National Weather Service provide websites that illustrate the latest radar maps, and allow looping of recent scans to get an idea of the motion of storms. For researchers and agencies that want access to the actual radar data the National Weather Services provides two real-time options, the first being a fee-based subscription to a multicast service that will push data to a receiving agency over the Internet, the second option for access is a free service via a FTP server per radar station and data product. The access point to download the latest DPA data for the Buffalo (KBUF) station, as well as, the previous 24 hours of data scans is the following: **ftp://tgftp.nws.noaa.gov/SL.us008001/DF.of/DC.radar/DS.81dpr/SI.kbuf/**

For archived radar data, the National Climate Data Center (NCDC), a department under the NOAA, operates a free data download service for accessing radar data on per station basis, up to 7 days at a time. NCDC operates a Hierarchical Data Storage System (HDSS) that uses robotic devices to retrieve media from its library. The NCDC's massive archive uses multiple tape drives and robotically managed storage cabinets that are addressable as a single, massive storage system. The public access point for downloading archived NEXRAD radar data is the following: **http://hurricane.ncdc.noaa.gov/pls/plhas/has.dsselect**

3.2.3 Differences Between NEXRAD and Environment Canada Radar

NEXRAD data was selected over radar data from Environment Canada for several reasons; the primary being the availability of real-time and archival data. Environment Canada has limited data available in its archive, with the data stored on CDROM diskettes at the Environment Canada radar research centre in King City Ontario. There was no viable means to acquire the data in timely manner from the vast library of CDROM's. The other major factor is the cost to access a data feed from Environment Canada. Canadian radar products can only be acquired in real-time from a subscription service that costs $200 per month per station. The Environment Canada data is processed and delivered on 10 minute intervals on the hour. Through the Grand River Conservation Authority data from the Exeter (WSO) and King City (WKR) radar stations were acquired for 2008, however, given that an archival data equivalent to the NEXRAD archive was not readily available NEXRAD was the sole source of radar data used in this research project.

Environment Canada uses a 5 cm or “C-band’ wavelength which is less expensive to operate compared to the NEXRAD 10 cm system. However, the 5 cm wavelength is more likely to suffer from attenuation of the radio signal. This is especially important with an intense rainfall rate typical of convective storms. A storm producing intense rainfall can effectively block the signal, rendering the radar unable to detect rainfall beyond the storm (Donaldson 2008). This is a critical factor in the use of the Environment Canada radar for tracking multiple storm cells, and highlights the need for overlapping radar coverage from multiple stations.

Other key differences of the Canadian a system include no algorithms for reducing radars errors and no calibration of the rainfall estimate with ground based rain gauge data. Yet, with the lower reliability of C-band radar over distance there is a greater need to have ground based measurements to calibrated rainfall estimates.

For southern Ontario the Exeter and King City stations are well positioned to augment and supplement radar data from the Buffalo and Detroit stations. However, given the significant differences in the technologies, data processing steps and data dissemination policies, the integration of both sources of radar in southern Ontario would be difficult.

3.2.4 Limitations and Sources of Error in Radar Data

Weather radar is a remote sensing monitoring system that is prone to various types of errors that can lead to inaccuracies in the final rainfall estimates. There are several types of errors that can be introduced into the subsystems; there are errors of hardware and calibration, calculation, external multi-sensors, and beam propagation.

The operators of the NEXRAD systems have made adjustments to the NEXRAD system over the time interval of the data that was analyzed. These adjustments include hardware upgrades and changes to the equipment, and variations to the algorithms and scan strategies. These variations are not accounted for in the analysis, and there is no way to quantify the impact of adjustments on the DPA data. Between 2002 and 2005 there were a number of improvements to subsystems, including improvements to quality control on the data (Saffle, Cate and Istok 2009).

Errors of calculation of the Z/R relationship are tightly coupled with the calibration to rainfall estimates. Improper use of constants in the calculation can lead to over or under estimation of the rainfall rate. Calibration of the NEXRAD system relies in part on external measurements from tipping bucket rain gauges. Story (2006) cites a number of potential errors associated with ground-based measurements including mis-matching of rain gauge clocks to radar clocks, rain gauge under catch due to extremely high rain rates or power outages associated with thunderstorms, high winds around the gauge, mechanical failures, hardware/software data transmissions and errors in the reported geographic location of the rain gauge. These errors can lead to erroneous bias factors applied against the radar values.

The reliability of radar data is based on assumptions using standard parameters for atmospheric conditions. When conditions deviate from normal, beam propagation errors may be caused by false echoes from targets other than precipitation beneath cloud bases. The following is a summary of the most common beam propagation errors as illustrated in Figure 3-3.

Ground clutter is commonly caused by low elevation beam angles striking objects on or above the ground, such as buildings. The echoes are recognizable by a lack of motion and are generally close to the station. In Ontario, the Niagara escarpment and built-up area in and around the Greater Toronto Area are typically prone to this error (Donaldson 2008). NEXRAD employs tests of low elevation scans to check for contamination from the surface.

Super refraction, also referred to as ducting, is the bending of the radar beam toward the earth's surface whereby it interacts with ground targets. The backscatter of the signal can appear as high reflectivity values on the radar. Similar to ground clutter, this type of anomalous propagation (AP) is detected by the stationary nature of targets whereby rainfall generally tends to have motion within the prevailing air flow. Super refraction is commonly caused by an atmospheric inversion whereby a low lying air mass is cool, often moist, and the air aloft is dry and warmer. This effect is common under late evening and early morning conditions, as well as, temperature inversions ahead of the leading edge of warm fronts. In the instance of frontal conditions, the error can cause confusion when real rainfall is mixed with AP effects.

WSR-88D employs automated clutter suppression and the radar operator has further manual tools to adjust for AP if it is recognized.

Under refraction is the opposite case of super refraction and occurs when the atmosphere is unstable and cools at a much faster rate than a standard atmosphere. This effect causes the beam to bend upward faster than normal which subsequently identifies the precipitation at a much higher elevation than it actually is.

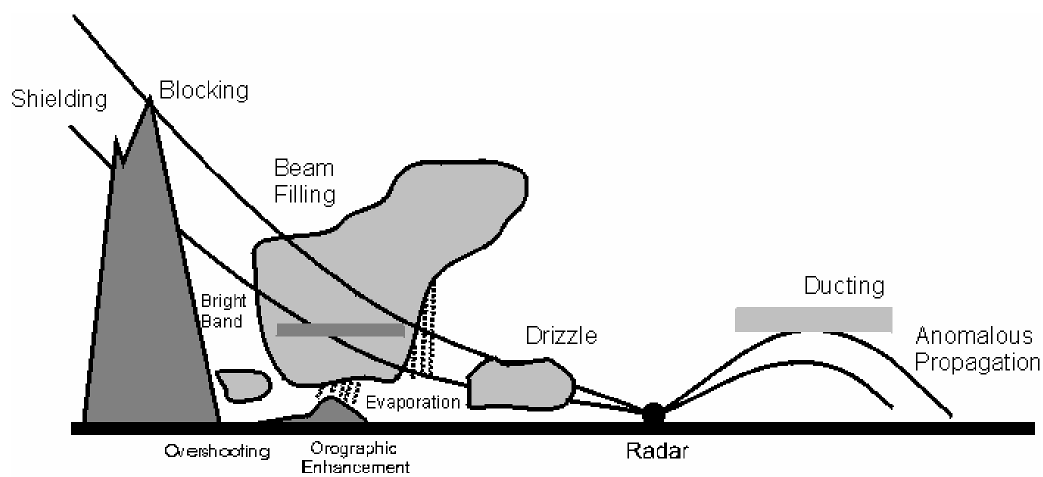

Figure 3-3: Radar beam propagation errors

(Source: http://upload.wikimedia.org/wikipedia/commons/3/3a/Radar-artefacts.PNG)

Bright band errors occur as high reflectivity values caused by either hail or when ice crystals falling through the freezing level of the cloud melt and form ice pellets. High or bright reflection values from water-coated ice crystals can lead to overestimation of rainfall nearer to the radar and underestimation at greater distances due to beam attenuation.

Range degradation errors have several aspects to it that include **partial beam filling** and **beam overshooting.** At far ranges the radar beam spreads outward and may suffer from underestimation since fewer hydrometeors (precipitation droplets) are struck by the signal. Stratiform rainfall, typical of warm front systems, deliver precipitation over a large area with a fairly constant vertical profile. The ‘wet’ layer of clouds can cause a bright band effect which in turn blocks more distant signals. This leads to signal degradation and an underestimate of rainfall accumulation at further distances. According to Story (2006) underestimates can also occur during stratiform rain events and low-topped convection due to the radar beam overshooting above the rainfall at far ranges.

Beam blockage is a problem of high terrain or mountains shielding the signal beyond. This is not a problem in Ontario.

Attenuation of the signal strength is not considered a major factor with 10 cm S-band wavelength, with the exception of bright band. However, it is a factor for 5 cm C-band used in Canada. It is also not clearly understood, but rain falling directly on the radar dome is also expected to have some degradation on the radar signal.

Chapter 4
Spatial Analysis Methodology

The first sections of this chapter provide a description of data processing methods used to derive daily precipitation and temperature surfaces from the MSC climate station data from 1960 to 2005 and the subsequent analysis of those surfaces for storm events. The second half of the chapter describes the processing and analysis of data from NEXRAD radar from Detroit and Buffalo stations for storm events between 1996 and 2008.

4.1 Deriving Daily Climate Surfaces

A raster-based approach was adopted for the spatial analysis of the MSC climate station data. Instead of examining weather stations discretely, neighbourhood analysis was used to interpolate available station data into continuous daily surfaces for the entire study area. With this approach the statistics reported in the results of Chapter 5 are area-based and influenced by the spatial interpolation of rainfall between climate stations. The software processing environment used was ArcInfo GIS software with functions of the Grid module for the raster processing. Algorithms for automated processing of data through various steps of data preparation and analysis were written in the Arc Macro Language (AML).

In 2007 the author, working at the Grand River Conservation, conducted a project that analyzed climate variables recorded daily at MSC climate stations across southern Ontario between 1960 and 1999. The variables of interest were daily accumulation values for precipitation (in millimeters), and daily maximum and minimum air temperature (degrees Celsius). A total of 1293 weather stations operated during the 40 year study period within the study area covered by the 2007 project. However, many of the stations were not in operation for the entire duration. Stations not reporting on a given date were excluded from the creation of the daily surface for that day. A value of zero measured precipitation was considered a valid value.

As part of this thesis research the original 40 year study was extended with an additional six years of MSC climate data for the years 2000 to 2005. Only the western portion of the 2007 study was examined using a subset of 1054 climate stations.

4.1.1 Spline Interpolation

Raster surfaces representing each daily variable were generated using a Spline interpolation. A similar approach was used by Shen (Shen et al. 2001) for a comparable project of deriving daily surfaces for temperature and temperature in Alberta. Shen et al. (2001) found that the Spline interpolation was well suited for accurately representing large widespread rainfall events, however, the authors noted with smaller localized storm events, such as summer convective storms, that the results had a smearing effect on the derived rainfall surfaces.

There are some notable shortcomings to the interpolation of a point cloud of distributed stations into a continuous surface. First, it should be noted that the Spline algorithm was run against daily accumulations not individual storm events. Multiple rainfall events within a daily reporting interval could skew the spatial representation of the actual events. Other potential sources of error are related to the spatial distribution of station locations. Small storms detected by one or only a few stations would be expected to create a curved surface of rainfall values out into the void between stations that reported little or no rainfall. The surface created could misrepresent the event whereby the discontinuity of wet and dry areas would likely be fairly abrupt in reality whereas the Spline interpolation would stretch decreasing values over a wider distance based on the slope between station values. In another instance, two adjacent stations experiencing two different convective storms cells could falsely fill the void between the stations with rainfall values when in fact little or no rain occurred there. Lastly, some storms could miss stations completely, or at least miss the most intense core of the storm, such that a local intense rainfall event may not represented in the daily surfaces at all. These potential sources of error need to be considered in the interpretation of the analysis results.

Aside from Spline, other interpolation techniques that were evaluated and considered were inverse distance weighting (IDW) and kriging. IDW surfaces were found to have a strong “bull’s eye” effect, indicative a non-smoothed linear weighted analysis. Surfaces created from a kriging interpolation had reasonably good spatial results; however, the algorithm parameters needed to be adjusted for each day to account for the semi-variance of input data and angular trends in the data due to the movement of storms. Kriging was also found to modify the original input values at station locations based on weighting values within the neighbourhood of stations. Altering the original values was considered an undesirable effect, whereas the Spline algorithm with the “tension” option was found to force the output surface to pass exactly through the observed value of the variable at each station.

It should be noted while the surfaces accurately represent the station data at their locations, that the spatial pattern of derived rainfall between stations is a factor of the distance and arrangement of available stations on any given date and the parameters of the Spline interpolation. There is a degree of error and uncertainty in any interpolated surface. In the case of the Spline algorithm, edge effects are particularly notable since the Spline fits a curved trend surface to the data. At the edge of the point data, the trend established from the point cloud propagates outward beyond the edge of input points. For example if an inland station reported a low rainfall value and a station near the shoreline of one of the Great Lakes reported a high value, the trend surface would continue to increase values beyond the shoreline over the lake. To reduce edge effect, the resultant surfaces are clipped to the extent of land area in the study area so that erroneous values over the Great Lakes are excluded.

The cell size of the output Spline surfaces was 1 km x 1 km. The number of climate stations that were available to contribute to any cell in the grid was set to 8. This value was chosen based on nearest neighbour analysis of the climate stations. The maximum number of points permitted by the software was 12, but it was found that the average distance between 12 contributing stations for was unacceptably high, whereas at a value of 8 stations the average high was deemed acceptable, although still larger than preferred at 22 Km. Note the decreasing number of climate stations as discussed in Chapter 3.

4.2 Analysis of Climate Surfaces

The processing of the daily climate surfaces involved the following steps:

1) Daily rainfall surfaces were accumulated for each month between March and September. Statistics were calculated from monthly surface totals to extract mean, maximum, minimum and standard deviation for each month for each year. The statistics were plotted on graphs with a linear trend line fitted using a least squares method. These results are meant as exploratory only, and do not account for serial correlation and non-symmetrical values, as dealt with by methods of trend analysis by Vincent and Mekis (2006) and Zhang, Vincent, Hogg and Niitsoo (2000). The graphs are shown in Chapter 5 and in the appendices.

2) Daily rainfall was evaluated by selecting cells from each daily surface where the total rainfall exceeded threshold values of 12.5 mm, 25 mm, 50 mm and 75 mm. The cells that exceeded these values were converted into raster masks and then the masks were totaled for each month and for the two 23 year intervals between 1960-1982 and 1983-2005, as well as, for the complete 46 year period.

By summing raster masks of different daily thresholds the hypothesis was the locations of more frequent storms of varying accumulations would be highlighted by higher summed values. Daily accumulations of higher totals were assumed to represent more severe storms. However, rainfall totals over an interval less than 24 hours cannot be directly expressed by the surfaces. The masks of different thresholds were turned in single bit rasters surfaces, whereby cells of a value equal to or above the threshold were assigned 1 and other 0. This allowed summation of the number of occurrences of events of each threshold total by month and by year.

4.3 NEXRAD Radar Processing

The methodology to prepare the radar data was less complicated than the Spline surfaces. However, aspects of the radar processing had other challenges, the main being the large amount of data to import and analyze. Whenever rainfall was detected anywhere in the 230 Km swath of the NEXRAD radar swath, a Digital Precipitation Array (DPA) data file was generated on 6 minute intervals. Each six minute interval was converted into a raster surface. For the 214 days during the months of March to September over the 13 year period of data, there is a theoretical maximum of 1,684,000 intervals of data for each station. In reality it was not always raining, whereas actually 1,048,000 six minute interval DPA files were processed for both Buffalo and Detroit over the 13 year period. Each DPA file was converted into an ASCII grid format using a Java based utility downloaded from a NOAA website (**http://www.ncdc.noaa.gov/oa/radar/jnx/jnt-install.php**). The ASCII file was imported into ArcInfo raster format and the study area mask was applied against the complete dataset and checked for non-zero values. If there were non-zero values within the study area for the six minute interval, the data was further processing to convert from the stereographic map project to Universal Transverse Mercator, Zone 17, and the rainfall value in inches converted to millimeters. A system folder was created for each year/month/day for each of Buffalo and Detroit stations to store the data for each day.

The DPA data is time stamped in Coordinated Universal Time (UTC) so a secondary processing step converted from UTC to local time, accounting for the specific date for the time difference between daylight savings and standard time.

A third step was to isolate hourly intervals in the DPA data. Because DPA data is the average of the previous hours moving average, selecting data spaced by hourly intervals effectively provides 24 discrete hourly intervals for a day. However, since the scan strategy for NEXRAD switches between short intervals of six minutes to ten minute intervals for clear air mode, the scans do not always evenly fall on the hours of the clock. Do deal with this, an algorithm selectively looked for DPA data closest to the hour using one minute steps on either side of the hour, and then extracted that raster as a one hour summary. If it was raining the range of minute values would be [:58, :59] of the previous hour or [:00, :01,:02,:03] from the next hour. From the hourly rasters for Buffalo and Detroit an hourly mosaic was created that stitched the surfaces together, with the rule that in the overlap area that the highest rainfall value would take precedence.

4.4 NEXRAD Radar Analysis

In a manner similar as described in 4.2 daily thresholds were set for 12.5, 25, 50 and 75 millimetres of daily rainfall and masks summed for the 13 period. However, radar offers a much finer temporal granularity of the data on a six minute moving one hour average of rainfall and a further analysis of rainfall intensity was conducted.

An algorithm was written in AML to step through all the 6 minute DPA rasters from March 1996 to September 2008. The algorithm performed a difference analysis on each grid looking for the maximum value for each 1 Km x 1 Km cell. When the value in the maximum grid was exceeded, the date and time of the record maximum was recorded in a different raster grid. Maximum one hour surfaces were generated for each month, each year, for each month over 13 years and for the total of all the data for 13 years. The CPU processing of this task ran for approximately 170 hours.

4.4.1 Anomalous Propagation Handling

False echoes were checked against the monthly maximums and then cross-referenced with daily climate surfaces when they were suspected to have occurred. Meetings with Environment Canada staff in November 2008 helped to identify the presence of AP artifacts in the NEXRAD data. Environment Canada (Klaassen 2008)(Donaldson 2008) also highlighted anomalies in some of the summaries. A complete review was done of all the monthly maximum one hour surfaces to check for the presence of AP errors. The NOAA Climate Toolkit was used to render animations of the DPA to check for stationarity of the data. Nine occurrences of AP were detected between 1997 and 2003. Figure 4-1 shows the AP effects for March 1997. Table 4-1 lists AP occurrences and their date and time when they were detected. A mask was created around the suspected AP contamination, and the one hour intensity was re-run for the month and the 13 year totals were updated to reflect the corrections. Detection of AP was a manual exercise of looking at maximum intensities. NEXRAD was expected to handle AP errors, whereas in 2004 upgrades to the system appear to have improved the handling since no occurrences were found after 2003.

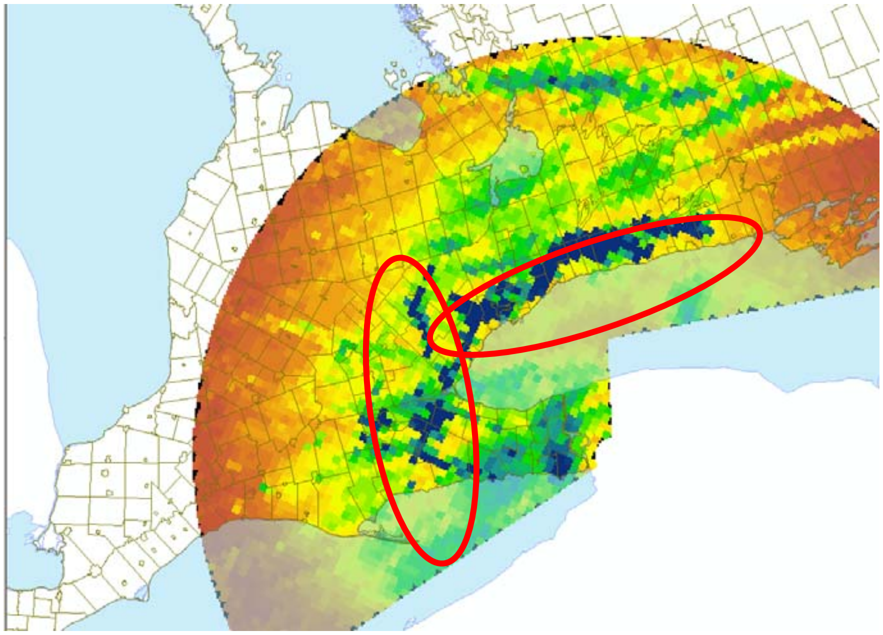

Figure 4-1: Effect of anomalous propagation shown in dark blue for Buffalo NEXRAD radar, March 1997

Station	Year	Start Month	Start Day	Start Hour	End Month	End Day	End Hour	Description
KBUF	1997	03	25	0900	03	25	1200	apparent ground clutter GTA, Oak Ridges moraine, and Niagara escarpment
KBUF	1997	03	29	0000	03	29	0500	Niagara escarpment, Hamilton and Brantford area
KBUF	1997	07	21	0500	07	21	1000	SW Ontario, unusual, not on Detroit radar, no movement
KBUF	1999	08	10	1000	08	10	1500	apparent ground clutter in the GTA area and the Oak Ridges moraine east of the GTA
KBUF	2002	03	09	0000	03	09	0500	Niagara escarpment
KBUF	2002	03	29	0500	03	29	0900	Niagara escarpment
KBUF	2003	03	15	0030	03	15	0500	Niagara escarpment, Hamilton
KBUF	2003	09	26	2100	09	26	2359	apparent ground clutter in the GTA area and the Oak Ridges moraine east of the GTA
KBUF	2003	09	27	0000	09	27	0400	apparent ground clutter in the GTA area and the Oak Ridges moraine east of the GTA

Table 4-1: Detected and fixed occurrences of anomalous propagation

Chapter 5
Spatial Analysis Results

This chapter presents the results from the analysis of 46 years of climate surfaces and 13 years of rainfall radar data. Prior to presenting the overall results, a look at the differences in the data sources from a single event will serve to provide context to later sections.

5.1 Rainfall Mapped from Spline Versus Radar – Case Study of July 14, 1997

The spline interpolation of rainfall on July 14, 1997 is illustrated in Figure 5-1. On that date two separate convective storms delivered significant rainfall. The first storm formed late afternoon from a lake breeze convergence and the second later in the evening moved southeastward from Lake Huron. The points in Figure 5-1 are climate stations used to generate the spline surface, with their point size as a relative indication of total daily rainfall.

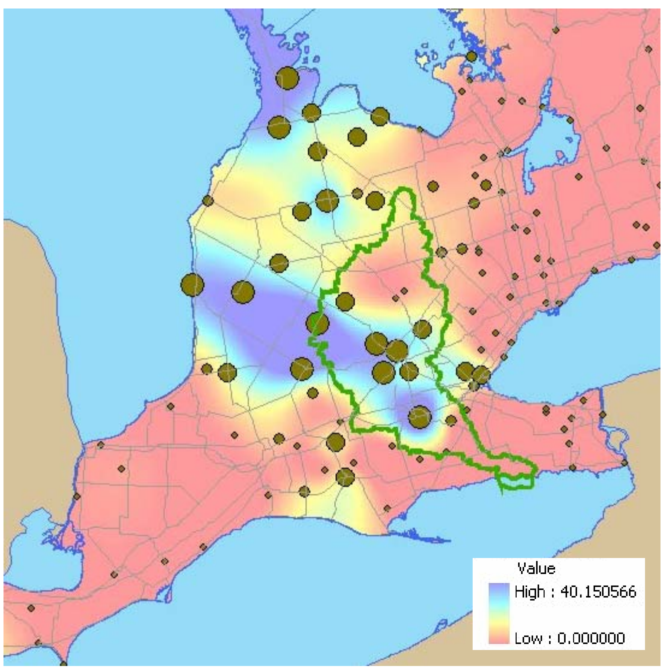

Figure 5-1: Daily precipitation surface for July 14, 1997 (value in millimeters)

The spline interpolation for July 14th is shown in a three dimensional perspective in Figure 5-2 to illustrate the curved nature of the spline output. In comparison,

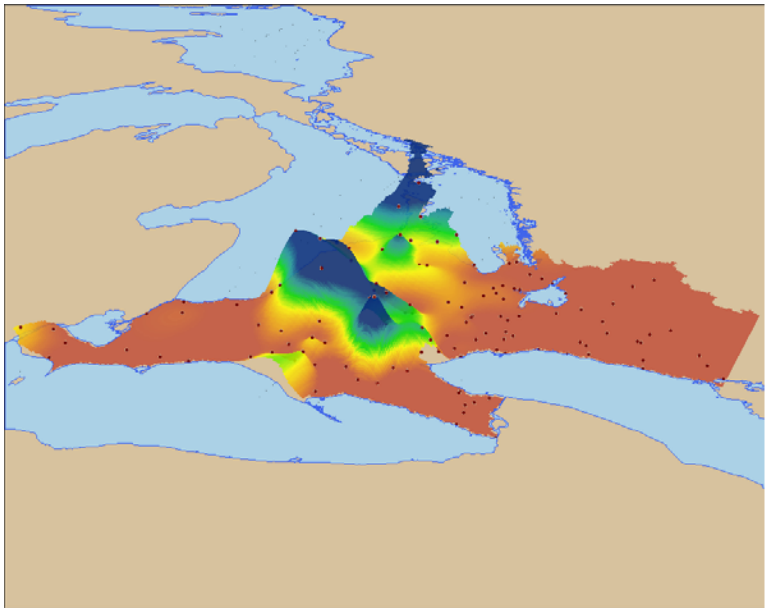

Figure 5-2: 3-D perspective of spline surface for July 14, 1997, with data points shown.

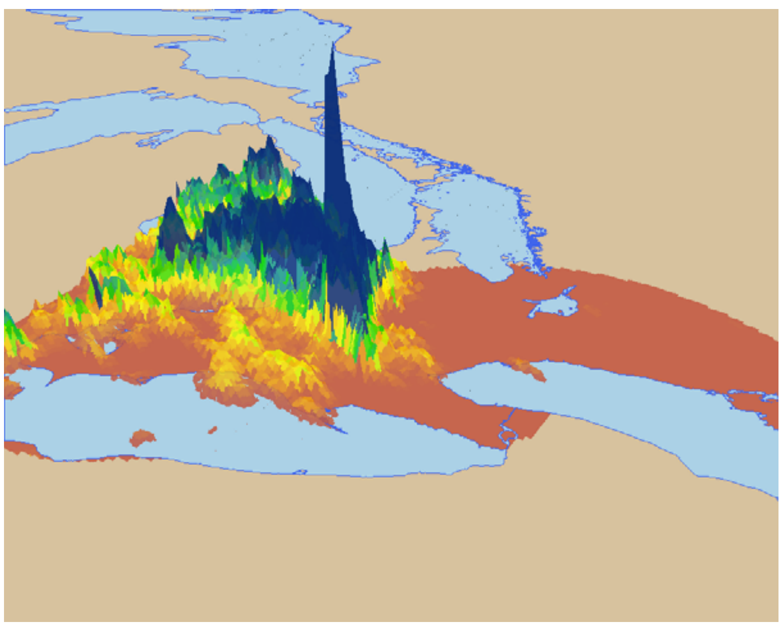

Figure 5-3: 3-D perspective of daily precipitation surface from NEXRAD July 14, 1997

the daily precipitation total for July 14, 1997 from the NEXRAD radar data is shown in Figure 5-3. Both figures 5-2 and 5-3 use the same vertical scale for total rainfall, however, note the steeper slope and rougher texture of the radar surface and the high spike in the centre. The spike in the radar surface represents a small area 12 Km east of the City of Stratford where the radar reported total daily rainfall of 294 mm. However, the highest rainfall reported by any of the climate stations that day was only 40 mm. The Stratford MSC station only reported 30.6 mm, whereas Detroit radar at the same location reported 50 mm and Buffalo 32 mm. This was a unique event that was colloquially named the Punkeydoodles Corners storm by Environment Canada (Environment Canada 2005) since they had staff doing field work at the rural hamlet about 8 Km from where the radar reported the highest rainfall (Sills 2009). MSC staff reported 8 inches, or 203 mm, whereas Buffalo radar reported 205 mm at Punkeydoodles Corners that same day. The storm's maximum rain rate was recorded by Detroit radar at 18:48 local time, with a one hour accumulation of 97 mm, however the hourly rate measured by Buffalo was 71 mm at the same location.

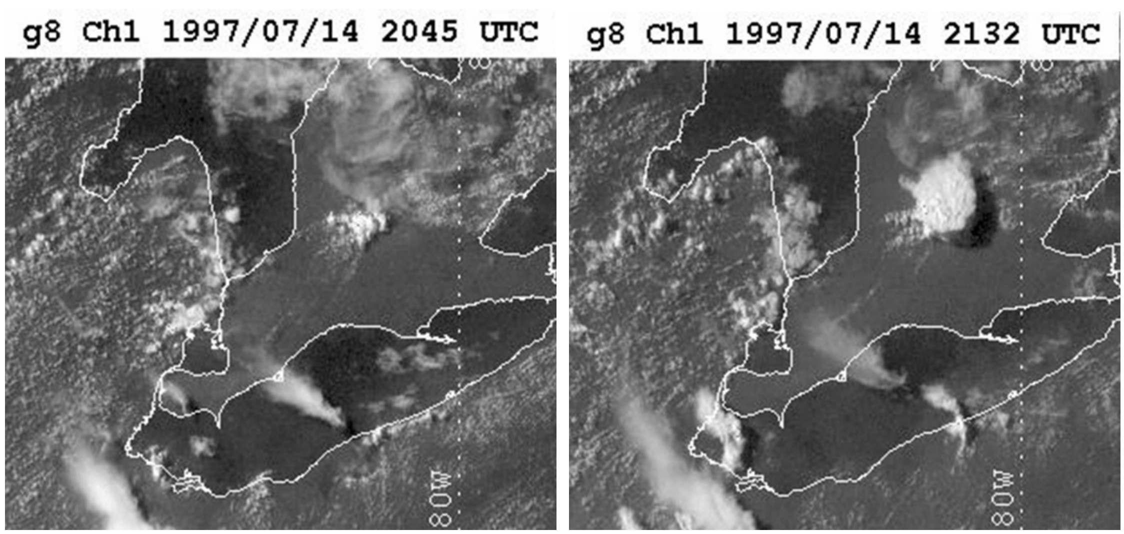

Figure 5-4: GOES images of 16:45 and 17:32 local time showing the development of the July 14, 1997 convection cell. Note the inverted Y cloud structures and the absence of cumulus clouds between the shoreline of the lakes and the storm cell.

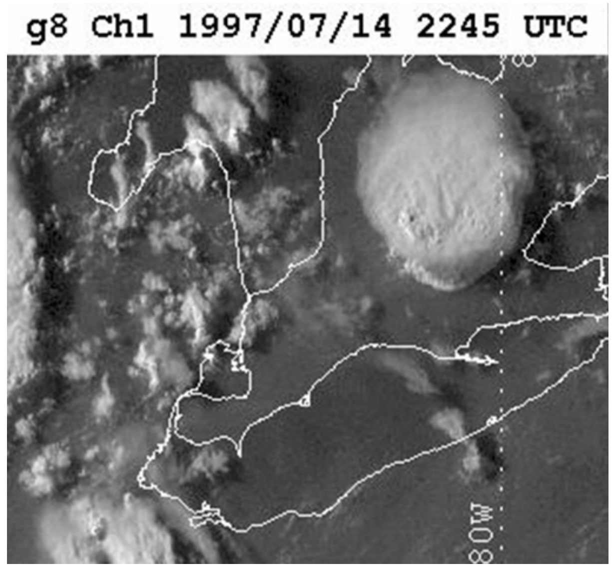

Figure 5-5: GOES image of the July 14, 1997 storm at 18:45 local, at the peak of the maximum rainfall rate at Punkeydoodles Corners.

Punkeydoodles Corners is near the 230 Km outer extent of the Detroit radar coverage whereas the Buffalo station is 70 Km closer than Detroit. At the spike that reported 294 mm of rain from Detroit, the Buffalo radar reported a total of 205 mm.

The comparison of measurements from MSC climate stations, two radar stations and anecdotal ground evidence demonstrates how different monitoring systems can produce different results for rainfall accumulation. It also shows a good correlation between the Buffalo radar values and ground measurements observed by the Environment Canada staff. The results also indicate a discrepancy between the Buffalo and Detroit radar results. It is only speculative, but the differences in radar values between stations could be the result of the differing distances to the stations and the effect distance may have had on beam height relative to the vertical profile of the storm. This case study also shows how a relatively small area between MSC climates station where a major downpour of 203 mm rainfall occurred was completely missed in the measurements from the closest climate station at Stratford, which only recorded 40 mm for the same event.

The differences between the spline surface and the radar show both the smearing effect of spline on local storms and the impact of sparse stations have on not fully characterizing a localized event. Figures 5-4 shows the early formation of convection and Figure 5-5 from the GOES satellite, at a time near to the storm's peak, shows the impressive magnitude of the storm cell. All the convection occurring in southwest Ontario was happening in the one updraft triggered by lake breeze and convergence. This storm tracked on a southwest to northeast path. The position of the storm cell relative to the Great Lakes is worth noting for later discussion.

5.2 Spline Interpolation Results

From the MSC climate station data between 1960 and 2005 a total of 16,800 surfaces for daily maximum and minimum temperature and 16,775 surfaces for daily precipitation accumulation were created and analyzed. The following sections will provide a summary of the analysis of daily minimum and maximum temperature and daily precipitation. The results are presented as monthly averages calculated for each year. The reader is referred to the Appendices for further results.

5.2.1 Monthly Temperature Trends 1960 to 2005

The generation of daily temperature surfaces was well suited to the spline interpolation technique due to the continuous nature of the variable. Whereas precipitation is generally a stochastic process that is prone to edge effects, temperature could be measured and reported for any active climate station. Figure 5-6 provides an example of daily minimum and maximum temperatures surfaces for July 14, 1997. The spatial patterns of warmer areas in red and cooler in blue highlight the complex nature of local and synoptic influences on daily temperature in southern Ontario.

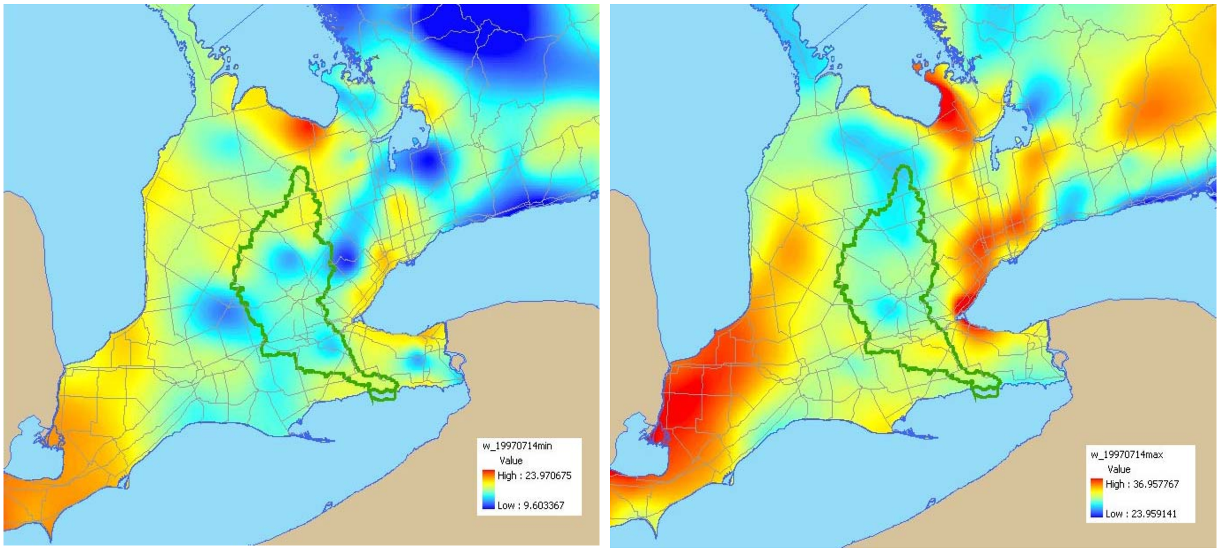

Figure 5-6: Daily minimum (left) and maximum (right) temperature surfaces, from July 14, 1997, generated from the spline interpolation

Monthly statistics for temperature were calculated by averaging the daily values for each month of each year and then reported on for maximum, minimum and average values for the monthly surfaces across the study area. The results are an ensemble from all the raster cells across the entire study area, and are not necessarily representative of any specific location. However, averaging raster surfaces values based on the spline interpolation of climate stations does favour dominate patterns of temperature distribution as contributing to the overall statistics.

The graphs and tables on the pages to follow present a summary of the temperature analysis. Monthly values were calculated using daily values averaged over each month. A best-fit linear trend is used to indicate linear change across all the data in the time series. The monthly averages over the 46 year period show a high degree of variability which is reflected by low R-squared values. While weak, the trend lines in the statistics show an upward shift in the temperature for each variable examined.

Figures 5-7 and 5-8 indicate an overall upward trend for March to September in the daily minimum temperature. This is likely the result of warmer temperatures in the evening and overnight. The changes in trend values are listed in Table 5-1. The greatest change in minimum temperature has occurred in the early spring and mid-summer. Based on the linear trend, on average the daily minimum temperature has increased by 1.4 degrees.

The monthly results for daily maximum temperature also indicate an overall upward warming trend for the period of data, as shown Figures 5-9 and 5-10. March shows the greatest change in maximum, average and minimum values, with an average change of 2.1 degrees. Table 5-2 lists the trend values for maximum temperature over the 46 year period of the data, with an average change of 1.0 degrees for the months listed.

Refer to Appendix A for monthly graphs showing minimum, maximum and mean values for both daily maximum and minimum temperatures. The minimum and maximum values represent the extreme values as averaged over the month for any given year. A linear trend line has been used to depict change over the 46 years. It is important to note the trend lines represent the averaging of the variation in the data and that the results showing change over time represent a smoothing of the extremes of variability and not necessarily the actual temperature one would necessarily expect at any given location. Nonetheless, the results clearly show that across the cyclic high and low values of annual variability that there has been an overall warming trend in southern Ontario between 1960 and 2005 for the months of March to September. One of the interesting aspects of the graphs in the Appendix A is that they shows the slope of change for all the months, with the exception of September was highest for changes to the minimum average daily temperature value. This suggests that areas that were generally cooler have warmed to a greater degree than areas that we generally already warmer. The graphs in Figure 5-11 illustrate this finding in gaps between the trend values from 1960 and 2005, showing the shifts that have occurred in the averages monthly temperatures. The results showing the highest increases in minimum daily temperature are consistent with findings by Vincent and Mekis (2006) and Zhang, Vincent, Hogg and Niitsoo

(2000) who found that in southern Canada that the greatest upward temperature trends are associated with increases in night-time temperature.

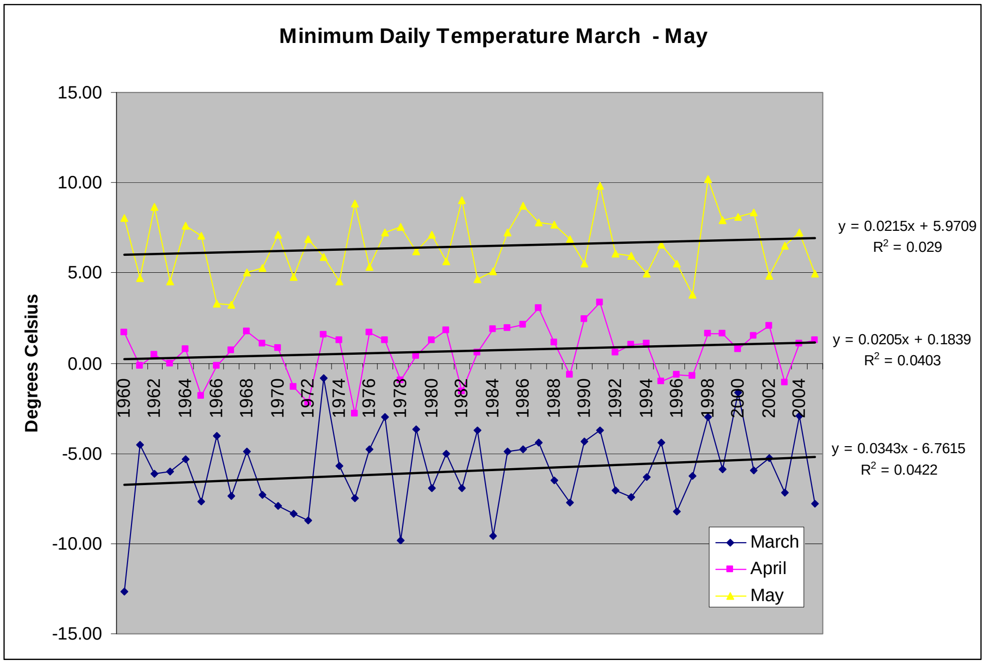

Figure 5-7: Graph of average daily minimum temperature 1960 – 2005 March to May

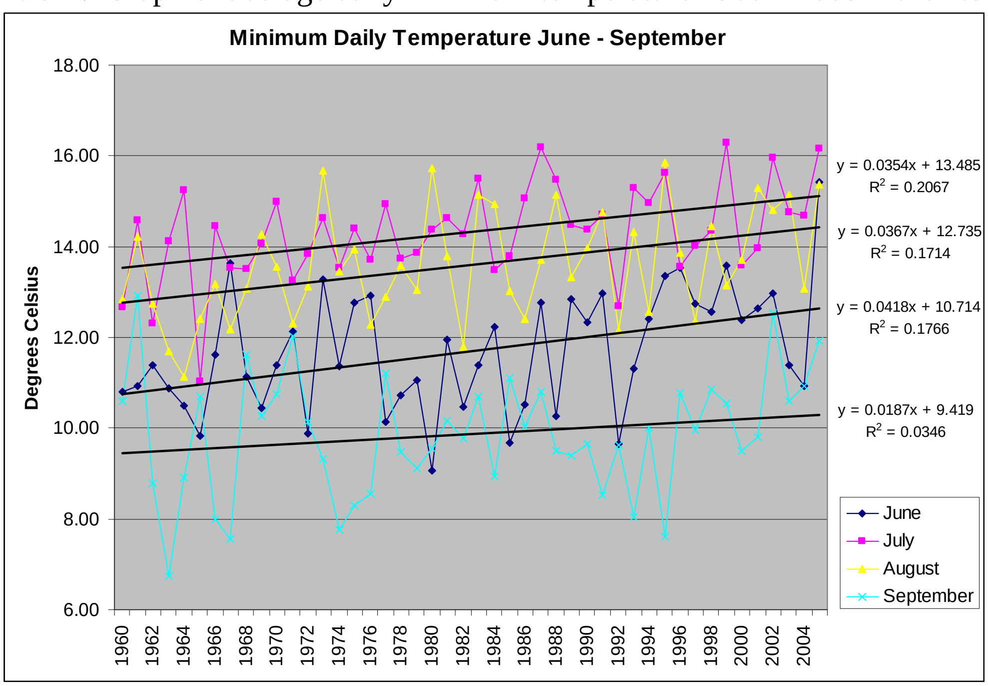

Figure 5-8: Graph of average daily minimum temperature 1960 – 2005 June to September

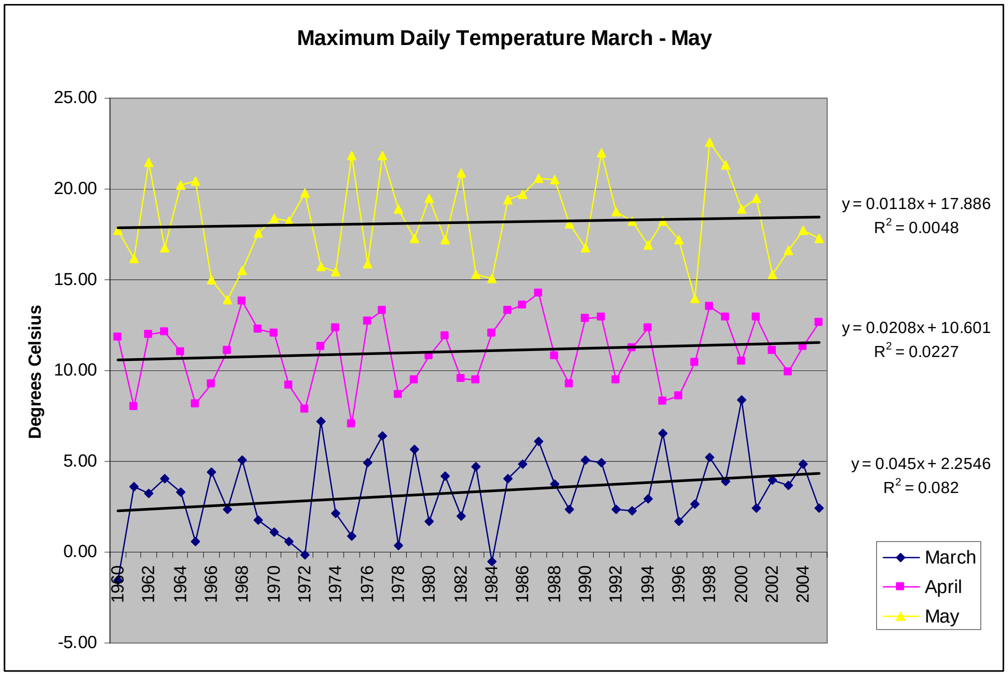

Figure 5-9: Graph of average daily maximum temperature 1960 – 2005 March to May

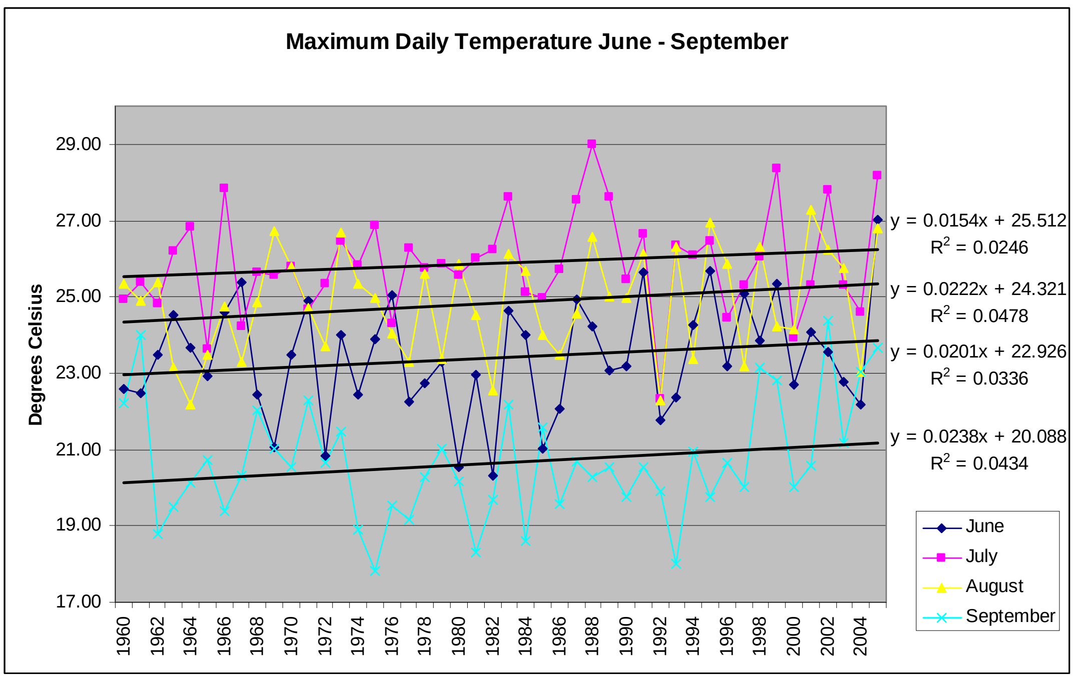

Figure 5-10: Graph of average daily maximum temperature 1960 – 2005 June to September

	Maximum			Average			Minimum		
Month	**1960**	**2005**	**Change**	**1960**	**2005**	**Change**	**1960**	**2005**	**Change**
March	-1.9	-0.7	1.2	-6.7	-5.1	1.6	-12.2	-11.1	1.1
April	3.8	5.1	1.3	0.2	1.1	0.9	-3.5	-2.8	0.7
May	10.1	10.6	0.5	6.0	7.0	1.0	2.5	3.5	1.0
June	15.7	16.6	0.9	10.8	12.7	1.9	6.6	8.8	2.2
July	18.7	19.1	0.4	13.5	15.1	1.6	9.6	11.2	1.6
August	18.1	18.7	0.6	12.8	14.5	1.7	8.8	10.6	1.8
September	14.6	14.9	0.3	9.4	10.3	0.9	4.9	6.2	1.3
Change			**0.7**			**1.4**			**1.4**

Table 5-1: Change in the monthly normals for daily minimum temperature

	Maximum			Average			Minimum		
Month	**1960**	**2005**	**Change**	**1960**	**2005**	**Change**	**1960**	**2005**	**Change**
March	5.8	8.1	2.3	2.3	4.4	2.1	-0.8	1.4	2.2
April	13.4	15.1	1.7	10.6	11.6	1.0	6.9	8.4	1.5
May	20.7	21.4	0.7	19.9	20.4	0.5	13.2	15.2	2.0
June	25.6	26.7	1.1	22.9	23.8	0.9	18.4	20.7	2.3
July	28.6	29.3	0.7	25.5	26.2	0.7	22.0	22.7	0.7
August	27.3	28.0	0.7	24.3	25.3	1.0	21.2	22.5	1.3
September	23.1	24.1	1.0	20.1	21.2	1.1	17.3	17.9	0.6
Change			**1.2**			**1.0**			**1.5**

Table 5-2: Change in the monthly normals for daily maximum temperature

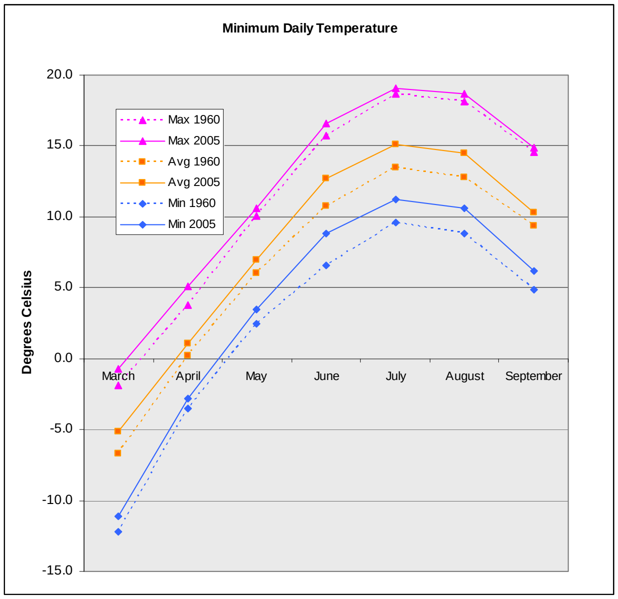

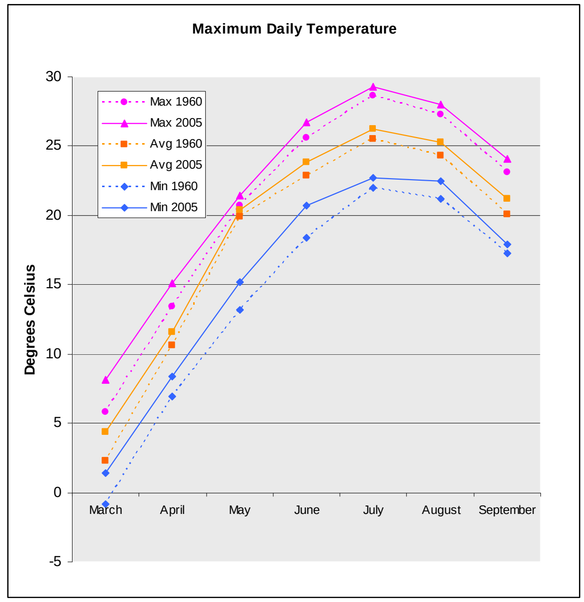

Figure 5-11: Graphs showing upward trend in daily minimum and maximum temperature between 1960 and 2005

5.2.2 Monthly Precipitation Trends 1960 to 2005

The results of the 46 year average monthly precipitation totals show a higher degree of annual variability than temperature and lower R-squared values. Graphs showing monthly precipitation totals from 1960 to 2005 are listed in Appendix B. The monthly totals were calculated by averaging the total monthly accumulation, summed from daily surfaces, for the entire study area for each year. The monthly trends vary with most months indicating slight upward trends or little change with few instances of downward change for the minimum, maximum and average precipitation values. It should be noted here that use of linear trends in climate data can lead to misperceptions and misleading conclusions since the trend line can be disproportionally influenced by outliers or extremes (Vincent and Mekis 2000). These results are a regional representation of the study area since they are an average of the monthly accumulation values of the surfaces interpolated from stations using the spline method. Extremes at individual stations are smoothed by the averaging of the results from the entire study area. These are exploratory statistics and do not represent any one location.

The trend values based on the end points of the best-fit linear trend from annual values for each month are listed in Table 5-3. For March the 24.7 percent increase in minimum average precipitation suggests that normally drier areas have been receiving more rain. March also shows a 7.6 percent increase in maximum and 7.1 percent increase in average values. April has had a 12 percent increase in average rainfall. May shows a considerable increase of 38.2 percent for average rainfall and 53.3 percent increase in minimum values. These results suggest a marked trend of substantially more rainfall during the month of May. June also showed an upward trend in average and minimum values. July had a 20.9 percent increase in the maximum rainfall values and a 9.5 percent average increase, possibly from more frequent and intense summer storms. The minimum values for July did not change suggesting that areas that are generally dry in July have remained dry. In August there is a clear drying trend with decreases in maximum and average values, with a slight increase in minimum values. September resumes a wetter trend with a 17.8 percent increase for maximum, 40.5 percent average and 82.0 percent for minimum values.

	Maximum				Average				Minimum			
Month	**1960**	**2005**	**Chg**	**%**	**1960**	**2005**	**Chg**	**%**	**1960**	**2005**	**Chg**	**%**
March	129.32	139.2	9.9	7.6	66.6	71.3	4.7	7.1	22.7	28.3	5.6	24.7
April	143.8	144.2	0.4	0.3	72.2	80.9	8.7	12.0	29.5	31.4	1.9	6.4
May	147.5	156.5	9.0	6.1	69.2	95.6	26.4	38.2	27.0	41.4	14.4	53.3
June	186.3	182.3	-4.0	-2.1	80.8	87.4	6.6	8.2	26.7	31.9	5.2	19.4
July	184.6	223.1	38.5	20.9	77.1	86.6	9.5	12.3	20.0	20.1	0.1	0.5
August	220.7	187.6	-33.1	-15.0	93.6	83.9	-9.7	-10.4	23.6	25.7	2.1	8.9
September	166.7	196.3	29.6	17.8	74.9	105.2	30.3	40.5	23.3	42.4	19.1	82.0
Change			**7.2**				**10.9**				**6.9**	

Table 5-3: Change in monthly precipitation averages between 1960 and 2005

With the exception of August, the trend in monthly precipitation shows an overall increase in rainfall across the months examined. Figure 5-12 plots the monthly trends over the period of data. The most notable months are May with a large increase in the average rainfall, July with an increase in the average and maximum values and September, which showed an increase in rainfall for the minimum, average and maximum values.

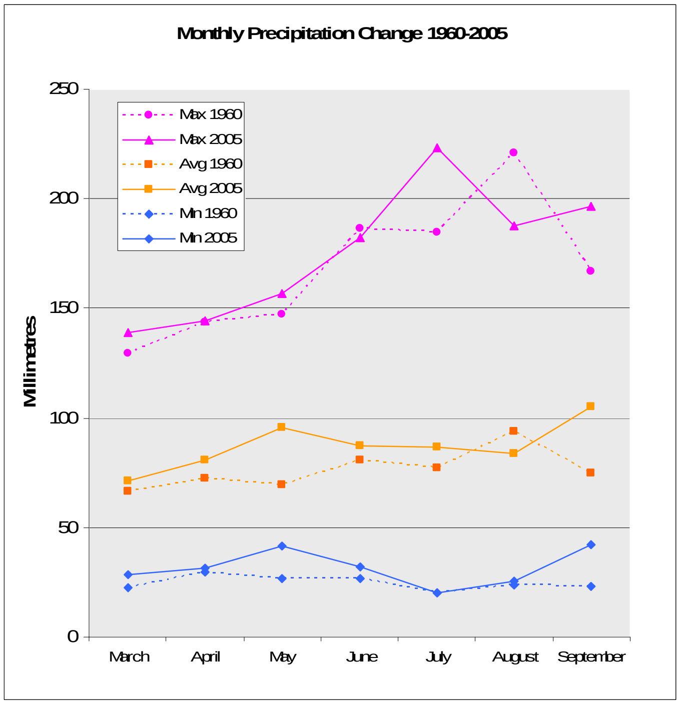

Figure 5-12: Graph of overall changes in monthly precipitation

5.2.3 Average Annual Precipitation

The results from the previous section represent statistics for the entire study area and do not necessarily represent the climate or a change in climate at any specific location. However, with the continuous surfaces it is possible to represent a spatial normal of precipitation for the period of data. The average annual rainfall for the months of March to September is shown on the map in Figure 5-13. The values are smoothed across 46 years of data, however the map does show local patterns of rainfall. The area west of the Niagara Escarpment is generally wetter than the area east of the escarpment. The one notable exception to this is a small area about 75 Km northeast of Toronto. Perhaps this may be an indication of urban heat island effect from Toronto, effect of terrain, lake breeze or a combination of all these. It would require further research into the type of storms events that occurred there, as well as an examination of the MSC climate data and other factors.

The gradient to wetter normal values in the far northeastern extent of the study area has the appearance of possibly being an artifact of the spline interpretation and edge effect due to sparse climate stations in that area. This requires further research to be conclusive.

The gradient to wetter areas inland from Lake Huron and Lake Erie in the southwest region of the study area represents reality since a consistent set of MSC stations persisted throughout the period of data. It also shows a southwest to northeast trend toward wetter averages, with a ridge of higher values extending eastward to the escarpment in the Cambridge area. The Lake Erie shoreline also shows clusters of wetter areas.

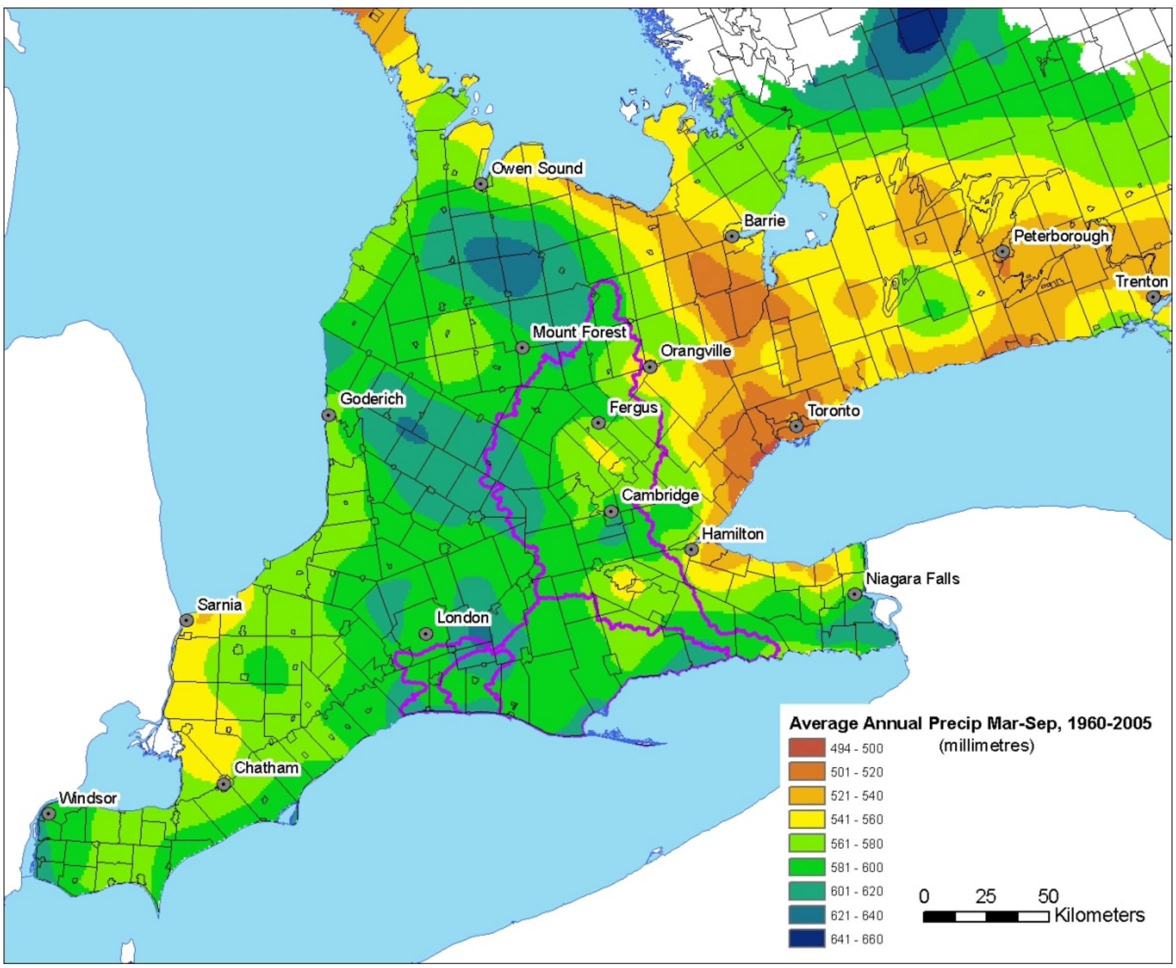

Figure 5-13: Map of average annual precipitation between March and September for the years 1960 to 2005.

5.2.4 Patterns of Changing Rainfall Averages

The monthly average for rainfall was calculated for the precipitation surfaces for two intervals of time during the 46 year data record to determine whether spatial patterns of average rainfall had changed. For each raster cell an average value for rainfall was calculated for each month from 1960 to 1982 and from 1983 to 2005, with the earlier average subtracted from the later to calculate the difference. Positive values indicated an increase in average precipitation in the most recent 23 years and negative values a decrease. Figure 5-14 shows the overall change in the average precipitation for the months of March to September. The map shows that most areas across the study area experienced an increase in average rainfall for the seven month duration. Refer to Appendix C for figures showing the change in average precipitation for each month.

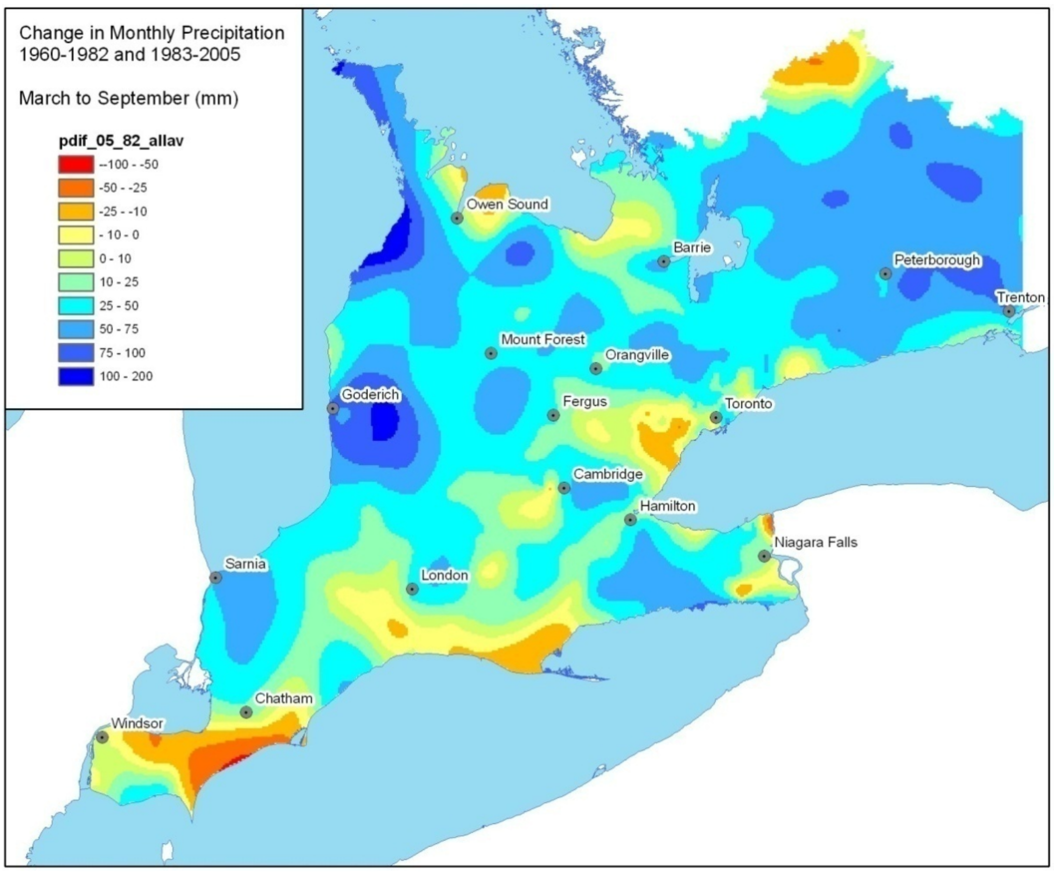

Figure 5-14: Change in average precipitation between 1960-1982 and 1983-2005

The maps in Appendix C provide a spatial context to the statistics of the monthly precipitation trends. The maps with notable changes in monthly precipitation averages are May, July, August and September. The map for May shows an increase in average precipitation across the entire study area in the later period. The map for July shows a concentration of higher rainfall occurring in central southwestern Ontario. August on the other hand shows a significant drying trend on average, with September showing increased rainfall in the more northern extent of the study area.

5.2.5 Spatial Patterns of Severe Rainfall Events

The number of occurrences of daily precipitation values meeting or exceeding the thresholds of 12.5, 25, 50 and 75 millimetres was totaled across the raster surfaces for each month for the entire 46 year period and for two 23 year periods from 1960-1982 and 1983-2005. The maps shown in this section illustrate the total occurrences for threshold occurrences of 25, 50 and 75 mm for the months of March to September. Appendix D shows the maps per month and the change for the 25 mm daily occurrences and Appendix E shows the monthly maps and the change for the 50 mm occurrences.

The maps on the following Figures 5-15 and 5-16 show the total number of occurrences of each daily threshold value for all the months between March and September for the entire 46 year period. The accompany map on the right shows the change in occurrences between the first and second 23 year periods. The total occurrences from the earlier were subtracted from the later period to generate the difference map, blue indicating an increase, brown a decrease in daily occurrences of the threshold values.

The maps in Figure 5-16 show a concentration of occurrences of 50 mm of daily rainfall inland from Lake Erie and Lake Huron, as well as, in the Chatham area. A similar pattern higher frequency locations on Figure 5-16 are continued on Figure 5-17 showing the map of 75 mm rainfall events.

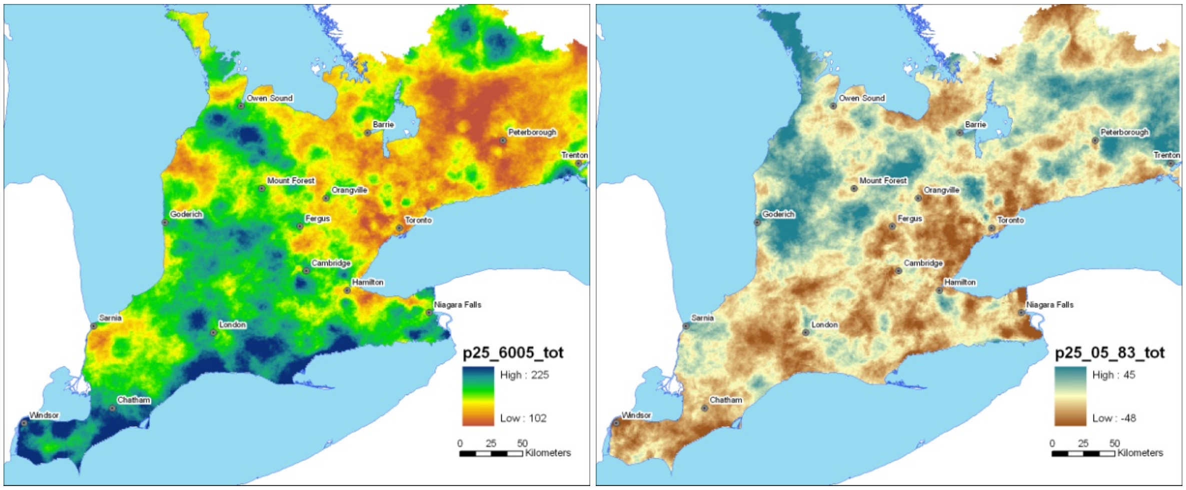

Figure 5-15: Total occurrences of 25 mm or more of daily precipitation from 1960-2005 and the change in the number of occurrences between 1960-1982 and 1983-2005. Blue means more occurrences and brown fewer in the most recent 23 year period.

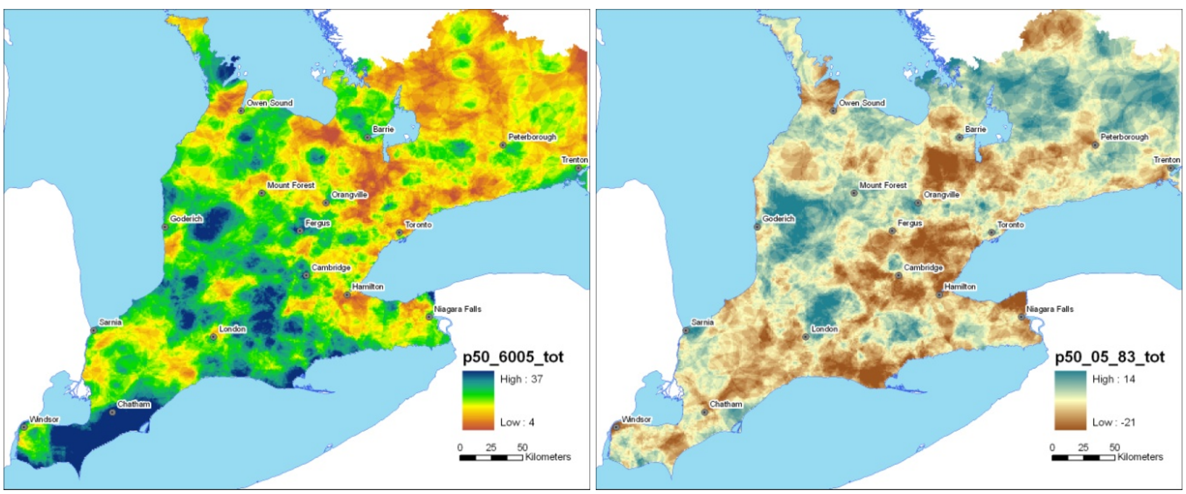

Figure 5-16: Total occurrences of 50 mm or more of daily precipitation from 1960-2005 and the change in the number of occurrences between 1960-1982 and 1983-2005.

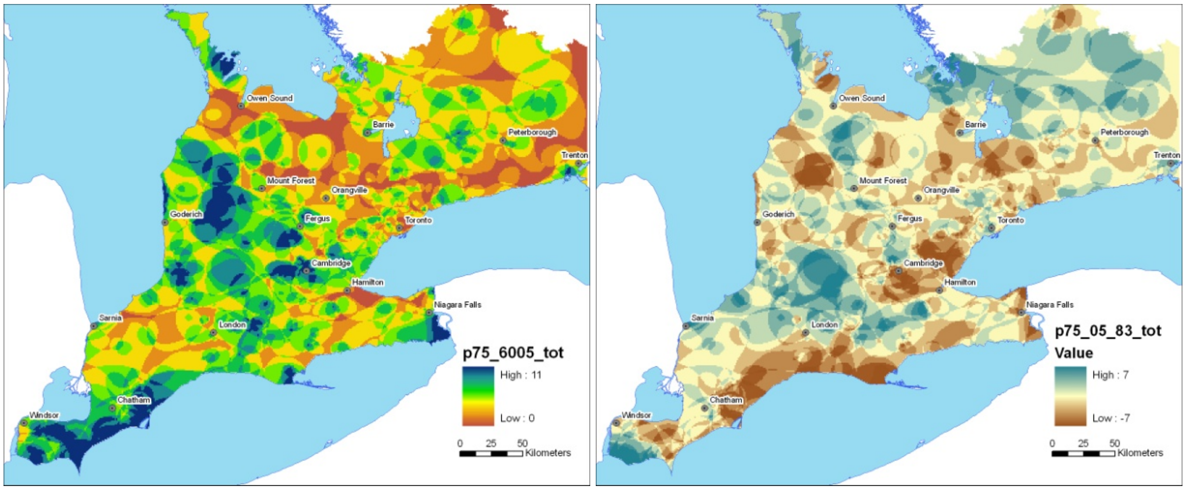

Figure 5-17: Total occurrences of 75 mm or more of daily precipitation from 1960-2005 and the change in the number of occurrences between 1960-1982 and 1983-2005. These events primarily occurred between June and September and no monthly maps are in the appendices.

The results of the daily threshold analysis indicate a heterogeneity in the patterns of heavy daily rainfall, highlighting areas that have more frequently experienced severe rainfall events. The change analysis also indicates shifting storm patterns whereas an increasing frequency of heavier rainfall events in the later period between 1983-2005 shows a concentration of severe rainfall in the central region of southwestern Ontario, inland from Lake Huron in the Goderich area and in the region east and northeast of Toronto.

There is a decreased consistency in the spatial pattern of storms in March and April for the 1983-2005 versus 1960-1982, indicating a shift to more organized storm patterns with similarity to the May pattern. Both March and April show a northerly shift of storm occurrences and decreases in occurrences in the southern extent of the study area. However, the change in storm pattern in May is different from the previous months.

Of the monthly maps show in Appendices D and E, some of the notable results are as follows:

- Both March and April show a shift of 25 mm daily rainfall northward in the later 23 year period.
- A northward shift of 25 mm daily rainfall is also evident in June and August
- May shows a pattern of concentrated local areas with higher rainfall frequency, as well as, local shifts in those locations
- July shows a concentrated area of more frequent storms in the area bounded by Fergus, Hamilton, Lake Erie and London. Chatham and the Lake Erie shoreline to the southwest also show a high frequency of severe rainfall.
- In August the area of severe rainfall appears to shift northward and eastward, with a trend toward a higher frequency in the Peterborough area and less in the southwest.
- In September the severe rainfall seems to contract toward the southwest, with concentrated areas in central southwest, and along the shores of Lake Erie and Lake Huron. However, there is a trend to increased frequency in the east portion of the study area also.

5.2.6 Number of Rainfall Days

During the generation of the daily rainfall threshold masks, the date that different rainfall accumulation thresholds were exceeded was tracked and statistics were generated for the number of days that a threshold event occurred. This provided the ability to examine the total number of daily occurrences of rainfall accumulations per month and year for the period of data.

The graph in Figure 5-18 shows the total number of days each year between March and September that rainfall accumulation events of 12.5, 25, 50 and 75 mm were recorded at any location in the study area. A 2nd order polynomial line (dashed) was used to attempt to model trend in the data. For accumulations of 12.5 and 25 mm there does appear to be a trend that shows a peak in daily events from the mid-1970's to the early 1990's. Given the low R-squared values there does not appear to be any significant change in the occurrences of 50 and 75 mm events.

Appendix F presents graphs of rain-day totals that provide a breakdown for the months of March to May and from June to September. The peak around 1980 and the recent downward trend is present in each threshold value, with the strongest trend in 12 and 25 mm events. There is no apparent change over time in the 75 mm events. The results for the individual month of May does show a weak upward trend in daily 12.5 mm events, whereas July shows weak downward trend in all thresholds. These results exhibit a high degree of variability. It also notable that the trend showing a peak in the numbers of threshold events around 1980 also correlates to the same period when the number of MSC climate stations also peaked in numbers across the study area. It seems plausible that the results could be affected by the reducing number of stations of the period from the peak. This is more likely the case for smaller convective storms; however the highest accumulations of 50 and 75 mm do not show any significant change. Given that, the data is likely indicative of real changes in the 12.5-25 mm range of daily rainfall.

The results showing a minor downward trend in the number of rain-days in the later 23 years of the data counters the apparent upward trend in monthly average precipitation demonstrated in earlier sections. One could conclude that the two trends suggest that there have generally been fewer storm events occurring, but when they do occur, the storms are delivering increasingly more rainfall per event. This finding would be consistent with the climate change predictions discussed in Chapter 2.

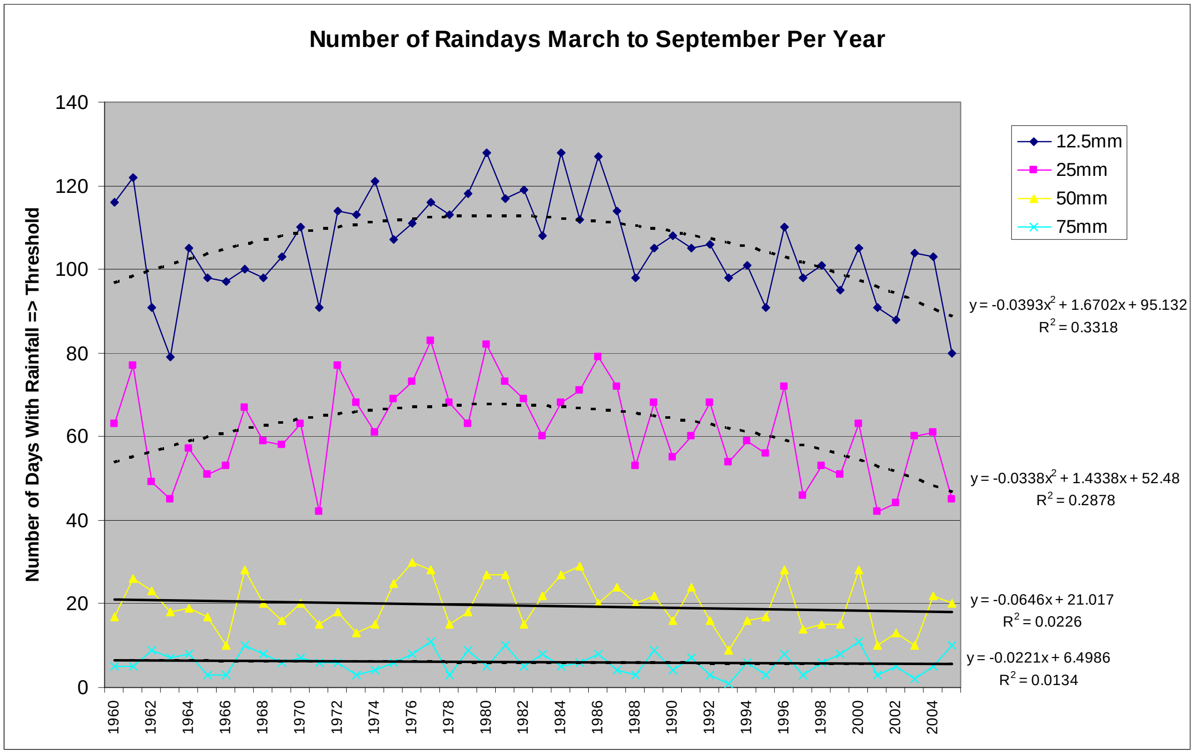

Figure 5-18: Number of days per year between March and September that rainfall threshold values occurred.

5.3 NEXRAD Radar Analysis

The results presented in this section provide a comparison of severe rainfall patterns derived from daily rainfall totals calculated from radar data versus precipitation surfaces derived from the spline interpolation. An analysis using the Getis Statistic (z-Gi*) compares the spatial clusters of daily rainfall events of 50 and 75 mm of rainfall between 1996 and 2005. An overview of the number of rain-days is also examined from the radar results. An analysis of one hour maximum rainfall intensity on the radar data is compared against the IDF values from Environment Canada. Finally, a case study compares the radar and rain-gauge measurements for July 2008, a month when numerous severe storms occurred in southwestern Ontario.

5.3.1 Spatial Patterns of Severe Rainfall Events 1996 to 2005

The spatial patterns of severe rainfall events from the radar data when compared to the results derived from the same years of 1996-2005 of spline surfaces show similarity in the clustering patterns in the frequency of storm events. The area northeast of London and in the Chatham area both show higher occurrences for 50 mm and 75 mm daily accumulation, as shown on Figures 5-19 and 5-20. However, the spline results show the area east of Goderich as significant whereas is does not appear on the radar results. This could be due to the area being on the outer edge of both Buffalo and Detroit NEXRAD, or perhaps an artifact in the spline interpolation. The reason for discrepancy is not certain.

In the area to the northeast of Toronto there is also similar patterns in the area southeast of Lake Simcoe and in the Peterborough area. The smoothing effect of the spline interpolation and a seemingly falsely extended coverage of heavy rainfall can be seen in the oval shape of the spline values. This effect highlights a weakness of the masking approach with the spline surfaces that could increase false positive clustering. If rainfall is artificially extended due to sparse number of stations, the repeated effect of this could create higher totals that may not be representative of real rainfall.

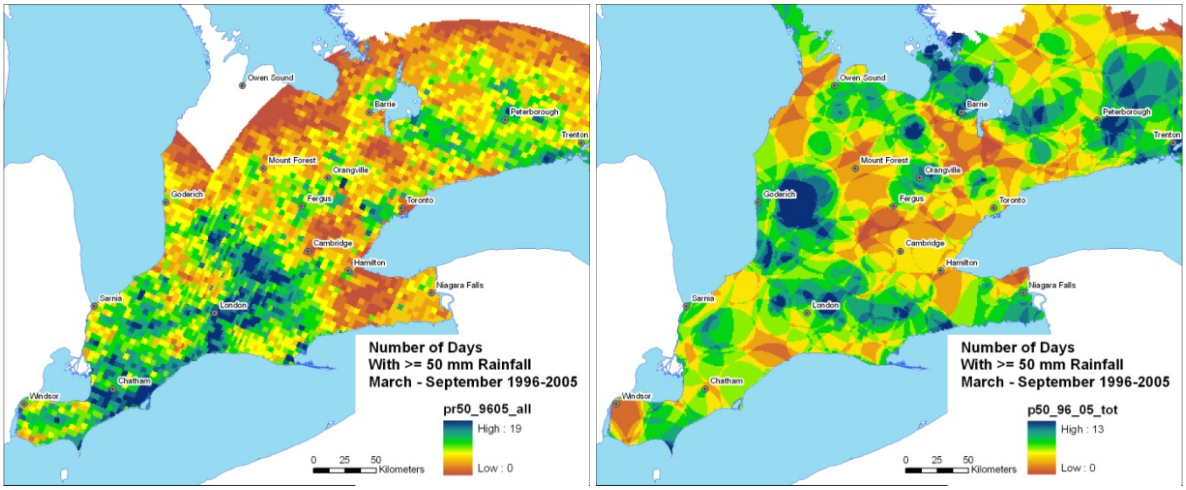

Figure 5-19: Maps of daily rainfall occurrences of 50mm or more from 1996-2005, radar on left and spline surfaces on right

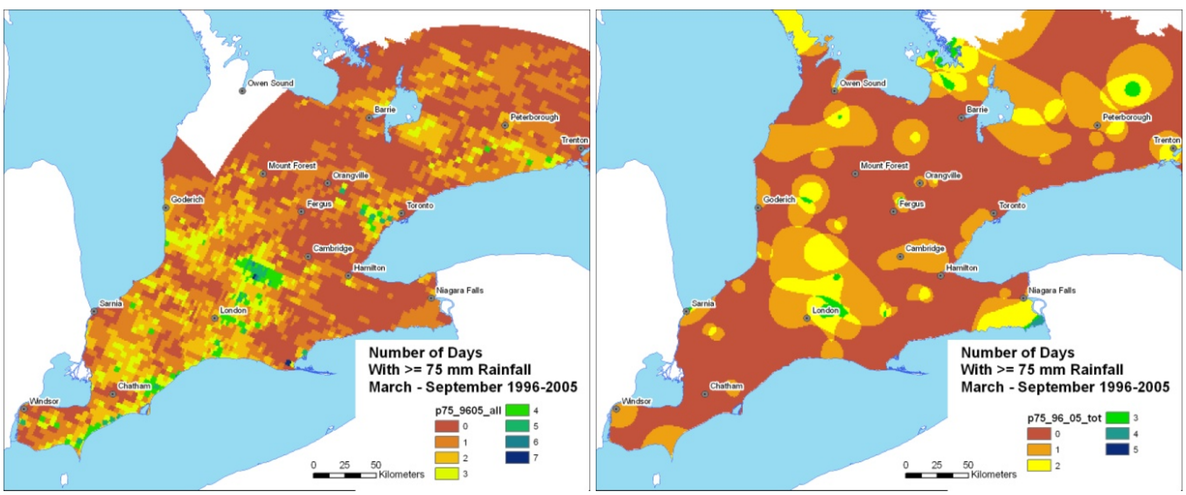

Figure 5-20: Maps of daily rainfall occurrences of 75mm or more from 1996-2005, radar on left and spline surfaces on right

5.3.1.1 Getis Clustering of the Severe Rainfall Patterns

A cluster analysis was run against the rainfall occurrences measured from radar and the spline MSC surfaces from 1996-2005. The Getis calculation is a statistical measurement of spatial autocorrelation. The resultant Z-score provides a measure of deviation from a normal random distribution whereby locations with either high or low Z-scores indicate the variable tends to be spatially clustered (Mitchell 2005). The algorithm works by looking at each feature within the context of neighboring features. A high Z-score value is only statistically significant if it is surrounded by other features with high values as well. The local sum for a feature and its neighbors is compared proportionally to the sum of all features; when the local sum is much different than the expected local sum, and that difference is too large to be the result of random chance, a statistically significant Z score results. The larger the Z score is, the more intense the clustering of high values. For statistically significant negative Z scores, the smaller the Z score is, the more intense the clustering of low values. For this analysis an inverse distance weight value of 10 Kilometres was used to define the extent of the neighbourhood to search within. The value of 10 Km was determined from an analysis of spatial lag in the data that showed that over 50% of the spatial autocorrelation could be accounted for in the first 10 Km of the data.

On the figures that follow in this section the Getis Statistic z-Gi*, where the conceptualization distance is less than or equal to 10 Km, is shown in shades of red and blue; where light to dark red shows areas of spatial autocorrelation of higher frequency of the rainfall events and light to dark blue areas with the lowest frequency occurrences.

Figure 5-21 shows the results for daily 50 mm events and some similarity and other differences between the radar and spline results. Notable are the discrepancy of the Chatham and Goderich areas, but some agreement in the area northeast of London and northeast of Toronto.

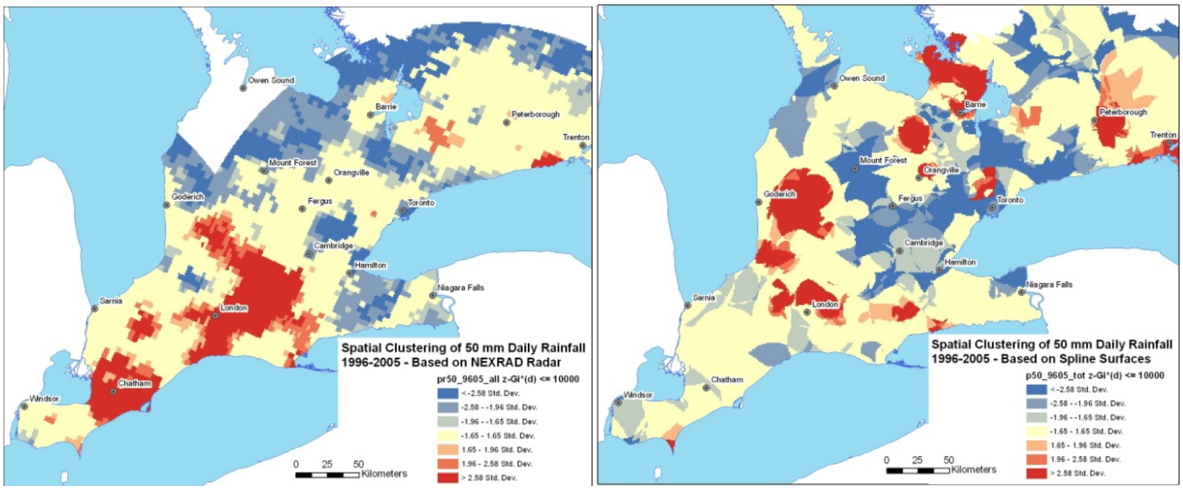

Figure 5-21: Spatial clustering of 50 mm rainfall 1996-2005 (radar left, spline right)

Figure 5-22 shows the Getis clustering for 50 mm events between 1983 and 2005 and a better agreement with the patterns shown on the radar data in Figure 5-21. Figure 5-23 shows the cluster results for daily 75 mm events and a good agreement between the results in the London area, yet a discrepancy in the area south of Niagara Falls in the Chatham area.

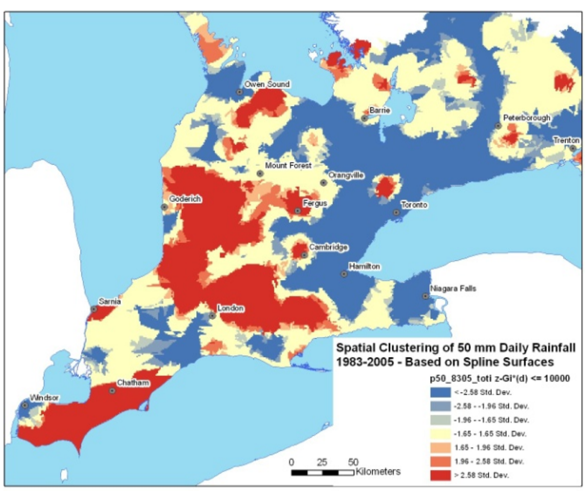

Figure 5-22: Spatial clustering of 50 mm rainfall 1983-2005 based on spline

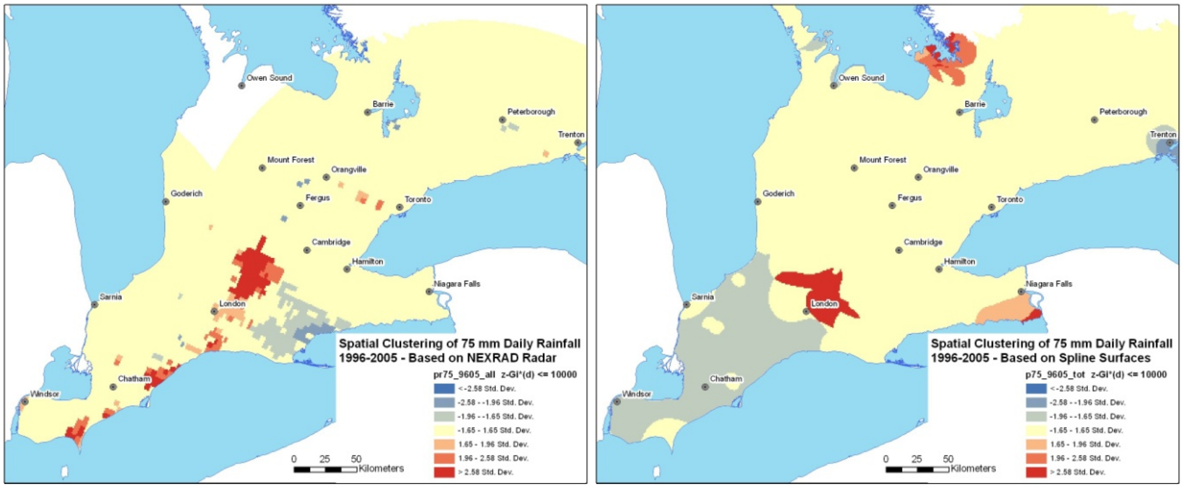

Figure 5-23: Spatial clustering of 75 mm rainfall 1996-2005 (radar left, spline right)

Figure 5-24 shows the cluster of 75 mm events between 1983-2005, expanding the extent of the cluster region northeast of London and better agreement with the radar in the Chatham area.

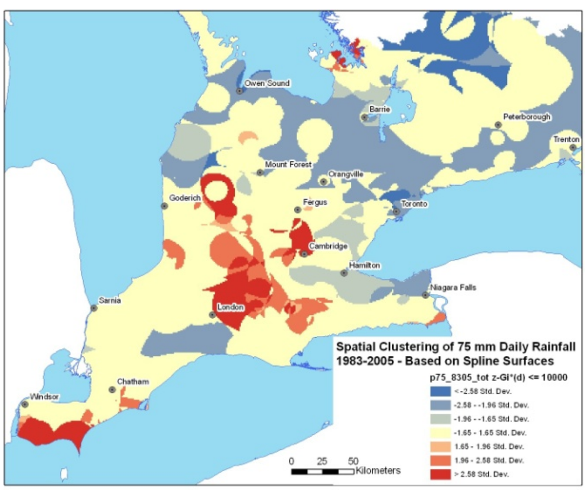

Figure 5-24: Spatial clustering of 75 mm rainfall 1983-2005 based on spline

5.3.2 Number of Rainfall Days

In a manner similar to the analysis of rain-days done on the spline surfaces, the number of occurrences of threshold values of daily rainfall where measured from the radar data. The results are plotted on Figure 5-25. The 13 year record of rainfall data from radar is likely too short to make any conclusive interpretations about trends. The seemingly upward trend in 12.5 to 50 mm occurrences is somewhat biased by the exceptionally stormy year of the 2008 season. If the 2008 values are removed, there is nearly no trend. However, the one interesting feature is the fairly strong correlation, albeit shallow slope, of the measurement of daily 75 mm events, showing an increase in these less frequent but very intense occurrences.

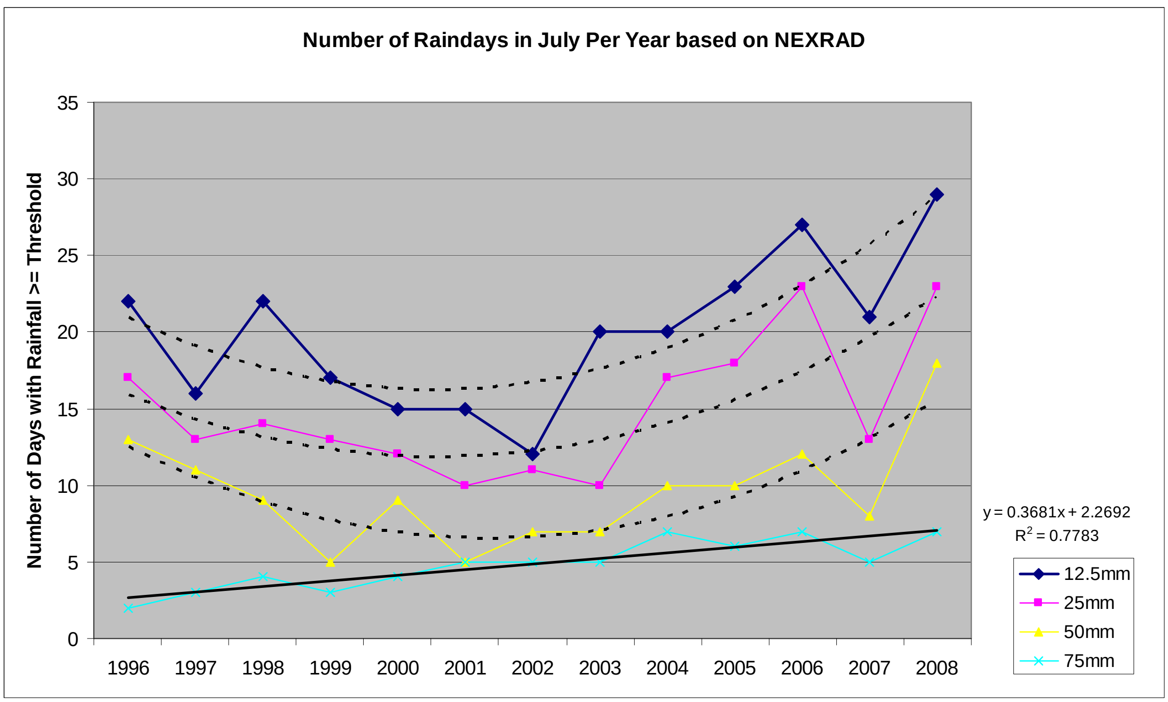

Figure 5-25: Number of rain-days for 12.5, 25, 50 and 75 mm events 1996-2008 based on NEXRAD

5.3.3 One Hour Rainfall Intensity Analysis

The DPA data from NEXRAD radar represents a moving one hour average of rainfall, updated every 6 minutes when rain is detected within range of the station. Every 6 minute raster surface between March and September for each year from 1996 to 2008 was analyzed for the maximum one hour rainfall intensity. For every raster cell across the study area for every month and for each year the maximum rainfall for that cell was recorded, along with the date and local time of day it was recorded. The following series of maps and graphs provide a visual summary of the results.

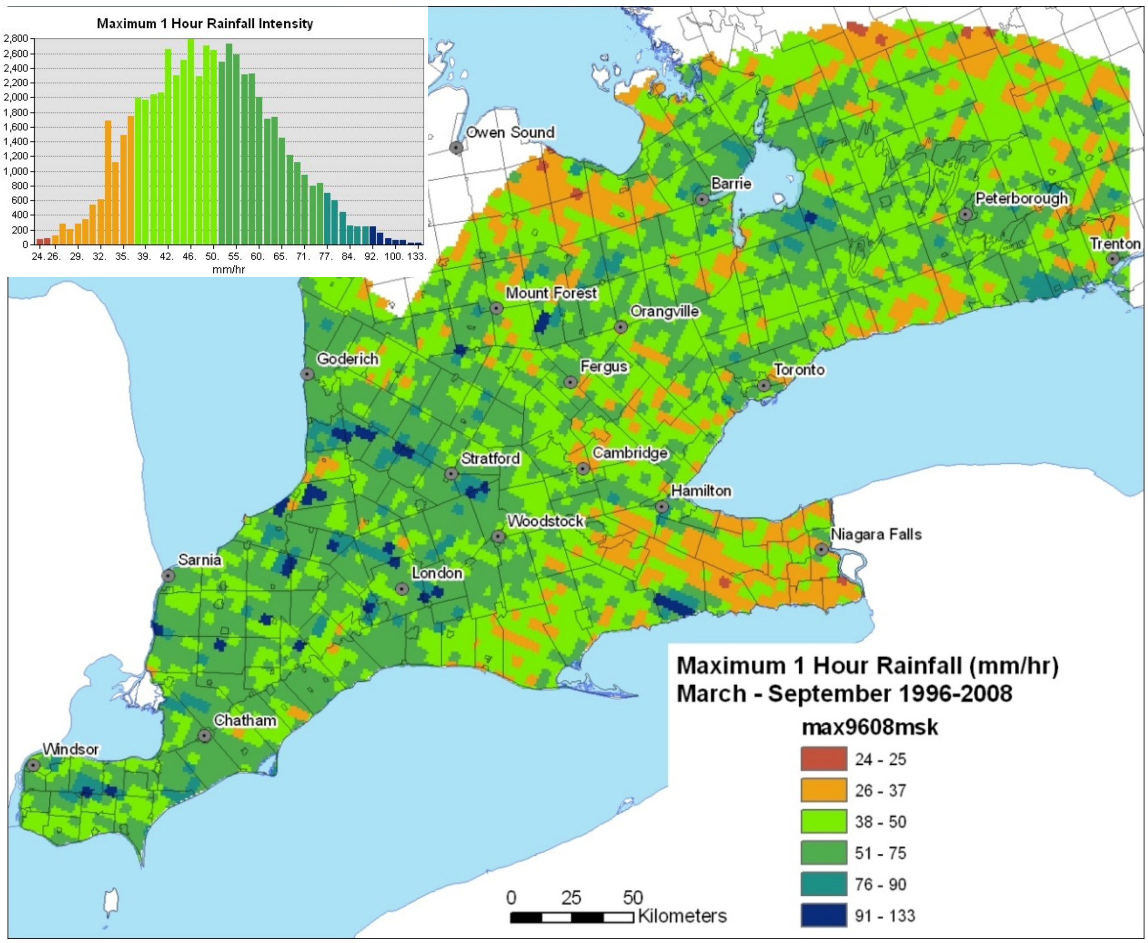

Figure 5-26: Maximum 1 hour rainfall intensity measured between March – September for the years 1996 to 2008, based on NEXRAD radar

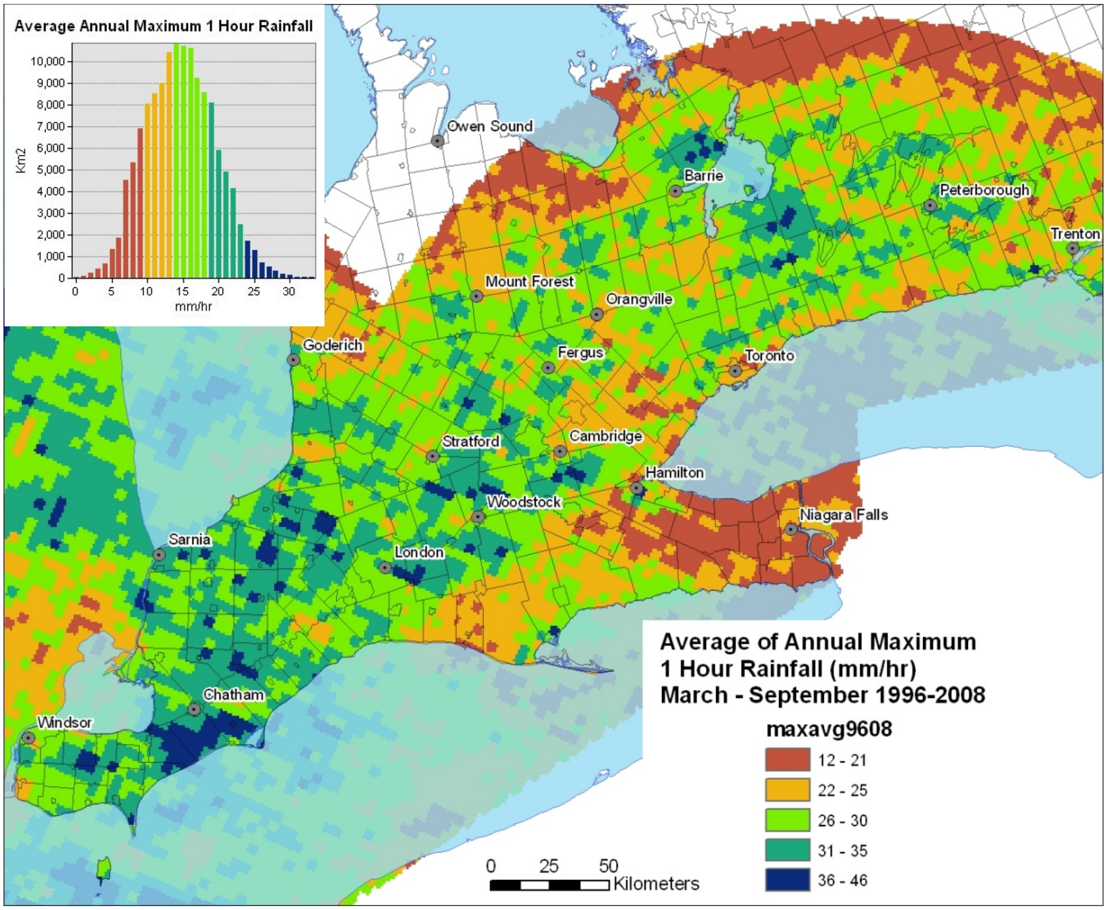

Figure 5-27: Average of annual maximum 1 hour rainfall intensity between March – September for the years 1996 to 2008, based on NEXRAD radar

Figure 5-26 shows the findings of the processing of all the 6 minute DPA data surfaces and represents the highest intensity 1 hour rainfall recorded for each cell over the 13 year period of data. The insert of the graph provides a distribution of the values across the study area. Figure 5-27 represents an average of the annual maximum detected for each of the 13 years. The higher average values suggest higher frequency of intense storms and show similar patterns found in the cluster analysis of the threshold occurrences.

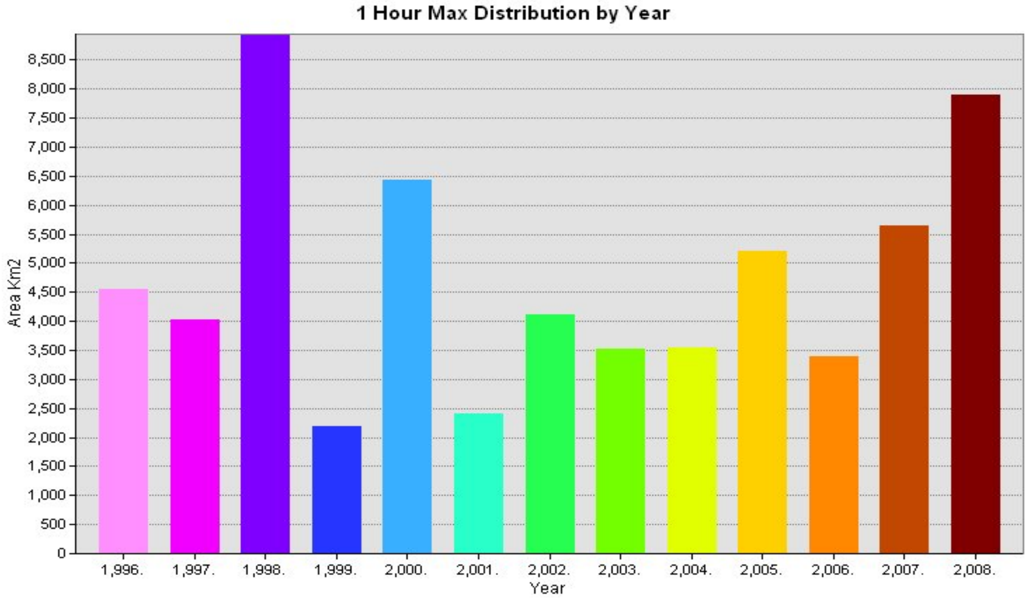

Figure 5-28: Distribution by area of the years contributing to the 1 hour maximum

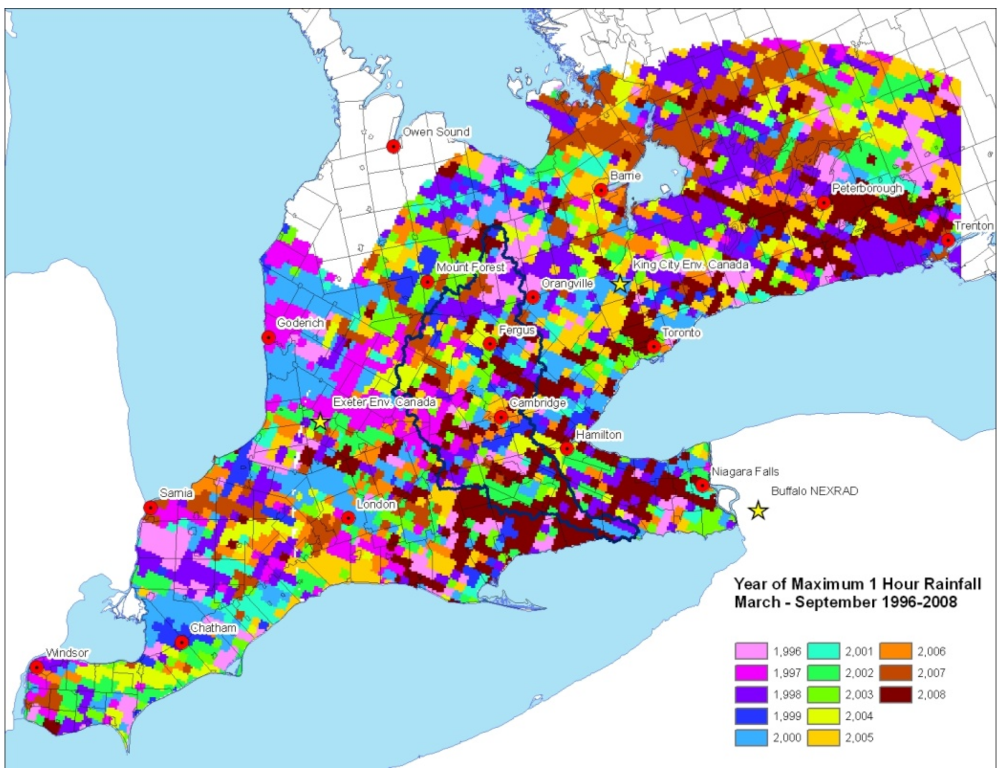

Figure 5-29: Distribution by study area of the years contributing to the 1 hour maximum

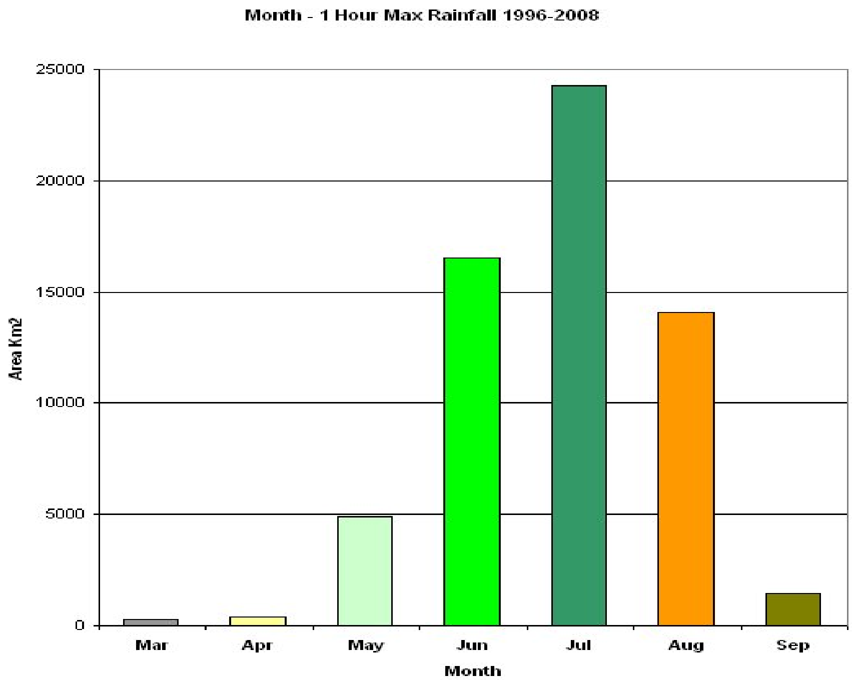

Figure 5-30: Distribution by area of the months contributing to the 1 hour maximum

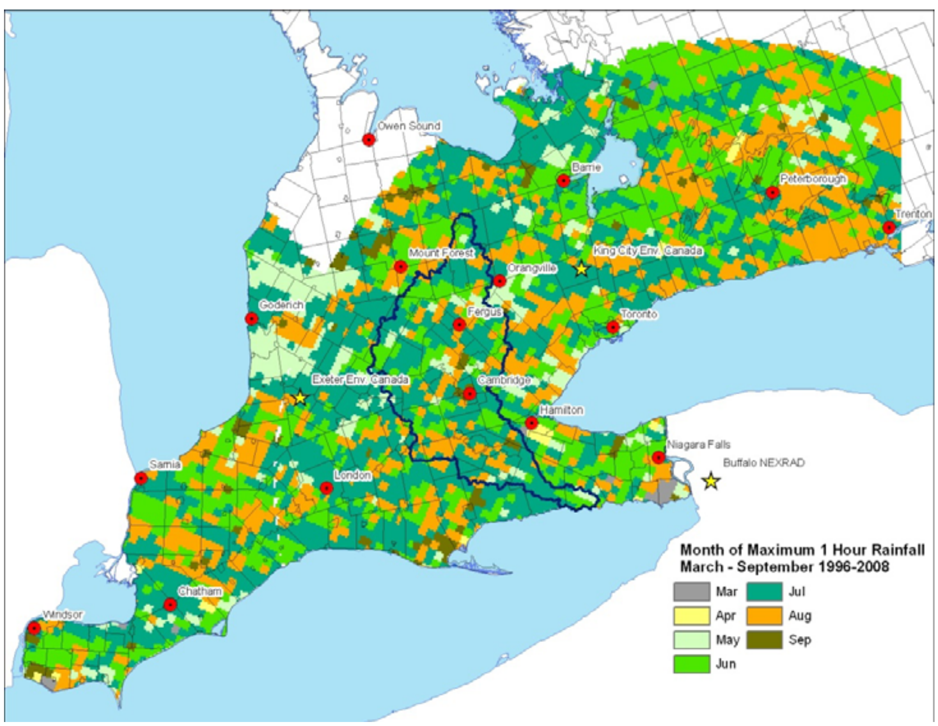

Figure 5-31: Distribution by study area of the months contributing to the 1 hour maximum

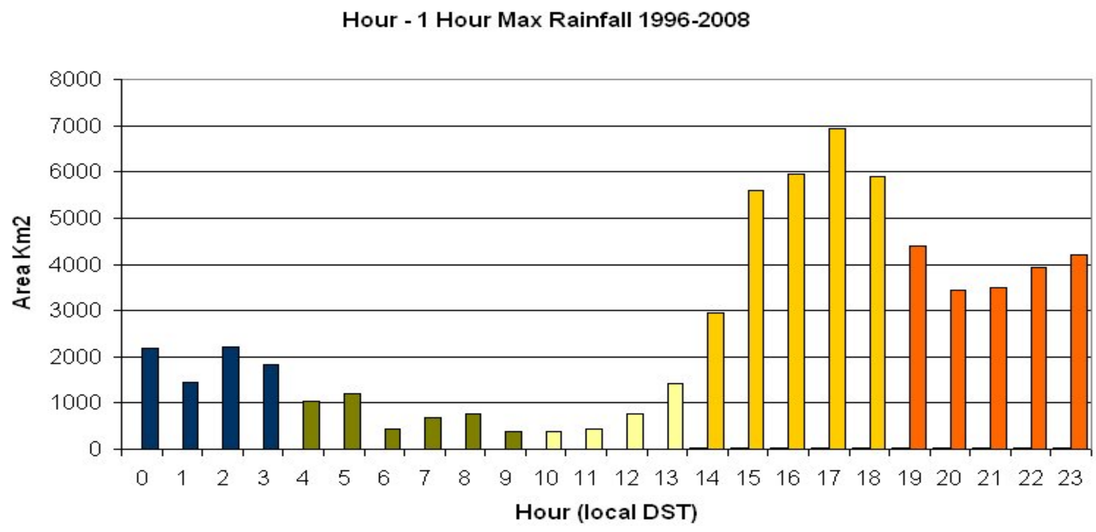

Figure 5-32: Distribution by area of the local time, rounded to the nearest hour, when the 1 hour maximum was detected

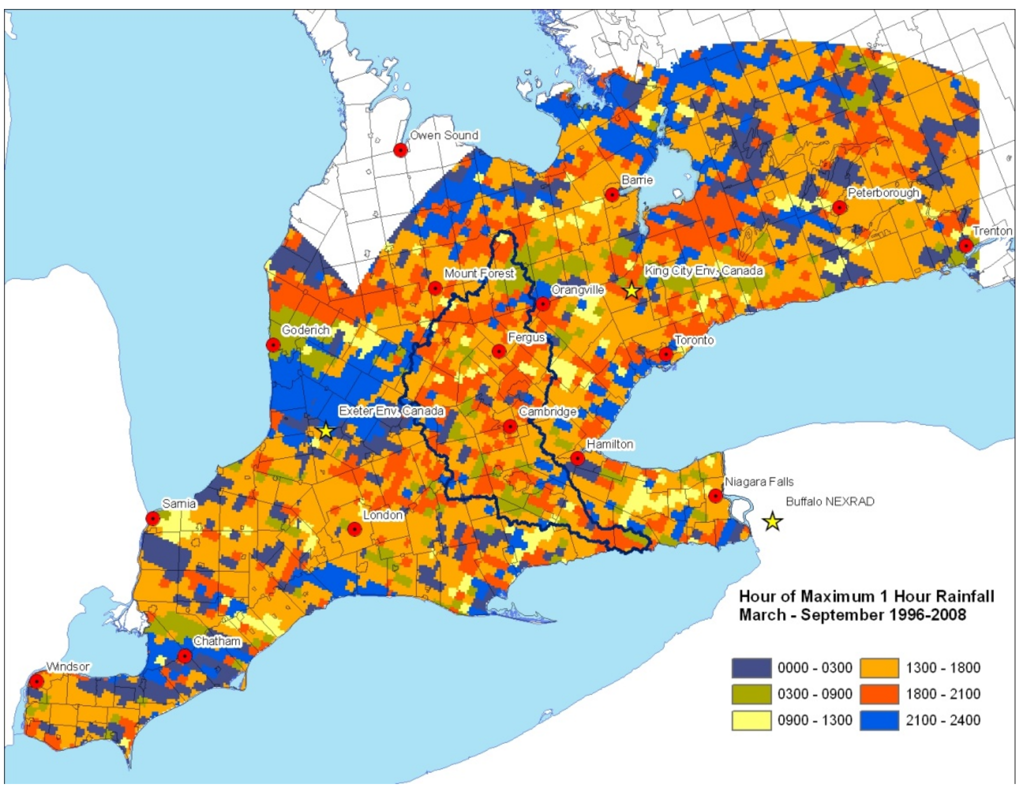

Figure 5-333: Distribution by study area of the local time, rounded to the nearest hour.

The maps in Figures 5-29, 5-31 and 5-33 show the year, month and time of day when the maximum 1 hour rainfall accumulation occurred. The distributions of the these values by area are presented in Figure 5-28 for the year, Figure 5-30 for the month and Figure 5-32 for the time of day. The graph of the maximum 1 hour rainfall by year provides some interesting characterization of the storm seasons of last 13 years. During 1998, the year with the most area of intense storms, a strong El Niño was setup in the Pacific ocean. Known to have a far reaching impact it would appear it did enhance the impact of storms in southern Ontario. The 2008 summer storm season was also significant; a map is shown in Appendix I. Whereas 1999 and 2001, known as dry years (Boyd 2008), were also reflected on the graph.

The monthly summary of the results clearly show the connection between solar input during the summer months and the impact on convection storms, with July clearly the peak month for the most intense rainfall, and the shoulder months of March – May and September with the least frequent intense 1 hour rainfall events. The hourly distribution correlates well with the expected behavior of convection driven storm events with storm occurrences peaking in the mid-afternoon to early evening. The sustained sill of values between 20:00 to midnight and into the early hours is likely the result of meso-scale self-perpetuating convective storm systems that are likely related to squall line formations.

5.3.4 Comparison of Radar to 1 Hour IDF Values from Environment Canada

The results up to this point have examined spline and radar results to characterize storm patterns and trends in rainfall. This section presents a comparison of the 1 hour maximum rainfall from the radar data to the 1 hour Intensity Duration Frequency (IDF) values as calculated by Environment Canada. The objective of the analysis was to determine if there are areas within the study area where the rainfall measured from radar between 1996 and 2008 has exceeded the official IDF values, and by what amount.

The IDF data for 1 hour rainfall was available for 42 MSC climate stations that sparsely spread out across the study area. An Inverse Distance Weighted (IDW) interpolation was used to create surfaces representing the 1 hour rainfall value for each of the frequency return intervals of 10, 25, 50 and 100 years. The maps on Figures 5-34 and 5-35 present a comparison of the 1 hour maximum to the IDF rainfall values for the 10 year and 100 year intervals. Maps of the 25 and 50 year intervals, as well as, a table of the IDF values and radar values are available in Appendix J. The areas in blue indicate where the radar surface exceeds the IDF value and brown is where it is less.

Figure 5-36 plots the 1 hour maximum rainfall from the radar against the 10 and 100 year IDF interval values, as well as, the average maximum from the 13 years of radar data against the average maximum from the IDF data. The maximums of two dataset are weakly correlated, with a better correlation between the averages. This suggests a discrepancy between the characterization of storm events in IDF curves versus actual events detected by radar, notwithstanding errors in the radar values.

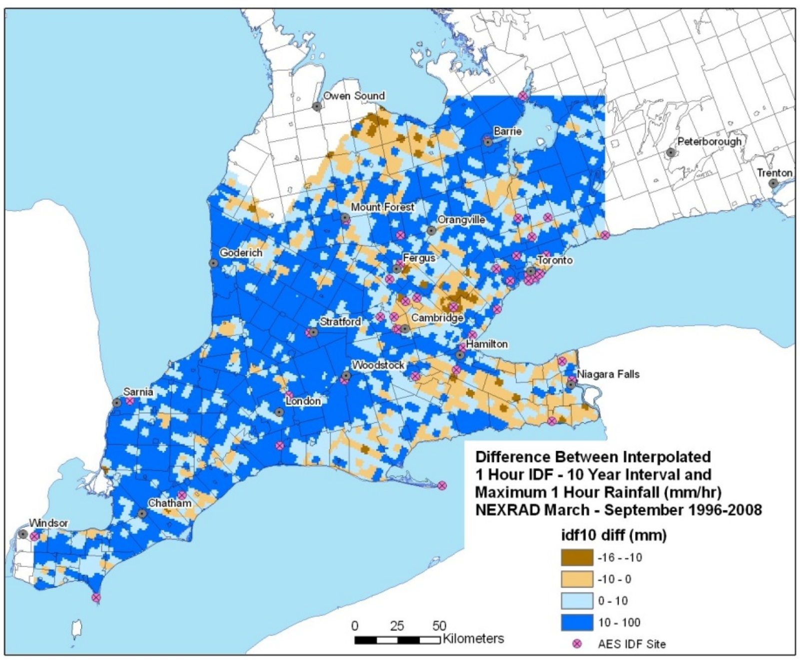

Figure 5-344: Difference between radar 1 hour maximum and IDF 10 year value

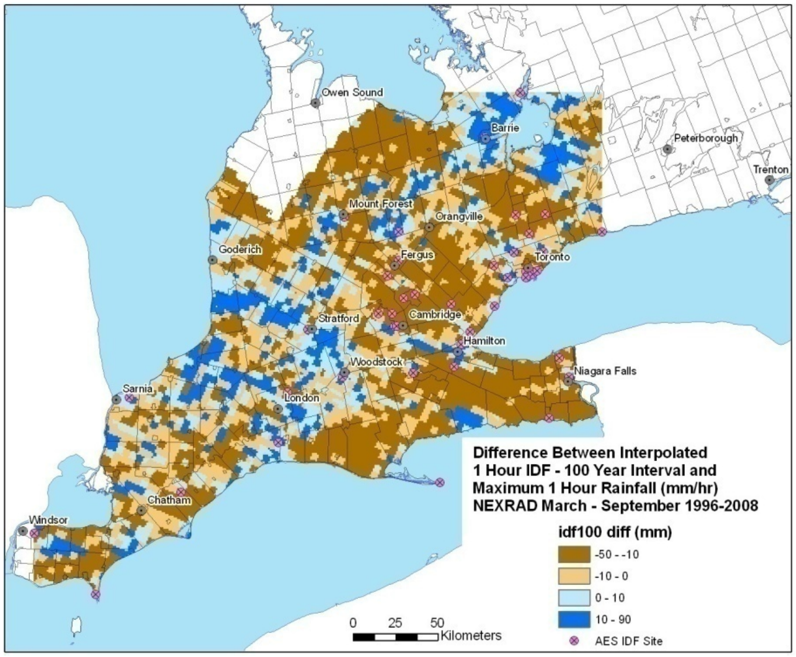

Figure 5-355: Difference between radar 1 hour maximum and IDF 100 year value

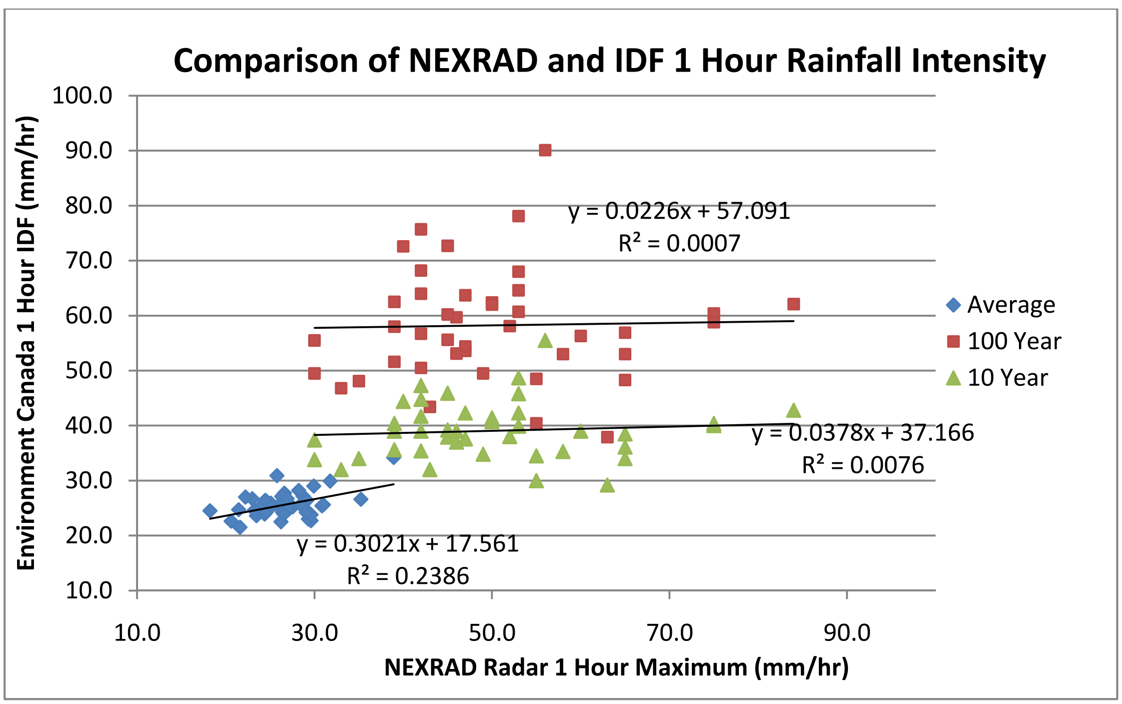

Figure 5-366: Graph of 1 hour maximum between radar and 10, 100 and average IDF

On the map in Figure 5-34 showing the difference in the 10 year interval it is not surprising that most areas exceeded the 10 year return value. It should be noted that the IDF values at the Milton station are considerably higher than the rest of the IDF stations, which have skewed the values in the vicinity of that station. The dark blue areas on the 100 year map in Figure 5-35 shows areas where the radar has detected storms that have exceeded the local and interpolated IDF value. There is little overall agreement between the radar results and the IDF values. The plot of the two date sets in Figure 5-33 shows mixed results between the radar above and below the 10 year and 100 IDF values. However, if the radar is accurate these results indicate that there have been storm events between 1996 and 2008 that have exceeded the 100 year return interval value for 1 hour IDF.

5.3.5 Comparison of NEXRAD and Rain Gauge – Case Study of July 2008

The potential value of radar data for rainfall analysis is dependent on the accuracy of the rainfall estimate and its spatial extent. As mentioned in Chapter 3 qualitative rainfall estimation (QPE) using radar can be affected by a number of factors. While the Precipitation Processing System (PPS) used by the National Weather Service takes steps to minimize errors in the NEXRAD system differences between ground and radar data are inevitable. To address this, calibration techniques between radar data and rain gauge data is widely used (Over and others 2007)(Sribimawati, Brown, Hogg 1992)(Ramkellawan, Gharabaghi, Winter 2009) to both assess the accuracy of the radar and to adjust radar values to better correlate with ground estimates. This section will present a comparison of rainfall measured from three different sources of ground based measurements including Environment Canada, the Grand River Conservation Authority (GRCA) and anecdotal private measurements. Monthly data is compared for July 2008, a month when a number of significant storm events crossed the study area, including a single event from July 11, 2008 that is examined.

The graph shown in Figure 5-37 compares NEXRAD results of the total rainfall accumulation for the month of July against measurements taken by the two methods at the GRCA, hourly measurement from tipping bucket rain gauges and daily totals from manually operated gauges. The tipping bucket and manual gauges are in different locations so the results are not comparable between them. The manual gauges are located at dam sites operated by the conservation authority. Rainfall is measured daily from manual rain gauges at 8am by the dam operation staff. The tipping bucket rain gauge (TBRG) data is collected from automated devices that report hourly accumulations back the GRCA head office. The results for July accumulation show the radar values with a good correlation with the manual gauges, and a lower correlation with the TBRG network. As mentioned earlier, TBRG are prone to different types of errors, whereby under catch due to intense rain and the effects of wind can skew the values. It should also be noted that the TBRG data is raw and has not undergone any level of quality assurance. Any temporary malfunctions during the month are not accounted for.

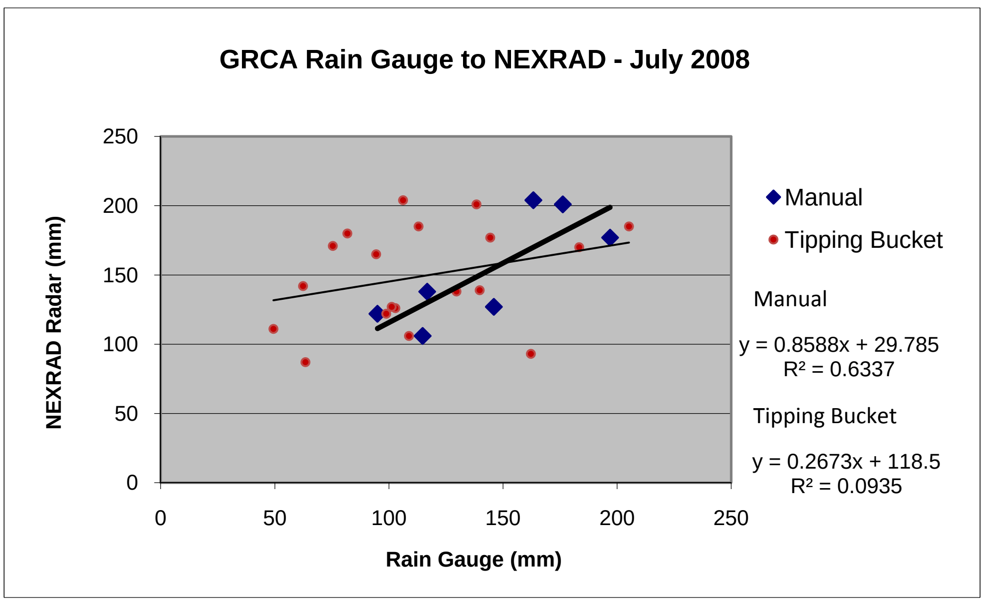

Figure 5-37: Comparison of GRCA rain gauge to NEXRAD for July 2008

The daily rainfall values for 39 stations from Environment Canada were downloaded from the National Climate Data and Information Archive for the month of July 2008 and assembled into a database that could be used to compare to the radar data. The website used was **http://www.climate.weatheroffice.ec.gc.ca/climateData/dailydata_e.html.** Figure 5-38 plots a comparison of the monthly total for July between the climate station and radar totals. The correlation is relatively good with a high R-squared value and few outliers. Environment Canada maintains a standard of quality assurance as well as standards for the rain gauge operation. There is a good fit of the data between accumulation values of approximately 75 to 200 mm of rainfall. The distance of the stations from the radar antenna varied between 40 and 216 Km from the radar. The range of distances provided an opportunity to look at whether the distance had any impact on the overall correlation. Figure 5-39 plots the percent difference between the radar and the rain gauge data and shows little impact over distance. It should be noted that the storm events of July 2008 were relatively local convective storms. Strataform rainfall would likely show more impact of distance. The spatial pattern of where the significant accumulation of rainfall occurred during July 2008 is shown in Figure 5-40.

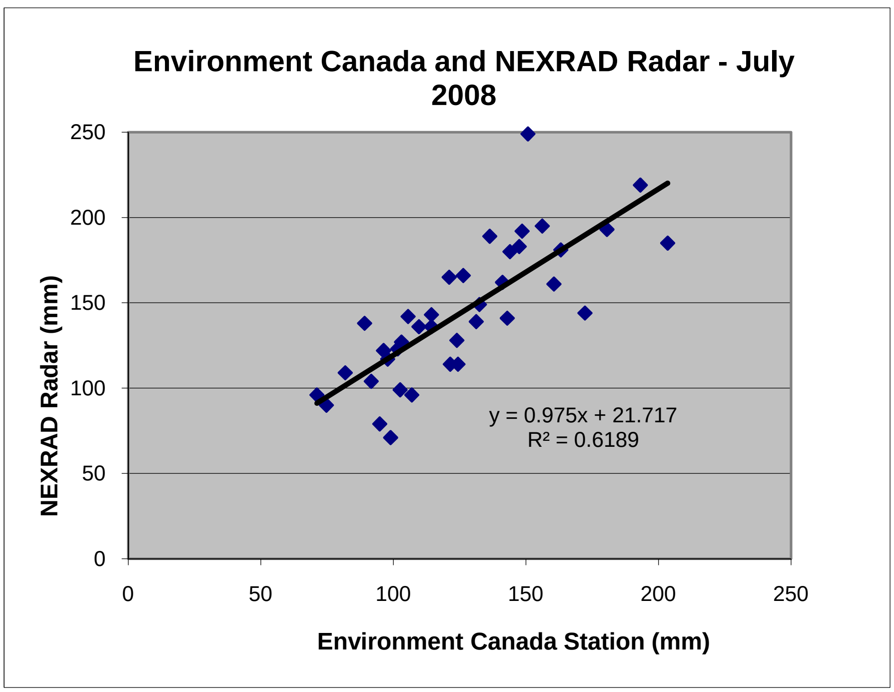

Figure 5-38: Comparison of Environment Canada rain gauge stations to NEXRAD radar for July 2008

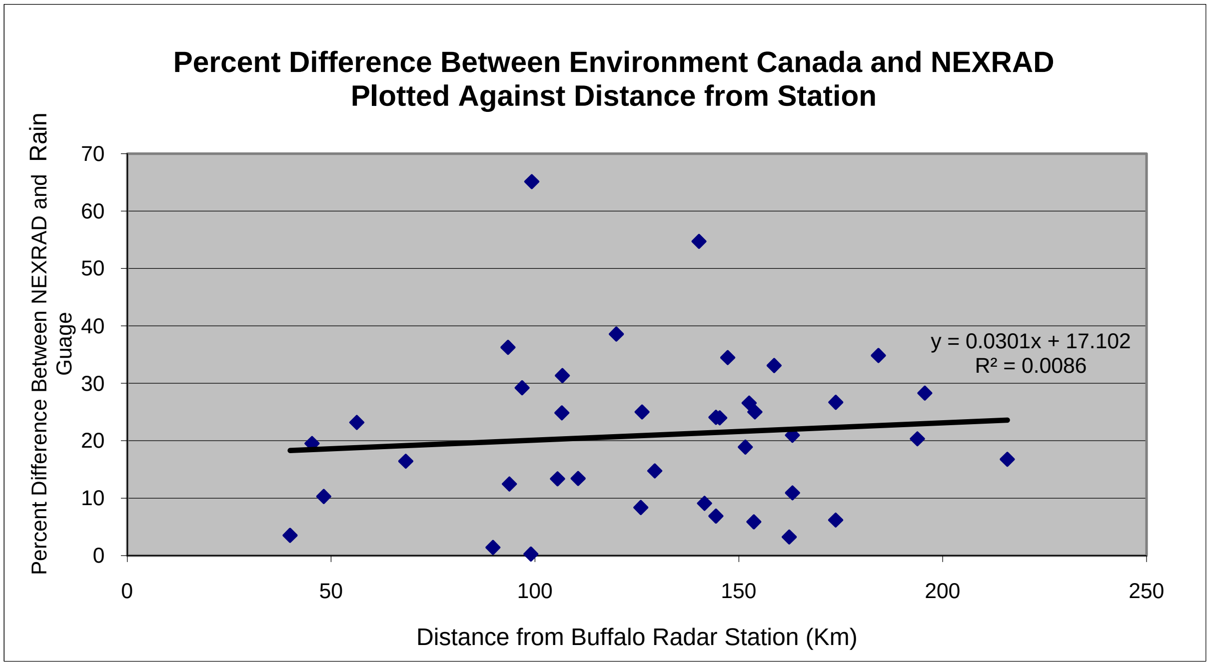

Figure 5-39: Percent Difference between Environment Canada rainfall and NEXRAD for July 2008, plotted against distance from the radar station

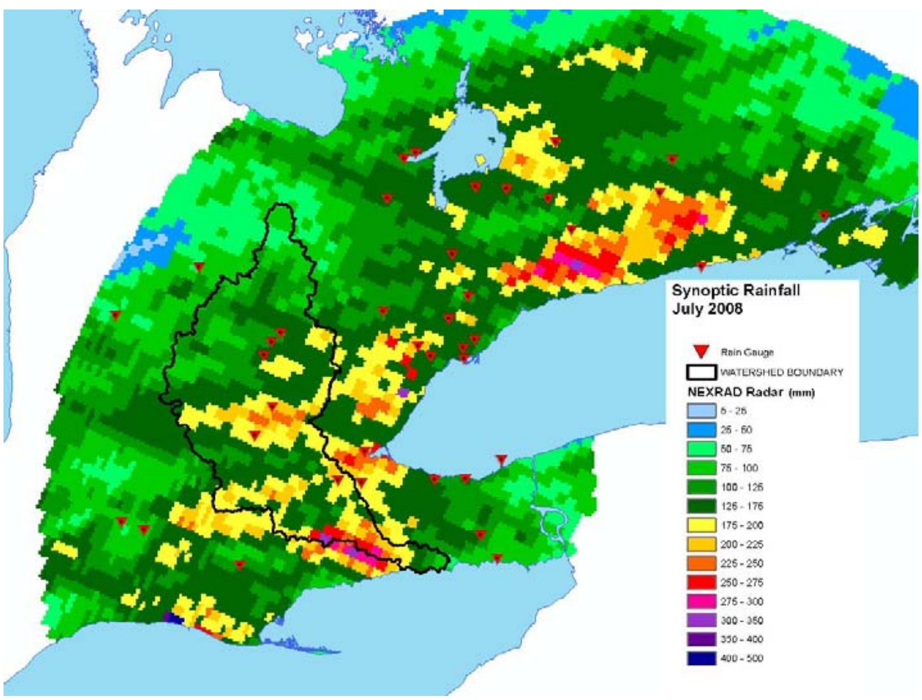

Figure 5-40: Map show total accumulation of rainfall for July 2008 from Buffalo NEXRAD

One of the events that contributed to high July rainfall within the Grand River watershed occurred in the early hours of July 11th when a major storm travelling on easterly track delivered very intense rain in an area between Stratford and Hamilton in a swath about 13 Km wide, Figure 5-41. The storm reached its peak between 3 am and 6 am, with the highest accumulations exceeding 100 mm. There were two active rain gauges near the region of the highest accumulation, a gauge operated by the GRCA in New Hamburg recorded 82 mm and another by Environment Canada at Roseville recorded 97 mm. Staff at the GRCA (Boyd 2008; Loeffler 2008) were able to acquire from a number of residents in the area of the core of the storm ground-based measurements of rainfall from their private rain gauges. The ground values are listed in Table 5-4 along with the radar value recorded at each location. The radar values compared to the private measurements had a mean field bias (MFB) of 0.73, calculated by the sum of the radar divided by the sum of gauge values. The radar was generally lower than the gauges, as shown on Figure 5-42.

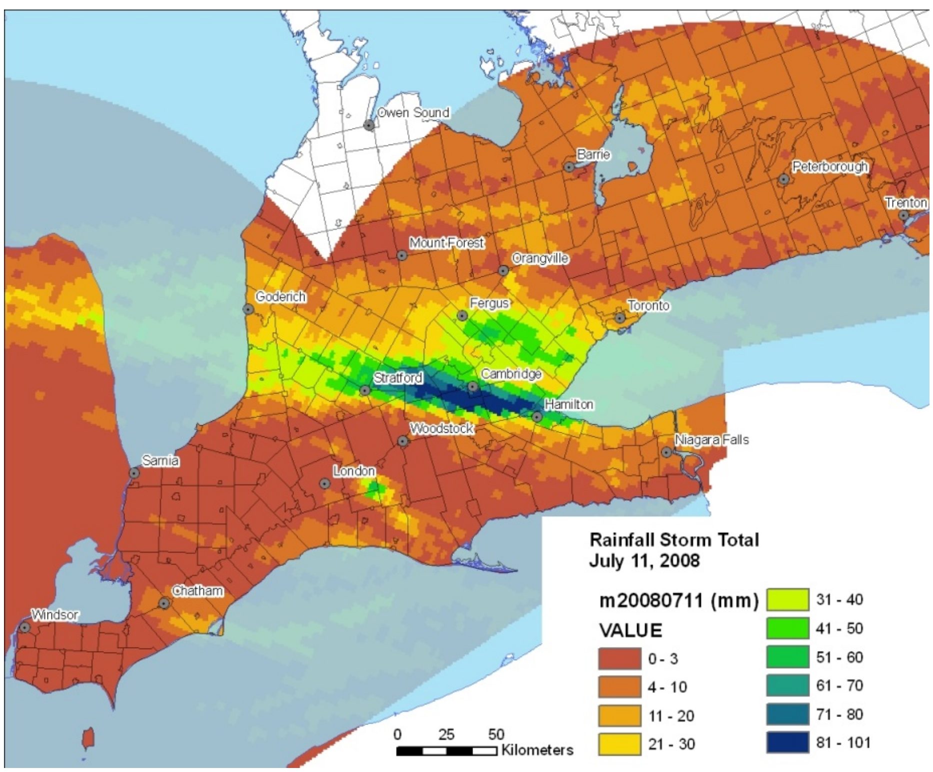

Figure 5-41: Rainfall total from July 11, 2008 storm from NEXRAD radar.

Rain Gauge	Gauge(mm)	Radar (mm)	Radar - MFB Adjusted (mm)
Private	63.5	56	77
Private	83.8	90	123
Private	88.0	80	110
Private	88.9	64	88
Private	96.5	87	119
Private	96.5	78	107
Private	101.6	91	125
Private	109.2	91	125
Private	114.3	78	107
Private	114.3	90	123
Private	114.3	80	110
Private	114.3	91	125
Private	114.3	91	125
Private	114.3	91	125
Private	120.0	76	104
Private	120.0	91	125
Private	127.0	76	104
Private	127.0	78	107
Private	127.0	64	88
Private	127.0	76	104
Private	127.0	76	104
Private	134.6	78	107
GRCA New Hamburg	103.8	82	n/a
Env. Canada Roseville	97.0	92	n/a

Table 5-4: Rainfall measures from radar compared to private measurements, GRCA and Environment Canada for July 11, 2008

It is notable that the radar has good correlation to the Environment Canada gauge at Roseville with values of 97 mm from the gauge and 92 mm from the radar. However, the two closest private measurements, within 3 Km of the Roseville gauge had values of 114 and 127 mm. This discrepancy could be the results of a number of factors related to both the gauges and the radar. First, the storm could have had very localized variability that resulted in significant differences over short distances. The gauge at Roseville may have had an under catch, more likely if it was a tipping bucket gauge. Whereas the private gauge were more likely manual buckets. The types of gauges were not known. The GRCA's tipping bucket rain gauge at New Hamburg was 21 mm higher than the radar suggesting that under catch was less likely a factor. Wind associated with the storm and the site conditions of the gauges could also have contributed to differences.

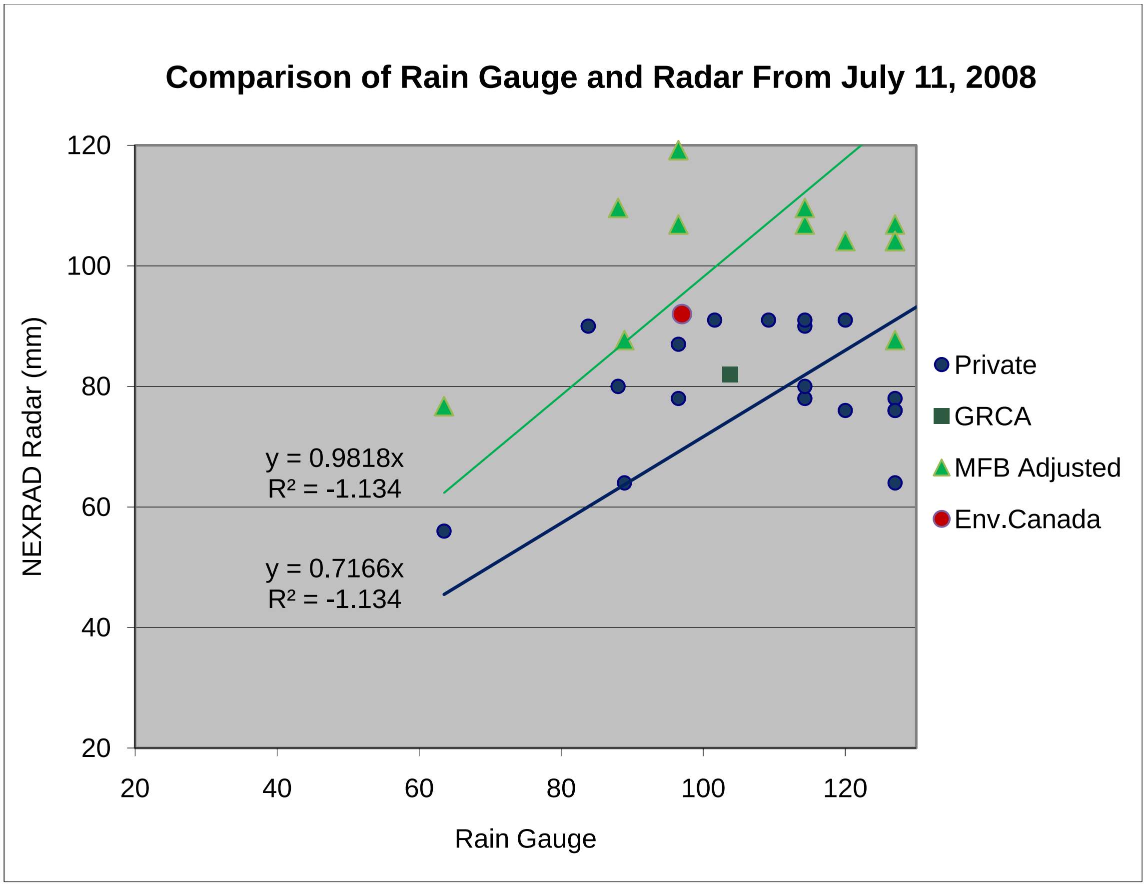

Figure 5-42: Graph of radar and gauge measurements from July 11, 2008

From the standpoint of the NEXRAD radar there are several important considerations when comparing its values to ground measurements. The cell resolution of DPA data is 4x4 Km representing an averaging of reflectivity within that area. It is also a measure of average hourly intensity, meaning that short bursts of heavy rainfall are averaged over on hour, smoothing their effect on DPA values. The bias factor adjustment used by NEXRAD is based on ground-based measurements in the United States, variations in atmospheric conditions over Ontario do not contribute to the calibration of NEXRAD radar. Lastly, the track of the storm was aligned directly with the beam from Buffalo (Figure 5-41). If the heaviest rain fell in area masked by heavy fall on the southeast leading edge of the storm, it is likely that beam filling could have been a factor in reducing the reflectivity measured deeper into the storm on the angle it was travelling and thus showing lower rainfall than the ground based measurements. It is an interesting case study since it demonstrates the uncertainty present in both measurement systems, and also challenges some assumptions about the accuracy of each. If one were to assume that the Roseville station was functioning properly and actually did not experience factors that have biased the 'catch', it suggests that the private measurements had errors. The range of values from the private gauges between the highest and lowest values was 71.1 mm whereas the radar had range of only 36 mm.

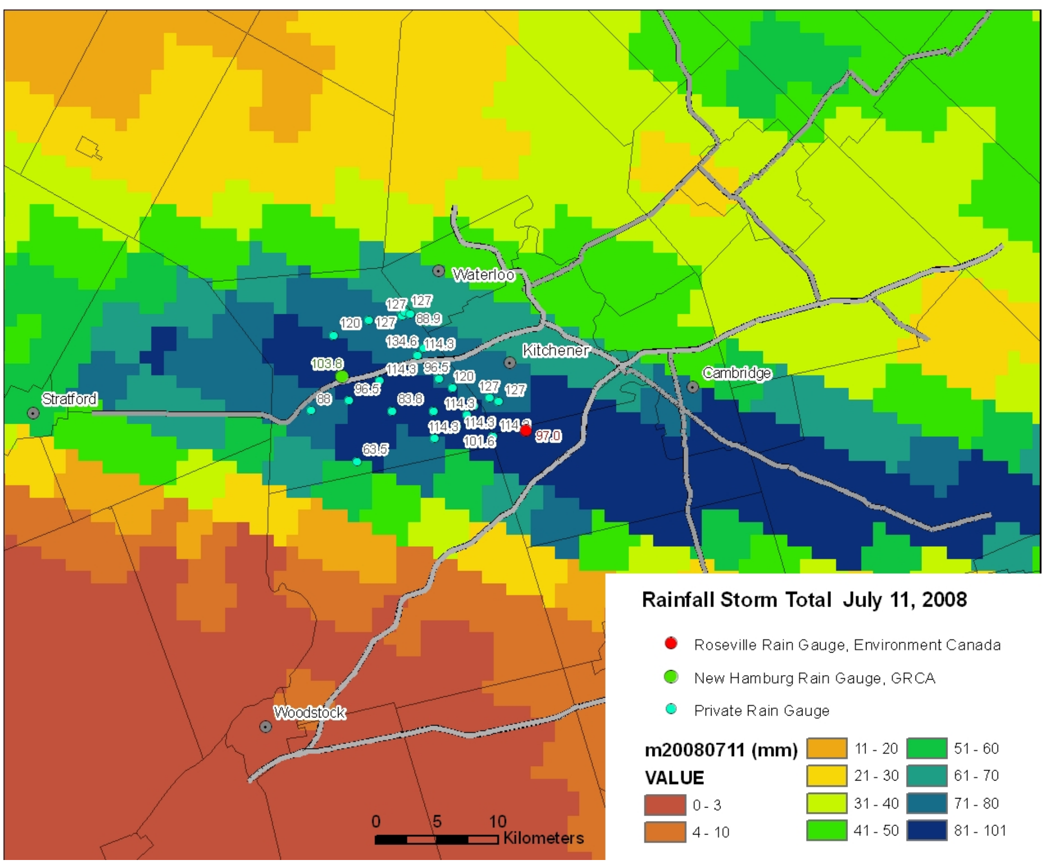

Figure 5-43: Map showing location of gauges and radar values from July 11, 2008

5.4 Summary of Results and Findings

The results presented in this chapter are the outcome from an extensive analysis against an exceptionally large amount of data. The following sub-sections attempt to provide a synopsis of some of the significant findings.

5.4.1 Normals for Monthly Temperature and Precipitation

While containing a high degree of variability as indicated by low R-squared values, the results on monthly averages for maximum and minimum temperature show a consistent upward trend of warming across the 46 years between 1960 and 2005. The results show a change in average minimum temperature of 1.4 degrees Celsius and 1.0 degrees for the maximum temperature. The results are averaged across the entire study area and it is likely that in specific locations the amount of change would vary. It is notable that the statistics for the minimum daily temperature values showed the highest amount of change, from 1.4 degrees to 1.5 degrees between the low and high averages. This suggests that areas that were cooler on average have experienced a greater degree of overall warming, whereas areas that are generally the warmest have not warmed as much. It also suggests an overall warming trend of night-time temperatures, a finding that concurs with predictions presented by the IPCC (Parry 2007) and findings of a similar studies in Canada (Zhang X, Vincent LA, Hogg WD, Niitsoo A. 2000)(Vincent LA and Mekis E. 2006). Another significant finding shows March with greatest temperature change for average daily maximum of 2.1 degrees. This implies a potentially earlier and more rapid snowmelt in the spring, with the negative impacts outlined in Chapter 2.

The high degree of average monthly rainfall variability from year-to-year illustrates the relative smoothing of rainfall normals. Whereas a calculated normal of rainfall is more representative of the mid-point between large fluctuations across annual high and low accumulation averages. There is a seemingly cyclic frequency between high years, average years, and low years on the graphs of monthly precipitation values. These inter-annual fluctuations are worthy of further research since they may point to possible influence from larger patterns of global atmospheric circulations and oceanic oscillations. For example, Hurrell (2009) suggests that large scale oceanic oscillations are associated with pronounced changes in temperature and rainfall patterns across North and South America. However, he also states that the science of predicting the impacts of these fluctuations is still in its infancy.

The comparison of the 23 year average between 1960-1982 and 1983-2005 shows that average annual precipitation for the majority of the study area has increased. However, the trend toward increased monthly and annual average precipitation does not necessary imply more storms. The analysis of the number of rainfall days seem to suggest that there has been a decrease in the number of rain-days overall since the early 1990's. Given increased total accumulation and fewer storm events, the conclusion that could be drawn is that the storms are both larger, possibly more frequent on days with storms (more convection cells) and that the storms are overall delivering more rainfall. Again, the results agree with climate change predictions whereby the relationship between atmospheric warming and increased moisture results increased total water returning to the surface as precipitation.

5.4.2 Rainfall Patterns

Whereas the monthly statistics for both temperature and precipitation exhibit a degree of variability, the spatial results depict complex and variable spatial patterns. The change in rainfall averages between in 1960-1982 and 1983-2005 show spatial shifts in all months examined. The increasing frequency of severe storms occurring in the month of July in southwestern Ontario is significant, and could represent an enhancement of the lake breeze effect. The analysis of daily occurrences of rainfall concurs with the monthly averages, with a noticeable increase in the number of occurrences of daily rain above 75 mm. The location where the increased occurrences are indicated (in blue on Figure 5-17) is significant to the overall rainfall patterns in southwestern Ontario. These are areas where lake breeze effects are likely a dominant local factor.

In the area approximately between London and Cambridge exists a corridor that appears to be where the influence of the lake breeze has its maximum effect on rainfall events. The cluster of storms as indicated in Figure 5-21 to 5-24 clearly highlight the significance of the corridor for its frequency of severe rainfall events. These results align well with previous work by Environment Canada on the effect lake breezes (King and others 2003) on tornado development. This thesis demonstrates the influence on rainfall accumulation and suggests that there is a persistent underlying pattern. While these results are not necessarily indicators of climate change, it is likely that atmospheric changes caused by global warming could act to enhance storms formed in this region, delivering more intense and more frequent rainfall events.

Lake breezes are not the only driver for severe storms, however, day time heating leading to convection is certainly the driver behind the highest 1 hour rainfall intensities, with late afternoon in July being the peak season, and the most likely period of the year for the highest one hour rainfall accumulation.

Insofar as other notable local patterns, the relatively high average one hour rainfall in the Chatham area is notable, both for its position between Lake Huron, Lake Erie and Lake St.Clair, as well as, its close downwind proximity to Detroit and Windsor. The question of whether urban heat island and air pollution play are role is not answered by this study. However, this pattern, detected in the 46 years of station data and in the recent 13 years of radar data, highlight this area for possible future research. The same effect from the Greater Toronto Area (GTA) is certainly apparent in the July 2008 rainfall totals, whether it actually had an impact is unknown. The higher occurrences of severe daily rainfall between the southeast shore of Lake Simcoe and Peterborough is another area of interest. What affects the GTA has combined with lake breeze from Lake Ontario and Lake Simcoe are not clear. These results suggest local processes at play, worthy of further examination.

5.4.3 Rainfall Intensity Analysis of NEXRAD Radar Data

The analysis of one hour maximum rainfall highlights southwestern Ontario as having both the most frequent severe events as well as on average the highest rainfall rates for the study area. This region is where the influence of lake breeze and convergence is at its greatest, which seems to increase rainfall rates and their frequency about 70 to 80 Km east of the Lake Huron, with more variability within the Grand River watershed, and a noticeable drop extending east of the Niagara Escarpment from Orangeville to Niagara Falls. The City of Toronto shows higher rainfall on its west end and on a track that runs north of the city eastward along the southern slopes of the Oak Ridges moraine. This suggests lake breeze from Lake Ontario enhancing convective storms, likely with a primarily westerly flow, which seems to extend to Peterborough. The shores around Lake Simcoe also favor occurrences of severe weather, likely influenced by terrain north of Barrie and the likely local lake breeze convergences with Lake Ontario on its south end.

The analysis of the dates of the severe weather indicated that 2008 and 1998 were significant years for geographic impact of storm events. However, the locations where the majority of the storm events occurred differed between these years. In 2008 the majority of the activity was in the central southwest, in and around the Grand River watershed, whereas in 1998 the Chatham area and in the northeast region of the study area were most affected. Based on the results on rain days, see Appendix H, 2008 had more days with rain than any year since 1996. The data also indicates a general increase in days with 75 mm of rain or more over the last 13 years. As far as seasonal variability, the month of the July dominates the occurrences of the severe rainfall, with late afternoon being the most likely time when a storm will occur.

The annual variability of storm patterns delivering intense rainfall suggest that synoptic conditions are a predominate factor for determining seasonal occurrences of severe storm events. Aside from the general trend favoring the southwest, over the 13 year period there were variable hot spots and cold spots across the study area for intense rain. However, local affects of lake breezes, land cover, terrain and urban heat island do appear to influence how general synoptic scale conditions interact with the local scale of the storm event.

5.4.4 Implications of Results for Land Management and Planning

The spatial and temporal characterization of intense storm patterns presented in the paper should have potential for application in various areas of land management. The following paragraphs lists proposed applications for the use of the results to improve land management and planning.

Stormwater management – The results indicate that Environment Canada IDF values are not representative of the storm events between 1996 and 2008 where over half of the area examined exceeded both the 25 year and 50 year frequency intervals, and many areas in the southwest exceeded the 100 year interval of intensity. The results indicate local patterns of frequency and intensity of rainfall. The spatial content of radar data could help define regional IDF values that would better represent short duration rainfall curves. Revised IDF values would allow new modeling of hydrologic responses of watersheds, leading to revised engineering specifications that account for the current climate.

Erosion control – Having knowledge of where and when intense rainfall is most likely to occur could help direct programs that promote practices that reduce the impact of intense rain on soil erosion and sedimentation of drainage systems.

Water Quality – Related in part to erosion control, programs for monitoring water quality and for promoting practices to improve it, should benefit from knowing when major events occurs for sampling and should be able to improve modeling the impact of rainfall with more representative rainfall data than from station data alone.

Agriculture – Rainfall monitoring is important for ensuring crop production and for applying best practices for soil and nutrient management. Agriculture is the primary land use in Southwestern Ontario. Planning for and managing surface runoff from the intense storm events that frequent that area can be more targeted with further examination of storm patterns.

Drought/low water – The results from this research also show areas where rain does not occur as often. By examining rainfall accumulations from radar, areas that have received below average rainfall could be detected and monitored.

Recreation – The management of recreational events during the storm season could use these results to choose dates when intense rainfall is less likely to impact, or at least take measures to be more prepared for the likelihood of intense weather in certain location and monthly intervals.

Chapter 6
Discussion and Conclusions

This chapter provides a synopsis of the objectives of this thesis and draws several key conclusions from the results and findings obtained from the research. Recommendations for future research and enhancements to this project are presented.

6.1 Review of Thesis and Objectives

This paper set out a number of objectives related to the history of rainfall in southern Ontario since 1960. Chapter 1 introduced the notion of climate normals and how the climate of the past may not be representative of the climate of the present or future. Chapter 2 put climate change and its overall impact into the context for the study area of southern Ontario and what some of the predicted impacts could be insofar as spring and summer precipitation. Chapter 3 reviewed the source climate data used from Environment Canada from 1960 to 2005. The rapid decline in the number of active climate monitoring stations from early 1990s onward highlights a growing information gap for ground based data sources. Chapter 3 also introduced NEXRAD weather radar as a source of precipitation data for southern Ontario, contrasting it with the Canadian radar, and provided background on the sources of error in radar rainfall measurement. Chapter 4 discussed the use of the Spline algorithm for spatial interpolation of daily surfaces for precipitation and temperature. The simpler but more voluminous analysis of the radar data was also presented. Chapter 5 presented the results of the primary objectives of the thesis, which were:

- To analyze the spatial patterns of rainfall events derived from interpolated rainfall surfaces and to examine trends and changes in patterns
- To analyze the spatial patterns of rainfall events derived from NEXRAD radar surfaces 1996 and 2008.
- To compare resulting spatial patterns from interpolated surfaces and from radar data. To examine whether there are similar or dissimilar cluster patterns.

- To build a spatial characterization of severe storm activity in southern Ontario by creating a spatial normal of 1 hour rainfall intensity using NEXRAD radar data.

6.2 Research Outcome and Contribution

The maps and the data presented in this paper have a greater richness of content than the general observations offered in the paper. The outcome of this project is a vast and rich set of data holdings that have research potential well beyond this thesis. The objective to derive rainfall patterns and characterize them both in temporal and spatial terms was successfully met. It was not the intent of this paper to explain in detail the meteorological processes that drive weather systems that cause the observed patterns nor to imply that the results are indicators of climate change due to global warming. However, for research related to rainfall in Ontario, the results should be relevant.

6.2.1 Climate Surfaces

The purpose of interpolating rainfall surfaces from climate stations was to create a spatial context to rainfall measurements. There is no question that there is a degree of uncertainty and of smoothing in the rainfall values. This is evident in the case study of the July 14, 1997 storm event. It is also likely that the surfaces underestimated the maximum rainfall delivered from the cores of intense storms when only infrequently would a station have a core pass over it. It is also likely that smaller storm events detected by stations were ‘smeared’ outward from the few stations that received rain, thus creating daily rainfall where none may have fallen. The fuzziness of the surfaces aside, the surfaces pass through the data values observed at climate stations, and therefore the results viewed as a whole for the study area, and not just one locality, do characterize clear trends that have occurred over the 46 years of measurements. Climate change was not a focus of this paper, however, the trends detected agree with climate change predictions of an overall warming trend, generally more precipitation on average, delivered by fewer storm events. In general the results seem to suggest that over the study period of 1960 to 2005 severe storms have become less frequent but that they are larger and deliver more intense rainfall when they occur.

6.2.2 Radar Data

Radar achieves what the spline interpolation of climate station could not with certainty, which is to provide complete spatial coverage content about the size, extent, intensity and timing of storm events. However, it does suffer from errors and therefore should be applied with knowledge of how different atmospheric conditions can affect rainfall estimation.

The analysis of radar for storm occurrences extracted patterns that generally agreed with the patterns derived from the climate surfaces. The Getis autocorrelation statistic highlighted the significant hot spot for severe weather in southwestern Ontario. This cluster is likely the result of lake breezes and their convergence from the surrounding lakes.

The analysis of one hour maximum rainfall for the 13 years of radar data derived maps of annual maximum rainfall rates. Again the southwest of the study area had the most consistency, however, it is also clear from looking at each year, the spatial patterns vary due to general synoptic conditions. Local factors, primarily the interaction of lake breezes appear to drive hot spots in different areas.

6.2.3 Uncertainty and Limitations

It is worth noting that the decline in the number of climate stations from 1990s onward is not addressed in this project. Whatever, if any, impact fewer stations had on the results from spline surfaces is unknown. Some confidence can be drawn from the good correlation of the rainfall occurrences between the radar and the surfaces between 1996 and 2005. However, given the fewer stations available presently, and the much richer data content from radar, the future applicability of interpolated rainfall from climate surfaces should be superseded by enhancing radar data analysis. Surface interpolation is more suitable for temperature analysis, whereas ground-based precipitation measurements should be focused for long term monitoring and as input for adjusting rainfall estimated from radar.

Radar data fills in the voids between climate stations. However, both radar data and rain gauges have their own sources of error and uncertainty. The case study of the July 11, 2008 storm demonstrated that even with ground-based measurements, a good correlation with radar cannot necessarily be achieved. In that case, uncertainty in the reliability of ground data is likely a contributing factor. It is interesting to note that the one Environment Canada station within the core area of highest rainfall had a good correlation with the radar. Statistically, one good data pair is not significant, however, the analysis of the one month accumulation of radar and Environment Canada stations for the month of July 2008 does show that the NEXRAD had an excellent fit with the station data. The precipitation processing system of NEXRAD that adjusts its output based on ground measurements sets it apart from the Environment Canada radar. In the United States radar data is used extensively for operational uses that include flood forecasting, tornado warning and hydrologic modeling. There is less equivalent work in Canada using radar data from Environment Canada. A recent study of total phosphorous on Lake Simcoe (Ramkellawan, Gharabaghi, Winter 2009) made use of NEXRAD data, even though the King City is less than half the distance from Buffalo.

6.2.4 Future Research Potential

This paper demonstrated the utility of using radar accumulation values as a source of rainfall measurement. While correlation to ground based measurements does have variability, the value of radar's ability to define the spatial extent of rainfall far surpasses what is possible to derive from ground-based data alone. There are many possible applications of NEXRAD radar information in southern Ontario, however, from a research standpoint future work to improve the understanding of rainfall patterns, maintaining archival data and improving the estimates from radar by calibrating it with ground-based measurements should continue.

The temperature surfaces that were generated from this project were only examined to determine if overall indications of warming trends had occurred across the study area. The spatial patterns of temperature would be interesting to examine further and could be correlated with other weather observations, land cover change and temperature recordings of the Great Lakes. The data could be useful for examining evapotranspiration as well as temperature effects on surface water temperature.

Further to the surfaces analysis, it would have been preferable to have used the standard WMO 30 year interval to examine differences between long term averages, rather than 23 year periods of data used in this project. Earlier MSC data does exist, and using station data from 1950 onward it would be possible to look at 30 year intervals from the last 60 years up to data from 2009. Given that there were substantial changes in average monthly precipitation detected in the analysis between 1960 to 1982 and 1983 to 2005, it would be interesting to examine the data more closely to determine how weather patterns changed and to explore possible causes.

The graphs that plot annual variability appear to display some regularity in the occurrences for years of extreme high and low values of temperature and precipitation. Atmospheric teleconnection patterns such as the North Atlantic Oscillation (NAO), the Pacific–North American (PNA) pattern and the west Pacific occurrences of the El Niño Southern Oscillation (ENSO) are known to influence weather patterns in North America (Feldstein 2000). The question of correlating the results from this thesis with historical fluctuations is likely difficult to address due to a complex interaction of factors. A study of annual droughts in Ontario by Klassen (2002) concluded that atmosphere-ocean circulations such as El Niño, La Niña and the North Atlantic Oscillation are not consistently and are not necessarily attributable to local drought conditions. On longer time scales, Hurrell (2009) suggests that anthropogenic climate change will be strongly modulated by natural climate variability, especially by slow variations driven by oceans on decadal time scales, thus masking change within non-uniform spatial and temporal variability. Supporting this idea, Zhang, Delworth and Held (2007) suggest that variability in the mean surface temperature record during the 20th century for the northern hemisphere can be partially attributed to fluctuations in sea surface temperature of the Atlantic Ocean. This suggests for the period of data used in this study that caution should used in implying long term trends from the results. A more rigorous approach to analyzing trends and variability is likely better suited to non-linear methods and consideration given to the influence of teleconnection patterns.

Because radar provides such a fine granularity of data in temporal and spatial terms, it offers the ability to examine storm events in detail. Storm size, motion and frequency could be further examined. By narrowing the window of time to late afternoon and early evening more direct analysis of the affects of lake breezes could also be explored.

The IDF analysis was only run on a one hour interval but the same type of analysis could be extended to intervals from 6 minutes to 24 hour intervals or longer. It would also be useful to consider further calibration of the radar with time-series data from hourly rain gauges, where available. If calibrated radar could be integrated into formal IDF calculations, with appropriate confidence intervals to account for uncertainty in the radar/rain-gauge correlation, this could offer a new approach to deriving IDF curves in the future.

Environment Canada radar should be examined more closely and compared to the NEXRAD products. It would be helpful to quantify the differences between the sensors, from rainfall estimates, comparison to ground-based measurements and in the types of beam errors that occur. The results from this would help quantify the gaps with Canadian radar and lead to recommendations for building a business case to revise the system.

This thesis only looked at event based comparisons of rain gage and radar data. In the future the use of rain gauge sites located in Ontario for real-time correlation of NEXRAD radar should be promoted with the NWS. This should improve the bias factor applied to radar and improve the overall accuracy of rainfall estimates over Ontario. This initiative could be based on collaboration between Environment Canada and conservation authorities who both operate short duration rain gauge networks. The use of real-time and near real-time radar data offers potential for a range of other applications, including continuous flood forecasting and warning. By tracking the accumulation and extent of rainfall values with radar, preferably calibrated with rain-gauges, it would be possible to automate the input of rainfall estimates into hydrologic models to predict the potential impacts from flooding. This would assist water management and dam operations, as well as, local emergency response agencies with early warnings and more accurate predictions for initiating flood response procedures, and public notification.

6.3 Concluding Remarks

The scientific community working on climate change has expressed a high level of confidence that extreme precipitation events will increase in the future climate under global warming (Houghton 2001). However, the spatial and temporal resolution of Global Climate Models (GCMs) is not sufficient to determine the location, timing and size of local and regional changes in extreme precipitation (Klaassen and Seifert 2004). Regional climate models (RCMs) have a finer resolution (about 40 Km in Ontario) than GCMs and do account for local climate forcing features and processes, but according to Klassen and Seifert (2004), they suffer from errors propagated from GCM scale parameters. This thesis attempted to characterize changes in climate normals since 1960 and the effects that local processes and landscape scale effects may have on weather that produces intense precipitation. The results from the pattern analysis suggest a persistent influence of lake breezes and the concentration of severe storms in southwestern Ontario. However, variations in patterns elsewhere also suggest other factors at play that have caused shifts in storm pattern occurrences. One of the potential uses of this research is to compare the results from this work with the predictions of RCMs to serve both as validation and calibration of those models for future scenarios.

Given the dynamic and complex nature of severe weather occurrences in southern Ontario the importance of continuous monitoring cannot be understated. Yet in Ontario today we find a declining number of climate monitoring stations and a radar system that is not well suited for long duration analysis, in comparison to the NEXRAD system. These shortcomings leave gaps in information about climate and suggest a lack of federal commitment to maintain a mandate that should reside with Environment Canada.

In the last six years of the study period, from 2000 to 2005, the number of active federal climate stations in Ontario dropped below the number from before the Second World War. This would seem illogical given the high profile and the importance of weather monitoring, including maintaining long term records. This could be forgiven in part if the Canadian radar network operated on par with the American NEXRAD system, with S-band radar for long range detection, calibration with ground-based data and an effective and free distribution of data. At a minimum, in the heavily populated areas of Canada, such as southern Ontario, it would make sense for Environment Canada to further invest into its radar technology so that it is on par with NEXRAD.

Weather is complex phenomena. As much as science and modern technology is able to determine, it will never be fully characterize weather, uncertainty will remain. This study used ground-based data and remotely-sensed radar data, two vastly different technologies, to examine weather and the patterns of precipitation it delivers. It is clear that ground-based data alone is insufficient as a tool for examining severe precipitation patterns. Radar offers the ability to measure rainfall over a large area from one location, however, is not a replacement for ground-based rain gauges. If fewer ground-based stations are going to be operating in the future, it is critical that those stations adhere to the highest standards to ensure the most accurate measure of rainfall. It would also make sense to position continuous ground-based monitoring stations in locations that most frequently experience severe weather. With accurate ground data, calibrated radar can fulfill a critical role of filling in the gap between stations. Southern Ontario is fortunate to have coverage from the NEXRAD network; however, its extent is limited whereas the Exeter and King City are ideally located to help offsite beam errors from Buffalo and Detroit. Environment Canada should give serious consideration to migrating its radar hardware and data processing into a system compatible with NEXRAD. It would be a laudable move on the part of the Federal government of Canada to invest into severe weather monitoring in the form of enhanced radar and data processing systems for the densely populated areas of southern Ontario.

Appendix A

Daily Minimum and Maximum Temperature 1960 to 2005

The graphs in this appendix present the monthly average for daily maximum and minimum temperature over the period of 1960 to 2005 for the entire study area.

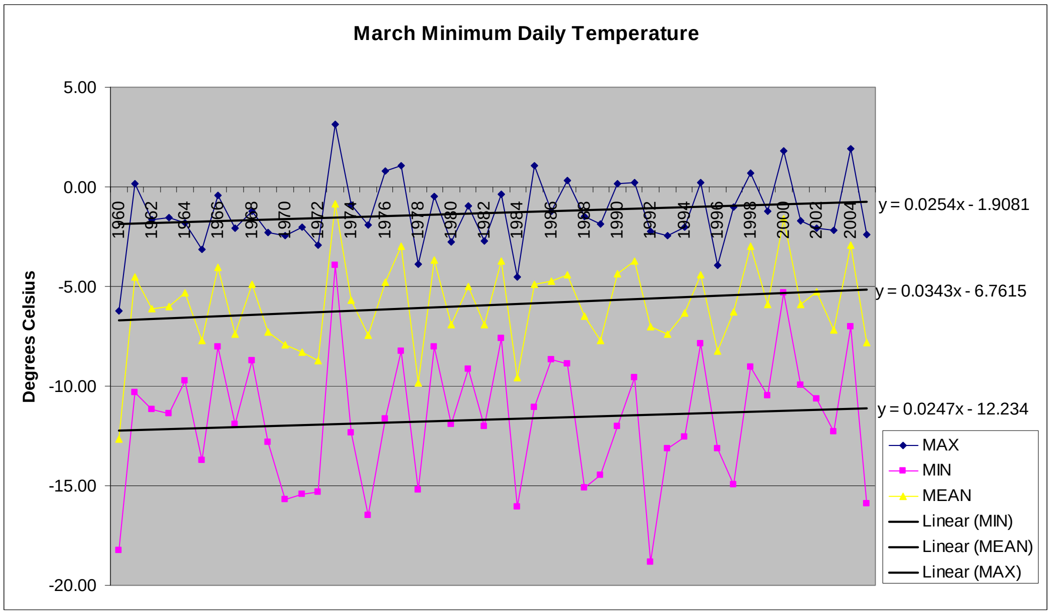

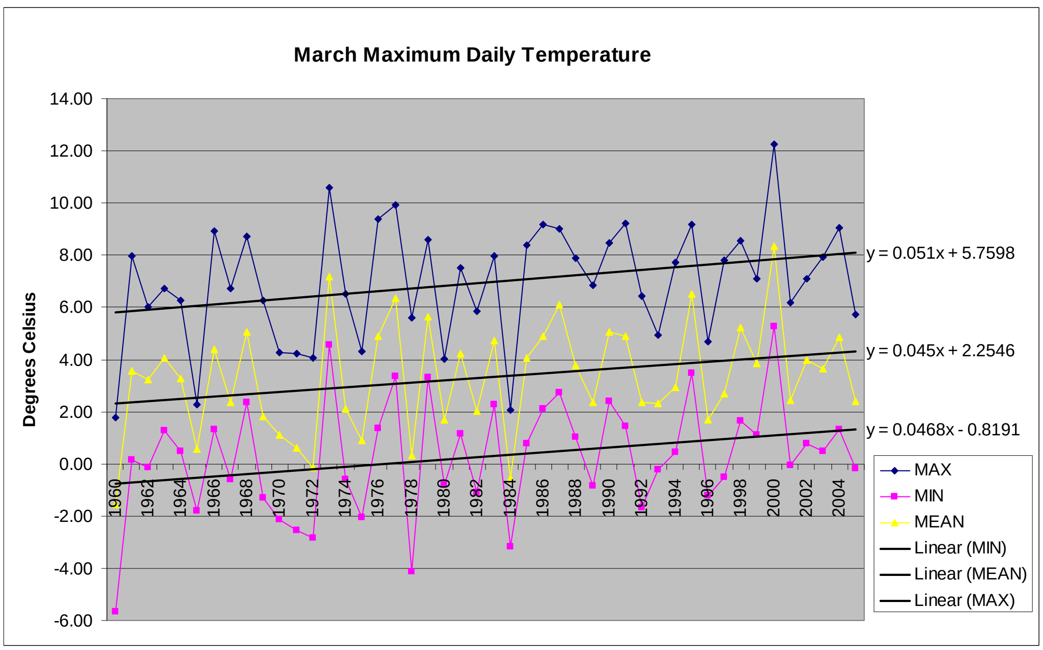

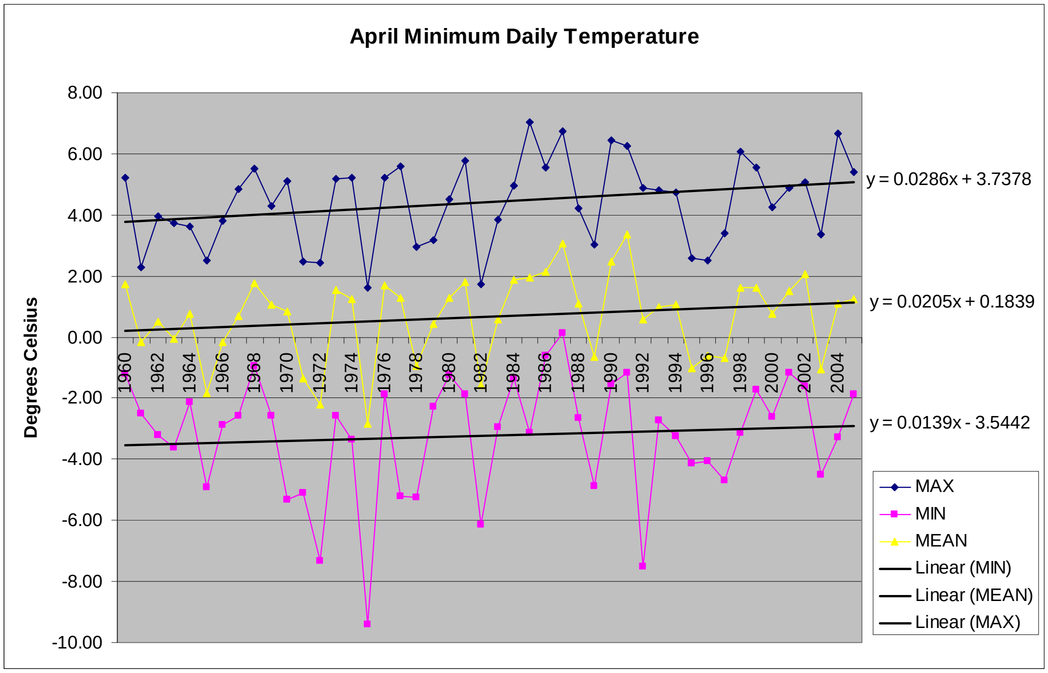
April Minimum Daily Temperature
Degrees Celsius
y = 0.0286x + 3.7378
y = 0.0205x + 0.1839
y = 0.0139x - 3.5442
MAX
MIN
MEAN
Linear (MIN)
Linear (MEAN)
Linear (MAX)

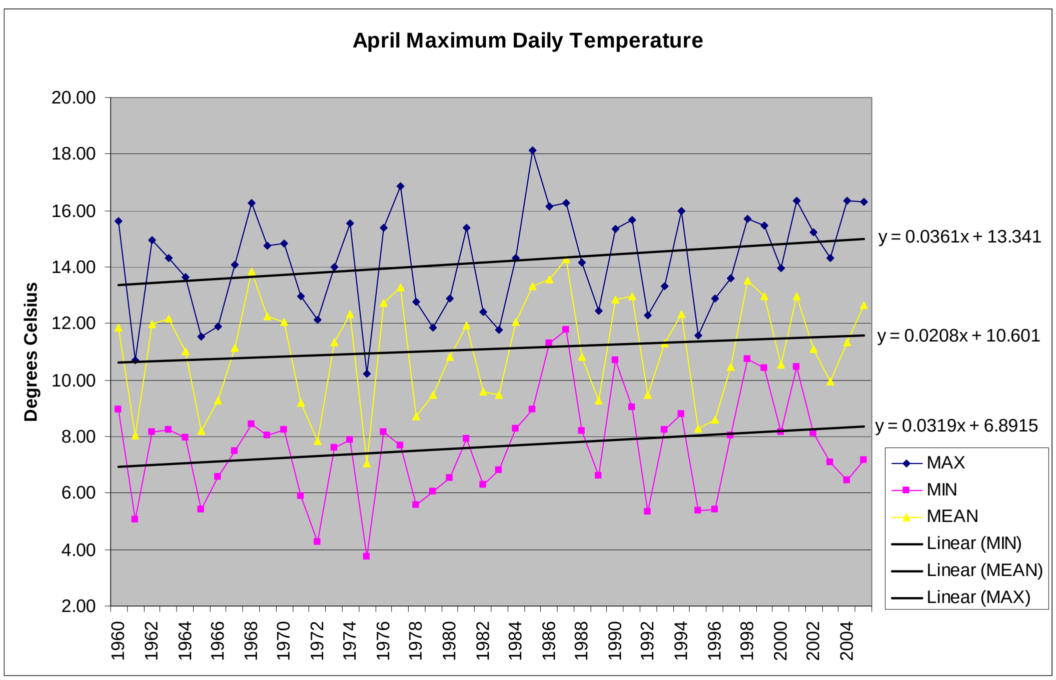
April Maximum Daily Temperature
Degrees Celsius
y = 0.0361x + 13.341
y = 0.0208x + 10.601
y = 0.0319x + 6.8915
MAX
MIN
MEAN
Linear (MIN)
Linear (MEAN)
Linear (MAX)

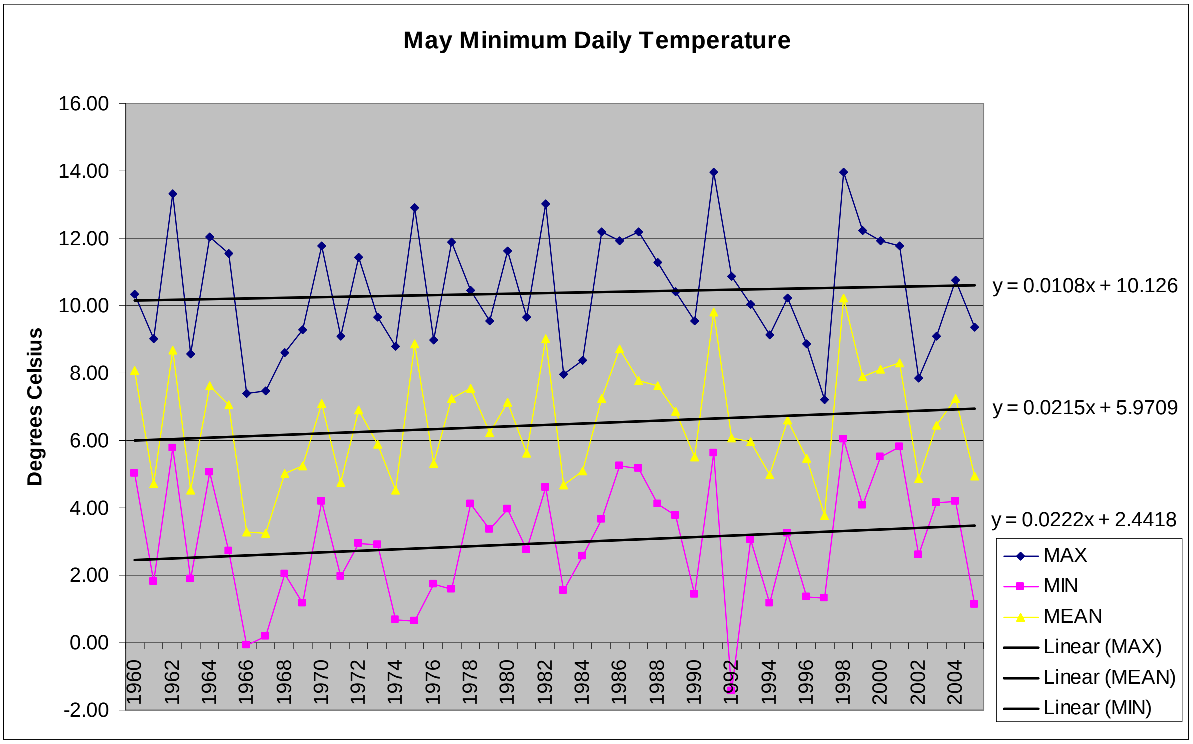
May Minimum Daily Temperature
Degrees Celsius
y = 0.0108x + 10.126
y = 0.0215x + 5.9709
y = 0.0222x + 2.4418
MAX
MIN
MEAN
Linear (MAX)
Linear (MEAN)
Linear (MIN)

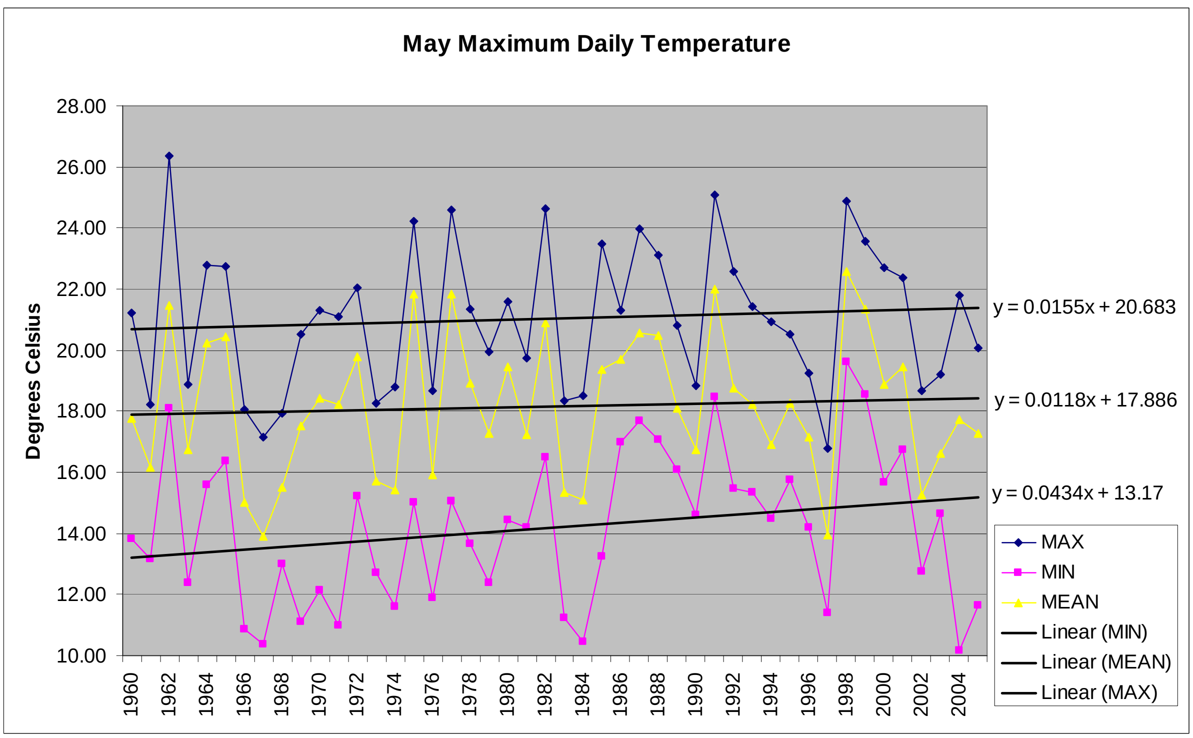
May Maximum Daily Temperature
Degrees Celsius
y = 0.0155x + 20.683
y = 0.0118x + 17.886
y = 0.0434x + 13.17
MAX
MIN
MEAN
Linear (MIN)
Linear (MEAN)
Linear (MAX)

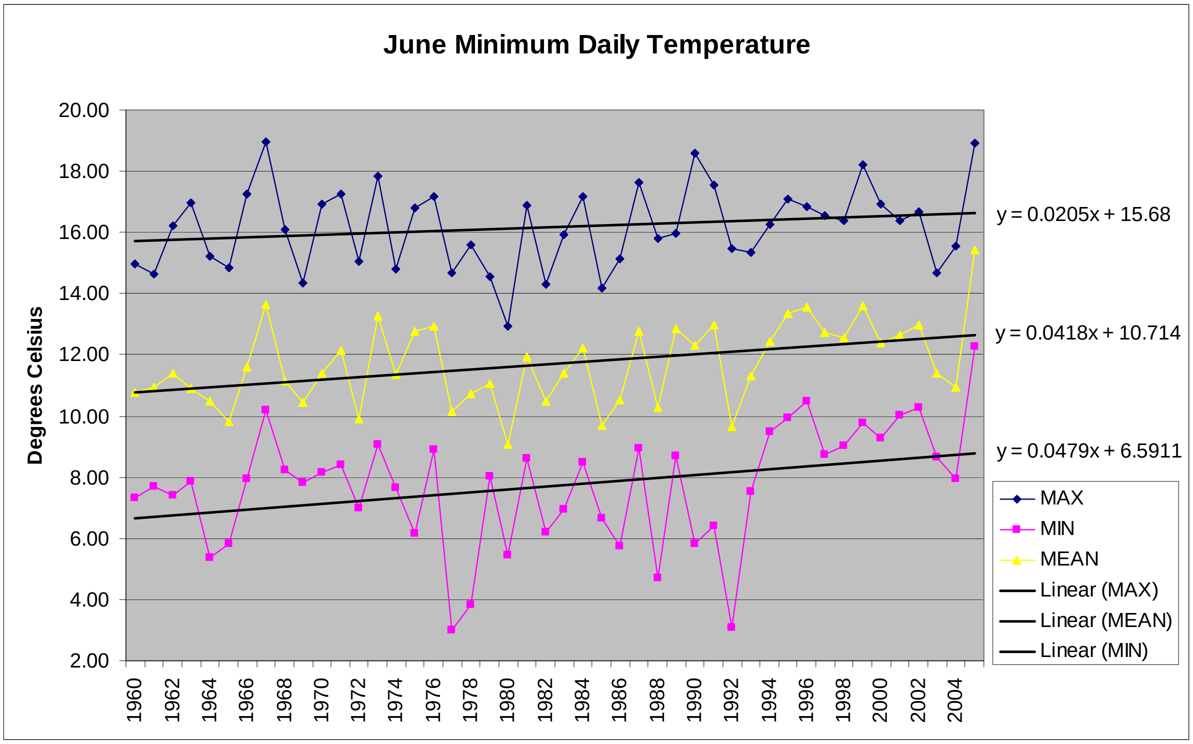

June Minimum Daily Temperature
Degrees Celsius
20.00
18.00
16.00
14.00
12.00
10.00
8.00
6.00
4.00
2.00
1960
1962
1964
1966
1968
1970
1972
1974
1976
1978
1980
1982
1984
1986
1988
1990
1992
1994
1996
1998
2000
2002
2004
y = 0.0205x + 15.68
y = 0.0418x + 10.714
y = 0.0479x + 6.5911
MAX
MIN
MEAN
Linear (MAX)
Linear (MEAN)
Linear (MIN)

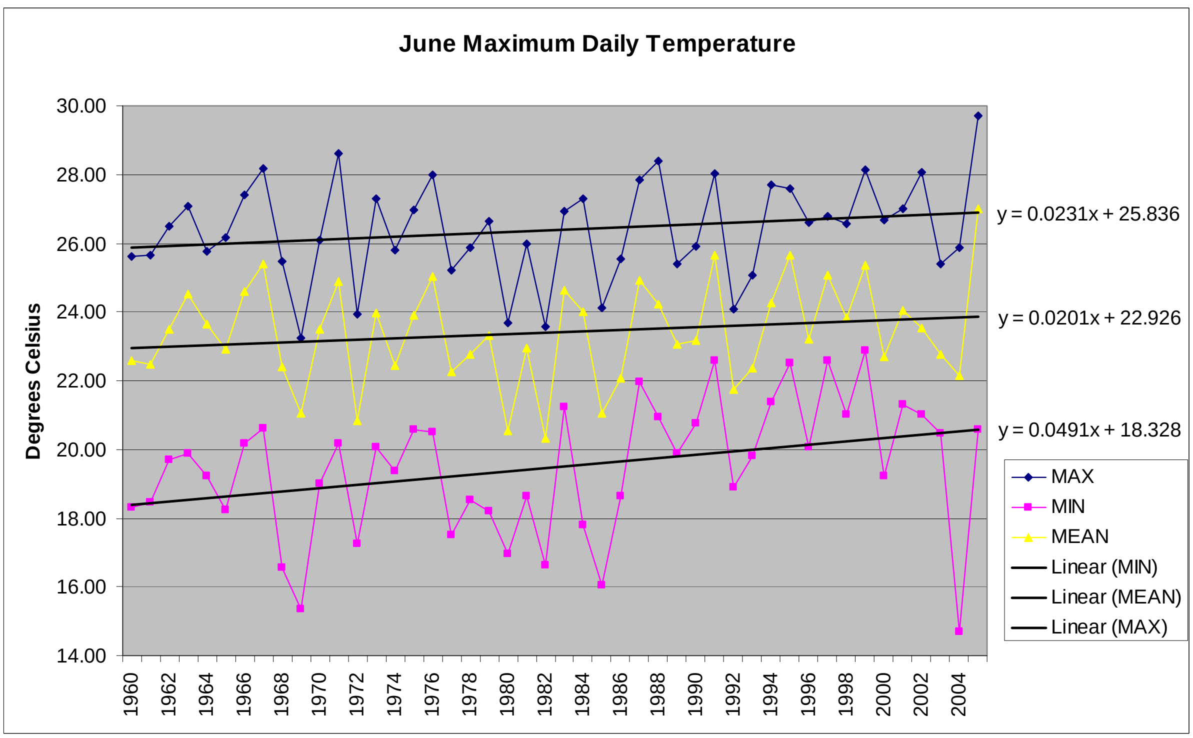

June Maximum Daily Temperature
Degrees Celsius
30.00
28.00
26.00
24.00
22.00
20.00
18.00
16.00
14.00
1960
1962
1964
1966
1968
1970
1972
1974
1976
1978
1980
1982
1984
1986
1988
1990
1992
1994
1996
1998
2000
2002
2004
y = 0.0231x + 25.836
y = 0.0201x + 22.926
y = 0.0491x + 18.328
MAX
MIN
MEAN
Linear (MIN)
Linear (MEAN)
Linear (MAX)

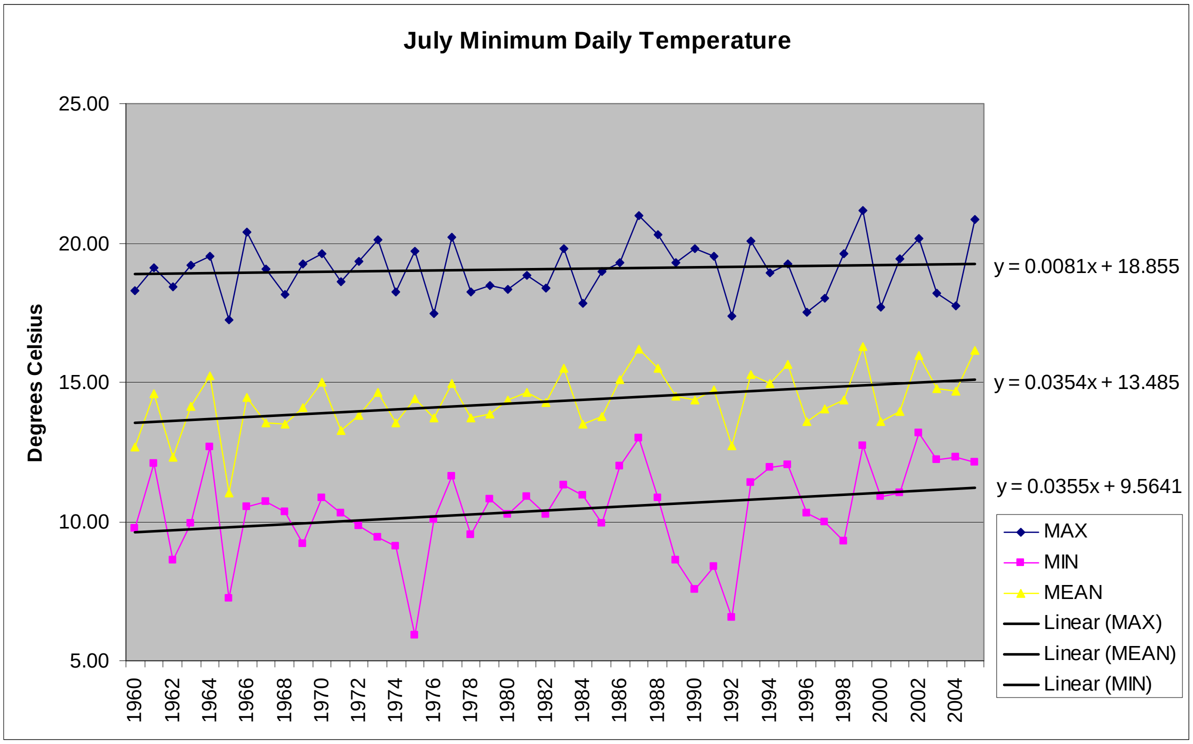

July Minimum Daily Temperature
Degrees Celsius
25.00
20.00
15.00
10.00
5.00
1960
1962
1964
1966
1968
1970
1972
1974
1976
1978
1980
1982
1984
1986
1988
1990
1992
1994
1996
1998
2000
2002
2004
y = 0.0081x + 18.855
y = 0.0354x + 13.485
y = 0.0355x + 9.5641
MAX
MIN
MEAN
Linear (MAX)
Linear (MEAN)
Linear (MIN)

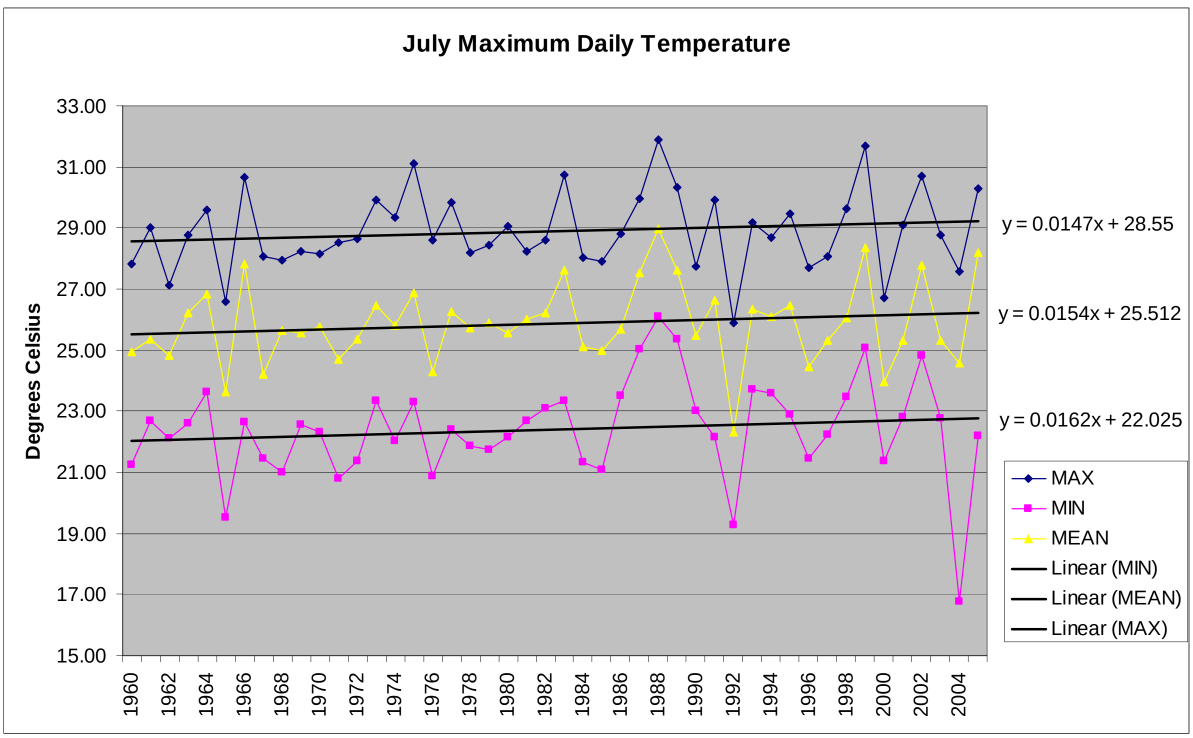

July Maximum Daily Temperature
Degrees Celsius
33.00
31.00
29.00
27.00
25.00
23.00
21.00
19.00
17.00
15.00
1960
1962
1964
1966
1968
1970
1972
1974
1976
1978
1980
1982
1984
1986
1988
1990
1992
1994
1996
1998
2000
2002
2004
y = 0.0147x + 28.55
y = 0.0154x + 25.512
y = 0.0162x + 22.025
MAX
MIN
MEAN
Linear (MIN)
Linear (MEAN)
Linear (MAX)

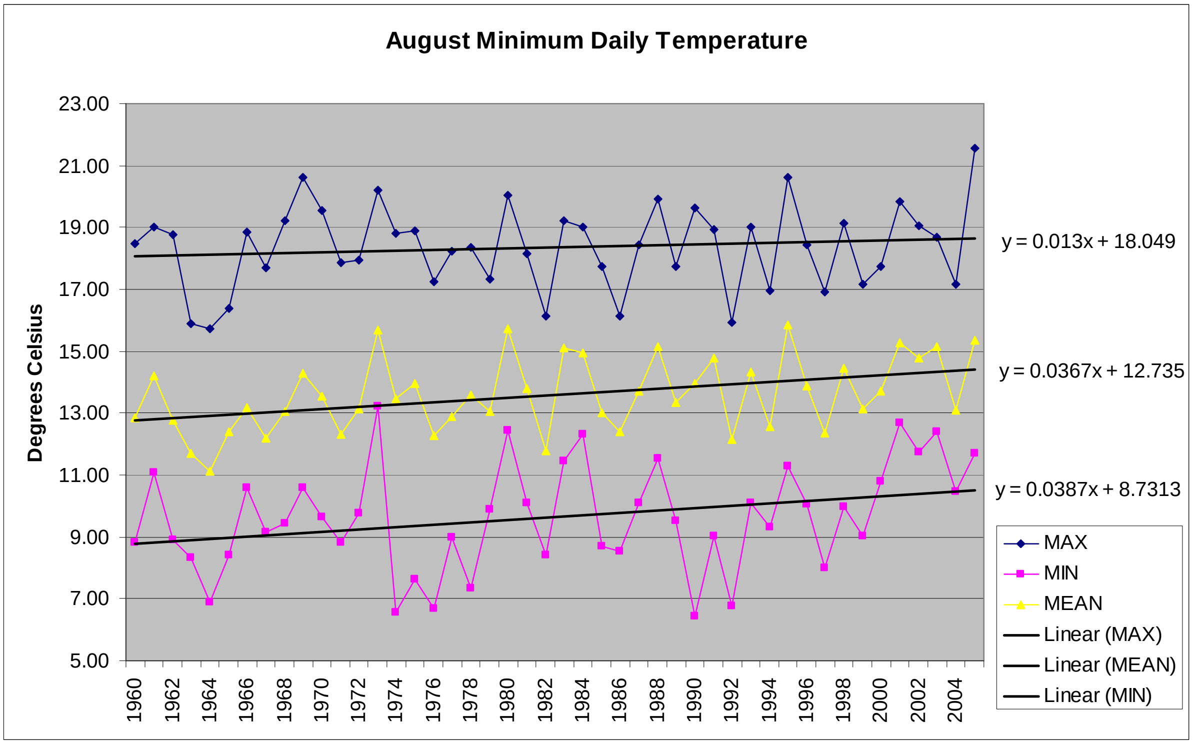
August Minimum Daily Temperature
Degrees Celsius
23.00
21.00
19.00
17.00
15.00
13.00
11.00
9.00
7.00
5.00
1960
1962
1964
1966
1968
1970
1972
1974
1976
1978
1980
1982
1984
1986
1988
1990
1992
1994
1996
1998
2000
2002
2004
y = 0.013x + 18.049
y = 0.0367x + 12.735
y = 0.0387x + 8.7313
MAX
MIN
MEAN
Linear (MAX)
Linear (MEAN)
Linear (MIN)

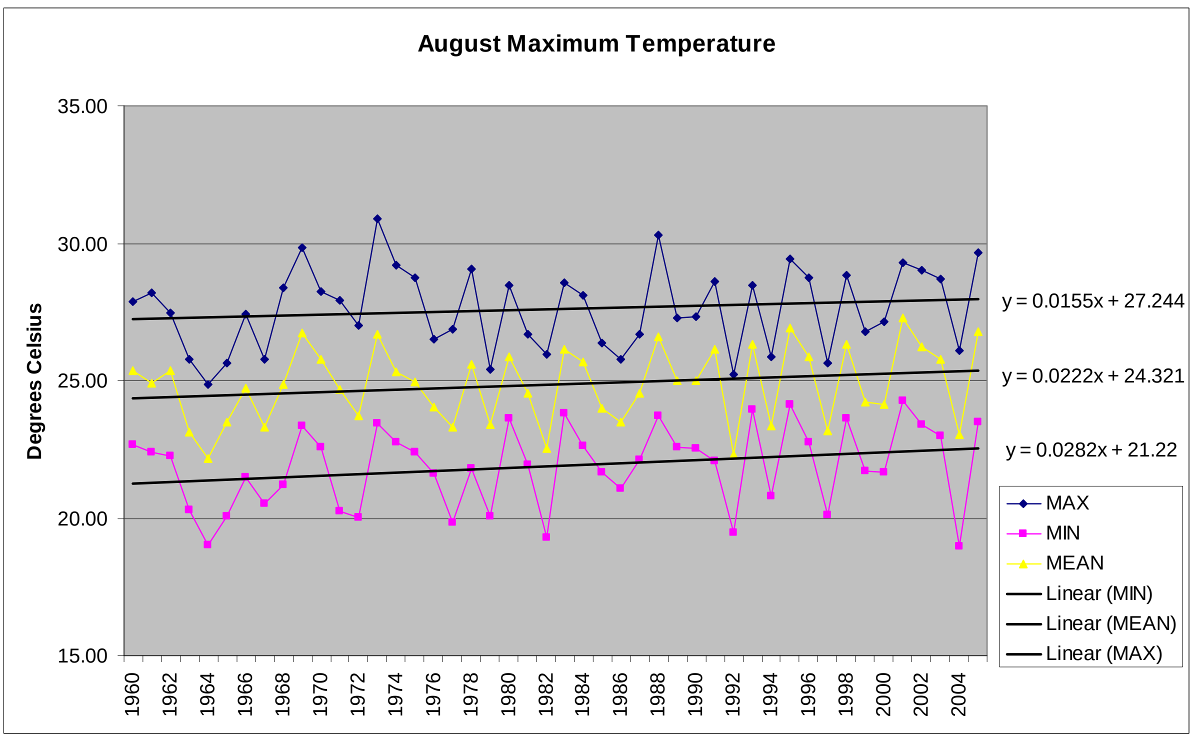
August Maximum Temperature
Degrees Celsius
35.00
30.00
25.00
20.00
15.00
1960
1962
1964
1966
1968
1970
1972
1974
1976
1978
1980
1982
1984
1986
1988
1990
1992
1994
1996
1998
2000
2002
2004
y = 0.0155x + 27.244
y = 0.0222x + 24.321
y = 0.0282x + 21.22
MAX
MIN
MEAN
Linear (MIN)
Linear (MEAN)
Linear (MAX)

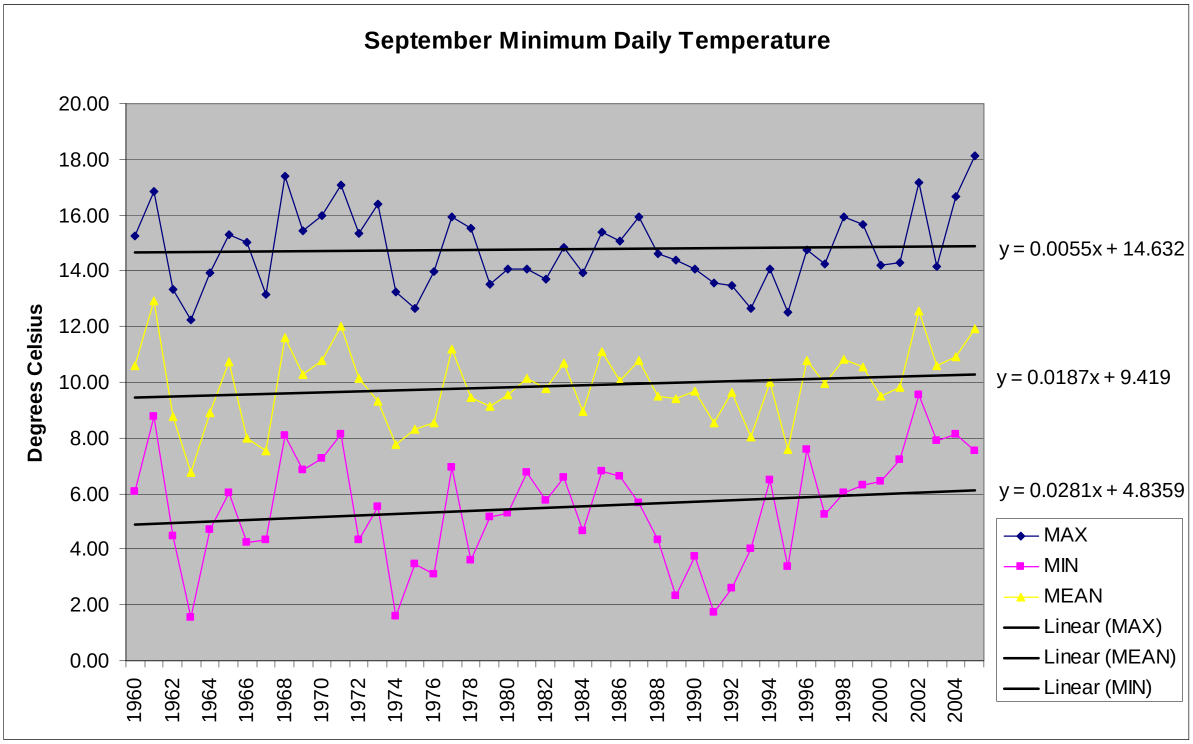
September Minimum Daily Temperature
Degrees Celsius
20.00
18.00
16.00
14.00
12.00
10.00
8.00
6.00
4.00
2.00
0.00
1960
1962
1964
1966
1968
1970
1972
1974
1976
1978
1980
1982
1984
1986
1988
1990
1992
1994
1996
1998
2000
2002
2004
y = 0.0055x + 14.632
y = 0.0187x + 9.419
y = 0.0281x + 4.8359
MAX
MIN
MEAN
Linear (MAX)
Linear (MEAN)
Linear (MIN)

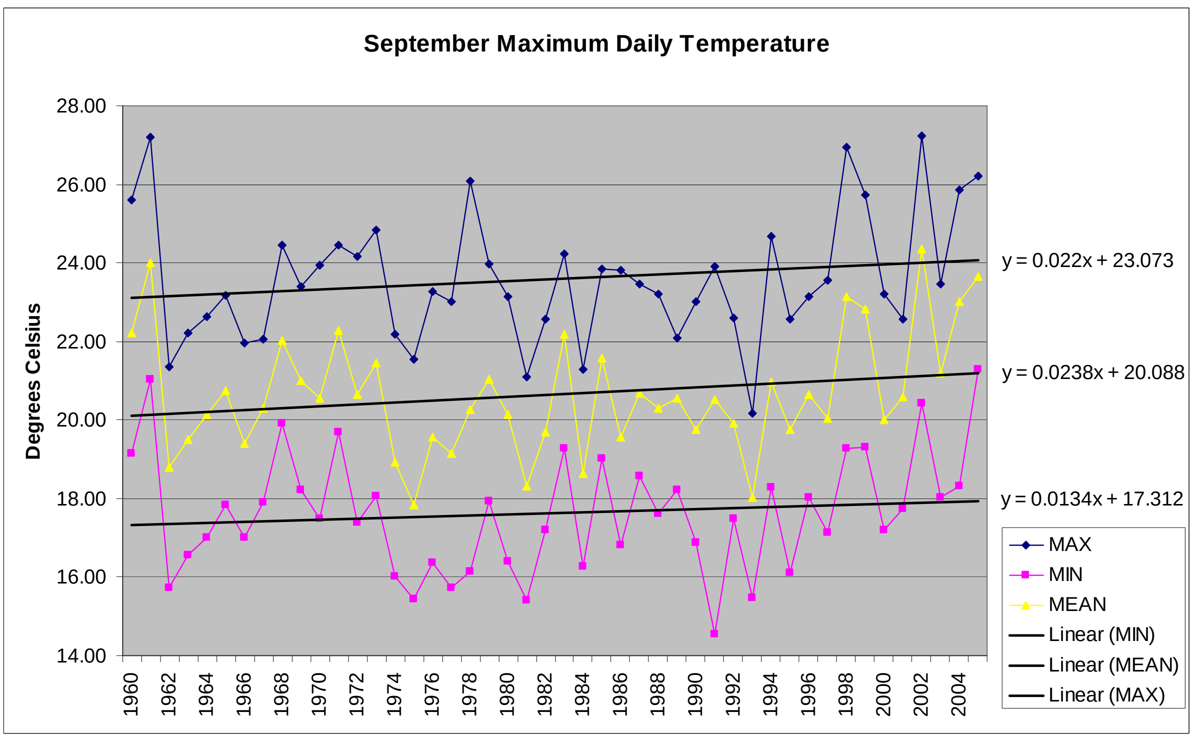
September Maximum Daily Temperature
Degrees Celsius
28.00
26.00
24.00
22.00
20.00
18.00
16.00
14.00
1960
1962
1964
1966
1968
1970
1972
1974
1976
1978
1980
1982
1984
1986
1988
1990
1992
1994
1996
1998
2000
2002
2004
y = 0.022x + 23.073
y = 0.0238x + 20.088
y = 0.0134x + 17.312
MAX
MIN
MEAN
Linear (MIN)
Linear (MEAN)
Linear (MAX)

Appendix B

Monthly Precipitation 1960 to 2005

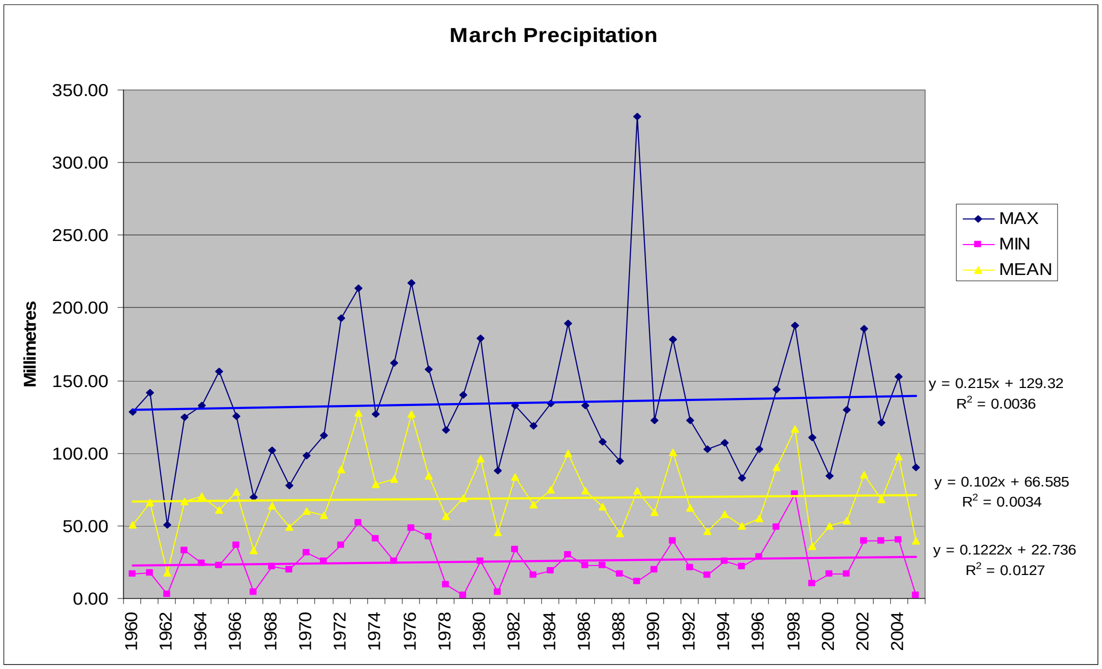

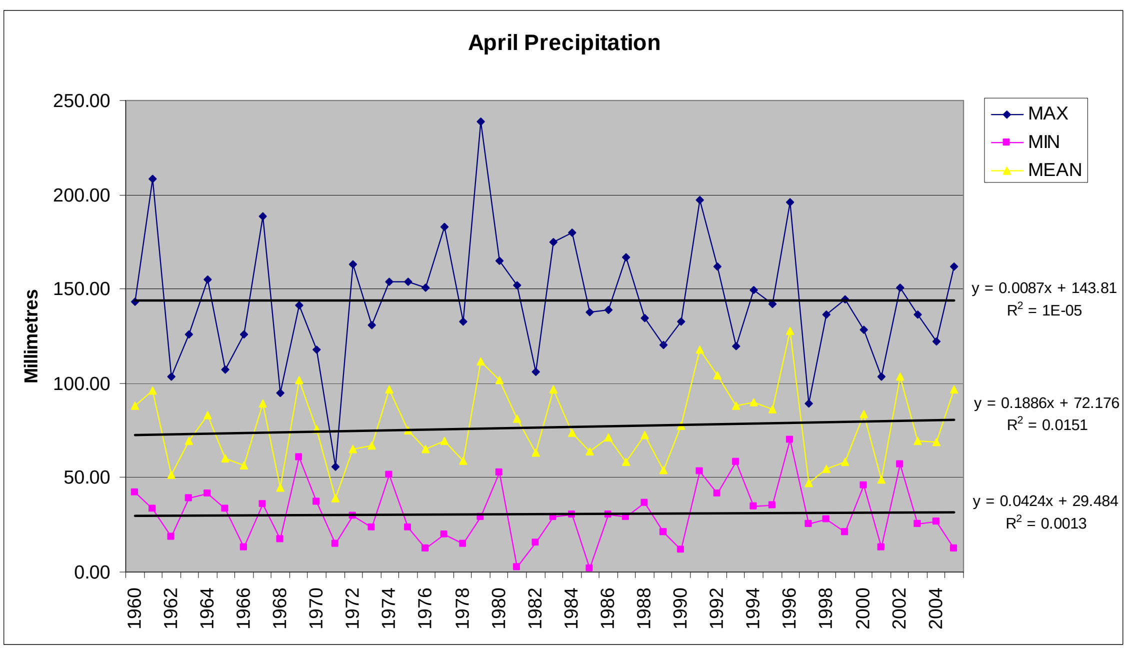

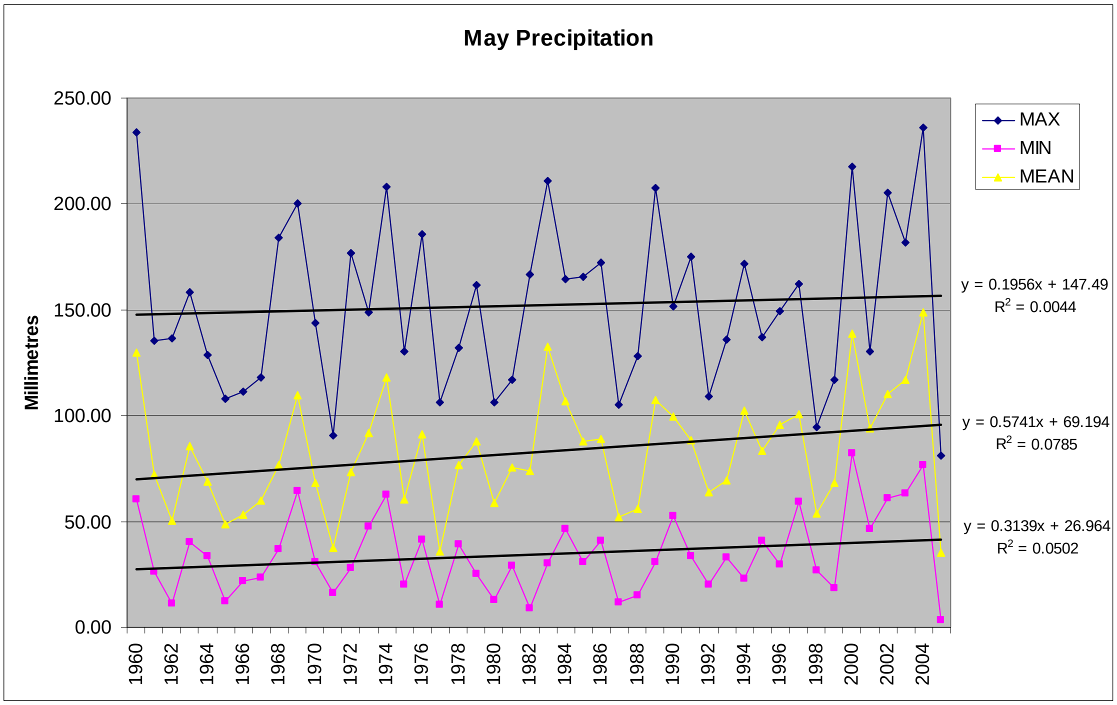
May Precipitation
Millimetres
MAX
MIN
MEAN
y = 0.1956x + 147.49
R^2 = 0.0044
y = 0.5741x + 69.194
R^2 = 0.0785
y = 0.3139x + 26.964
R^2 = 0.0502

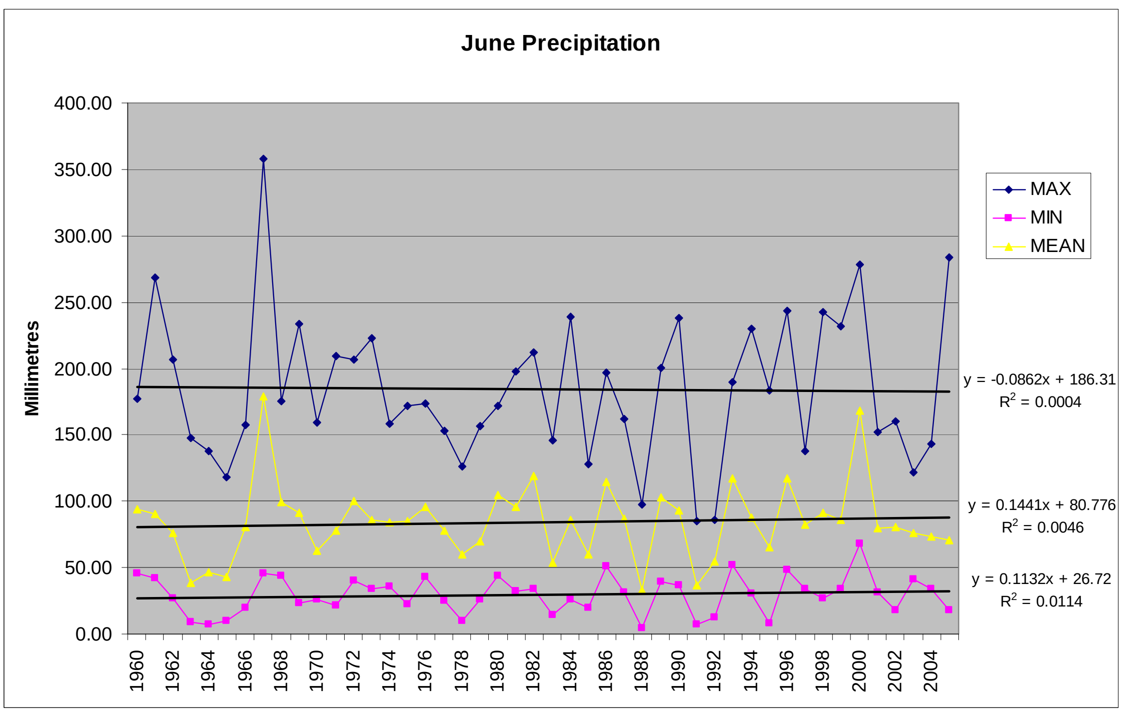
June Precipitation
Millimetres
MAX
MIN
MEAN
y = -0.0862x + 186.31
R^2 = 0.0004
y = 0.1441x + 80.776
R^2 = 0.0046
y = 0.1132x + 26.72
R^2 = 0.0114

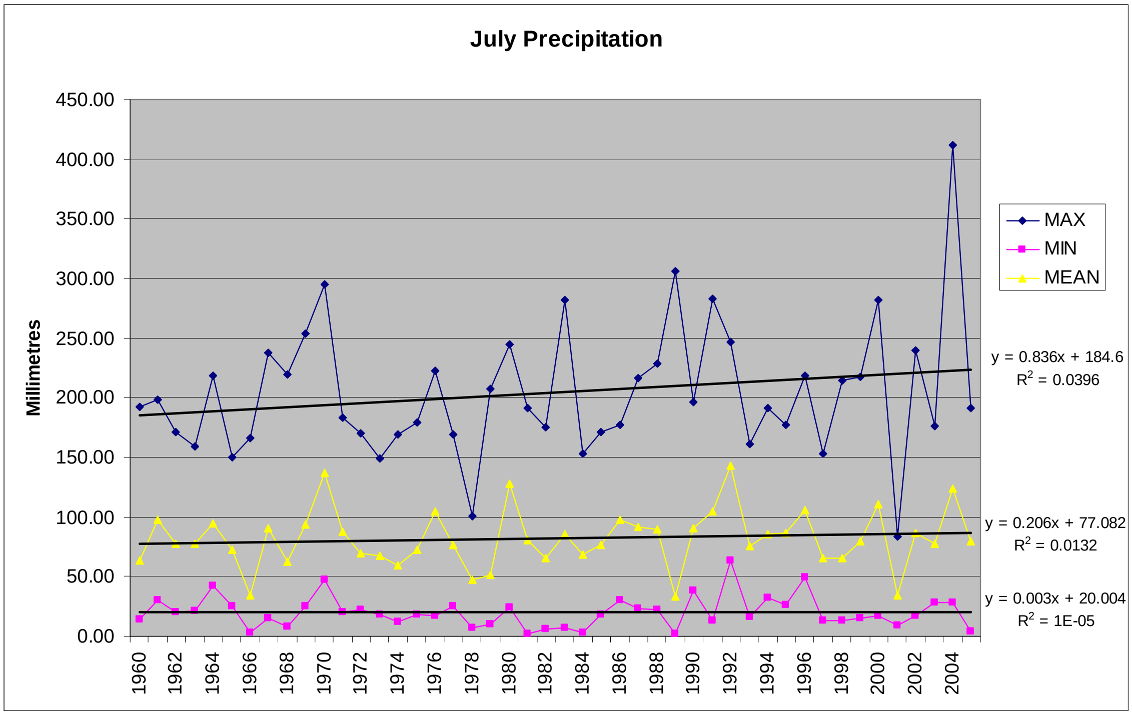
July Precipitation
Millimetres
450.00
400.00
350.00
300.00
250.00
200.00
150.00
100.00
50.00
0.00
1960
1962
1964
1966
1968
1970
1972
1974
1976
1978
1980
1982
1984
1986
1988
1990
1992
1994
1996
1998
2000
2002
2004
MAX
MIN
MEAN
y = 0.836x + 184.6
R^2 = 0.0396
y = 0.206x + 77.082
R^2 = 0.0132
y = 0.003x + 20.004
R^2 = 1E-05

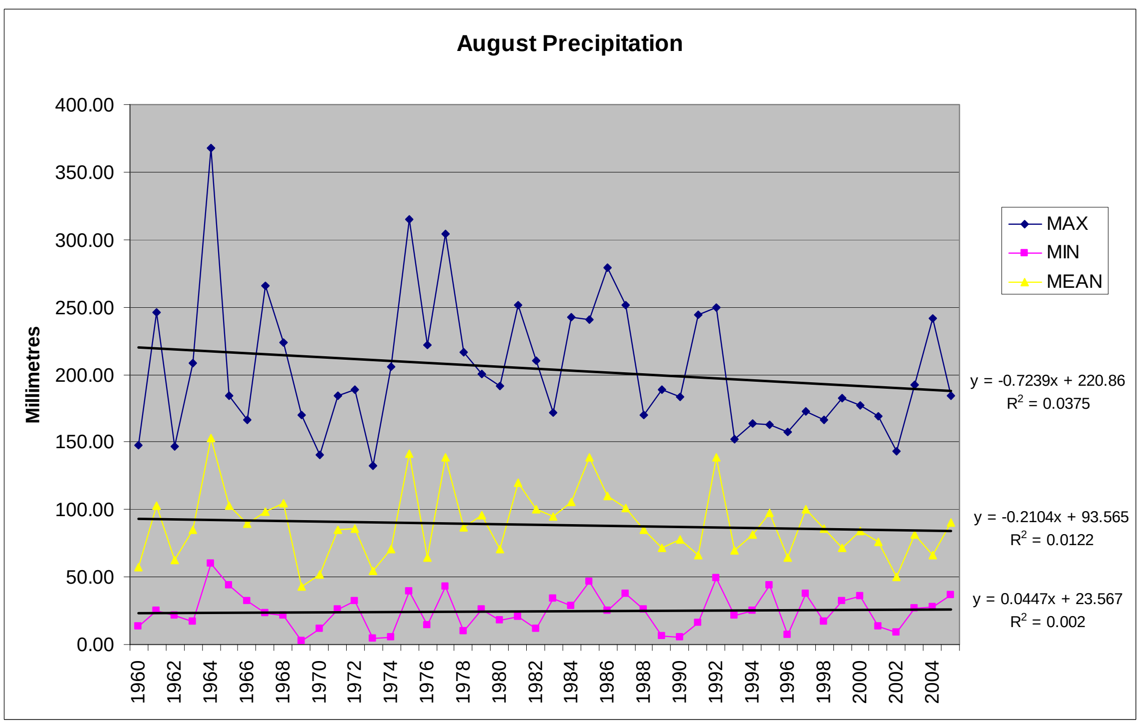
August Precipitation
Millimetres
400.00
350.00
300.00
250.00
200.00
150.00
100.00
50.00
0.00
1960
1962
1964
1966
1968
1970
1972
1974
1976
1978
1980
1982
1984
1986
1988
1990
1992
1994
1996
1998
2000
2002
2004
MAX
MIN
MEAN
y = -0.7239x + 220.86
R^2 = 0.0375
y = -0.2104x + 93.565
R^2 = 0.0122
y = 0.0447x + 23.567
R^2 = 0.002

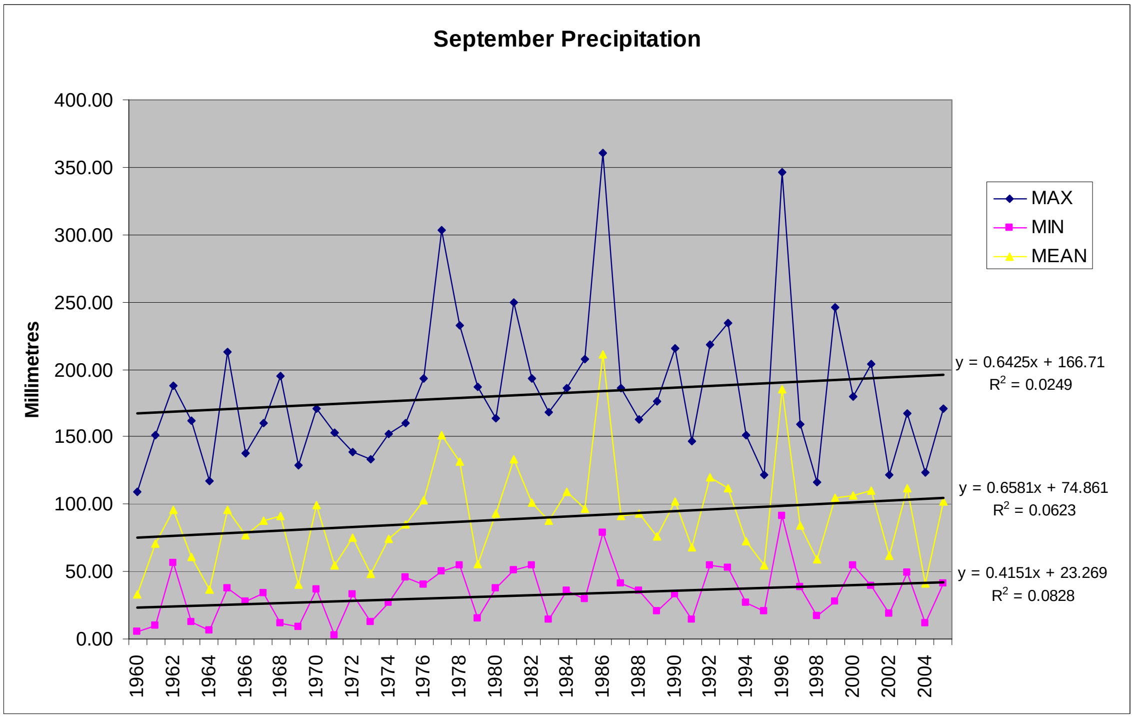

September Precipitation
Millimetres
400.00
350.00
300.00
250.00
200.00
150.00
100.00
50.00
0.00
1960
1962
1964
1966
1968
1970
1972
1974
1976
1978
1980
1982
1984
1986
1988
1990
1992
1994
1996
1998
2000
2002
2004
MAX
MIN
MEAN
y = 0.6425x + 166.71
R2 = 0.0249
y = 0.6581x + 74.861
R2 = 0.0623
y = 0.4151x + 23.269
R2 = 0.0828

Appendix C

Maps Showing Change in Average Monthly Precipitation Between 1960 to 1982 and 1983 to 2005

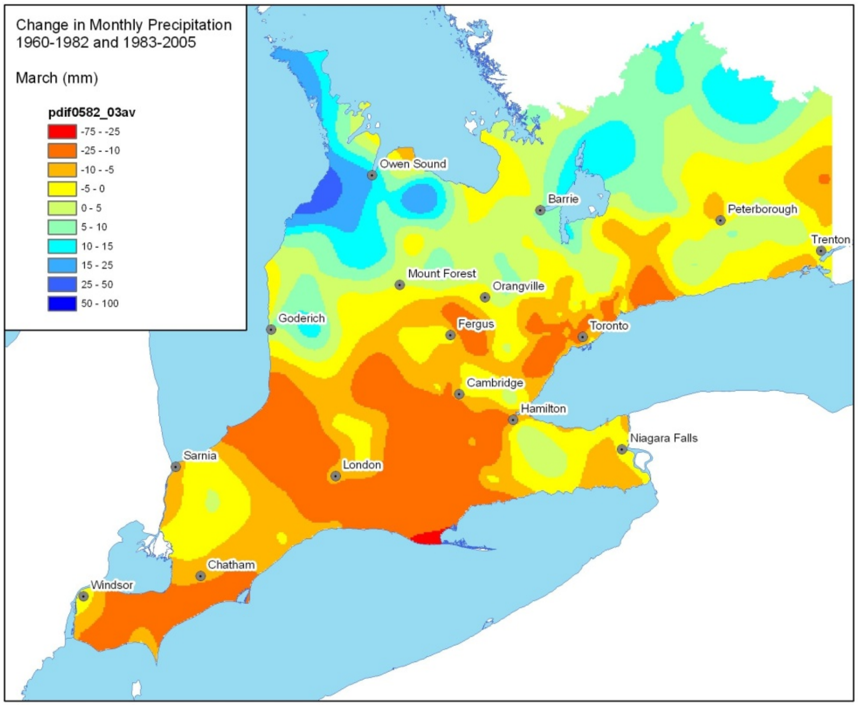

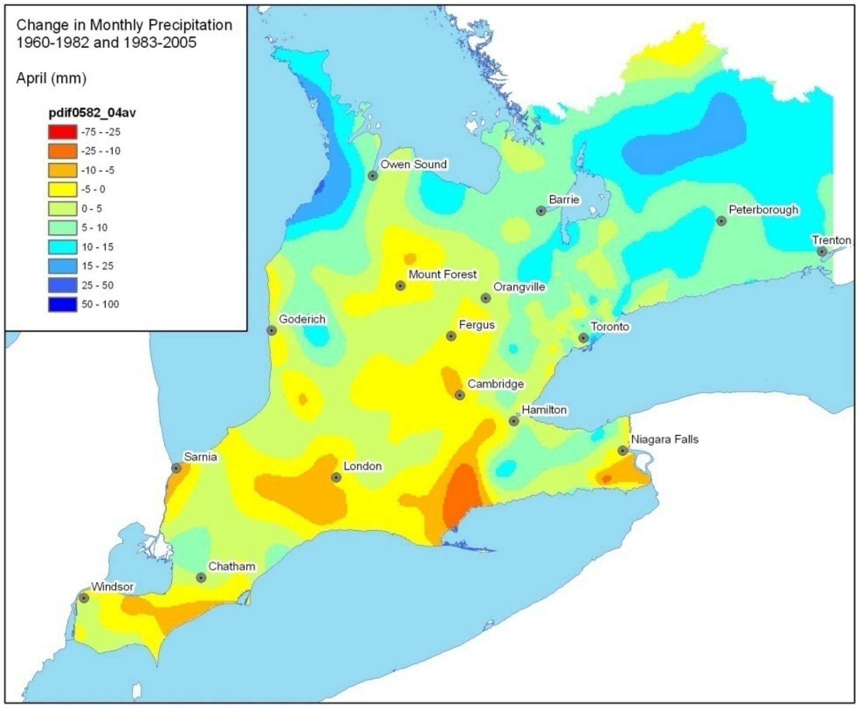

Change in Monthly Precipitation
1960-1982 and 1983-2005
April (mm)
pdif0582_04av
-75 - -25
-25 - -10
-10 - -5
-5 - 0
0 - 5
5 - 10
10 - 15
15 - 25
25 - 50
50 - 100
Owen Sound
Barrie
Peterborough
Trenton
Mount Forest
Orangville
Goderich
Fergus
Toronto
Cambridge
Hamilton
Niagara Falls
Sarnia
London
Chatham
Windsor

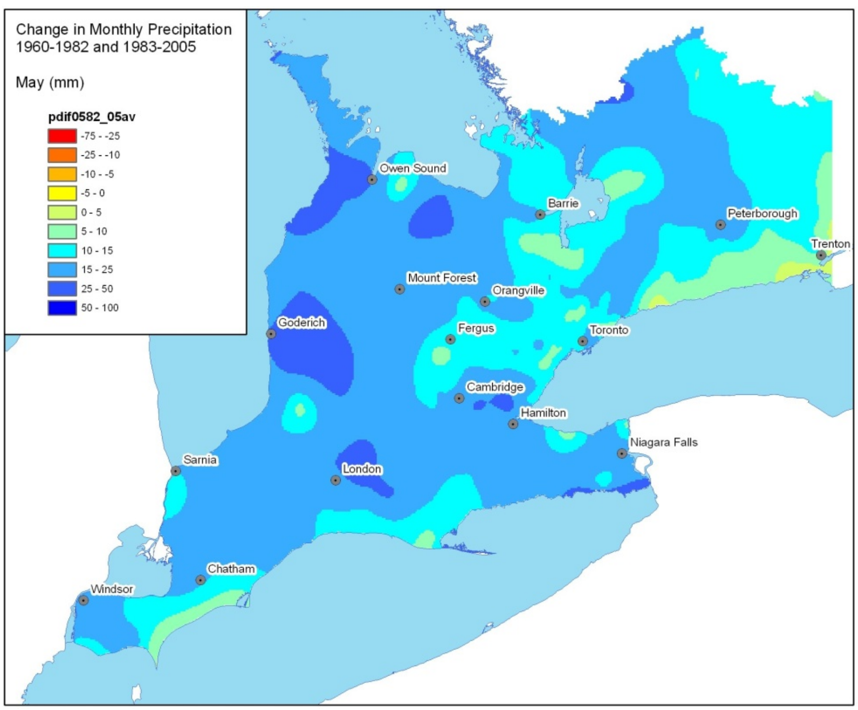

Change in Monthly Precipitation
1960-1982 and 1983-2005
May (mm)
pdif0582_05av
-75 - -25
-25 - -10
-10 - -5
-5 - 0
0 - 5
5 - 10
10 - 15
15 - 25
25 - 50
50 - 100
Owen Sound
Barrie
Peterborough
Trenton
Mount Forest
Orangville
Goderich
Fergus
Toronto
Cambridge
Hamilton
Niagara Falls
Sarnia
London
Chatham
Windsor

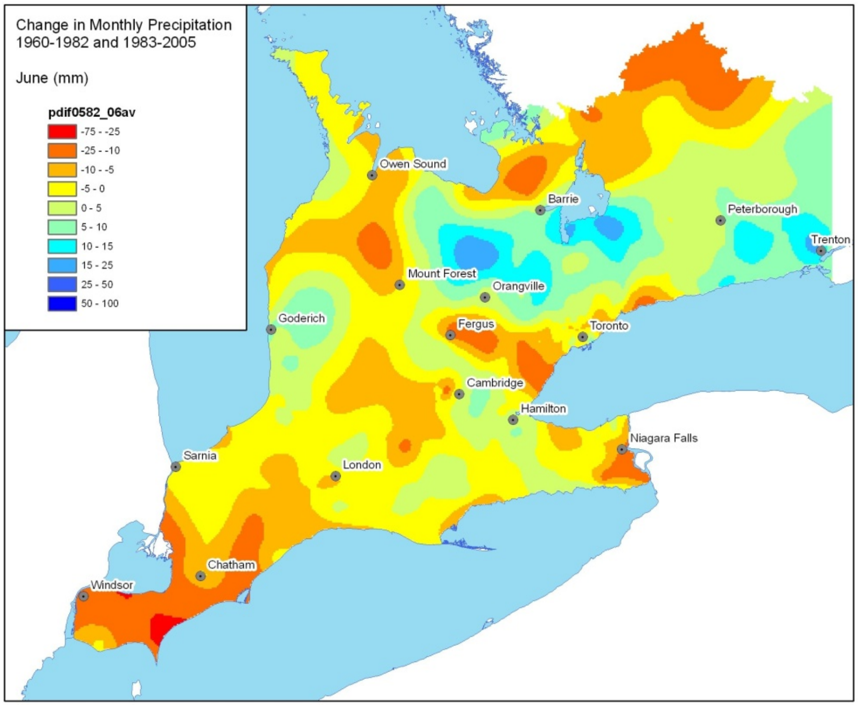
Change in Monthly Precipitation
1960-1982 and 1983-2005
June (mm)
pdif0582_06av
-75 - -25
-25 - -10
-10 - -5
-5 - 0
0 - 5
5 - 10
10 - 15
15 - 25
25 - 50
50 - 100
Owen Sound
Barrie
Peterborough
Trenton
Mount Forest
Orangville
Goderich
Fergus
Toronto
Cambridge
Hamilton
Niagara Falls
Sarnia
London
Chatham
Windsor

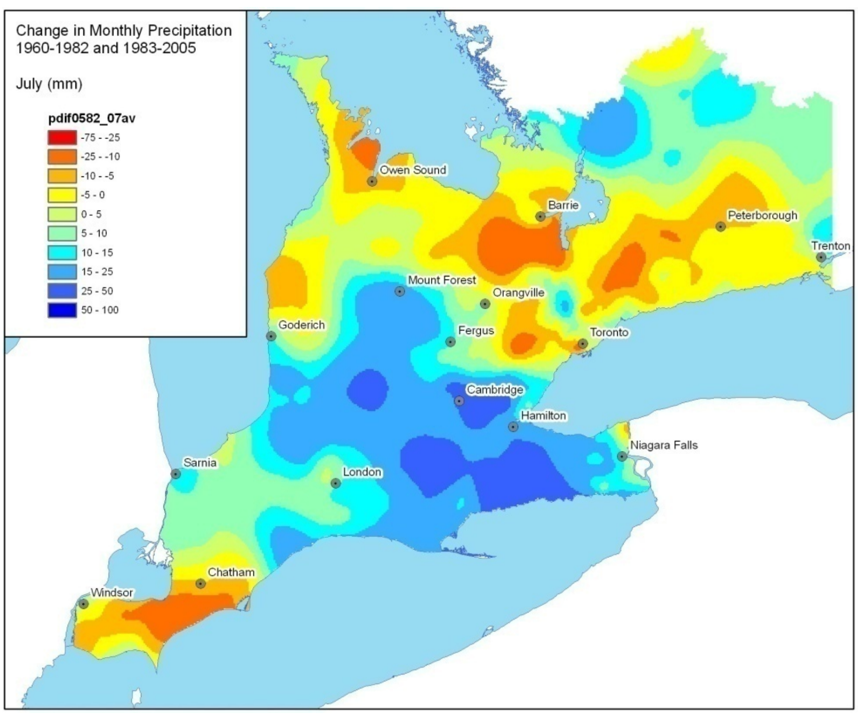
Change in Monthly Precipitation
1960-1982 and 1983-2005
July (mm)
pdif0582_07av
-75 - -25
-25 - -10
-10 - -5
-5 - 0
0 - 5
5 - 10
10 - 15
15 - 25
25 - 50
50 - 100
Owen Sound
Barrie
Peterborough
Trenton
Mount Forest
Orangville
Goderich
Fergus
Toronto
Cambridge
Hamilton
Niagara Falls
Sarnia
London
Chatham
Windsor

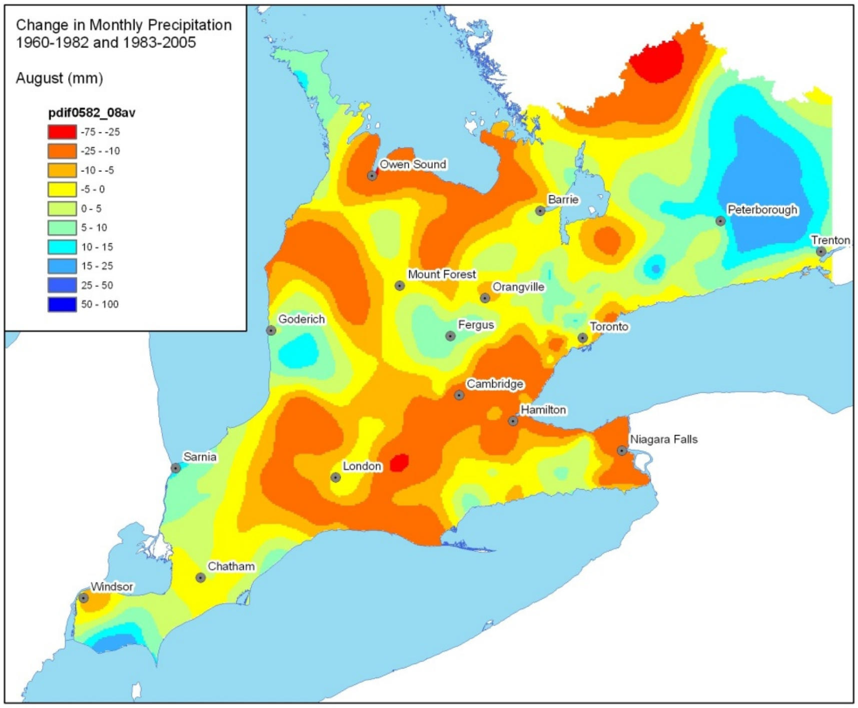

Change in Monthly Precipitation
1960-1982 and 1983-2005
August (mm)
pdif0582_08av
-75 - -25
-25 - -10
-10 - -5
-5 - 0
0 - 5
5 - 10
10 - 15
15 - 25
25 - 50
50 - 100
Owen Sound
Barrie
Peterborough
Trenton
Mount Forest
Orangville
Goderich
Fergus
Toronto
Cambridge
Hamilton
Niagara Falls
Sarnia
London
Chatham
Windsor

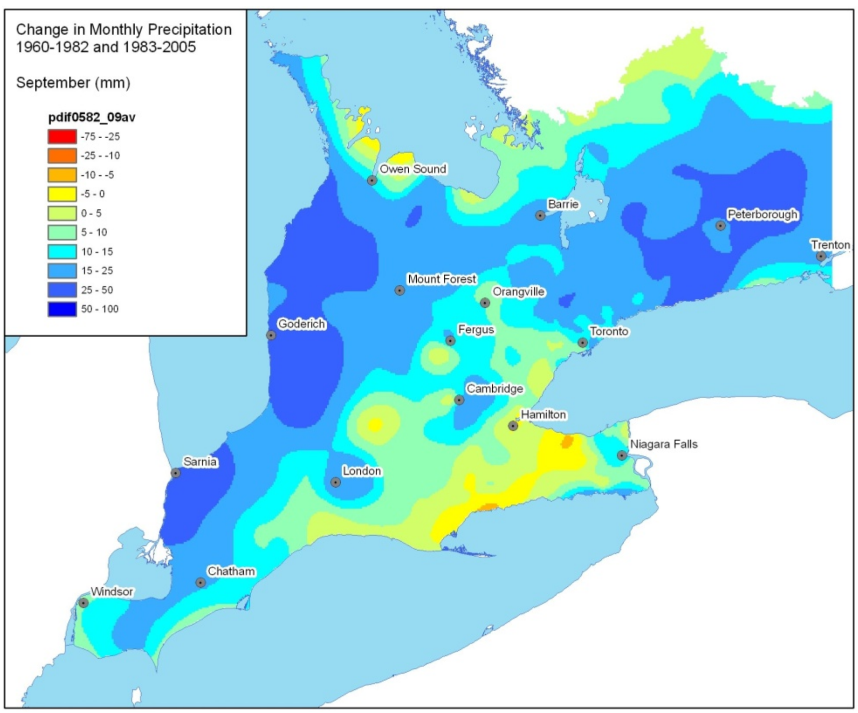

Change in Monthly Precipitation
1960-1982 and 1983-2005
September (mm)
pdif0582_09av
-75 - -25
-25 - -10
-10 - -5
-5 - 0
0 - 5
5 - 10
10 - 15
15 - 25
25 - 50
50 - 100
Owen Sound
Barrie
Peterborough
Trenton
Mount Forest
Orangville
Goderich
Fergus
Toronto
Cambridge
Hamilton
Niagara Falls
Sarnia
London
Chatham
Windsor

Appendix D

Maps Showing Number of Occurrences of Daily Precipitation Over 25 Millimetres between 1960 to 2005

The map on the left shows the total occurrences of daily precipitation of 25 mm or more per month. The map on the right shows the change between 2005-1983 and 1960-1982, blue means an increase and brown a decrease.

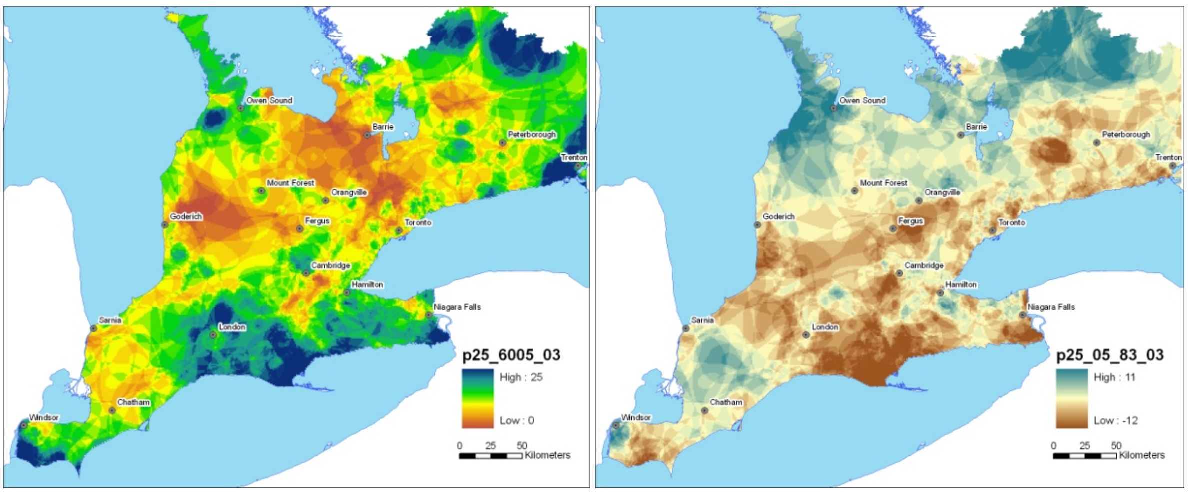

March

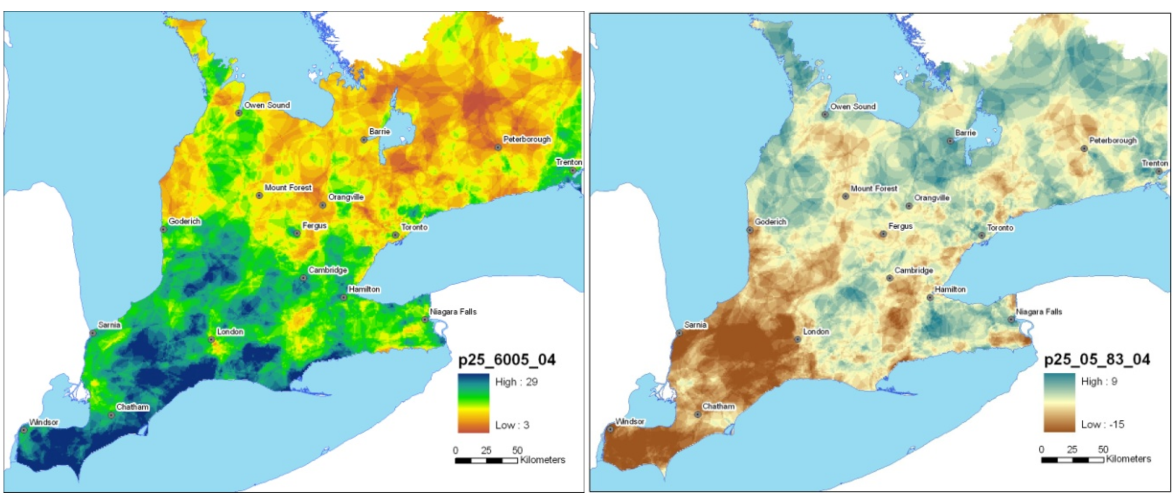

April

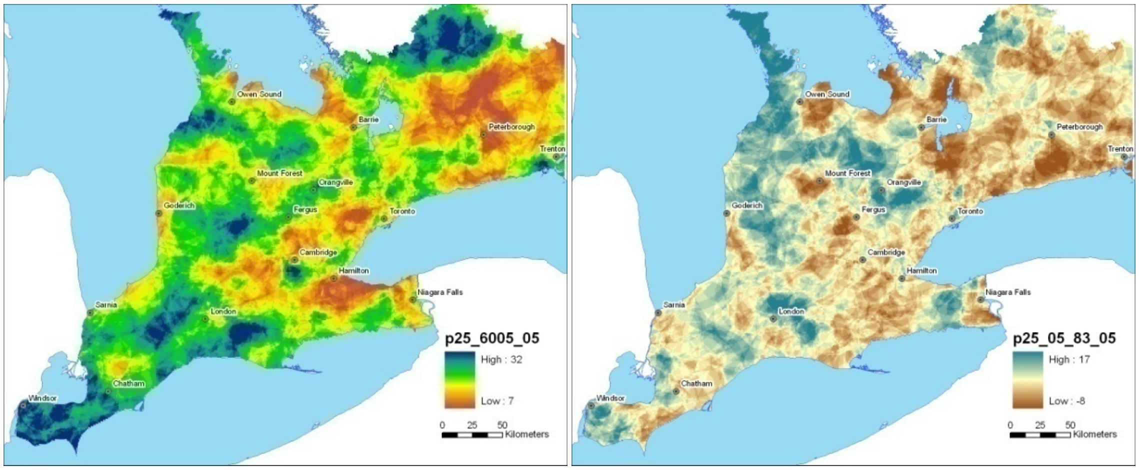

May

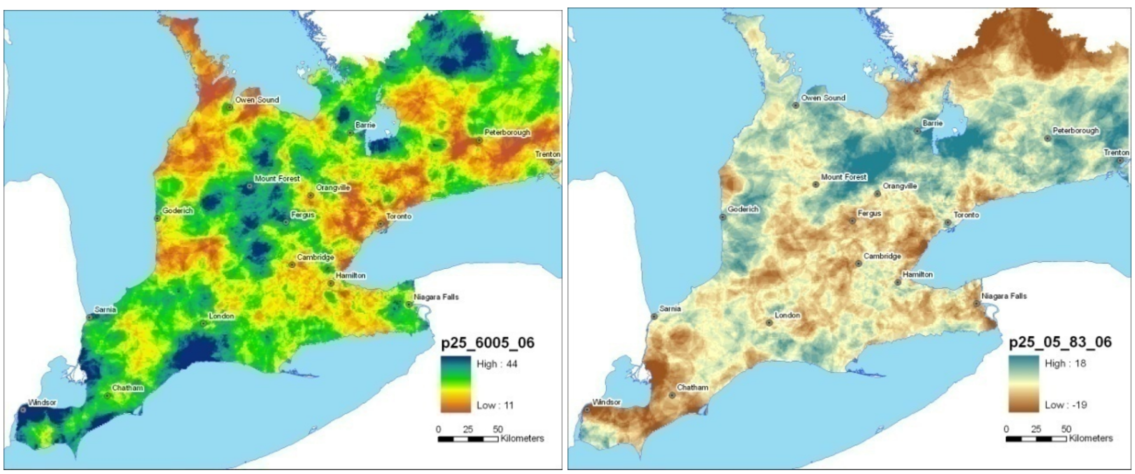

June

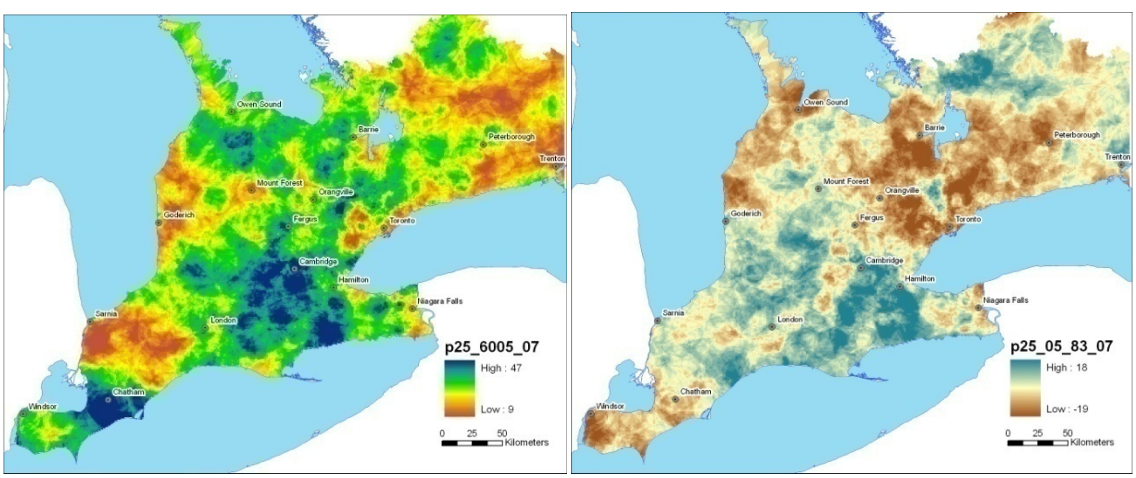

July

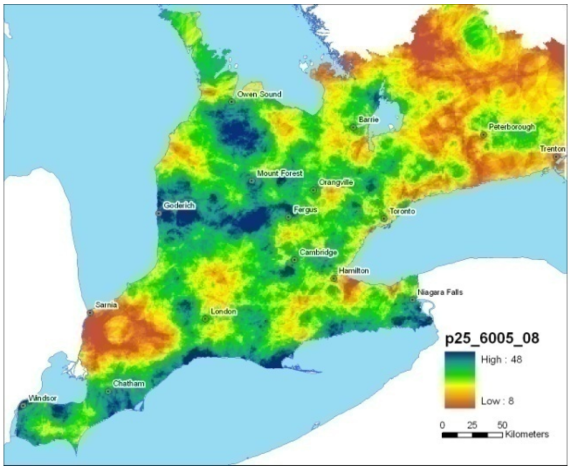

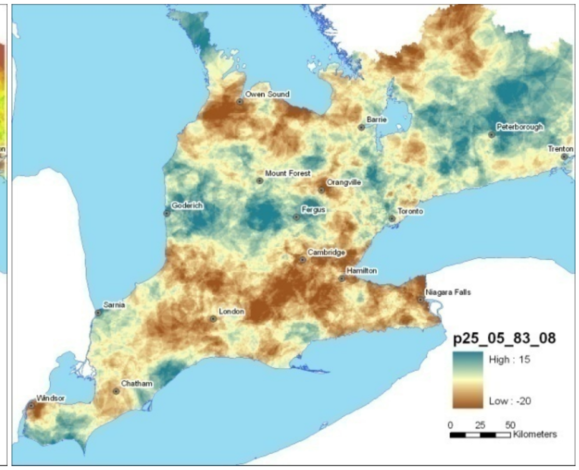

August

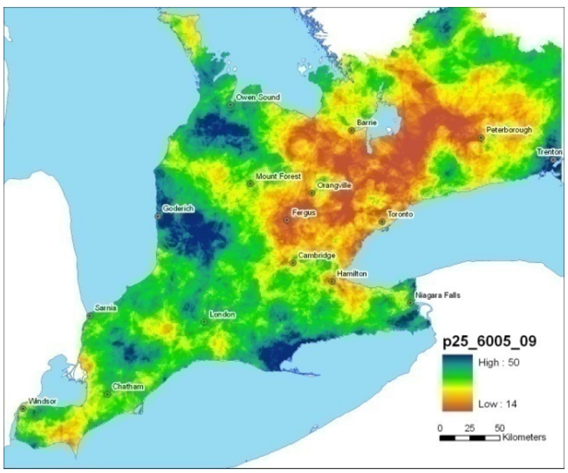

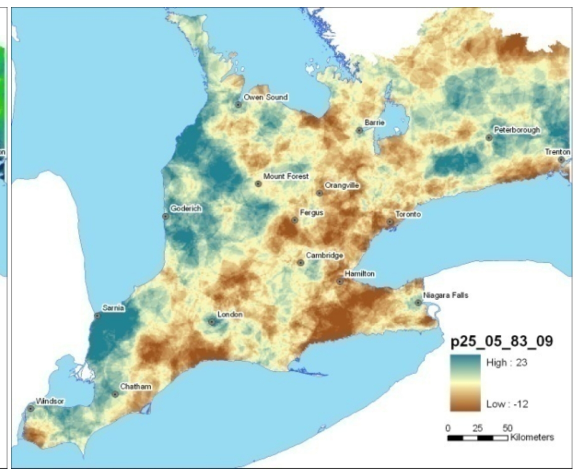

September

Appendix E

Maps Showing Number of Occurrences of Daily Precipitation Over 50 Millimetres between 1960 to 2005

The map on the left shows the total occurrences of daily precipitation of 50 mm or more per month. The map on the right shows the change between 2005-1983 and 1960-1982, blue means an increase and brown a decrease.

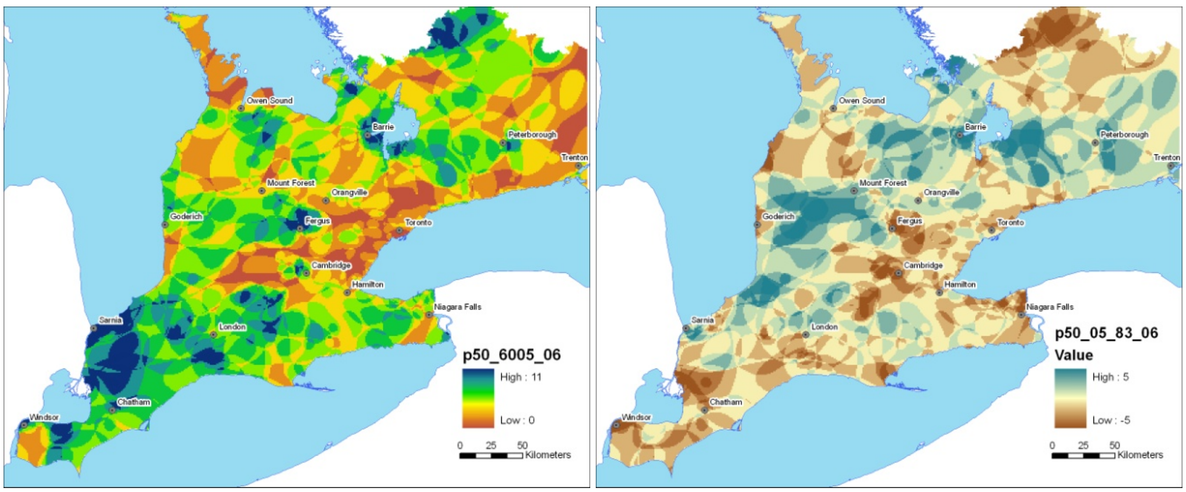

June

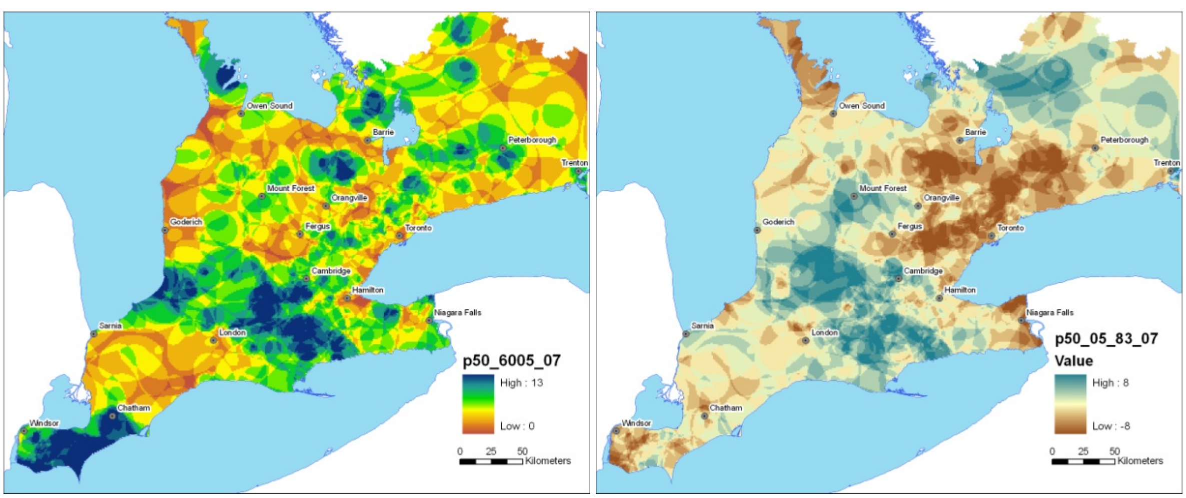

July

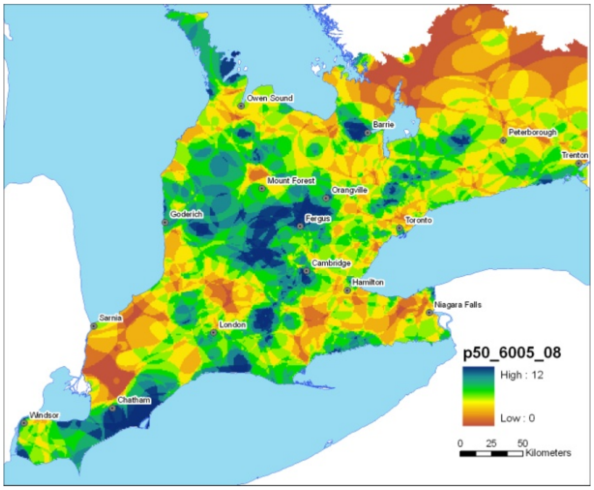

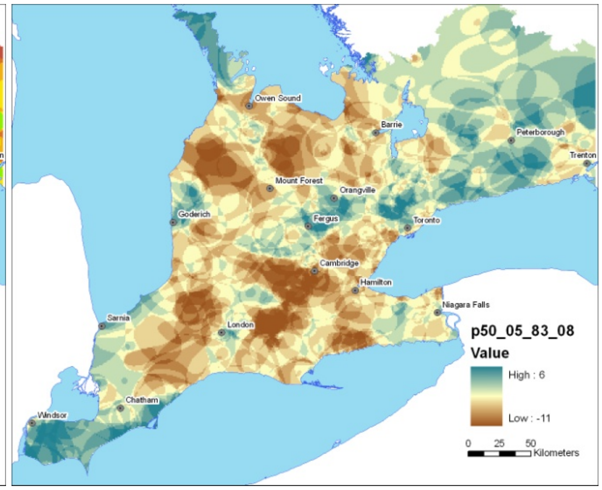

August

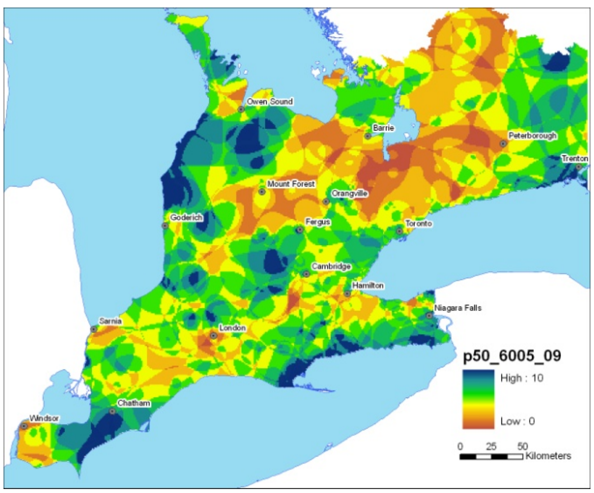

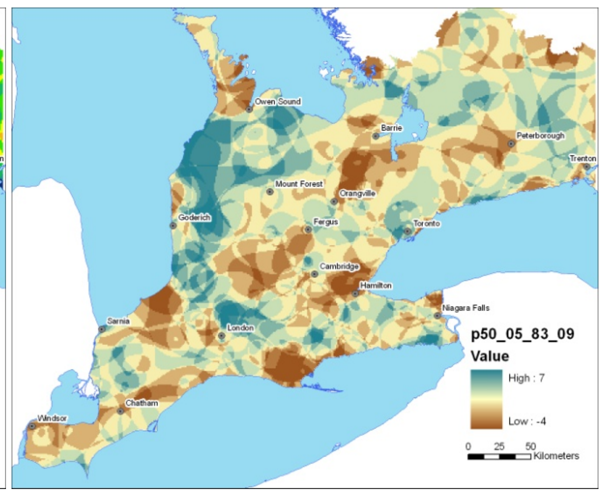

September

Appendix F

Number of Raindays 1960 to 2005 Based on Spline Surfaces

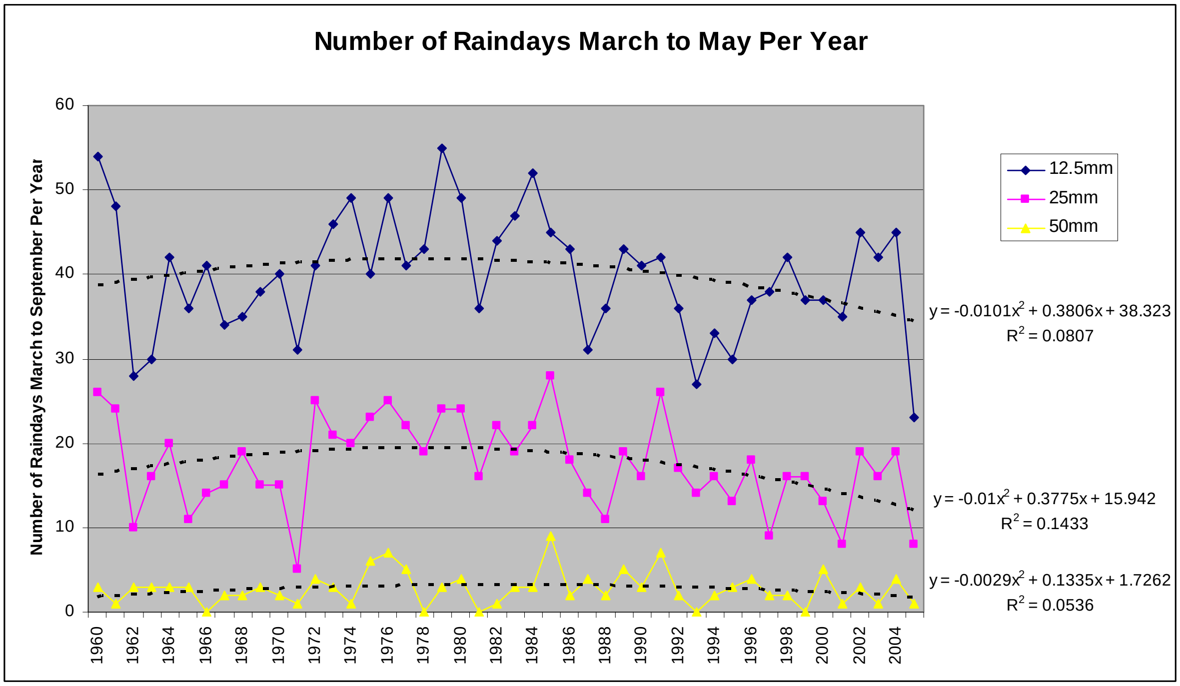

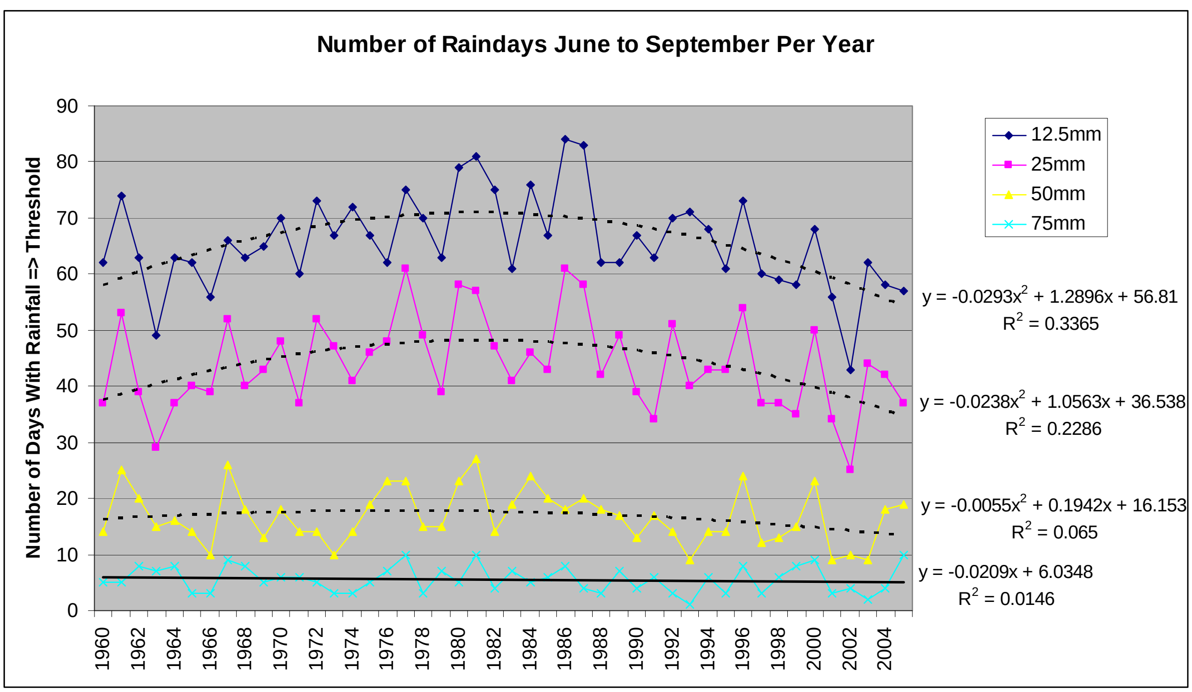

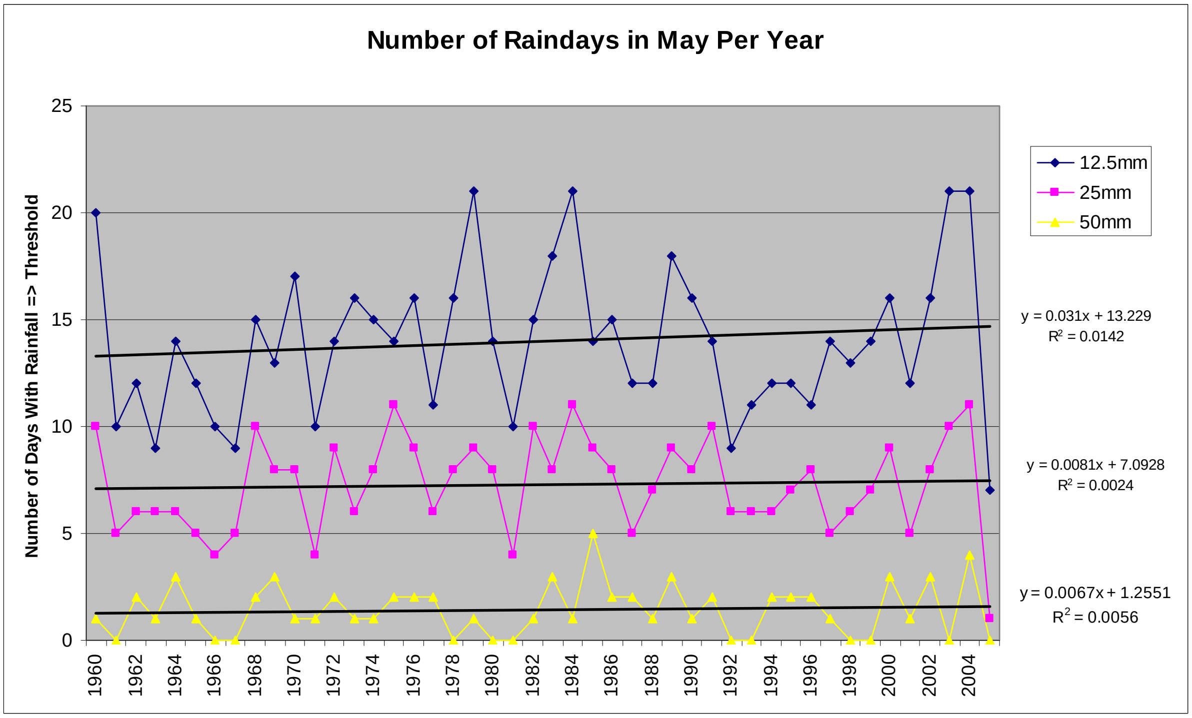
Number of Raindays in May Per Year
Number of Days With Rainfall => Threshold
12.5mm
25mm
50mm
y = 0.031x + 13.229
R2 = 0.0142
y = 0.0081x + 7.0928
R2 = 0.0024
y = 0.0067x + 1.2551
R2 = 0.0056

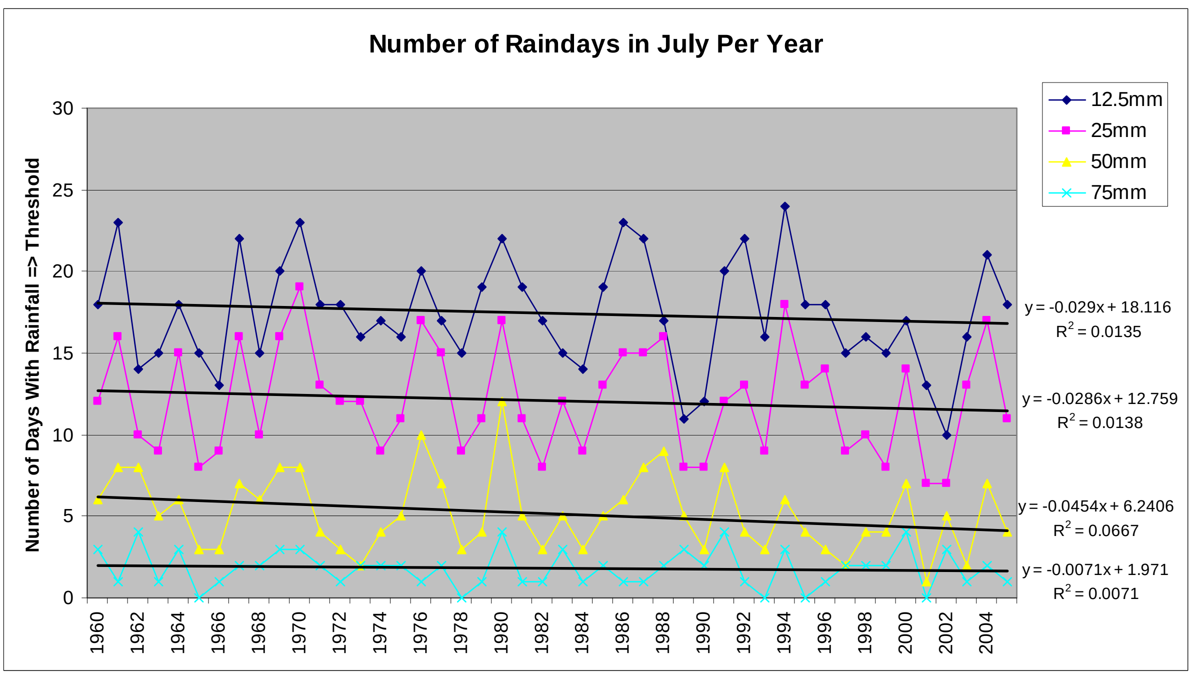
Number of Raindays in July Per Year
Number of Days With Rainfall => Threshold
12.5mm
25mm
50mm
75mm
y = -0.029x + 18.116
R2 = 0.0135
y = -0.0286x + 12.759
R2 = 0.0138
y = -0.0454x + 6.2406
R2 = 0.0667
y = -0.0071x + 1.971
R2 = 0.0071

Appendix G

Maps Showing Number of Occurrences of Daily Precipitation Over 50 and 75 Millimetres between 1996 to 2008 based on NEXRAD

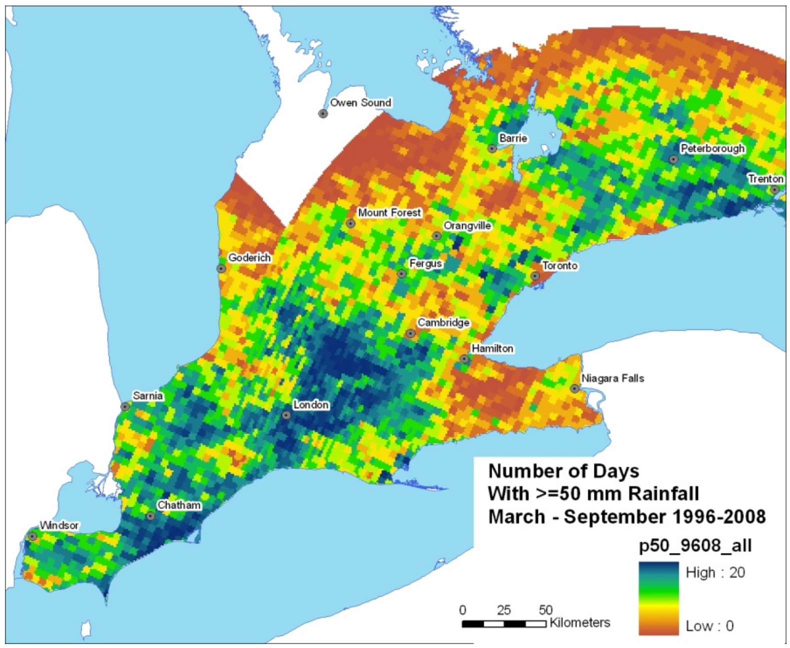

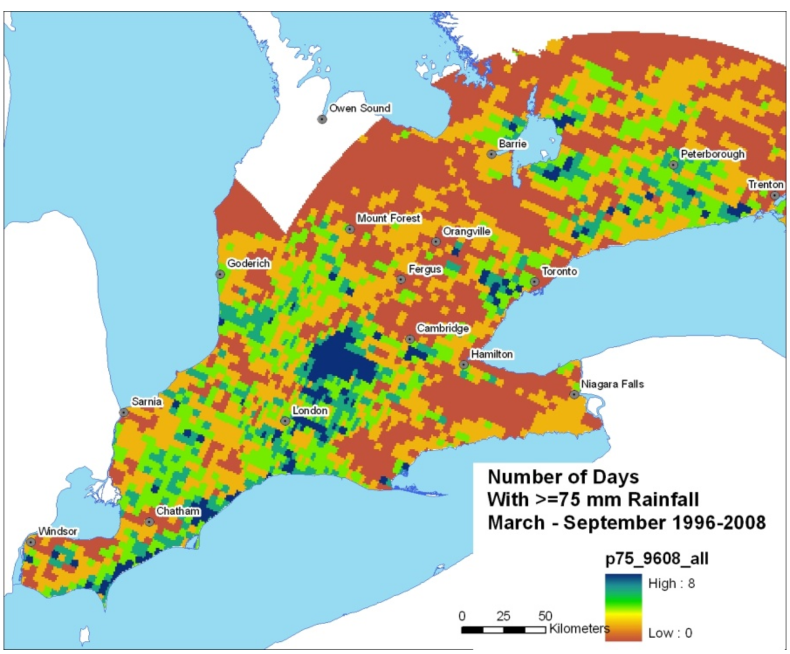

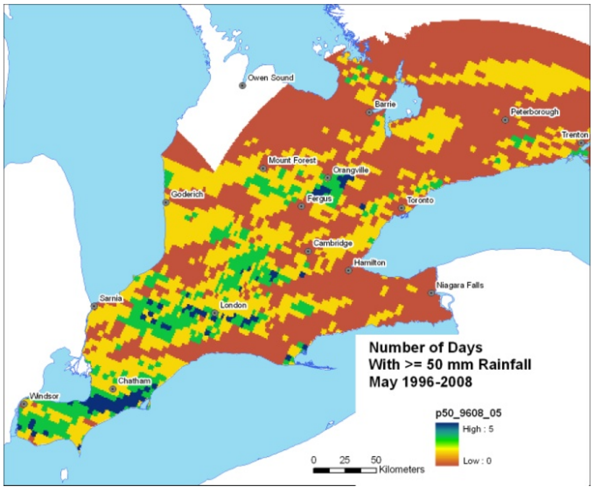
Owen Sound
Barrie
Peterborough
Trenton
Mount Forest
Orangville
Goderich
Fergus
Toronto
Cambridge
Hamilton
Niagara Falls
Sarnia
London
Chatham
Windsor
Number of Days
With >= 50 mm Rainfall
May 1996-2008
p50_9608_05
High : 5
Low : 0
0 25 50
Kilometers

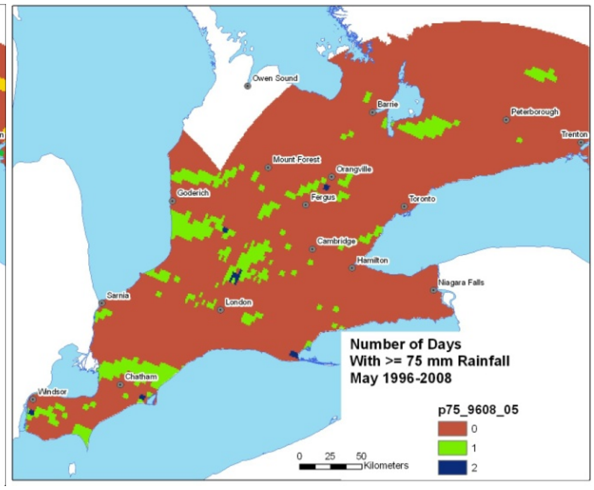
Owen Sound
Barrie
Peterborough
Trenton
Mount Forest
Orangville
Goderich
Fergus
Toronto
Cambridge
Hamilton
Niagara Falls
Sarnia
London
Chatham
Windsor
Number of Days
With >= 75 mm Rainfall
May 1996-2008
p75_9608_05
0
1
2
0 25 50
Kilometers

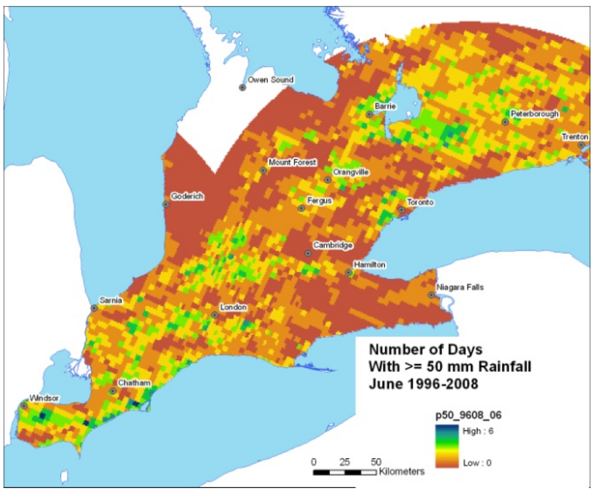
Owen Sound
Barrie
Peterborough
Trenton
Mount Forest
Orangville
Goderich
Fergus
Toronto
Cambridge
Hamilton
Niagara Falls
Sarnia
London
Chatham
Windsor
Number of Days
With >= 50 mm Rainfall
June 1996-2008
p50_9608_06
High : 6
Low : 0
0 25 50
Kilometers

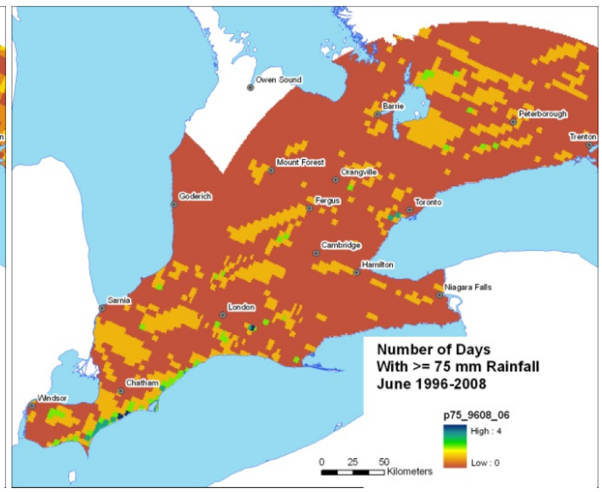
Owen Sound
Barrie
Peterborough
Trenton
Mount Forest
Orangville
Goderich
Fergus
Toronto
Cambridge
Hamilton
Niagara Falls
Sarnia
London
Chatham
Windsor
Number of Days
With >= 75 mm Rainfall
June 1996-2008
p75_9608_06
High : 4
Low : 0
0 25 50
Kilometers

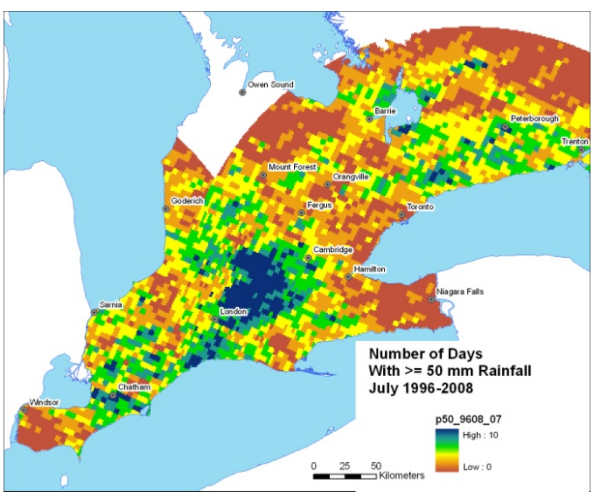
Owen Sound
Barrie
Peterborough
Trenton
Mount Forest
Orangville
Goderich
Fergus
Toronto
Cambridge
Hamilton
Niagara Falls
Sarnia
London
Chatham
Windsor
Number of Days
With >= 50 mm Rainfall
July 1996-2008
p50_9608_07
High : 10
Low : 0
0 25 50
Kilometers

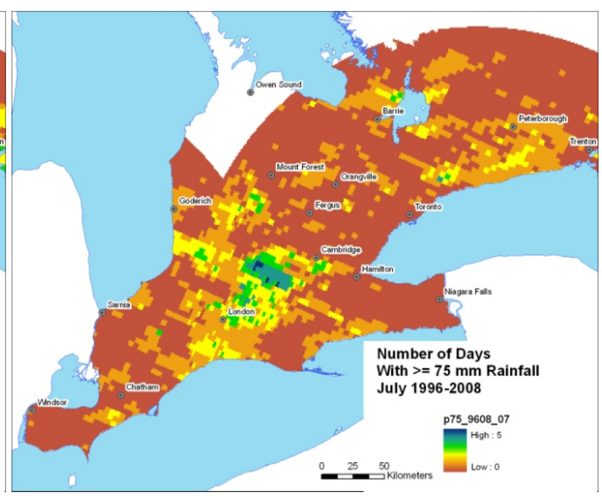
Owen Sound
Barrie
Peterborough
Trenton
Mount Forest
Orangville
Goderich
Fergus
Toronto
Cambridge
Hamilton
Niagara Falls
Sarnia
London
Chatham
Windsor
Number of Days
With >= 75 mm Rainfall
July 1996-2008
p75_9608_07
High : 5
Low : 0
0 25 50
Kilometers

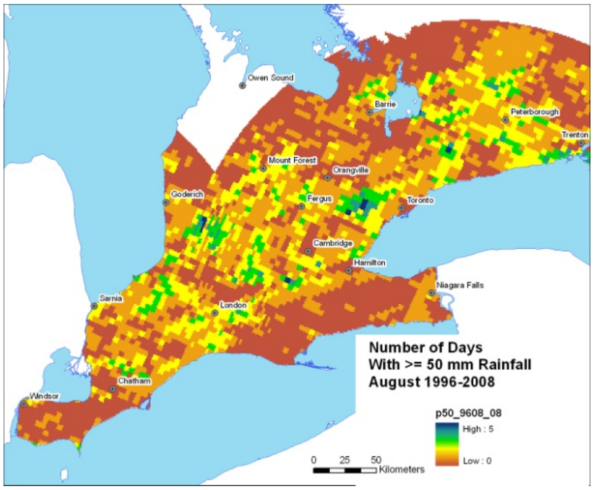
Owen Sound
Barrie
Peterborough
Trenton
Mount Forest
Orangville
Goderich
Fergus
Toronto
Cambridge
Hamilton
Niagara Falls
Sarnia
London
Chatham
Windsor
Number of Days
With >= 50 mm Rainfall
August 1996-2008
p50_9608_08
High : 5
Low : 0
0 25 50
Kilometers

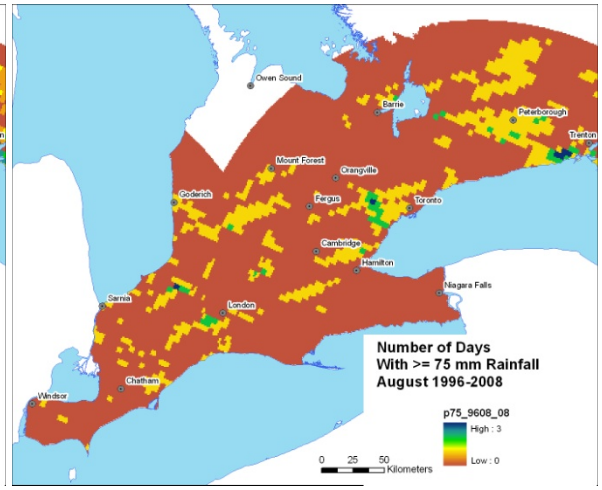
Owen Sound
Barrie
Peterborough
Trenton
Mount Forest
Orangville
Goderich
Fergus
Toronto
Cambridge
Hamilton
Niagara Falls
Sarnia
London
Chatham
Windsor
Number of Days
With >= 75 mm Rainfall
August 1996-2008
p75_9608_08
High : 3
Low : 0
0 25 50
Kilometers

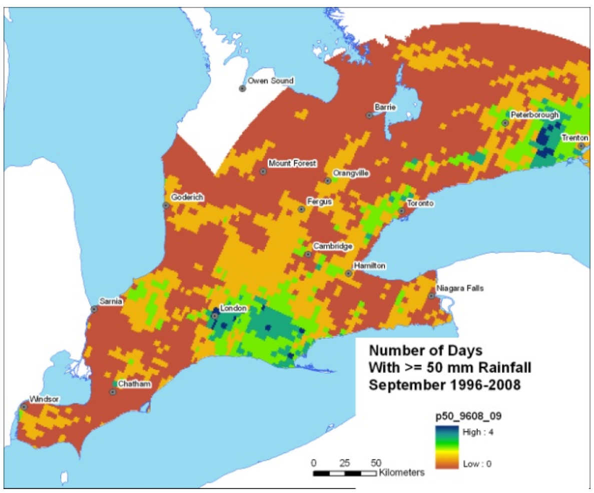
Owen Sound
Barrie
Peterborough
Trenton
Mount Forest
Orangville
Goderich
Fergus
Toronto
Cambridge
Hamilton
Niagara Falls
Sarnia
London
Chatham
Windsor
Number of Days
With >= 50 mm Rainfall
September 1996-2008
p50_9608_09
High : 4
Low : 0
0 25 50
Kilometers

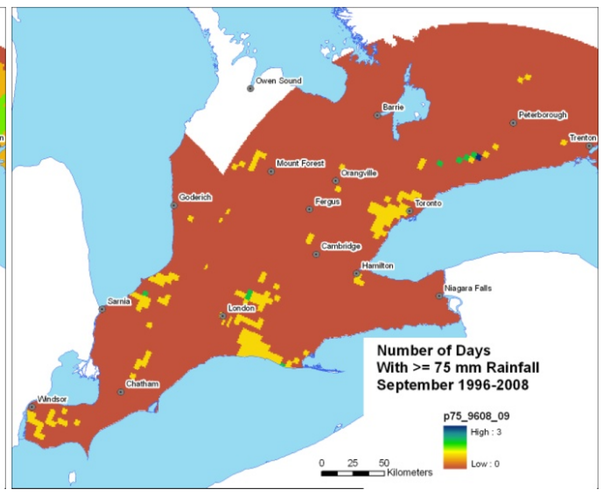
Owen Sound
Barrie
Peterborough
Trenton
Mount Forest
Orangville
Goderich
Fergus
Toronto
Cambridge
Hamilton
Niagara Falls
Sarnia
London
Chatham
Windsor
Number of Days
With >= 75 mm Rainfall
September 1996-2008
p75_9608_09
High : 3
Low : 0
0 25 50
Kilometers

Appendix H

Number of Rain-days From 1996 to 2008 Based on NEXRAD

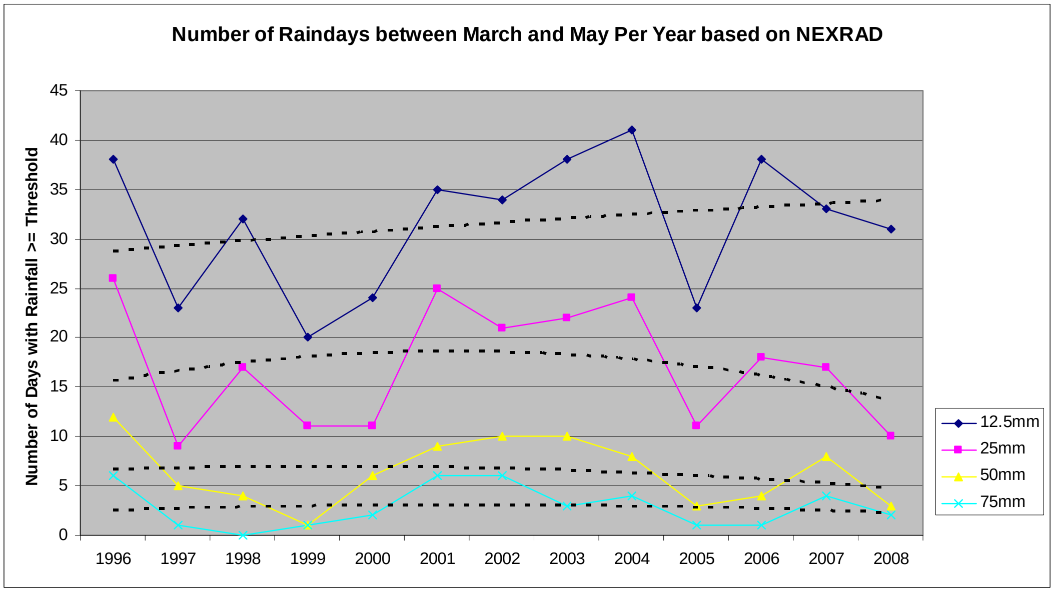

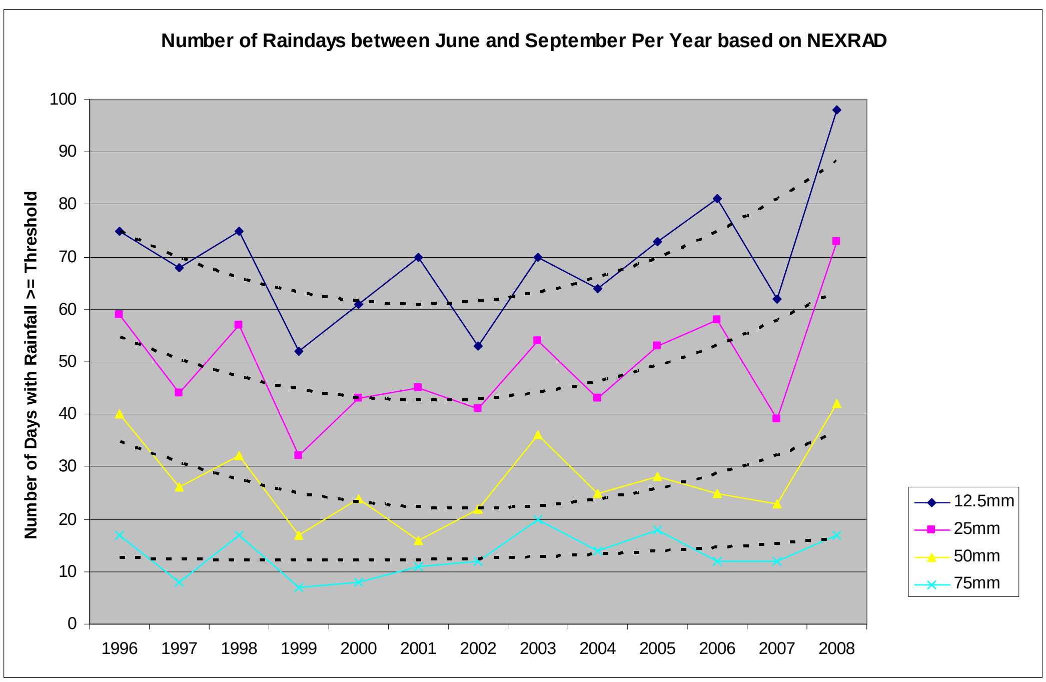

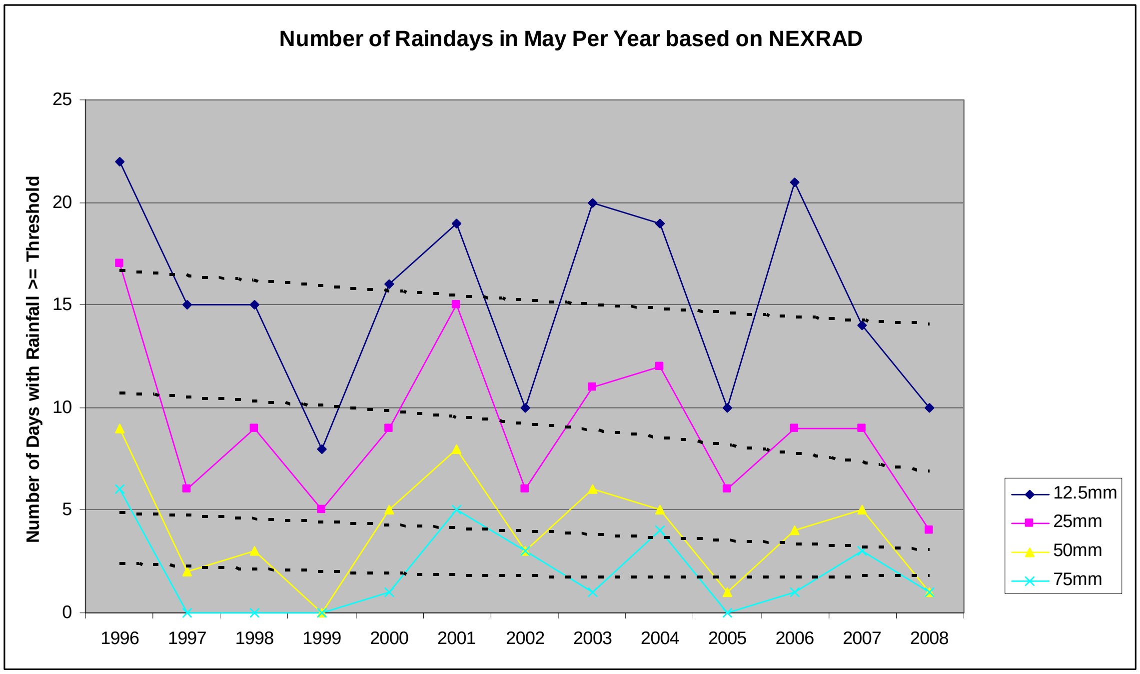
Number of Raindays in May Per Year based on NEXRAD
Number of Days with Rainfall >= Threshold
25
20
15
10
5
0
1996
1997
1998
1999
2000
2001
2002
2003
2004
2005
2006
2007
2008
12.5mm
25mm
50mm
75mm

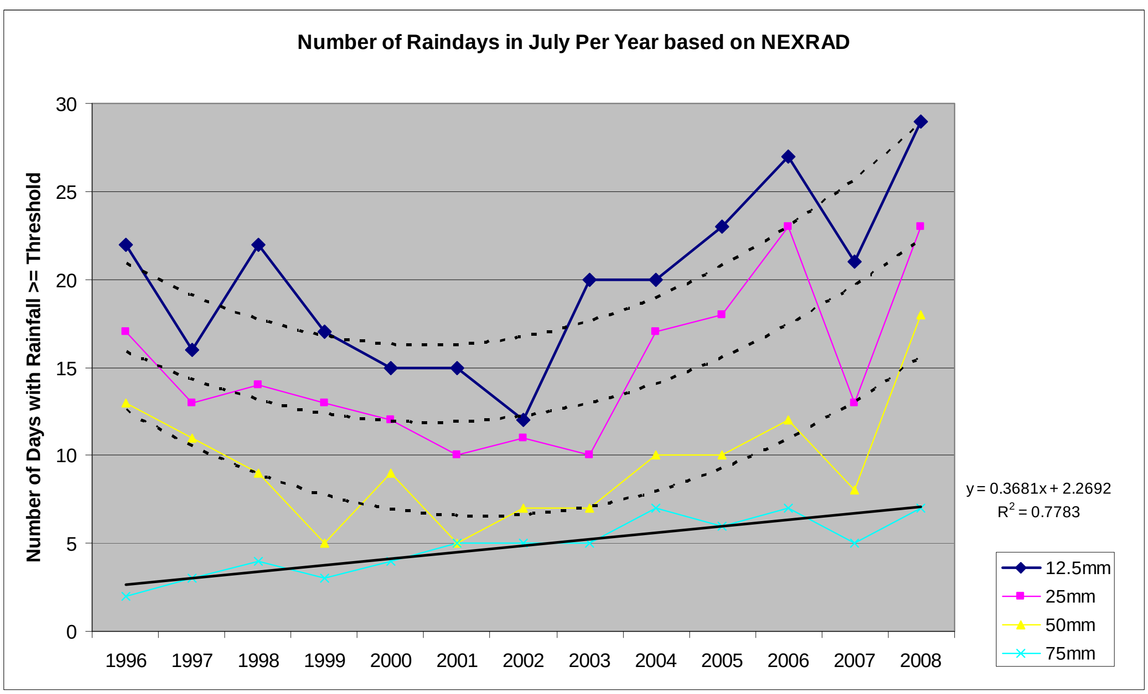
Number of Raindays in July Per Year based on NEXRAD
Number of Days with Rainfall >= Threshold
30
25
20
15
10
5
0
1996
1997
1998
1999
2000
2001
2002
2003
2004
2005
2006
2007
2008
y = 0.3681x + 2.2692
R^2 = 0.7783
12.5mm
25mm
50mm
75mm

Appendix I

1 Hour Rainfall Intensity Based on NEXRAD Radar 1996 to 2008

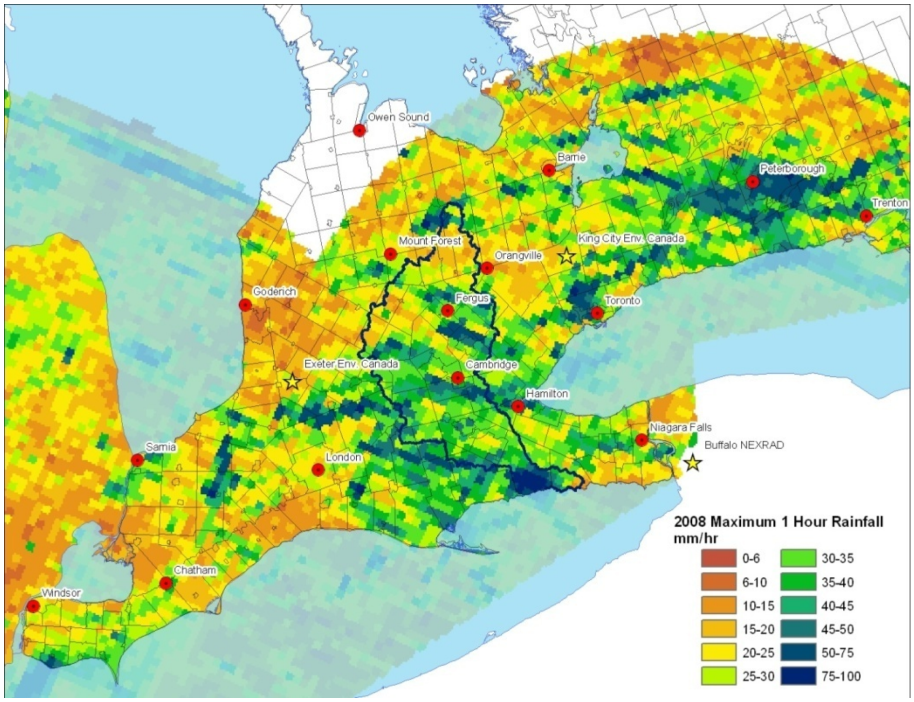

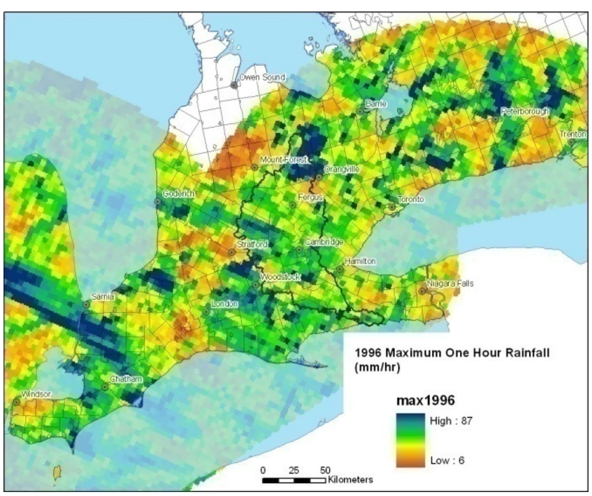

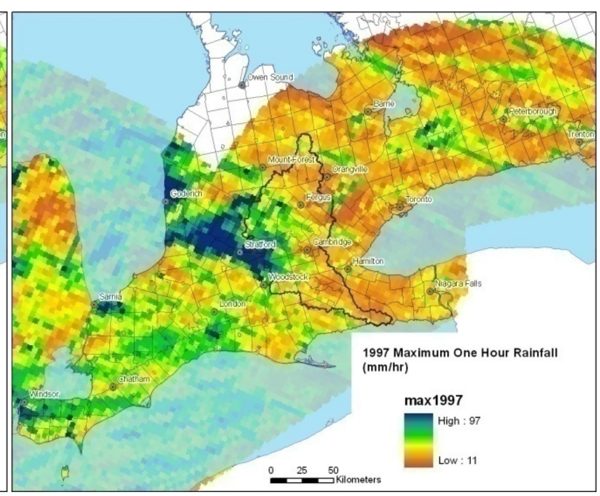

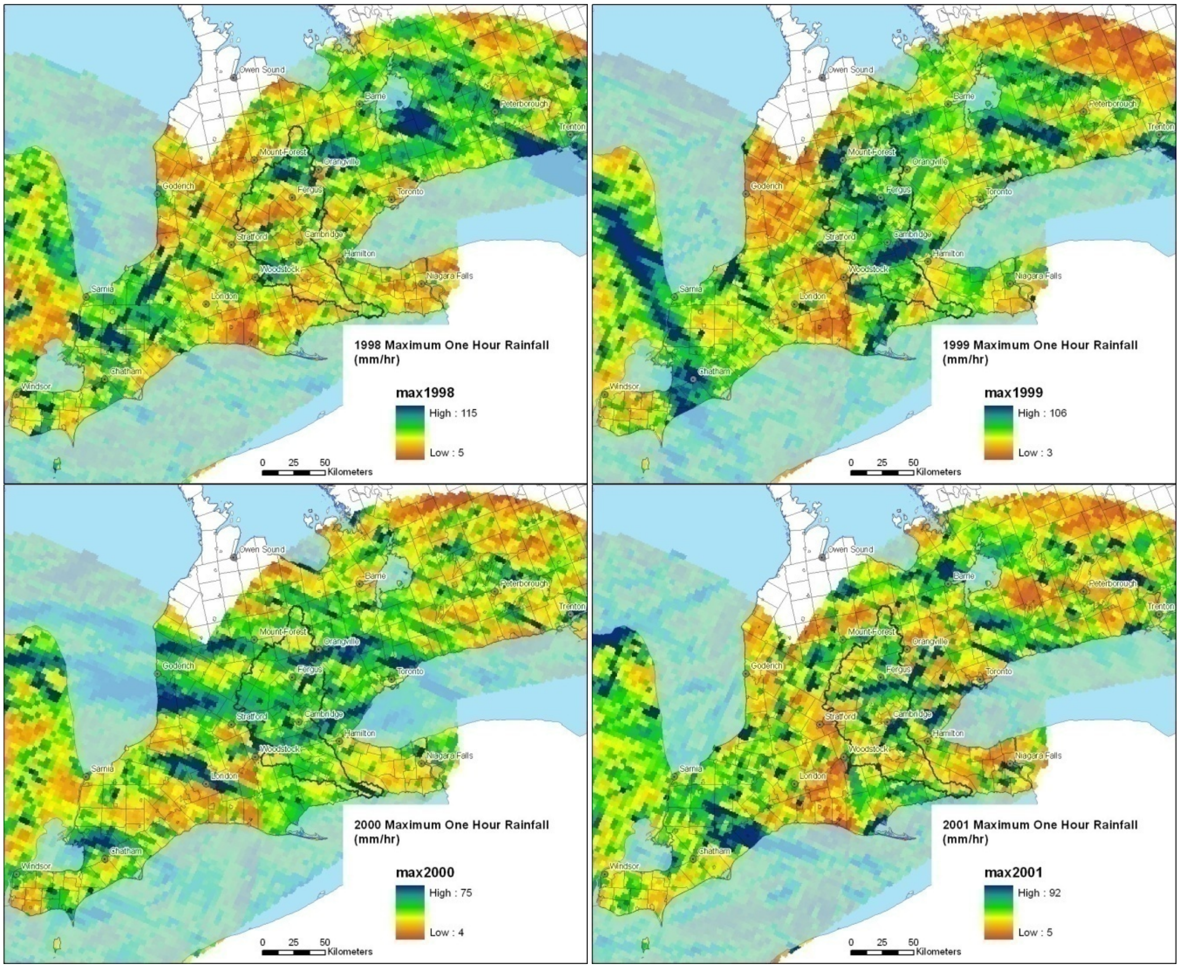

1998 Maximum One Hour Rainfall (mm/hr)
max1998
High : 115
Low : 5
1999 Maximum One Hour Rainfall (mm/hr)
max1999
High : 106
Low : 3
2000 Maximum One Hour Rainfall (mm/hr)
max2000
High : 75
Low : 4
2001 Maximum One Hour Rainfall (mm/hr)
max2001
High : 92
Low : 5
0 25 50 Kilometers
Owen Sound
Barrie
Peterborough
Trenton
Mount Forest
Orangeville
Goderich
Fergus
Toronto
Stratford
Cambridge
Hamilton
Woodstock
Niagara Falls
Sarnia
London
Chatham
Windsor

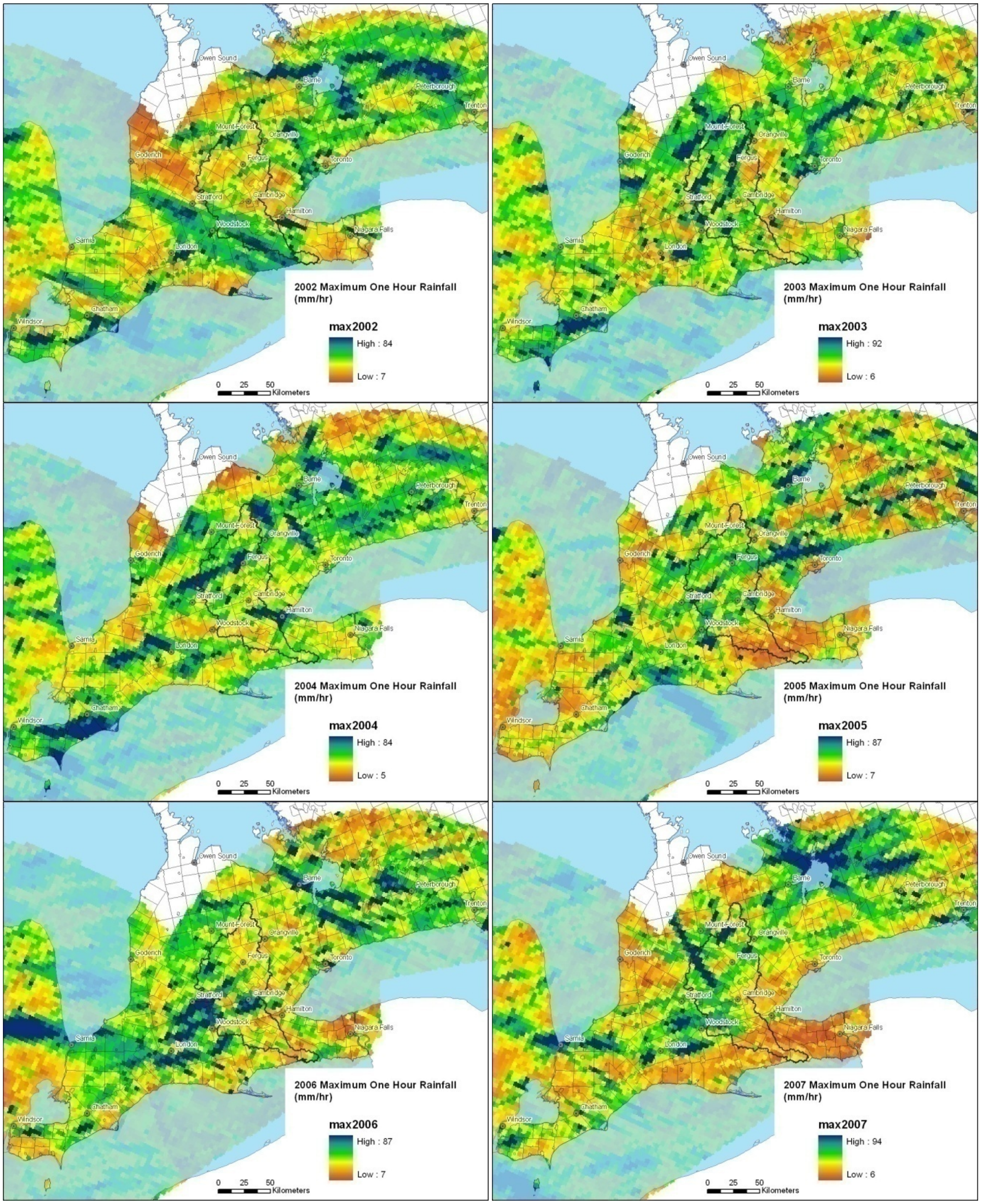
2002 Maximum One Hour Rainfall (mm/hr)
max2002
High : 84
Low : 7
0 25 50 Kilometers
2003 Maximum One Hour Rainfall (mm/hr)
max2003
High : 92
Low : 6
0 25 50 Kilometers
2004 Maximum One Hour Rainfall (mm/hr)
max2004
High : 84
Low : 5
0 25 50 Kilometers
2005 Maximum One Hour Rainfall (mm/hr)
max2005
High : 87
Low : 7
0 25 50 Kilometers
2006 Maximum One Hour Rainfall (mm/hr)
max2006
High : 87
Low : 7
0 25 50 Kilometers
2007 Maximum One Hour Rainfall (mm/hr)
max2007
High : 94
Low : 6
0 25 50 Kilometers

Appendix J

Difference Between Environment Canada 1 Hour IDF Maximums and 1 Hour Rainfall Intensity Based on NEXRAD Radar 1996 to 2008

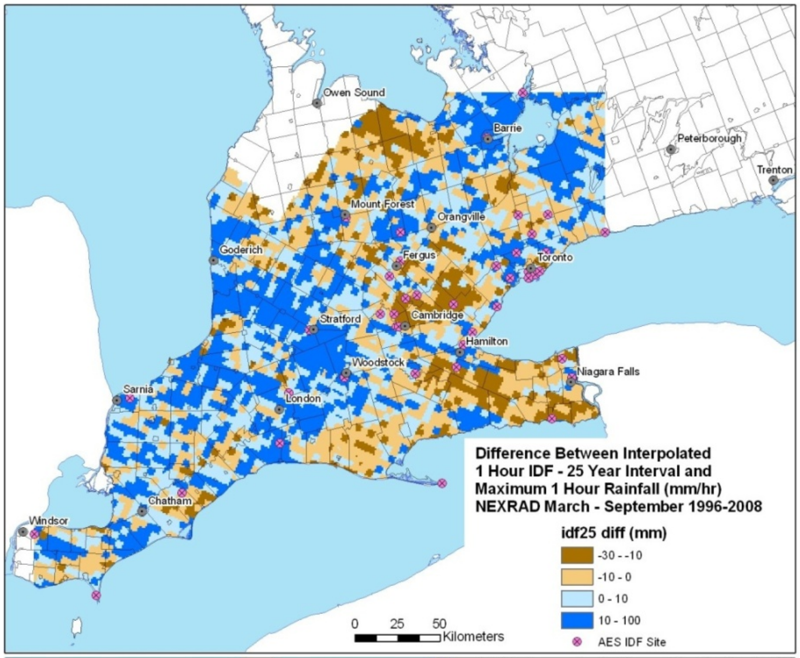

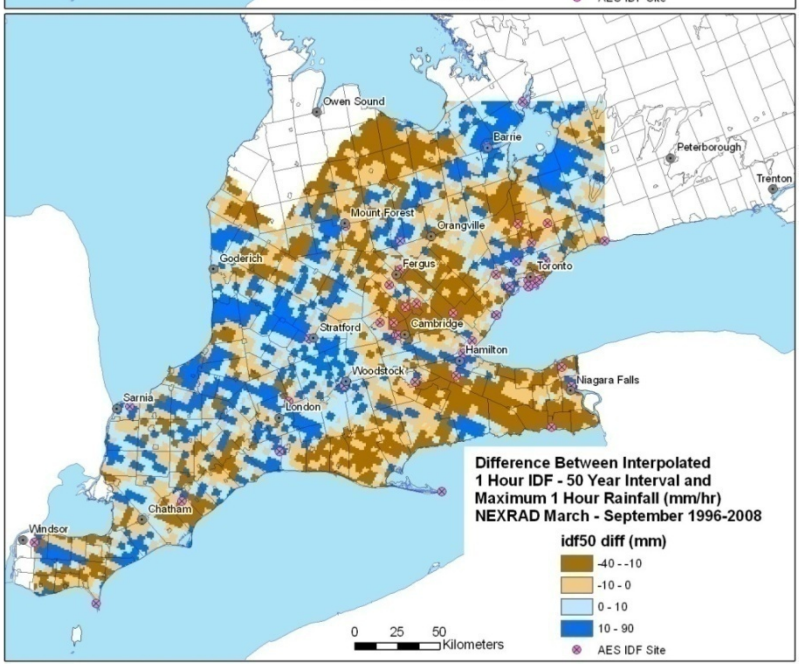

Table of Environment Canada 1 Hour IDF Values Compared to 1 Hour Maximum From NEXRAD

MSC IDF Station				NEXRAD 1996-2008		MSC IDF Statistics			MSC IDF 1 Hour Intensity By Interval					
AES_STID	NAME	start_yr	end_yr	1 Hr max	1 Hour avg	hr_max	max_yr	hr_avg	2-yr	5-yr	10-yr	25-yr	50-yr	100-yr
6127514	SARNIA A	1962	2002	60	35.2	48.3	1962	26.6	25.1	33.4	39.0	46.0	51.1	56.3
6155722	OAK RIDGES	1927	1948	42	25.1	64.8	1946	25.9	23.9	34.6	41.7	50.7	57.4	64.0
6155878	OSHAWA WPCP	1970	2003	33	21.6	41.2	1979	21.5	20.2	27.3	32.0	38.0	42.4	46.8
6158084	STOUFFVILLE WPCP	1961	1989	50	27.5	47.8	1967	25.2	23.3	33.7	40.7	49.5	56.0	62.4
6158350	TORONTO	1940	2003	65	30.8	50.0	1974	25.4	23.8	32.6	38.5	45.9	51.4	56.9
6158406	TORONTO BOOTH	1966	1992	39	23.2	61.2	1974	24.6	22.7	33.3	40.4	49.3	55.9	62.5
6158520	TORONTO ELLESMERE	1966	1994	58	29.6	47.8	1977	22.7	21.1	29.7	35.3	42.5	47.8	53.0
6158525	TORONTO ETOBICOKE	1964	1980	65	29.4	49.0	1968	24.1	22.6	30.7	36.1	43.0	48.0	53.0
6158575	TORONTO GREENWOOD	1966	1981	52	23.5	47.0	1974	23.6	21.8	31.5	38.0	46.1	52.1	58.1
6158665	TORONTO ISLAND A	1971	1994	50	23.0	55.1	1974	26.7	24.9	34.8	41.4	49.7	55.9	62.0
6158718	TORONTO KEELE-FINCH	1964	1987	75	38.8	48.6	1980	25.5	23.7	33.5	40.0	48.3	54.4	60.4
6158733	TORONTO MALTON A	1950	2003	39	24.1	47.5	1970	34.2	22.7	30.4	35.6	42.0	46.8	51.6
6110557	BARRIE WPCC	1979	1990	63	29.3	32.3	1986	23.0	22.2	26.4	29.2	32.7	35.3	37.9
6115820	ORILLIA TS	1965	2003	47	24.6	44.7	1967	26.2	24.8	32.5	37.6	44.0	48.8	53.6
6134610	LONG POINT	1967	1984	40	23.5	78.4	1980	24.3	21.8	35.4	44.4	55.8	64.2	72.6
6135638	NIAGARA FALLS	1965	1990	30	20.6	47.0	1983	22.6	21.2	28.7	33.8	40.1	44.8	49.5
6136606	PORT COLBORNE	1964	2000	30	18.2	60.0	1991	24.5	22.9	31.6	37.4	44.7	50.2	55.5
6137147	RIDGETOWN	1959	2003	53	31.8	68.6	1962	29.9	27.9	38.7	45.8	54.8	61.4	68.0
6137287	ST CATHARINES A	1954	2003	42	21.5	49.3	1972	24.7	23.4	30.6	35.4	41.5	46.0	50.5
6137362	ST THOMAS WPCP	1926	2002	75	28.7	60.2	1935	27.2	25.6	34.5	40.4	47.8	53.3	58.8
6139525	WINDSOR A	1946	2003	84	29.9	56.7	1995	29.0	27.2	36.6	42.8	50.6	56.4	62.1
613FN58	POINT PELEE	1975	2003	42	28.2	63.2	1989	28.2	26.1	37.4	44.8	54.2	61.2	68.2
6140954	BRANTFORD OWRC	1961	2001	35	24.4	42.9	1977	23.9	22.6	29.5	34.0	39.7	43.9	48.1
6141095	GALT	1980	1992	39	26.0	48.4	1987	25.5	23.9	33.0	39.0	46.7	52.3	58.0
6142400	FERGUS SHAND DAM	1962	2003	53	26.6	86.9	1967	27.7	25.1	39.2	48.7	60.5	69.3	78.1
6142991	GRAND VALLEY STP	1980	1991	65	29.6	42.8	1984	23.8	22.6	29.5	34.0	39.8	44.1	48.3
6143069	GUELPH ARBORETUM	1954	2003	46	24.5	55.8	1982	24.2	22.3	32.3	39.0	47.3	53.6	59.7
6143087	GUELPH SMALLFIELD FARM	1954	1964	42	26.3	63.5	1964	27.1	24.6	38.2	47.3	58.8	67.3	75.7
6144241	KITCHENER CITY ENG 2	1955	1967	49	26.4	43.7	1960	24.3	22.9	30.1	34.8	40.7	45.1	49.5

AES_STID	NAME	start_yr	end_year	1 Hr max	1 Hour Avg	hr_max	max_yr	hr_avg	2-yr	5-yr	10-yr	25-yr	50-yr	100-yr
6144475	LONDON A	1943	2003	53	29.2	83.3	1953	26.4	24.4	35.2	42.3	51.3	58.0	64.6
MSC IDF Station				NEXRAD 1996-2008		MSC IDF Statistics			MSC IDF 1 Hour Intensity By Interval					
AES_STID	NAME	start_yr	end_year	1 Hr max	1 Hour Avg	hr_max	max_yr	hr_avg	2-yr	5-yr	10-yr	25-yr	50-yr	100-yr
6145503	MOUNT FOREST	1962	1986	42	24.5	49.2	1985	26.4	24.8	33.3	39.0	46.1	51.4	56.7
6146714	PRESTON WPCP	1971	1996	45	25.2	43.1	1990	25.3	23.7	32.2	37.9	45.1	50.4	55.6
6148105	STRATFORD OWRC	1966	2003	53	27.1	65.2	2002	25.1	23.2	33.2	39.9	48.3	54.5	60.7
6149387	WATERLOO WELLINGTON A	1971	2003	45	26.9	61.5	1988	26.7	24.3	37.3	45.9	56.7	64.7	72.7
6149625	WOODSTOCK	1962	2003	82	31.5	42.9	1970	24.6	23.4	30.1	34.5	40.2	44.3	48.5
614B2H4	ELORA AUTOMATIC CLIMATE STATION	1970	2002	47	31.0	46.0	1982	25.6	24.1	32.2	37.6	44.4	49.4	54.4
6151059	BURLINGTON FIRE HQ'S	1970	1982	46	28.5	41.4	1982	25.6	24.2	31.9	37.0	43.5	48.3	53.1
6153194	MOUNT HOPE A	1971	2003	47	22.2	77.0	1989	27.0	25.1	35.4	42.3	50.9	57.3	63.7
6153300	HAMILTON RBG	1963	2003	55	26.2	37.1	1974	22.5	21.6	26.6	30.0	34.2	37.3	40.4
6155187	MILTON KELSO	1960	1974	56	25.8	72.1	1969	30.9	27.8	44.5	55.5	69.5	79.9	90.1
615HMAK	TORONTO BUTTONVILLE A	1986	2003	45	29.1	57.6	1986	24.2	22.3	32.4	39.2	47.7	54.0	60.2
615N745	OAKVILLE SOUTHEAST OWRC	1965	1976	43	26.5	33.5	1971	23.9	22.8	28.3	32.0	36.6	40.0	43.4

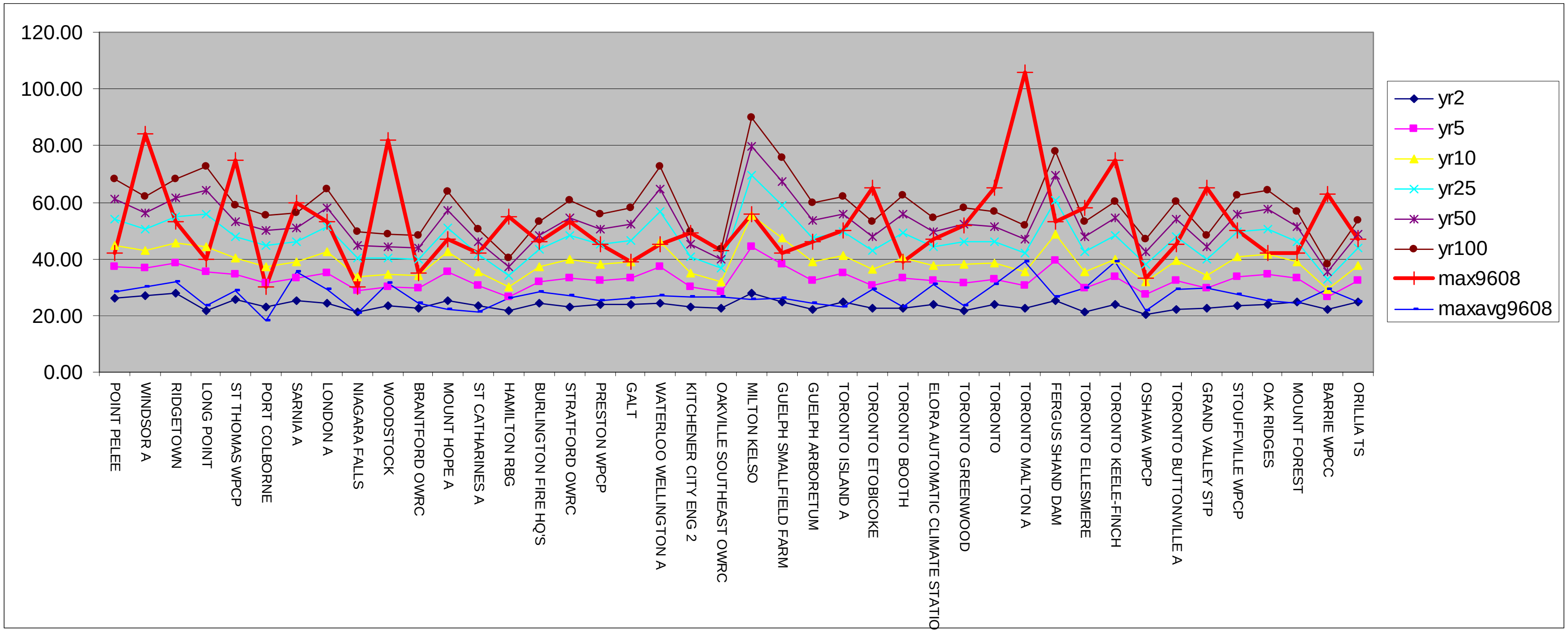

120.00
100.00
80.00
60.00
40.00
20.00
0.00
POINT PELEE
WINDSOR A
RIDGETOWN
LONG POINT
ST THOMAS WPCP
PORT COLBORNE
SARNIA A
LONDON A
NIAGARA FALLS
WOODSTOCK
BRANTFORD OWRC
MOUNT HOPE A
ST CATHARINES A
HAMILTON RBG
BURLINGTON FIRE HQ'S
STRATFORD OWRC
PRESTON WPCP
GALT
WATERLOO WELLINGTON A
KITCHENER CITY ENG 2
OAKVILLE SOUTHEAST OWRC
MILTON KELSO
GUELPH SMALLFIELD FARM
GUELPH ARBORETUM
TORONTO ISLAND A
TORONTO ETOBICOKE
TORONTO BOOTH
ELORA AUTOMATIC CLIMATE STATIO
TORONTO GREENWOOD
TORONTO
TORONTO MALTON A
FERGUS SHAND DAM
TORONTO ELLESMERE
TORONTO KEELE-FINCH
OSHAWA WPCP
TORONTO BUTTONVILLE A
GRAND VALLEY STP
STOUFFVILLE WPCP
OAK RIDGES
MOUNT FOREST
BARRIE WPCC
ORILLIA TS
yr2
yr5
yr10
yr25
yr50
yr100
max9608
maxavg9608

Appendix K
Spline Algorithm

Software used for the processing was ArcGIS 9.1 command line with the GRID (Spatial Analyst) extension.

The spline formula used the following formula for the precipitation and temperature surface interpolation:

$$S(x,y) = T(x,y) + \sum_{j=1}^{N} \lambda_j R(r_j)$$

where:

$j = 1, 2, 3, \ldots, N$

N is the number of points

λ_j are the coefficients found by the solution of a system of linear equations

r_j is the distance from the point (x,y) to the j^{th} point

$$T(x,y) = a1$$

$$R(r) = -\frac{1}{2\pi\varphi^2}\left[\ln\left(\frac{r\varphi}{2}\right) + c + K_o(r\varphi)\right]$$

where

τ^2 and ϕ^2 are the parameters entered at the command line

K_o is the modified Bessel function

c is a constant equal to 0.577215

a_i are the coefficients found by the solution of a system of linear equations

The following section provides a detailed description of which parameters were used with the spline interpolation formula.

Method	= tension
Weight	= 1.0
# of points	= 8 nearest points
Cell size	= 1 km

a. *Weight*

Weight parameter defines the weight of tension. It influences the character of the surface interpolation. Default is 0.1.

Higher weight values reduce the stiffness and produce coarser surfaces that more closely conform to the input points.

Weight values ranging from 0 to 5 were tested. Setting the weight parameter at **1.0** provided a balance between staying close to the range of observed values without getting too coarse.

b. *Number of points*

This parameter specifies how many points are used for local approximation. The default is 12.

The greater the number of points specified, the greater the influence from stations that lie further from the input point. This generally results in a smoother surface, but may mask any local variation.

Nearest neighbour analysis was completed using the ArcVeiw 3x extension Nearest Features v3.8. (www.jennessent.com). Diagrams showing the nearest stations were generated to assist in determining how many points should be used for this parameter.

Setting this parameter at **8** prevents distant stations from influencing the estimated surface, but also provides adequate coverage given the irregular and sometimes sparse distribution on input points. See Figure 5a and 5b

Figure 5a and 5b:

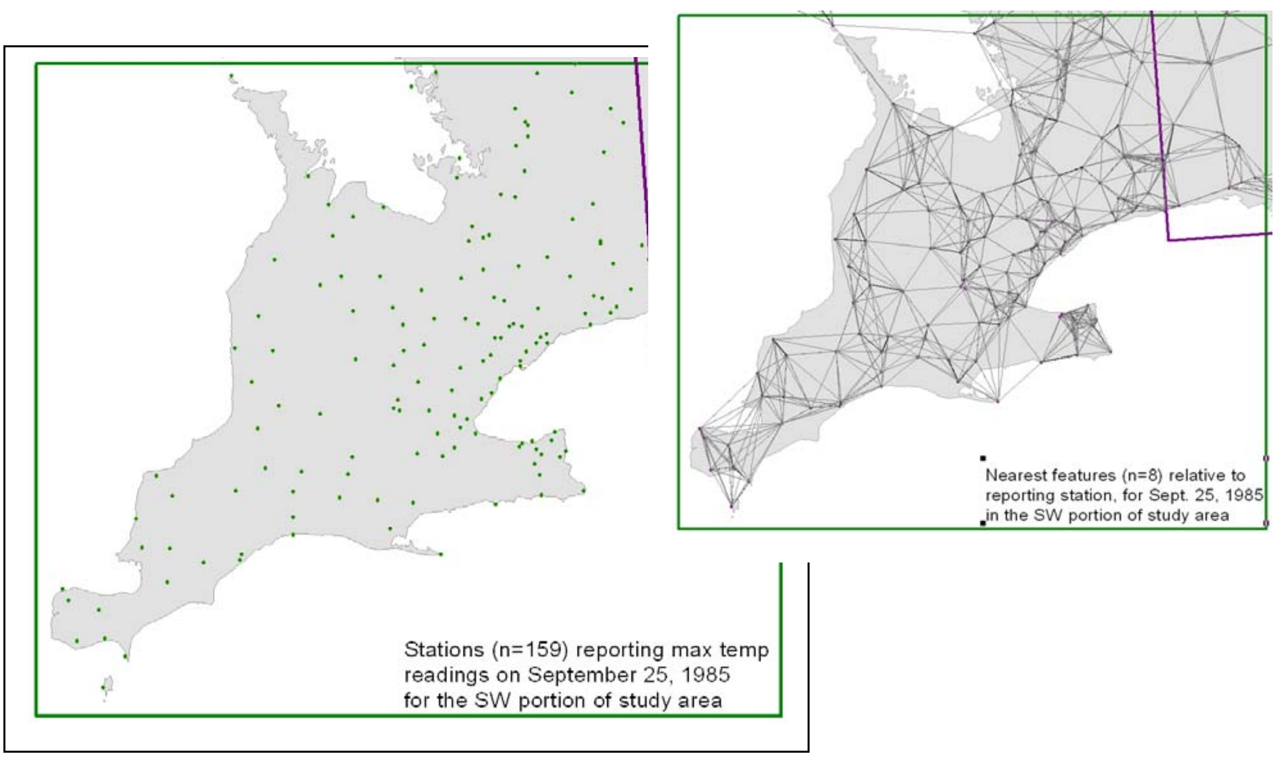

c. *Cell size*

Cell size of **1000m** was used, resulting in 1km x 1km raster surfaces.

d. *Area of interpolation* – xmin, ymin, xmax, ymax

When using the spline method of interpolation with ArcGIS, it is not possible to use a polygon layer to define the extent of the area to be interpolated. The coordinates of a rectangle (xmin, ymin, xmax, ymax), however, can be specified.

The following coordinates were used when generating interpolated surfaces for the study area:

Extent of W region:

xmin	316000
ymin	4605000
xmax	780000
ymax	5030000

Extent of E region:

xmin	700700
ymin	4842000
xmax	1053000
ymax	5084000

* Surfaces created in UTM 17 and projected to UTM 18

Given the shape of southern Ontario, its location adjacent to the Great Lakes, and the fact that observed climate variables were only recorded at land-based climate stations, edge effect cannot be overlooked. Any extension of the interpolated surface beyond the land base and over the Great Lakes is not an estimation of temperature in that location, but merely an artifact of processing resulting from the coordinates used to define the extent of the interpolation. For areas close to the shoreline the interpolation is weaker due to the lack of data over the lakes.

The parameters chosen for the spline method will help minimize deviation from the observed values and ensure that the interpolated surface passes exactly through the input points (climate stations), but a mask was applied to the Great Lakes (i.e. Great Lakes assigned NO DATA value) so that further analysis would not be skewed.

Bibliography

Atlas D et al. 1963. Severe local storms. Boston: American Meteorological Society. 247 p. illus. 29 cm p.

Barry RG and Chorley RJ. 1987. Atmosphere, weather and climate. 5th ed ed. London ; New York: Methuen. xxii, 460 p., [31] p. of plates : ill., maps p.

Bates BC, Kundzewicz ZW, Wu S, Palutikof JP, Eds. 2008. Climate change and water. technical paper of the intergovernmental panel on climate change. Geneva: IPCC Secretariat. 210 p. .

Boyd D. 2008. Senior water resources engineer, grand river conservation authority, personal communication. .

Brown ME and McCann B. 2004. Relating clustered convective events to land-surface features in mississippi. .

Brown DM, McKay GA, Chapman LJ. 1968. The climate of southern ontario. 2nd -- ed. Ottawa: Queen's Printer. 50 p.

Bruce JP, Dickinson WT, Rudra RP, Wall GW, Kazim SM. 2006. Planning for extremes: Adapting to impacts on soil and water from higher intensity rains with climate change in the great lakes basin. Ontario Chapter of the Soil & Water Conservation Society.

Changnon SAJ. 1980. More on the la porte anomaly: A review. Bulletin American Meteorological Society 61(7):702-17.

Connor S. 2007 Carbon dioxide rate is at highest level for 650,000 years. <http://www.independent.co.uk/environment/climate-change/carbon-dioxide-rate-is-at-highest-level-for-650000-years-434809.html>. Accessed 2008 November 15.

Conservation Ontario. 2009. Protecting people and property: A Business case for investing in flood prevention & control. Newmarket, Ontario: Conservation Ontario. 56 p. .

Cumming Cockburn Limited. 2000. Hurricane hazel and extreme rainfall in southern ontario. Toronto, ON: Institute for Castastrophic Loss Reduction.

De Loë RC and Berg A. 2006. Mainstreaming climate change in drinking water source protection in ontario. Ottawa, Ontario: Pollution Probe and the Canadian Water Resources Association (Ontario Branch).

Desjardins RL, Sivakumar MVK, de Kimpe C. 2007. The contribution of agriculture to the state of climate: Workshop summary and recommendations. Agricultural and Forest Meteorology 142:314-24.

Donaldson N. 2008. Radar research scientist.

Ellis RT and Chen SS. 2004. Effects of sea breeze and local winds on rainfall in south florida. 26th conference on hurricanes and tropical meteorology; May 2004; Miami, FL. American Meteorological Society.

Environment Canada. 2008 11-Jan-08. Canadian climate normals - climate information. <http://www.climate.weatheroffice.ec.gc.ca/climate_normals/climate_info_e.html>. Accessed 2008 11/01.

Environment Canada. 2007a Environment canada short-duration rainfall IDF (intensity-duration-frequency) tables and graphs – availability of electronic files december 2007. Accessed 2008 08/28.

Environment Canada. 2007b 2007-09-10. Fact sheet - winter weather warnings. <http://www.on.ec.gc.ca/severe-weather/winterwx_factsheet_e.html>. Accessed 2009 02/07.

Environment Canada. 2005 2005-05-24. Fact sheet - summer severe weather warnings. <http://www.on.ec.gc.ca/severe-weather/summerwx_factsheet_e.html>. Accessed 2009 02/07.

Environment Canada. 2001. Tracking key environmental issues : Air and water, nature, climate change and severe weather. Ottawa: Environment Canada. TML PUBLIC "-//W3C//DTD HTML 4.0 Transitional//EN" "http://www.w3.org/TR/REC-html40/loose.dtd"> p.

Farwell J, Boyd D, Ryan T. 2008. Making watersheds more resilient to climate change: A response in the grand river watershed, ontario canada. Cambridge, Ontario: Grand River Conservation Authority.

Feldstein SB. 2000. The Timescale, Power Spectra, and Climate Noise Properties of Teleconnection Patterns. Journal of Climate, 13, 4430-4440.

Francis D and Hengeveld H. 1998. Extreme weather and climate change. Ottawa: Minister of Supply and Services Canada. TML PUBLIC "-//W3C//DTD HTML 4.0 Transitional//EN" "http://www.w3.org/TR/REC-html40/loose.dtd"> p.

Grand River Conservation Authority. 2008. The grand - fall 2008 report. Cambridge, Ontario: Grand River Conservation Authority. 11 p. .

Hogg WD, Carr DA, Routledge B. 1989. Rainfall intensity-duration frequency values for canadian locations. Environment Canada. Report nr CLI-1-89.

Houghton JT. 2001. Climate change 2001 : The scientific basis : Contribution of working group I to the third assessment report of the intergovernmental panel on climate. New York : Cambridge, Eng.: Cambridge University Press.

Hurrell JW et al. 2009. Decadal Climate Prediction: Opportunities and Challenges. Community White Paper. National Center for Atmospheric Research, Climate Analysis Section, Boulder CO

IPCC 2000. IPCC Special Report on Emission Scenarios. [Nebojsa Nakicenovic and Rob Swart (Eds.)] Cambridge University Press, UK. pp 570

IPCC 2007. Climate Change 2007: The Physical Science Basis. Contribution of Working Group I to the Fourth Assessment Report of the Intergovernmental Panel on Climate Change [Solomon, S., D. Qin, M. Manning, Z. Chen, M. Marquis, K.B. Averyt, M. Tignor and H.L. Miller (eds.)]. Cambridge University Press, Cambridge, United Kingdom and New York, NY, USA, 996 pp.

Keeling CD and Whorf TP. 2004 Atmospheric CO2 concentrations (ppmv) derived from in situ air samples collected at mauna loa observatory, hawaii <http://cdiac.ornl.gov/ftp/ndp001/maunaloa.co2>. Accessed 2008 04/10.

Kharin, VV and Zwiers FW. 2005. Estimating Extremes in Transient Climate ChangeSimulations. Journal of Climate, 18 (8): 1156-1173.

King PWS, LEDUC MJ, Sills DML, Donaldson NR, Hudak DR, Joe P, Murphy BP. 2003. Lake breezes in southern ontario and their relation to tornado climatology. Weather and Forecasting 18(5):795-807.

Klassen J. 2002. A Climatological Assessment Of Major 20th Century Drought In Southern Ontario, Canada. 13th Conference on Applied Climatology; May 2002, Portland OR. American Meteorological Society.

Klaassen J. 2008. Senior Climatologist/Meteorologist. .

Klaassen J and Seifert M. 2004. Extreme rainfall in ontario: The summer 2004 storms study. Downsview, Ontario: Meteorological Service of Canada, Environment Canada.

Loeffler A. 2008. Conservation specialist, grand river conservation authority, personal communication. .

Mead C, Murdoch G, Turnage TJ. 2008 October 24, 2008. A severe weather climatology for the NWSO midland, texas county warning area. <http://www.srh.noaa.gov/ssd/techmemo/sr-191.htm>. Accessed 2009 03/19.

Mikko IJ and Sykes JF. 2007. The impact of climate change on spatially varying groundwater recharge in the grand river watershed. Journal of Hydrology 36(2).

Milly PCD, Betancourt J, Falkenmark M, Hirsch RM, Kundzewicz ZW, Lettenmaier DP, Stouffer RJ. 2008. Stationarity is dead: Whither water management? Science 319(February).

Mitchell, A. 2005. The ESRI Guide to GIS Analysis, Volume 2. ESRI Press

Mortsch L, Alden M, Klaassen J. 2005. Development of Climate Change Scenarios for Impact and Adaptation Studies in the Great Lakes – St. Lawrence Basin. Report prepared for the International Joint Commission, International Lake Ontario – St. Lawrence River Study Board, Hydrologic and Hydraulic Modeling Technical Working Group, 21 pp., Toronto, Ontario, Canada.

Murdoch PS, Baron JS, Miller TL. 2000. Potential effects of climate change on surface-water quality in north america. Journal of the American Water Resources Association 36(2):347-366.

National Oceanic and Atmospheric Administration, Ocean Service Education. 2009 July 29, 2009. Climate resources, factsheets. <http://oceanservice.noaa.gov/education/pd/climate/>. Accessed 2009 09/02.

National Research Council of Canada. Associate Committee on Hydrology, Watt WE, Lathem KW, Neill CR. 1989. Hydrology of floods in canada: A guide to planning and design. 1989: . 245 p p.

National Weather Service. 2008 June 13, 2008. Does the urban heat island affect rainfall variability across the phoenix, AZ metropolitan area during the monsoon season?

<http://www.wrh.noaa.gov/psr/general/monsoon/MonsoonPMA.php>. Accessed 2009 03/18.

Nuttle WK. 1993. Adaptation to climate change and variability in canadian water resources. [Downsview, Ont.]: Canadian Climate Centre. TML PUBLIC "-//W3C//DTD HTML 4.0 Transitional//EN" "http://www.w3.org/TR/REC-html40/loose.dtd"> p.

Ontario Ministry of Natural Resources. 2008. Southern ontario land resource information system (SOLRIS)
phase 2 - data SpecificationsVersion 1.2. Remote Sensing Specialist, Science and Information Branch, Ontario Ministry of Natural Resources.

Ontario Ministry of Natural Resources. 1985. Technical guidelines for flood plain management in ontario. Toronto, ON: .

Over TM, Murphy EA, Ortel TW and Ishii AL. 2007. Comparisons between NEXRAD radar and tipping-bucket gage rainfall data: A case study for DuPage county, illinois. ; May 15, 2007; ASCE. 274 p.

Parry ML. 2007. Climate change 2007 : Impacts, adaptation and vulnerability : Contribution of working group II to the fourth assessment report of the intergovernment. Cambridge, UK ; New York: Cambridge University Press.

Pearce D. 2008. Violent thunderstorm causes flooding, barn fire in boston. Brantford Expositor;Sect News:.

Phillips DW and O'Donnell BJ. 1975. Storm agnes in the lake ontario basin june 2-25, 1972. Downsview: Environment Canada, Atmospheric Environment. Report nr CLI-2-75.

Raddatz RL. 2007. Evidence for the influence of agriculture on weather and climate through the transformation and management of vegetation: Illustrated by examples from the canadian prairies. Agricultural and Forest Meteorology 142:186-202.

Ramanujan K. 2007 November 30, 2007. Are cities changing local and global climates? <http://www.nasa.gov/vision/earth/environment/Changing_Cities.html>. Accessed 2009 March/2009.

Ramkellawan J, Gharabaghi B, Winter JG. 2009. Application of weather radar in estimation of bulk atmospheric deposition of total phosphorus over lake simcoe. Canadian Water Resources Journal 34(1):37-60.

Rosenfeld D. 2000.
Suppression of rain and snow by urban and industrial air pollution. Science 287(5459):1793-6.

Saffle RE, Cate GS and Istok MJ. 2009. Nexrad product improvement – update 2009. 25th conference on international interactive information and processing systems (IIPS) for meteorology, oceanography, and hydrology; January 14, 2009; Phoenix, AZ. American Meteorological Society.

Sanderson M and Smith JV. 1993. Impact of climate change on water in the grand river basin, ontario. Waterloo, Ont.: University of Waterloo, Dept. of Geography. TML PUBLIC "-//W3C//DTD HTML 4.0 Transitional//EN" "http://www.w3.org/TR/REC-html40/loose.dtd"> p.

Schroeter H. 2007. Meteorological data missing-value fill-in for ontario. Cambridge, Ontario: Grand River Conservation Authority.

Science Daily. 2007. 2007-12. Top 11 warmest years on record have all been in last 13 years. <http://www.sciencedaily.com/releases/2007/12/071213101419.htm>. Accessed 2008 10/28.

Shen SP, Dzikowski P, Li G, Griffith D. 2001.
Interpolation of 1961–97 daily temperature and precipitation data onto alberta polygons of ecodistrict and soil landscapes of canada. Journal of Applied Meteorology 40:2162-77.

Sills DML. 2009. Severe weather scientist – severe local storms, mesoscale meteorology. .

Smith J and Lavender B. 1998. Adapting to climate variability and change in ontario. volume IV of canada country study: Climate impacts and adaptation. Downsview, Ontario: Environment Canada.

Southam CF, Mills BN, Moulton RJ, Brown DW. 1999. The potential impact of climate change in ontario's grand river basin: Water supply and demand issues. Canadian Water Resources Journal 24(4):307-330.

Story GJ. 2006. Determining WSR-88D precipitation algorithm performance using the stage III precipitation processing system. :July 21, 2008 .

Sumner GN. 1988. Precipitation : Process and analysis. Chichester [West Sussex] ; New York: Wiley. TML PUBLIC "-//W3C//DTD HTML 4.0 Transitional//EN" "http://www.w3.org/TR/REC-html40/loose.dtd"> p.

Sribimawati T, Brown DM, Hogg WD. 1992. Rainfall distribution during extended periods in mid-summer in southwestern ontario. Climatological Bulletin 26(3):135.

Troutman BM. 1981. The effect of input errors in using precipitation-runoff models for runoff prediction. Statistical analysis of rainfall and runoff; May 18-21, 1981; Mississippi State University. Baton Rouge, Louisiana: Louisiana State University.

Vincent LA and Mekis E. 2006. Changes in Daily and Extreme Temperature and Precipitation Indices for Canada over the Twentieth Century. Atmosphere-Ocean 44 (2) 177-193

Worldwatch Institute. 2006. Vital signs 2006-2007 : The trends that are shaping our future. 1st ed. New York: Norton. 160 p.

Zhang R, Delworth TL, Held IM, 2007: Can the Atlantic Ocean drive the observed multidecadal variability in Northern Hemisphere mean temperature? *Geophysical. Research Letters,* **34**, L02709, doi:10.1029/2006GL028683

Zhang X, Vincent LA, Hogg WD, Niitsoo A. 2000. Temperature and Precipitation Trends in Canada During the 20th Century. Atmosphere-Ocean 38 (3) 395-429